Integrative analysis of CD8 T-cell responses in the context of adaptive immunity to acute Hepatitis C virus infection

David Wolski

UNIVERSITÉ DE STRASBOURG

UNIVERSITÉ DE STRASBOURG

École Doctorale des Sciences de la Vie et de la Santé STRASBOURG

ÉCOLE DOCTORALE des sciences de la vie et de la santé (ED 414)

UMR 1110 Interactions virus-hôte et maladies hépatiques

THÈSE

présentée par:

David WOLSKI

soutenue le: **16 Mai 2017**

pour obtenir le grade de: **Docteur de l'Université de Strasbourg**

Discipline: **Sciences de la Vie et de la Santé**

Spécialité: **Immunologie**

Integrative analysis of CD8 T-cell responses in the context of adaptive immunity to acute Hepatitis C virus infection

DIRECTEUR DE THÈSE
Mr BAUMERT Thomas — Professeur, Université de Strasbourg

CO-DIRECTEUR DE THÈSE
Mr LAUER Georg — Professeur, Harvard Medical School

RAPPORTEURS:
Ms VAN BAARLE Debbie — Professeur, University Medical Center Utrecht
Mr LOHMANN Volker — PD, University of Heidelberg

AUTRE MEMBRE DU JURY (EXAMINATEUR):
Mr GEORGEL Philippe — Professeur, Université de Strasbourg

<u>Mühsal der Besten</u>

»Woran arbeiten Sie?« wurde Herr K. gefragt.

Herr K. antwortete: »Ich habe viel Mühe, ich bereite meinen nächsten Irrtum vor.«

- Bertolt Brecht -

Gewidmet meiner Mutter Hilde,

ihr verdanke ich meine Liebe zur Wissenschaft,

und Emily,

sie hat mir geholfen, das Licht am Ende des Tunnels zu sehen.

Ihr wart der Fels in der Brandung auf beiden Seiten des Ozeans.

Acknowledgments

First and foremost, I would like to thank my supervisors Prof. Thomas Baumert and Prof. Georg Lauer, without whose support and guidance this thesis would not have been possible. For their help in shaping and realizing this project, keeping me on track and focused, and for inspiring and challenging me to grow both personally and as a scientist, I am eternally grateful.

I would also like to express my sincerest appreciation for Prof. Debbie van Baarle, Dr. Volker Lohmann, and Prof. Philippe Georgel, who have graciously agreed to be members of my thesis committee and have sacrificed their time to participate in my defense.

Special thanks go to Dr. Catherine Schuster for her help and advice, to Catherine Corbel for her help in organizing my defense, and to Géraldine Schverer, Anne Zeter, and Mélanie Muser for their administrative support in organizing a PhD project from across the ocean.

I would like to acknowledge Dr. Peter Foote, Dr. Diana Chen, and Dr. Catherine Fauvelle, whose hard work was integral to the success of this project, as well as Dr. Arthur Kim and Dr. Lia Lewis-Ximenez, whose dedication to the patients that made this work possible has been an inspiration.

I extend my most heartfelt gratitude to Pierre and Julie, who have been great friends and were a tremendous help in the creation of this thesis.

Furthermore, I would like to thank all my friends and colleagues, past and present, who have accompanied me on this journey and helped to make the past years a wonderful experience. In order of appearance, I thank Daniela and Donatella, Garrett, Michelle, Jennifer, Stephanie, Jasneet, Joelle, Lyndon, Brandon, Michaela, Tess, Almudena, Juliana, and Ruben.

Lastly, I would like to thank the University of Strasbourg and the National Institutes of Health for providing me with the opportunity and financial support to perform my research and present this work.

Table of Contents

Table of Figures

Abbreviations

ADP	Adenosine diphosphate
AMP	Adenosine monophosphate
ATP	Adenosine triphosphate
CAMERA	Correlation Adjusted MEan RAnk gene set test
CD4	Cluster of differentiation 4
CD8	Cluster of differentiation 8
CD39/ENTPD1	Cluster of differentiation 39/Ectonucleoside triphosphate diphosphohydrolase-1
CD127/IL7R	Cluster of differentiation 127/Interleukin 7 Receptor
CD160	Cluster of differentiation 160
CD244/2B4	Cluster of Differentiation 244
CREB1	cAMP responsive element binding protein 1
CXCL2	Chemokine (C-X-C motif) ligand 2
CXCL8	Chemokine (C-X-C motif) ligand 8
DAA	Direct-acting antiviral
DAVID	Database for Annotation, Visualization, and Integrated Discovery
EBV	Epstein-Barr virus
FLI1	Fli-1 proto-oncogene, ETS transcription factor
GAGE	Generally Applicable Gene-set Enrichment
GSEA	Gene Set Enrichment Analysis
HBV	Hepatitis B Virus

HCMV	Human cytomegalovirus
HCV	Hepatitis B Virus
HIV	Human immunodeficiency virus
IFN-α	Interferon alpha
IFN-γ	Interferon gamma
IL1-β	Interleukin 1 beta
IL28B	Interleukin 28B/interferon-λ 3
IRES	Internal ribosome entry site
IRF3	Interferon regulatory factor 3
LAG-3	Lymphocyte-activation gene 3
LCMV	Lymphocytic choriomeningitis virus
MAVS	Mitochondrial antiviral-signaling protein
MDA5	Melanoma Differentiation-Associated protein 5
nAb	Neutralizing antibody
NF-κB/NFKB1/2	Nuclear factor kappa-light-chain-enhancer of activated B cells
ORF	Open reading frame
PD-1	Programmed cell death protein 1
pDC	Plasmacytoid dendritic cells
RFX5	Regulatory factor 5
RIG-I	retinoic acid-inducible gene 1
RNA	Ribonucleic acid
STAT1	Signal transducer and activator of transcription 1

STAT5	Signal transducer and activator of transcription 5
TCR	T cell receptor
TGFB1	Transforming growth factor beta 1
Tim-3	T-cell immunoglobulin and mucin-domain containing-3
TLR3	Toll-like receptor 3
TLR7	Toll-like receptor 7
TNF/TNFα	Tumor necrosis factor alpha
TP53	Tumor protein p53
TRIF	TIR-domain-containing adapter-inducing interferon-β
USP18	Ubiquitin-specific peptidase 18
UTR	Untranslated region
WGCNA	Weighted gene co-expression network analysis

Page intentionally left blank

Résumé

Le virus de l'hépatite C (VHC) est un petit virus enveloppé de la famille des Hepacivirus (Gould, 1999). Son génome viral se compose d'un ARN monocaténaire de polarité positive et présente une variabilité génétique élevée. L'identification de multiples génotypes et sous-types du VHC d'une part, et la détection de quasi-espèces virales chez un même sujet infecté d'autre part, témoignent de cette diversité génétique (Teschke, 2015). Celle-ci est notamment due au haut niveau d'erreurs induit au cours de la réplication, permettant notamment au virus d'échapper la réponse immune médié par les anticorps antiviraux et les lymphocytes T spécifiques du virus.

L'infection au VHC présente la particularité de pouvoir évoluer vers deux issues cliniques distinctes. En effet, dans environ 80% des cas, le virus persiste et l'infection devient chronique en l'absence de toute intervention thérapeutique. D'un autre côté, près de 20% des patients verront leur infection complètement éradiquée par leur système immunitaire dans les 6 à 8 mois suivant la primo-infection.

Une fois l'infection devenu persistante, la plupart des patients développe une hépatite C chronique et le risque d'évolution vers une cirrhose et une fibrose foie ou même un cancer se voie alors particulièrement augmenté (Poynard, Bedossa, & Opolon, 1997). Plusieurs facteurs ont été identifié comme pouvant influencer l'évolution de l'hépatite C incluant, le sexe et l'âge de l'hôte, sa consommation d'alcool ou encore l'existence d'éventuelles coïnfections avec le virus de l'immunodéficience humaine (VIH) ou avec le virus de l'hépatite B (HBV) (Sulkowski, 2003). A l'échelle mondiale, c'est plus de 150 millions de personnes qui sont atteints par l'infection au VHC sous sa forme chronique et dont l'évolution est devenue, dans de nombreux pays, la première indication vers la transplantation hépatique.

Bien que les transfusions sanguines contaminées aient longtemps été la principale cause de la transmission du virus (et le sont encore dans les pays en voie de développement), la grande majorité des transmissions dans les pays développés provient du partage des matériels d'injections contaminés par les

toxicomanes, élevant la prévalence de l'infection à 50% au sein de cette population à haut risque (UNODC, 2013).

L'introduction récente de traitements antiviraux très efficaces (Direct Acting Antivirals: DAA), permettant l'éradication du virus chez près de 90% des patients traités (Jayasekera, Barry, Roberts, & Nguyen, 2014), a révolutionné la prise en charge des patients infectés (Chung & Baumert, 2014). Jusqu'ici, et bien que présentant des effets secondaires importants, les traitements utilisant l'interferon-alpha, notamment sous sa forme pégylé, en combinaison avec de la Ribavirine, constituaient la principale option thérapeutique pour les patients infectés de façon chronique. Néanmoins, malgré la mise sur le marché des nouveaux traitements antiviraux, l'infections au virus de l'hépatite C restera un important problème de santé public pour plusieurs raisons; 1) la grande majorité des patients ne savent pas qu'ils sont infectés (Seeff, 2002), 2) la plupart des personnes infectées se trouve dans des pays en voies de développement et n'ont accès ni aux tests diagnostiques, ni aux traitements antiviraux aussi efficaces soient-ils (A. Hill & Cooke, 2014), 3) les patients infectés, même traités avec succès, demeurent à haut risque pour le développement de complications liées à leur infection tel que l'apparition d'un carcinome hépatocellulaire, 4) les populations à haut risque d'infection comme les toxicomanes demeurent à haut risque de réinfection après traitement (A. Y. Kim, Onofrey, & Church, 2013). Pour toutes ces raisons, la mise au point d'un vaccin prophylactique demeure une priorité de santé publique.

La réponse immunitaire contre le virus de l'hépatite C débute directement dans les hépatocytes infectés lorsque les RNA viraux sont détectés, induisant l'expression des interférons de types I et III ainsi qu'une variété de cytokines proinflamatoires (Bender et al., 2015). L'activation des récepteurs de l'interféron induit la stimulation d'une multitude de gènes (Interferon Stimulated Genes: ISGs) codant pour des protéines aux fonctions antivirales diverses (Schoggins et al., 2011). Cette réponse immunitaire

dite innée inclus également la mise en œuvre d'une variété de cellules spécialisés telles que les cellules NK, les cellules dendritiques ou encore les macrophages résidents du foie (Kupffer cells), produisant elles aussi une variété de cytokines pro-inflammatoires allant des interférons de type I (Dreux et al., 2012) à l'interleukine 1 bêta et bien d'autres (Negash et al., 2013). Les cellules NK, en plus de leur capacité à secréter de l'interféron gamma, impliqué dans l'inhibition de la réplication du virus (Golden Mason, Cox, Randall, Cheng, & Rosen, 2010; Jang et al., 2013; Sugden, Cameron, Mina, & Lloyd, 2014), ces cellules ont également pour fonction l'élimination des cellules infectées via la synthèse des protéines lytiques perforine et granzyme B. Bien que le VHC soit capable d'inhiber en partie la réponse immunitaire innée, la production continu d'interféron et l'induction des ISGs qui en résulte peuvent aboutir au blocage des voies de signalisations de l'interféron (G. Randall et al., 2006), réduisant ses propriétés antivirales (X. Zhang et al., 2014). Ainsi, la forte expression des ISGs chez des patients infectés de façon chronique a été associée à une plus faible réponse aux traitements utilisant l'interféron alpha (Dill et al., 2011). L'exposition prolongé à l'interféron a également pour caractéristique la différenciation des cellules NK, diminuant leur activité antivirale (Edlich et al., 2011; Miyagi et al., 2010).

La réponse immunitaire adaptative à l'encontre du VHC se compose de deux éléments principaux ; la réponse humorale résultant de la production d'anticorps antiviraux par les cellules B et la réponse cellulaire sous la forme des lymphocytes T CD8 dits cytotoxiques et des cellules T CD4 dits auxiliaires.

Bien que la contribution des anticorps neutralisants dans le control de l'infection ait été très longtemps jugé comme peu importante, notamment en raison de l'apparition tardive des anticorps lorsque l'infection en est déjà au stade chronique (Logvinoff et al., 2004), des études plus récentes rapportent l'induction rapide d'anticorps neutralisants au cours de la phase aiguë de l'infection et corrèle

la présence de ces anticorps avec le control de l'infection (Osburn et al., 2014; Pestka et al., 2007). Aussi, dans de rares cas, les anticorps neutralisants ont même été associés à la résolution tardive de l'infection chez des patients infectés de façon chronique (Raghuraman et al., 2012). En particulier, la détection d'anticorps neutralisants à réaction croisée, chez des patients capables d'éradiquer l'infection de façon spontanée malgré plusieurs réinfections (Osburn et al., 2010), suggère que l'induction d'anticorps à forte capacité neutralisante pourrait être un élément clé de la réponse induite par un vaccin potentiel.

Le rôle des cellules T, au cours des phases aiguë comme chronique de l'infection, a été largement étudié et les résultats de ces études, réalisées chez l'homme et dans des modèles expérimentaux utilisant le chimpanzé, ont tous démontré le rôle essentiel des lymphocytes T CD8 et CD4 pour la résolution de l'infection par le système immunitaire de l'hôte (Grakoui, 2003; Shoukry et al., 2003). Les réponses T spécifiques du VHC n'apparaissent que tardivement, 6 à 8 semaines suivant la primo-infection, et induisent le déclin rapide de la charge virale. Durant cette phase critique, le système immunitaire gagne et perd, par intermittence, le contrôle du virus (Rehermann, 2009), jusqu'à ce que le virus soit finalement dépassé par le système immunitaire ou la complète éradication du virus (Bowen & Walker, 2005). Bien que la réponse T semble être en tout point similaire au cours des premières semaines de la phase aiguë de l'infection, à la fois chez les patients qui élimineront spontanément le virus comme chez les patients qui progresseront vers une infection chronique (Cox, Mosbruger, Lauer, Pardoll, Thomas, & Ray, 2005a; Lauer et al., 2005), le phénotype des lymphocytes T diverge progressivement à mesure que l'issue clinique de l'infection se dessine. Ainsi, alors que le contrôle de l'infection est marquée par la présence de lymphocytes T CD8 hautement (poly-)fonctionnelles et l'émergence d'une population T CD4 mémoire (Schulze zur Wiesch et al., 2012), l'infection persistante diverge par la disparition progressive des lymphocytes T CD4, l'apparition de cellules T CD8 dysfonctionnels et l'émergence de quasi-espèces

virales limitant d'autant plus la visibilité des lymphocytes T par la mutation des épitopes viraux reconnus (Cox, Mosbruger, Mao, et al., 2005c; Erickson et al., 2001; Kuntzen et al., 2007). L'évasion du système immunitaire adaptatif par l'apparition de ces quasi-espèces virales est un mécanisme d'échappement majeur, affectant les réponses induites par les lymphocytes B et T de manière similaire (Timm et al., 2004).

Un mécanisme important par lequel un virus peut échapper à la réponse immunitaire est la dysfonction et l'épuisement des lymphocytes T (Angelosanto, Blackburn, Crawford, & Wherry, 2012; Wherry, 2011). Ce mécanisme, commun aux lymphocytes T CD4 et T CD8, n'a été que très peu étudié dans un contexte d'infection chronique au VHC (Kasprowicz et al., 2008; Kroy et al., 2014). L'épuisement des cellules T est le résultat de deux mécanismes principaux; l'autorégulation des cellules T via l'expression de récepteurs inhibiteurs (Barber et al., 2005; Blackburn et al., 2008), et l'allo-régulation via l'interaction avec des cellules T régulatrices (Boettler et al., 2005; Cabrera et al., 2004; Rushbrook et al., 2005; Smyk-Pearson et al., 2008). Ces mécanismes initialement destinés à maintenir une réponse T adaptée et proportionnée sont autant de voies potentielles pouvant être exploitées par le virus pour diminuer la réponse immune à son encontre (Belkaid, 2007; O'Garra & Vieira, 2004; Sakaguchi, Yamaguchi, Nomura, & Ono, 2008).

Ainsi, lorsque nos connaissances actuelles de ces mécanismes immunologiques résultent, pour la plupart, de recherches portant sur des mécanismes isolés, utilisant un seul type cellulaire, il semble de plus en plus relevant d'étayer ces connaissances par une vision plus global des mécanismes immunologiques mis en œuvre, ce qui implique la gestion d'un très grand nombre de données et l'utilisation de systèmes d'analyse complexe telle que la bio-informatique médicale (Aderem et al., 2010; Germain, Meier-Schellersheim, Nita-Lazar, & Fraser, 2011). Ce nouveau domaine, communément appelé immunologie

des systèmes (Shay & Kang, 2013) permet l'intégration de données provenant de techniques expérimentales à faibles et hauts débits. Ces approches utilisent un ensemble d'outils computationnels pour mieux comprendre au niveau holistique les interactions dynamiques entre les cellules immunitaires, les pathogènes, les cellules infectées ou malignes (Chaussabel & Baldwin, 2014).

Avec cette complexité en tête, le but de ma thèse était 1) de démontrer que l'on peut approfondir nos connaissances biologiques par des techniques analysant l'expression des gènes issus des rares populations de lymphocytes T CD8 spécifiques du virus et 2) d'étudier la régulation de ces gènes à différents stades de l'infection, eu égard de l'issue clinique, et de la réponse immune adaptative.

La première partie de mon travail était une étude de preuve de concept utilisant une cohorte pilote de 30 patients, tous en phase aiguë de l'infection mais évoluant vers différentes issues cliniques, dans le but de démontrer qu'il était possible d'obtenir des données d'expression génétiques de grande qualité à partir d'ARN provenant d'un petit nombre de cellules T CD8 spécifiques du virus (environ 1000) et d'identifier des gènes candidats impliqués dans la régulation des cellules T au cours de l'infection. L'analyse non-supervisée des résultats (non publiée) avait révélé une séparation claire entre les 2 issues cliniques (infection spontanément résolue ou persistance de l'infection) associée à l'expression de plusieurs gènes. Par validation des cibles identifiées par cytometrie en flux, nous avons observé que l'ectonucléoside triphosphate diphosphohydrolase-1 (ENTPD1) ou CD39, une enzyme impliquée dans l'hydrolyse des nucléosides tri- et diphosphates ((A/U)TP et (A/U)DP) en monophosphates ((A/U)MP), était bien différentiellement exprimée à la surface des cellules T CD8 spécifiques du virus selon l'issue clinique de l'infection. Jusqu'ici, l'expression de CD39 avait seulement été rapportée à la surface des cellules T CD4 régulatrices, où sa fonction enzymatique avait été associée à l'activité inhibitrice de ces cellules (Deaglio et al., 2007). Plus tard, l'analyse de l'expression de CD39 par les

lymphocytes T CD8 spécifiques du VHC, VIH, CMVh ou EBV ont démontré que l'expression de CD39 était corrélée avec l'expression du récepteur inhibiteur PD1 au cours de la réplication des virus VHC et VIH, suggérant une implication potentielle de CD39 dans l'activation et/ou la dysfonction des lymphocytes T. Cette hypothèse a ensuite été confortée par la confirmation de nos résultats dans un modèle murin d'infection virale chronique (LCMV), dans lequel CD39 est fortement exprimé par les cellules T CD8 dysfonctionnelles. Ces résultats ont donc montré le rôle clé de la protéine CD39 dans les mécanismes d'épuisements des lymphocytes T et soulignent l'importance de la régulation métabolique dans le fonctionnement des lymphocytes T (Gupta et al., 2015).

Dans la seconde partie de mon projet, j'ai appliqué les techniques de profilage d'expression des gènes mis en place plus tôt à une cohorte plus large de patients. Basée sur nos connaissances actuelles de la réponse immunologique au cours de la phase aiguë de l'infection, notre hypothèse était que la réponse immune adaptative se définie par une réponse multifactorielle, sujette à une fine régulation fonctionnelle et au cours du temps. L'analyse développée pour tester cette hypothèse est basée comme précédemment sur les lymphocytes T CD8, provenant de patients atteints d'infections chronique ou résolue, mais prend également en compte différents temps au cours de l'infection et identifie les cellules T CD8 spécifiques d'épitopes viraux conservés et mutés parmi les patients atteints d'infection chronique. L'analyse a également été étayée par l'identification, par cytometrie en flux, des cellules T CD4 spécifiques du VHC ainsi que par les titres d'anticorps neutralisants, obtenus par une méthode utilisant un système de pseudo-particules virales. Parmi les échantillons testés pour la présence d'anticorps neutralisants, seulement quatre ont montré une activité neutralisante et étaient reparti de façon équitable au sein des différents groupes de patients, empêchant leur corrélation avec les profils de transcription des gènes des lymphocytes T. L'absence de réponse forte par les anticorps neutralisants a néanmoins renforcé notre

conviction que toute association observée entre la régulation des gènes des lymphocytes T et l'issue clinique de l'infection pourrait résulter d'un lien de causalité direct.

L'analyse différentielle de l'expression des gènes a dans un premier temps confirmé la présence de différents profils d'expression en fonction de l'issue clinique de l'infection. Différents profils d'expression des gènes ont également été identifiés selon la capacité des cellules T à reconnaitre ou non (par exemple si un épitope apparait muté) les épitopes viraux. Parmi ces gènes differentiellement régulés, nous avons observé de nombreux régulateurs et effecteurs de la réponse immune et du stress cellulaire, renforçant notre argument selon lequel la régulation métabolique et la fonction des cellules T sont étroitement liées. Afin de poursuivre notre analyse, nous avons utilisé une approche non-supervisée d'apprentissage automatique pour construire un réseau de co-expression des gènes pour chaque groupe expérimental et définir des modules de gènes co-regulés. Nous avons observé une co-regulation des gènes liés aux voies metaboliques et immunes ainsi que des gènes impliqués dans l'assemblage du nucléosome et la répression de la chromatine. Differents profiles de connectivité et de co-régulation des gènes et groupes de gènes, au sein d'un même groupe et entre les differents groupes de patients, ont révélé le cœur de l'entité des cellules T ainsi que des profils d'expression uniques, associés à l'issue clinique de l'infection, indicant un dysfonctionnement précoce des réponses des cellules T CD8 spécifique du virus au cours de l'infection chronique. Plus précisément, nous avons identifié des différences majeures dans la régulation des processus métaboliques au cours de l'infection chronique précoce par le VHC ainsi que des profils d'expression des gènes impliqués dans la régulation de l'apoptose, la différenciation des lymphocytes T et la réponse à l'inflammation. De plus, ces différences présentaient de fortes associations avec l'âge et le sexe du patient, deux prédicteurs connus pour influencer l'issue clinique de l'infection, ainsi qu'avec le niveau d'aide apporté par les cellules T CD4 auxilliaires.

En résumé, les travaux présentés dans cette thèse démontrent que les événements transcriptionnels ayant lieu dans les cellules T CD8 spécifiques du virus au cours de cette phase critique qu'est la phase aiguë de l'infection, sont marquées par des changements dans la régulation des fonctions métaboliques de base, des voies de signalisation pro-inflammatoires, des processus liés à l'assemblage du nucléosome ainsi que dans le remodelage et la répression de la chromatine. Ces changements, fortement dépendants du temps, sont corrélés a l'augmentation de la dysfonction des cellules T CD8, à la présence des T CD4 auxiliaires et à la perte de la reconnaissance de l'antigène, suggérant que la perturbation des fonctions métaboliques pourrait conduire à une dysrégulation des processus transcriptionnels susceptible d'entraîner l'épuisement des cellules T et la perte des fonctions effectrices des lymphocytes T CD8 spécifiques du virus au cours de la phase aiguë de l'infection. Les travaux futurs devraient viser à mettre en oeuvre des modèles fonctionnels capables de fournir de plus amples réponses quant aux mécanismes de la régulation du métabolisme des lymphocytes T et leurs rôles dans le contrôle de l'intégrité fonctionnelle et transcriptionnelle des cellules T, dans les environnements à haut stress que sont les sites d'infection, ainsi qu'une meilleure compréhension du rôle des modifications épigénétiques de l'ADN et des histones dans la régulation de l'immunité par les lymphocytes T.

Introduction

Historical Background

In 1975, Harvey Alter and colleagues reported evidence that a heretofore undefined infectious agent was the likely cause of a large percentage of incidences of hepatitis after blood transfusions (Alter et al., 1975). This discovery was a direct result of the development of serological tests for hepatitis A virus (HAV) and hepatitis B virus (HBV), allowing to rule out these viruses as the cause of many cases of post transfusion hepatitis. These cases, caused by an unknown agent, were thus called non-A, non-B hepatitis. It was not until thirteen years later, in 1989, that a team of scientists around Michael Houghton and Qui-Lim Choo isolated a cDNA clone of a virus from a hepatitis patient that turned out to be the causative agent for most cases of non-A, non-B hepatitis. The virus was named Hepatitis C virus (HCV) (Choo et al., 1989).

Hepatitis C Virus

About 50nm in size, Hepatitis C virus is a small, enveloped, single-strand, positive-sense RNA virus of the genus Hepacivirus within the Flaviviridae family (Gould, 1999). Its ~9.6 kilobase genome contains a single long open reading frame (ORF) that codes for a large polyprotein precursor and is flanked by 5' and 3' untranslated regions (UTRs) (Figure 1, [Scheel & Rice, 2013]). The 5' untranslated region contains both an internal ribosome entry site (IRES), which facilitates ORF translation by the host cellular translation apparatus (Hoffman & Liu, 2011), and two binding sites for the host endogenous microRNA mir122 (Jangra, Yi, & Lemon, 2010). The HCV polyprotein is processed into 3 structural proteins (core, E1, E2) and 7 nonstructural proteins (p7, NS2, NS3, NS4A, NS4B, NS5A, NS5B). The core protein makes up the nucleocapsid, while the glycoproteins E1 and E2, together, form the viral envelope (Bartenschlager, Penin, Lohmann, & André, 2011). p7 is a viroporin with ion channel activity

that ensures successful viral assembly and exit from the host cell (Chandler, Penin, Schulten, & Chipot, 2012; Luik et al., 2009; Wozniak et al., 2010).

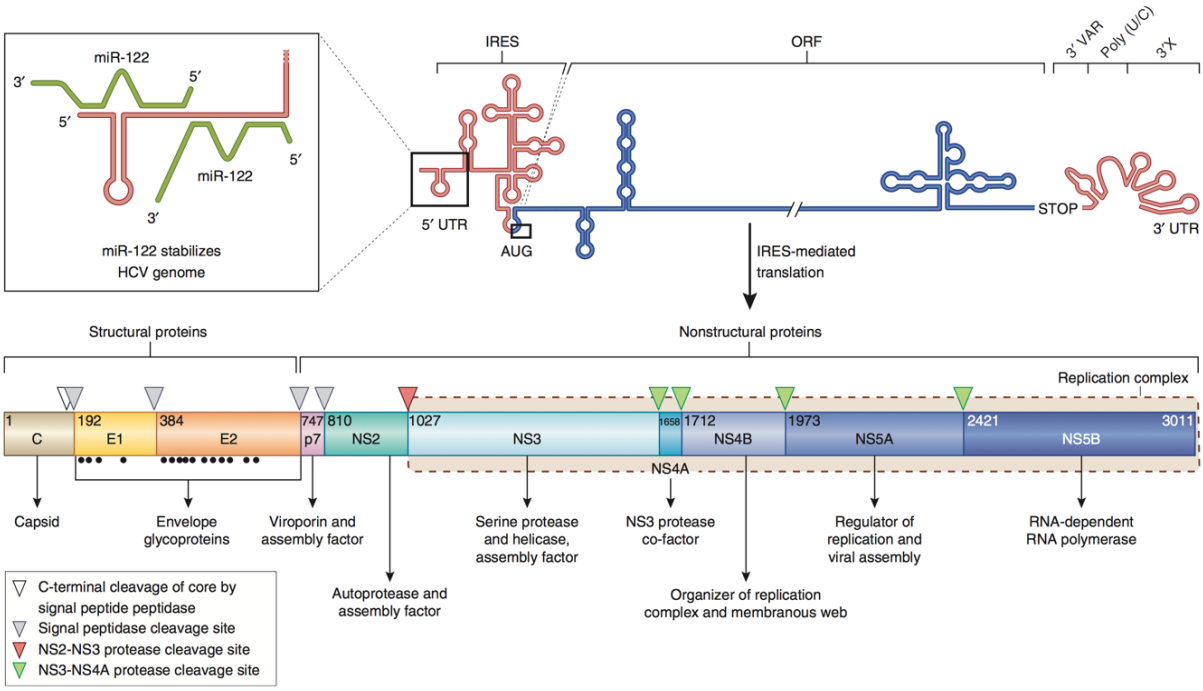

Figure 1. *Structural organization of the HCV genome and polyprotein (Scheel & Rice 2013).*

The autoprotease NS2 both interacts with p7 as part of the assembly module and cleaves itself from the protease NS3 (Lorenz, Marcotrigiano, Dentzer, & Rice, 2006), which, in turn, cleaves the remainder of the viral proteins from each other, with help from its cofactor NS4A. Both NS3 and NS4A also play a role in assembly of the virus (Morikawa et al., 2011; Phan, Kohlway, Dimberu, Pyle, & Lindenbach, 2011). NS4B organizes the replication complex and the membranous web at the endoplasmic reticulum (Egger et al., 2002), where it, together with NS5A, which regulates replication and viral assembly, provides the framework that allows the RNA-dependent RNA polymerase NS5B to synthesize, first, a negative-sense template, and then several copies of positive-sense RNA which are used further in either translation and replication or in the loading of new virus particles (Jones, Patel, Targett-Adams, & McLauchlan, 2009; Lohmann, 2013).

One of the most important features of HCV is its extensive viral diversity, reflected both on the population level, by significantly distinct viral genotypes, and within patients, by the quasispecies nature of the circulating vial population. HCV can be classified in at least 7 genotypes and 67 subtypes (Smith et al., 2013). Genotypes and subtypes differ from each other by 31-33% and 20-25% on the nucleotide level, respectively, resulting in extensive differences on the protein level as well (Simmonds et al., 2005). The heterogeneity of the circulating HCV strains by far dwarfs that of human immunodeficiency virus (HIV) and hepatitis B virus (HBV) and is a major obstacle to the development of an HCV vaccine (Figure 2, [Ray & Thomas, 2015]).

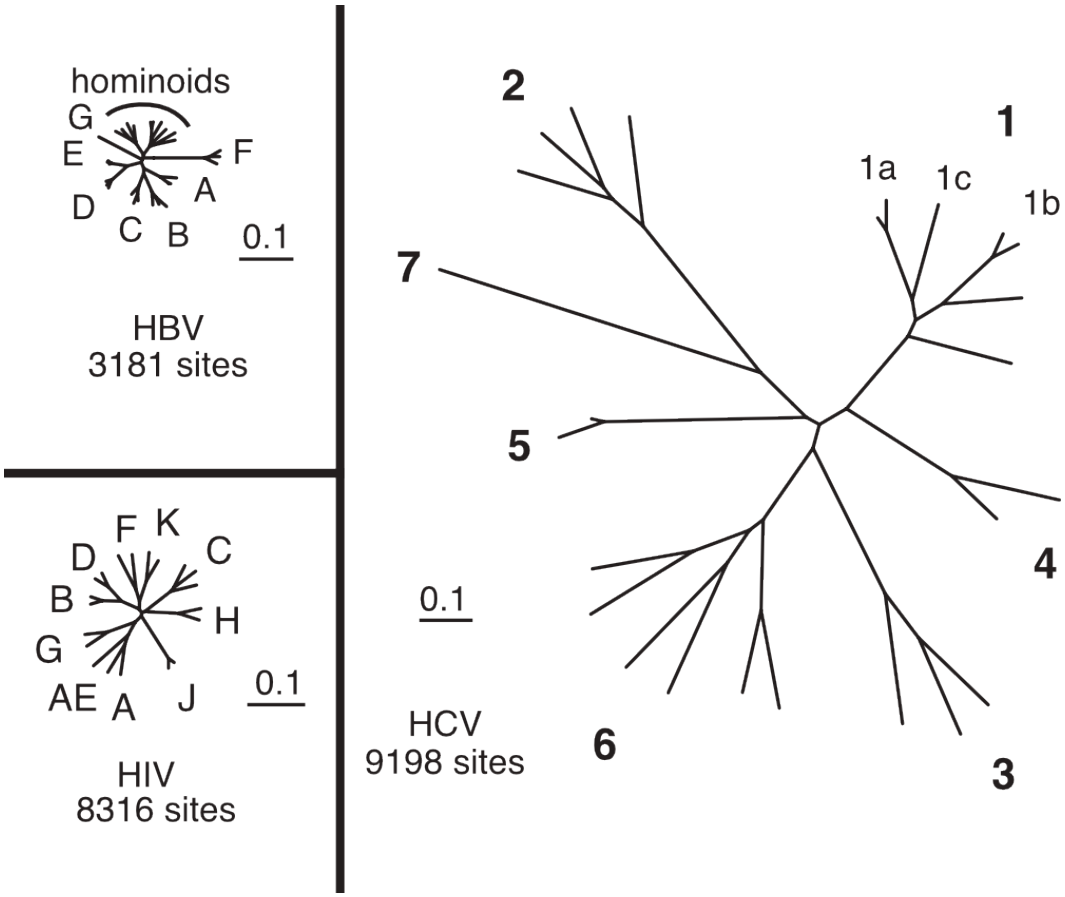

Figure 2. *Genetic diversity of HCV in comparison with HIV and HBV (Ray & Thomas, 2015)*

Because of the extremely high HCV replication level and the viral replication complex that lacks proofreading capacity, the virus also exists in a highly complex and continuously evolving spectrum of different mutants, called quasispecies, within a single patient (Teschke, 2015). This process, mostly driven by viral adaptations to the antiviral antibody and T cell response and subsequent mutations that restore viral replication fitness, is a major reason why HCV can persist in most patients in the presence of robust immune responses.

HCV Epidemiology

In 2016, an estimated more than 150 million people worldwide were infected with HCV, putting them at risk of developing chronic viral hepatitis, liver cirrhosis and, ultimately, end stage liver disease and liver cancer (Hajarizadeh, Grebely, & Dore, 2013). HCV-related liver disease has become the leading indication for liver transplantation in many countries. There are great differences in HCV prevalence between different regions of the world (Figure 3), with the highest prevalence of HCV being found in the Nile Delta in Egypt, where unsafe injection practices during comprehensive parenteral treatment programs for schistosomiasis have resulted in a prevalence of 18% and more in some communities (Guerra, Garenne, Mohamed, & Fontanet, 2012).

Overall, blood transfusions and other unsafe medical practices were the major driver of the early HCV pandemic, until the introduction of HCV antibody tests and better medical practices led to a sharp decline in HCV transmissions, at least in countries that were able to comprehensively establish such programs (Donahue et al., 1992). In these countries, most HCV transmissions now occur in people who inject drugs via contaminated drug paraphernalia, leading to a prevalence often exceeding 50% in these

populations (UNODC, 2013). In the USA, a recent countrywide surge of opioid use has led to a second wave of HCV infections in people under the age of 30 (Harris et al., 2016).

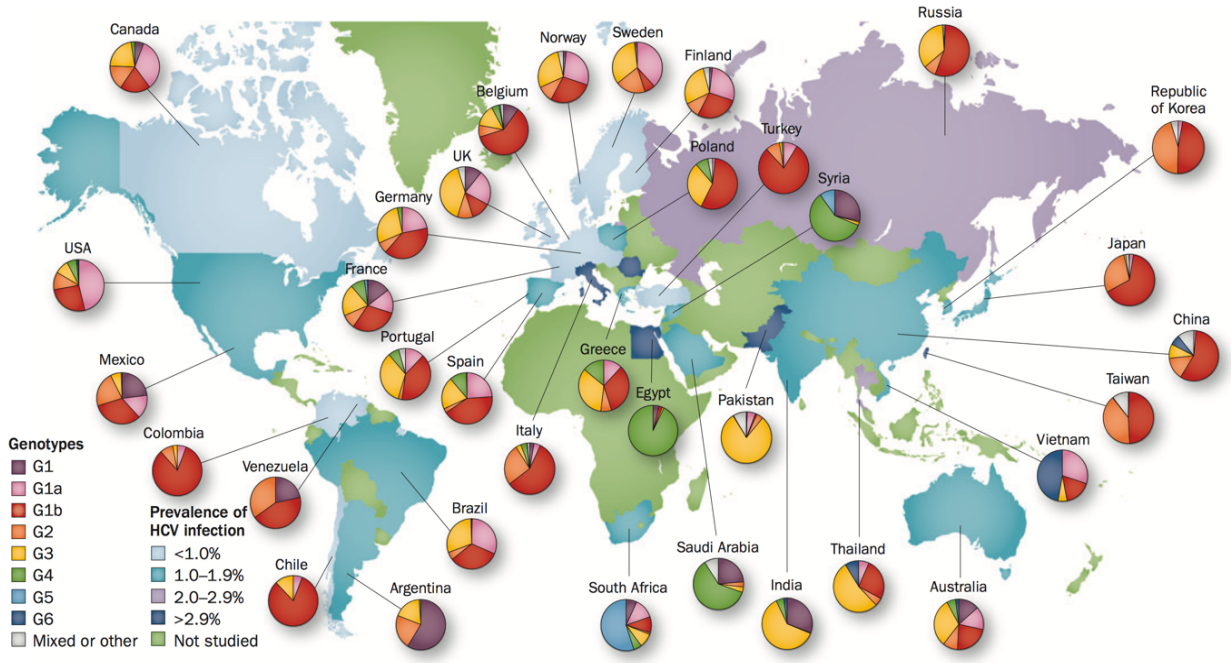

Figure 3. *Global estimates of HCV infection prevalence and genotype distribution (Hajarizadeh, Grebely, & Dore, 2013)*

The wide prevalence of HCV, especially in resource poor areas, together with the ongoing transmission in people who inject drugs, almost certainly guarantees that HCV will remain a major clinical challenge for many years, despite the recent introduction of extremely efficient directly acting antiviral therapies (DAA) achieving viral eradication in more than 90% of treated subjects (Jayasekera et al., 2014).

Natural History of HCV Infection

HCV infection is unique among chronic viral infections in that it can result in two completely dichotomous clinical and virological outcomes. In about ~70% of subjects, HCV viremia persist and will, in almost all of these subjects, continue to persist over the entire life span of the host without therapeutic

interventions (Figure 4, [Heim, 2013]). In the other ~30% of infections, however, the virus is completely eradicated by the immune system, akin to classical acute infections like influenza or hepatitis A. This almost always occurs in the first 6 to 8 months after viral exposure and depends on vigorous and sustained immune responses. Importantly, the same viral inoculum, or even the same viral clone, can lead to either outcome in humans and chimpanzees, indicating that host features play a key role in the outcome of infection (Lauer & Walker, 2001).

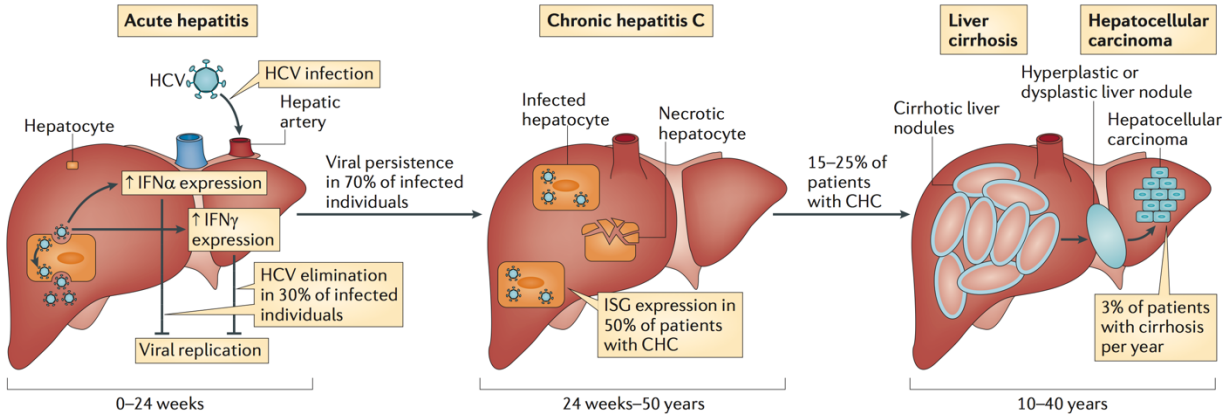

Figure 4. *Natural history of HCV infection (Heim 2013)*

Once chronic HCV infection is established, most patients will develop chronic hepatitis with elevated liver transaminases and inflammatory infiltrates observed in histological assessments of liver biopsies (Seeff, 2002). Beyond that, the clinical course and the timeline of disease progression is highly variable between patients, ranging from minimal hepatitis over several decades to very rapid progression, resulting in liver fibrosis and cirrhosis, liver failure and/or liver cancer within a few years. However, in most patients it takes several decades from HCV infection to overt signs of liver disease (Poynard et al., 1997), with key factors influencing disease progression being sex, age, alcohol use and co-infection, with younger age, female sex, and low alcohol consumption being predictors of slower rate disease progression.

In contrast, high alcohol consumption as well as HIV or HBV coinfection are known to increase the progression rate more than just additively (Blankley et al., 2014; Sulkowski, 2003).

HCV Treatment

Recent breakthroughs in HCV therapy have completely revolutionized the care of HCV patients (Chung & Baumert, 2014). Early treatment regimens based on the application of interferon alpha achieved a full virologic cure in not more than 10% of patients with genotype 1 infection, and even the more recent therapies using PEGylated interferons in combination with Ribavirin achieved a sustained virologic response only in a minority of subjects and came with severe side effects (Heim, 2013). In contrast, the introduction of different direct-acting antiviral agents (NS3/4A protease inhibitors, NS5B nucleoside polymerase inhibitors, NS5B non-nucleoside polymerase inhibitors, and NS5A inhibitors) that can be given alone or in combination, has led to cure rates of over 90%, even in difficult to treat patients (Bartenschlager, Lohmann, & Penin, 2013; Sarrazin, Hézode, Zeuzem, & Pawlotsky, 2012). Patients who are aware of their infection and live in societies that can provide these extremely costly drugs can now mostly rely on being cured.

Nevertheless, HCV infection will remain a significant global health issue for the foreseeable future for the following reasons: 1) The vast majority of HCV infected people are unaware of their infection (Seeff, 2002), 2) Most HCV infected persons live in resource poor country where diagnostic tools and, more so, new drugs will not be readily available (A. Hill, Khoo, Fortunak, Simmons, & Ford, 2014), 3) patients who are cured in later stages of liver disease are still at risk for complications such as hepatocellular carcinoma, and 4) people at high risk for infection and re-infection, such as the increasing population who injects drugs and people in high prevalence areas will continue to be at risk (A. Y. Kim

et al., 2013). These reasons imply the need for continued efforts in community outreach, testing programs and public health services, programs that allow diagnosis and testing in resource poor settings and, above all else, an effective prophylactic HCV vaccine.

Innate immunity in acute and chronic HCV

Defense against HCV infection begins with the innate immune response in the infected hepatocytes themselves (Figure 5, [Shin, Sung, & Park, 2016]). Viral RNA is sensed either by pattern recognition receptors retinoic acid-inducible gene I (RIG-I) and melanoma differentiation-associated protein 5 (MDA5) in the cytoplasmic compartment, or by toll-like receptor 3 (TLR3) in endosomes (Arnaud et al., 2011; Hiet et al., 2015; K. Li et al., 2012).

This sensory event triggers different downstream signaling pathways mediated through either mitochondrial antiviral-signaling protein (MAVS) (for RIG-I and MDA5) or Toll/IL-1 receptor-domain-containing adapter-inducing interferon-b (TRIF) (for TLR3), which converge in the induction of type I and type III interferon expression and the expression of pro-inflammatory cytokines by interferon regulatory factor 3 (IRF3) and nuclear factor kappa B (NF-κB) respectively (Bender et al., 2015). Signaling of released interferons through their receptors in turn induce the expression of interferon-stimulated genes (ISGs), whose products exert a range of antiviral effector functions (Schoggins et al., 2011).

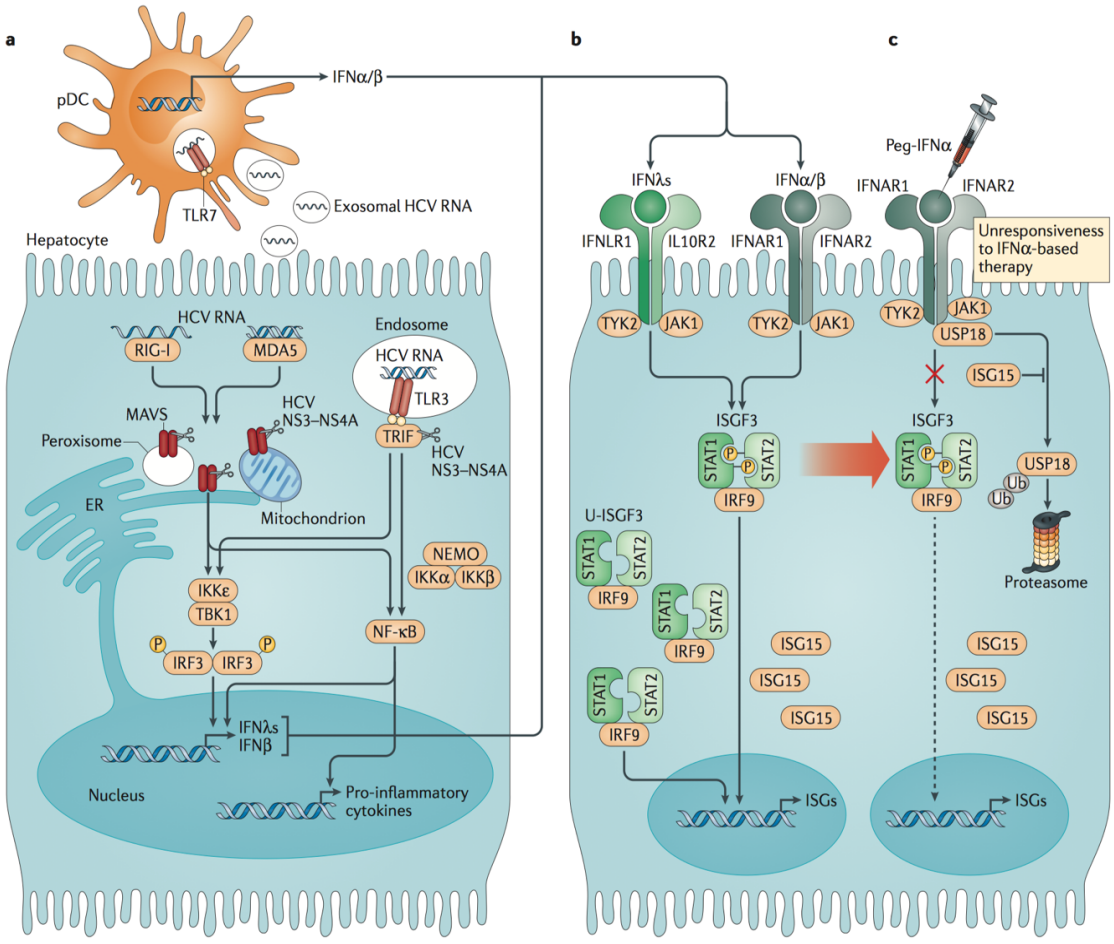

Figure 5. *Innate interferon response to HCV infection (Shin et al. 2016)*

The innate immune response to HCV also includes a range of innate immune cells, such as NK cells, dendritic cells and liver-resident macrophages (Kupffer cells). A recent study found that, like hepatocytes, plasmacytoid dendritic cells (pDCs) also produce type I interferons in response to the uptake of hepatocyte exosomes that contain viral RNA (Dreux et al., 2012) in a TLR7-mediated, is cell-to-cell contact dependent process. The TLR7 inflammasome is also the mechanism by which Kupffer cells produce an interleukin 1 beta (IL-1b) response to phagocytic uptake of HCV RNA in vivo (Negash et al., 2013). NK cells play a dual role in HCV infection, by both secreting cytokines such as interferon

gamma (IFN-γ), which inhibits HCV replication (Golden Mason et al., 2010; Jang et al., 2013; Sugden et al., 2014), and directly killing infected cells via perforin and granzyme B.

HCV is able to interfere with the innate immune response through cleavage of the signaling proteins MAVS and TRIF by HCV NS3/NSA4, but fails to abrogate it completely (Bellecave et al., 2009). Even with decreased interferon production, ISG induction continues, as signal transducer and activator of transcription 1 (STAT1), signal transducer and activator of transcription 2 (STAT2), and interferon regulatory factor 9 (IRF9), the molecules that make up IFN-stimulated gene factor 3 (ISGF3), are present in high enough numbers to allow the complex to induce ISG expression in the absence of STAT phosphorylation by interferon receptors (Sung et al., 2015).

This persistence of the virus with simultaneous prolonged induction of ISGs eventually leads to blockade of interferon signaling by the ubiquitin-specific peptidase 18 (USP18) which is stabilized by ISG15 (G. Randall et al., 2006), effectively desensitizing cells to interferon stimulation (X. Zhang et al., 2014), an effect that results in the poor prognosis for interferon therapy in patients with high baseline ISG induction (Dill et al., 2011). Another innate immunity hallmark of long-term interferon production is a shift in NK cell function to a more cytotoxic profile and away from production of IFN-γ, which is associated with their diminished ability to control HCV (Edlich et al., 2011; Miyagi et al., 2010).

Adaptive immunity in acute and chronic HCV

The adaptive immune response to HCV consists of two main components, the humoral response in the form of antibodies produced by B cells and the cellular response in the form of cytotoxic CD8 T cells and CD4 T helper cells (Figure 6, [Baumert, Fauvelle, Chen, & Lauer, 2014]).

While the contribution of neutralizing antibodies to control and resolution of HCV infection was controversial for a long time, as neutralizing antibodies seemed to appear mostly in patients with long-term chronic infection (Logvinoff et al., 2004), more recent studies have reported the rapid induction of neutralizing antibodies and its correlation with viral clearance in multiple cohorts of acutely infected individuals (Osburn et al., 2014; Pestka et al., 2007) as well as rare cases of broadly neutralizing antibodies overcoming long-term chronic infection and leading to resolution of disease (Raghuraman et al., 2012).

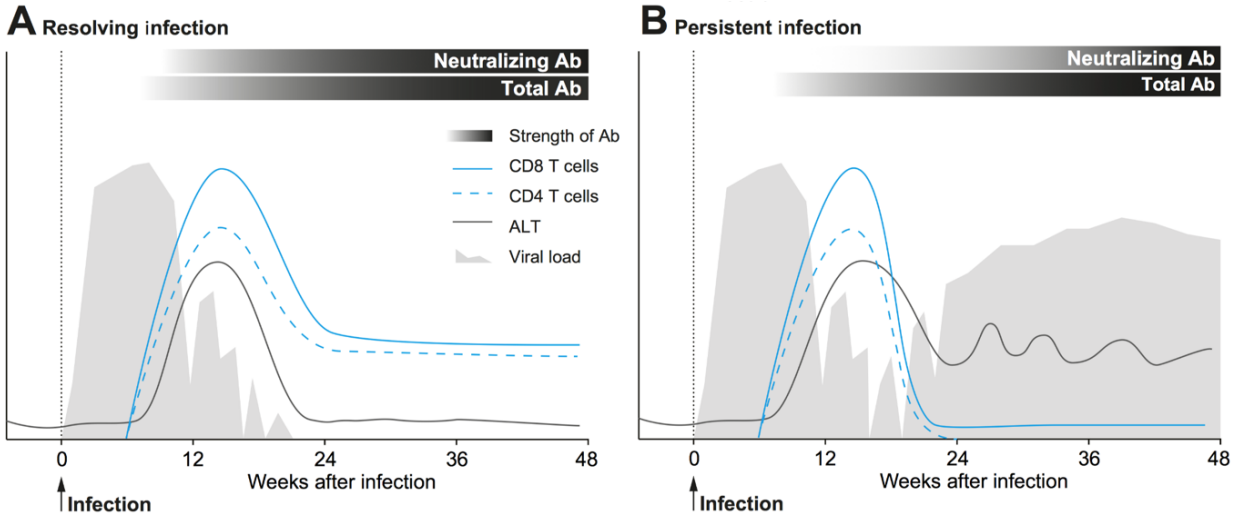

Figure 6. *Kinetics of the adaptive immune response in resolving and persistent HCV infection (Baumert, Fauvelle, Chen, & Lauer, 2014).*

Particularly the detection of cross-reactive nAbs in patients with a secondary HCV infection after previous clearance (Osburn et al., 2010) suggests that induction of high quality neutralizing antibodies aids in spontaneous resolution of infection and could be a vital part of the immune response elicited by a potential vaccine. However, part of the intra-host HCV dissemination strategy is direct cell-to-cell transmission of the virus, which limits the effect of neutralizing antibodies (Brimacombe et al., 2010), as well as that of direct-acting antivirals (Xiao et al., 2014), once the initial infection has taken place. At this point, a T cell response will be required to identify and cure or kill infected cells.

The role of T cells in the context of both acute and chronic infection has been studied extensively. Results from studies in both human infection and a chimpanzee infection model of T cell depletion have demonstrated that both CD8 and CD4 T cells are essential to successful immune response to HCV infection (Grakoui, 2003; Shoukry et al., 2003). Specific T cell responses to HCV do not appear until 6 to 8 weeks into infection, but their arrival is succeeded by a rapid decline in viral load. In this critical phase, the immune system intermittently gains and loses control of the virus in most subjects (Lauer, 2013; Rehermann, 2009), until finally, the virus either outpaces the immune system or is completely eliminated (Bowen & Walker, 2005).

While the T cell response in patients with resolving and persisting infection starts out with similar breadth of targeted epitopes and magnitude of response (Cox, Mosbruger, Lauer, Pardoll, Thomas, & Ray, 2005b; Schulze zur Wiesch et al., 2005), the response phenotype diverges as the infection progresses. Resolving infection is marked by highly (poly-)functional CD8 and CD4 T cells that eventually contract into a pool of long-lived memory cells (Day et al., 2002; Schulze zur Wiesch et al., 2012), whereas persistent infection is accompanied by the disappearance of CD4 T cells and a greatly diminished pool of CD8 T cells that either become exhausted or cannot exert antiviral activity as a result of dominant escape mutations manifesting in the viral quasispecies, which render the virus invisible to the cells (Cox, Mosbruger, Mao, et al., 2005c; Erickson et al., 2001; Kuntzen et al., 2007) and cause T cells that target escaped viral sequences in chronic infection to display a phenotype that, in certain aspects, resembles T cells in patients with resolved infection (Kasprowicz et al., 2010).

These viral escape mutations constitute a major factor in the evasion from the adaptive immune system by the virus, which affects B and T cells equally. The lack of proofreading and error correction

methods in the HCV replication machinery leads to a fast diversification of the virus and gives rise to variants that are not recognized by antibodies and or the T cell receptor (Timm et al., 2004).

T cell dysfunction and exhaustion

Another mechanism by which viruses escape the adaptive immune response is T cell dysfunction and exhaustion (Angelosanto et al., 2012; Wherry, 2011). This phenomenon likely applies to both CD4 and CD8 T cells in persistent HCV infection (Rutebemberwa et al., 2008), although it is not very well understood in the context of this particular viral infection (Kasprowicz et al., 2008; Kroy et al., 2014). T cell exhaustion and dysfunction is usually the result of either T cell auto-regulation in the form of inhibitory immune checkpoints (Barber et al., 2005; Blackburn et al., 2008) or T cell allo-regulation in the form of cytokines secreted by regulatory T cells or direct interaction with them (Boettler et al., 2005; Cabrera et al., 2004; Rushbrook et al., 2005; Smyk-Pearson et al., 2008). However, other cell environmental factors, including sources of metabolic stress, have been described to contribute to T cell exhaustion (Figure 7, [Wherry & Kurachi, 2015]).

All these mechanisms present important physiological roles in maintaining self-tolerance and fine tuning of the T cell response in order to avoid excessive T cell-induced damage to the host during infection, but are potential targets for exploitation by pathogens (Belkaid, 2007; O'Garra & Vieira, 2004; Sakaguchi et al., 2008).

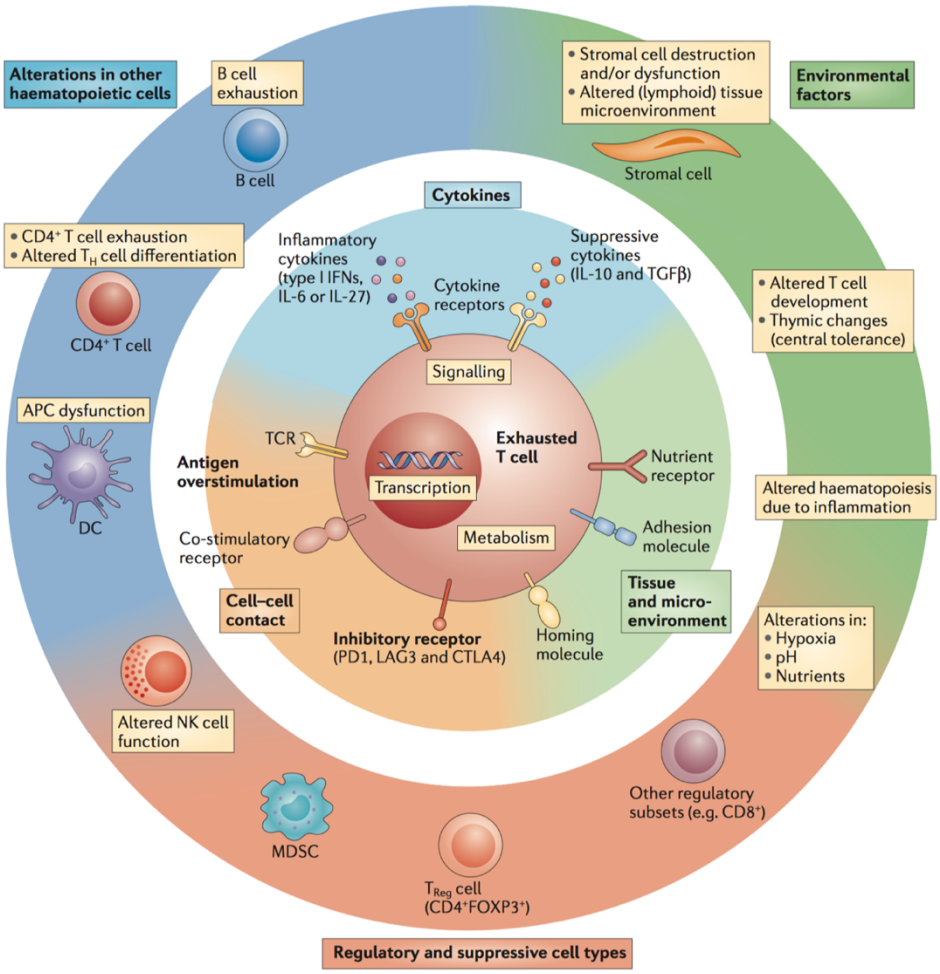

Figure 7. *Overview of T cell exhaustion mechanisms (Wherry & Kurachi, 2015)*

Systems Immunology

An increasing understanding of the complex interplay between different immune cells that orchestrate the response to invading pathogens has brought about a shift in focus towards experimental and analysis approaches that are better equipped to deal with this complexity (Aderem et al., 2010; Germain et al., 2011). This field, commonly referred to as systems immunology (Shay & Kang, 2013) is concerned with the integration of various types of data from different low- and high throughput experimental technologies using an array of innovative computational tools to better understand the tightly regulated

dynamic interactions that govern the precise targeting of pathogens and infected or malignant cells at a holistic level (Chaussabel & Baldwin, 2014).

Gene expression profiling

Data acquisition in systems biological approaches are fueled by an expansive array of quantitative experimental techniques that investigate function and dynamics of biological systems and are often collectively referred to as "omics" (Figure 8, [Ritchie, Holzinger, Li, Pendergrass, & Kim, 2015]). Their rise was largely brought on by technological advances in a) microfluidics that for the first time allowed the production of devices and chips that allowed for large numbers of small entities, such as RNA transcripts, to be measured in small volumes and with high resolution, and b) microprocessors providing enough computing power to deal with the wealth of data that the new experimental techniques were producing (Beebe, Mensing, & Walker, 2002; Kitano, 2002).

One of these technological advances was the development of DNA microarrays that allow for relative quantification of many RNA transcripts in very little time (Schena, Shalon, Davis, & Brown, 1995). In the case of single-channel arrays, transcripts are represented by a set of different perfect match and mismatch probe pairs that map to different locations within the transcript sequence. Based on intensity values of match/mismatch pairs for the different probes within a set, relative transcript abundance can be calculated.

In recent years, next-generation sequencing approaches reached cost levels at which they present an attractive alternative to microarrays, as they enable capture of all RNA transcripts, not just known ones, down to the single cell level. However, the long history of microarrays have created a wealth of

sophisticated and capable tools to analyze them, making microarrays an attractive tool for highly targeted application that can be compared to existing data sets (Bumgarner, 2001).

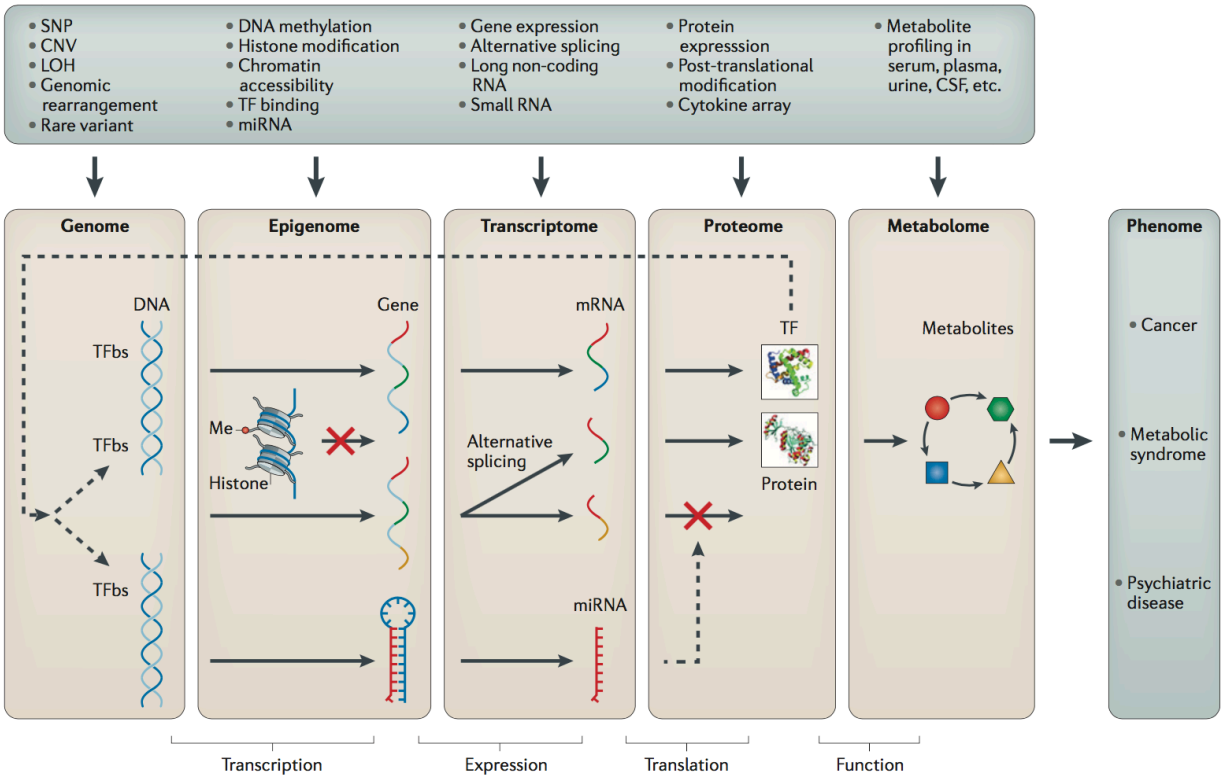

Figure 8. *Interrogation of biological systems by multi-omics approaches (Ritchie, Holzinger, Li, Pendergrass, & Kim, 2015)*

Computational transcriptome analysis

The tools to analyze transcriptional data sets range from simple supervised analyses of differential expression between two to several groups all the way to highly complex unsupervised machine learning approaches such as artificial neural networks (Schmidhuber, 2015). The wealth of published and freely available data sets that bear potential for highly informative meta-analysis as well as the rate at which large amounts of data from various high-throughput experimental technologies are generated, have created the need for both highly specialized as well as broadly applicable computational tools. This need has been met by rapidly growing communities of experimentalists, bioinformaticians, and statisticians, working

together and creating an expansive library of freely available tools that can be used with open-source software environments such as R and Python (C. Hill, 2016; Ihaka & Gentleman, 1996). For reference, the R bioinformatics software project Bioconductor currently offers over 1200 software packages (Huber et al., 2015), most of which are under active development and have rich user communities.

Gene co-expression networks

One of the most successful approaches for identification of co-regulation patterns in transcriptome data is the construction of gene co-expression networks, which employ a clustering-based machine learning approach to infer groups (modules) of co-regulated genes from correlations in their expression patterns across a group of samples in an unsupervised manner (Langfelder & Horvath, 2007; Langfelder, Zhang, & Horvath, 2008; Yip & Horvath, 2007; B. Zhang & Horvath, 2005). Some of these approaches apply weights to correlations by raising them to a power, thereby emphasizing stronger correlations and down-weighing weak ones. Weighted gene co-expression network analysis (WGCNA) effectively reduces noise in the data and simultaneously produces scale-free networks (Langfelder & Horvath, 2008), a concept that gained widespread attention after it was found to underlie the topology of the world wide web and has since been found in many real-world networks including gene networks (Figure 9, [Barabási & Oltvai, 2004]).

Scale free networks are characterized by following an approximate power law degree distribution and the relative commonness of nodes of a degree (defined as the number of connections from that node to others) that is much higher than the average degree of the network (Barabási & Albert, 1999). For gene regulatory networks, this scale-free property means that most genes exhibit few connections to other genes and only a small number of genes exhibit many connections. The most highly connected genes

within a network (nodes of a high degree) are referred to as hub genes and often serve in a regulatory capacity within the network (Langfelder, Mischel, & Horvath, 2013). These hubs are usually connected to a few smaller hubs, which are in turn connected to nodes with smaller degree, resulting in a network that is relatively robust to perturbations, as deletion of random nodes does not usually lead to disconnection of the network. This fault tolerant behavior is considered to be an important feature in the organization of real-world networks such as the ones found in biology (Albert, Jeong, & Barabási, 2000).

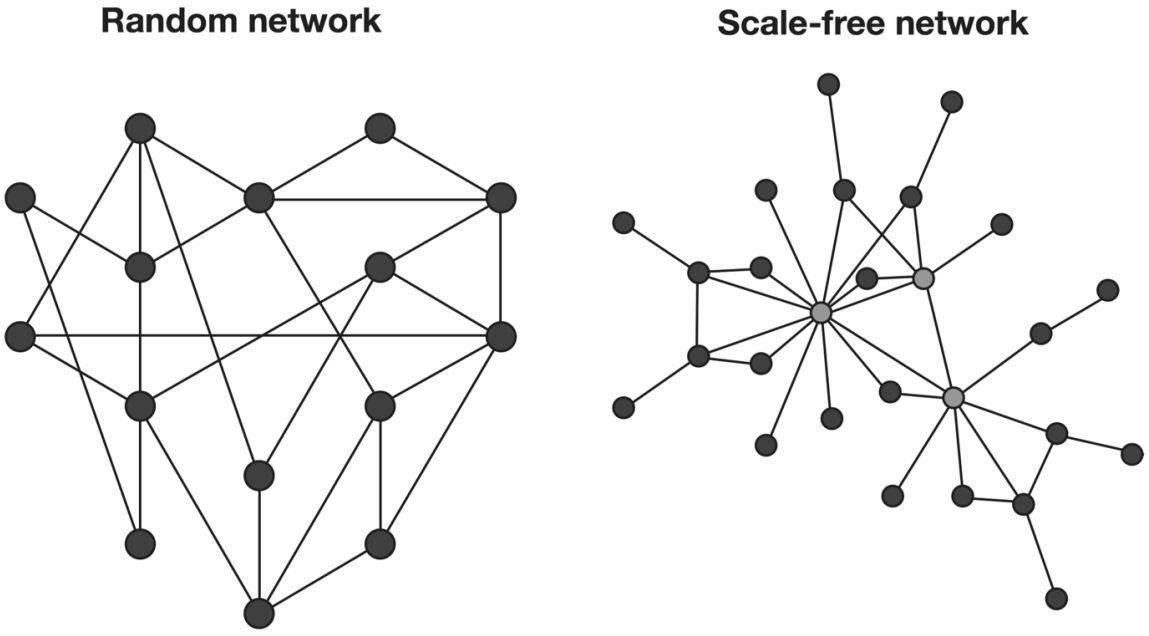

Figure 9. *Example illustrations of simple random and scale-free networks (Barabási & Oltvai 2004)*

Due to their correlation-based structure, gene co-regulation network approaches like WGCNA can be integrated well with other types of quantitative data, allowing identification of expression patterns that track with external variables such as complementary experimental or metadata. Furthermore, the incorporation of knowledge from external databases such as pathway and gene ontology repositories and protein-protein interaction networks can enhance these approaches by linking them to biological context and thereby aiding in hypothesis generation and determination of molecular targets for validation.

Insights from transcriptional profiling

Extraction of biological insights from both differential expression analysis and co-expression network analyses can be aided by combining them with powerful interpretative tools such as enrichment analysis and visualization tools. While all enrichment analysis tools are unified by their attempt to identify overrepresentation of genes from a reference set in the analyzed data, they span a wide range of applications and biological scopes. Some gene set enrichment tools like ROAST (Wu et al., 2010), CAMERA (Wu & Smyth, 2012), and GSEA (Subramanian et al., 2005) were designed to be used lists of ranked genes, e.g. by differential expression, while others, like GAGE (Luo, Friedman, Shedden, Hankenson, & Woolf, 2009), DAVID (Huang, Sherman, & Lempicki, 2008), and Enrichr (E. Y. Chen et al., 2013), can be used with unordered lists of genes. Another set of tools is specialized to perform enrichment analysis for specific pathway or gene ontology databases (Ashburner et al., 2000; Fabregat et al., 2016; Kanehisa, 2000; The Gene Ontology Consortium, 2015). These tools often offer more sophisticated algorithms that are tailored to unique features of the targeted database (Alexa, Rahnenfuhrer, & Lengauer, 2006).

Since differential expression analyses are very commonly performed, most tools that perform the analysis also offer visualization capabilities for heatmaps, volcano plots and Venn diagrams, which are standard visualizations of these results (Qu et al., 2016; Reich et al., 2006).

Tools for visualization of networks, however, usually stand on their own, as they are universally applicable in most cases and can be used in a variety of different fields. Two prominent and powerful examples of network visualization suites that offer a wide range of integrations with other bioinformatics tools are Cytoscape and the igraph package for R (Herrmann & Bucksch, 2014; Shannon, 2003).

Aims of the study

By recent estimates, chronic HCV infection affects over 150 million people worldwide. The infection is often not detected, as it can progress asymptomatically for years, until long-term hepatic inflammation results in complications such as liver fibrosis, cirrhosis and cancer. While the recent highly potent direct-acting antivirals have revolutionized HCV therapy, real concerns exist over whether a reactive strategy can realistically void the need for a prophylactic vaccine.

The feasibility of developing such a vaccine is supported by the fact that long-term viral persistence is contrasted by a substantial fraction of infections (~20%) that end in spontaneous immune-mediated clearance of the virus. Decades of work on deciphering the correlates of immunity to HCV infection have highlighted the importance of a competent adaptive immune response in this process, but have failed to deliver a definitive answer on what exactly defines a protective response and what differentiates it from a failing immune response, especially in the early phase of infection when the outcome is determined.

This has brought on a growing appreciation for the fact that the immune response to HCV is a multifactorial event regulated by highly complex processes whose elucidation will require novel, integrative experimental and analytical approaches.

With this complexity in mind, the aim of my thesis was to 1) establish that we can gain biological insight from gene expression profiling of rare HCV-specific CD8 T cells during early HCV infection, and 2) investigate the gene regulatory processes in these cells in the context of different disease outcomes and relate them to other components of the adaptive immune response (antibody and CD4 T cell response) in an integrative manner.

Results

Part 1: Early transcriptional divergence marks virus-specific primary human CD8 T cells in chronic versus acute infection

David Wolski, Peter Foote, Diana Chen, Lia L Lewis-Ximenez, Catherine Fauvelle, Jasneet Aneja, Andreas Walker, Pierre Tonnerre, Almudena Torres-Cornejo, Sabrina Imam, Michael T Waring, Damien C Tully, Todd M Allen, Raymond T Chung, Jörg Timm, W Nicholas Haining, Arthur Y Kim, Thomas F Baumert, Georg M Lauer

Manuscript submitted for publication [February 13, 2017]

Introduction

The goal for the main part of my PhD project was to design and perform a microarray experiment in a larger cohort of HCV-infected patients with more early infection samples and better defined infection time points, given our experience with a pilot study, described in Part 2 of this thesis, and its limitations. Based on existing knowledge of the events and immunology of the acute phase of HCV infection leading up to resolution or persistence, our hypothesis was that competent adaptive immunity to HCV infection is characterized by a multi-facetted response strategy and subject to tight regulation on a functional and temporal level.

Therefore, in addition to CD8 T cells from patients with chronic and resolving infections, the newly designed experiment included multiple time points from individual patients, as well as CD8 T cells from chronically infected individuals that targeted viral epitopes that had escaped the T cell response by viral sequence variation. In the same patients, we also quantified the HCV-specific CD4 T cells, by the

same flow-cytometric approach used to sort specific CD8 T cells, and neutralizing antibody titers using a HCV pseudoparticle system, to interpret the CD8 findings in the context of the immune response by other arms of the adaptive response. However, of the samples that were tested for neutralizing antibodies, only four displayed notable neutralizing activity above background, and these were distributed equally among the outcome groups, impeding our ability to detect associations between antibody titers and patterns in T cell transcription profiles. At the same time, the absence of strong neutralizing antibody responses during the early infection period that we analyzed increased our confidence that the observed associations between T cell gene regulation and outcome are indeed critical events for the subsequent development of viral control or persistent HCV viremia.

In a differential expression analysis, comparing gene expression profiles of CD8 T cells in three distinct immunological states (resolving infection, persisting infection with antigen recognition and persisting infection without antigen recognition) we confirmed our previous observation that CD8 T cells from patients with resolving and persistent infection display distinct transcriptional profiles. Importantly we also observed a third distinct expression profile for CD8 T cells targeting escaped HCV epitopes. Among the differentially regulated genes we observed a host of important regulators and effectors of both immune and cellular stress responses, strengthening the argument that metabolic regulation and T cell function are highly intertwined.

Expanding the complexity of our analysis, we used an unsupervised machine-learning approach to construct gene co-expression networks for each of the experimental groups and defined modules of tightly co-regulated genes, that we found to be highly enriched for genes related to metabolic and immune-related pathways as well as processes of nucleosome assembly and chromatin silencing.

Closer inspection of these modules and pathways revealed that the regulators and effectors identified by differential expression were embedded in functional subunits which varied greatly in their degree and directionality of gene regulation depending on outcome, showing up potential defects in regulation that have a high probability of being contributing factors to the gene regulatory events that lead to T cell dysfunction and viral persistence.

Distinct patterns of connectivity and co-regulation of genes and modules both within and between different modules and patient groups revealed a core T cell identity as well as unique outcome associated traits indicating early dysregulation of HCV-specific CD8 T cell responses in chronic infection. Specifically, we identified major differences in regulation of metabolic processes during early chronic HCV infection together with differential expression patterns of genes involved in regulation of apoptosis, T cell differentiation and the response to inflammation. Furthermore, these differences exhibited strong associations with subject age and sex, and levels of available CD4 T cell help, which are strong predictors of HCV disease outcome.

Results

Publication No. 2

Early transcriptional divergence marks virus-specific primary human CD8 T cells in chronic versus acute infection

David Wolski[1,2,3], Peter Foote[1], Diana Chen[1], Lia L Lewis-Ximenez[4], Catherine Fauvelle[2,3], Jasneet Aneja[1], Andreas Walker[5], Pierre Tonnerre[1], Almudena Torres-Cornejo[1], Sabrina Imam[6], Michael T Waring[7], Damien C Tully[7], Todd M Allen[7], Raymond T Chung[1], Jörg Timm[5], W Nicholas Haining[6], Arthur Y Kim[8], Thomas F Baumert[2,3,9], Georg M Lauer[1,10]

[1]Gastrointestinal Unit and Liver Center, Massachusetts General Hospital; Harvard Medical School; Boston, MA, 02114; USA.

[2]Inserm, U1110; Institut de Recherche sur les Maladies Virales et Hépatiques; Strasbourg, 67000; France.

[3]Université de Strasbourg; Strasbourg, 67081; France.

[4]Laboratory of Viral Hepatitis, Oswaldo Cruz Institute; FIOCRUZ, Rio de Janeiro, 21040; Brazil.

[5]Institute for Virology, University Hospital Düsseldorf; Heinrich Heine University; Düsseldorf, 40225; Germany.

[6]Department of Pediatric Oncology, Dana-Farber Cancer Institute, Boston, MA, 02115; USA.

[7]Ragon Institute of Massachusetts General Hospital, Massachusetts Institute of Technology and Harvard University; Boston, MA, 02139; USA.

[8]Division of Infectious Disease; Massachusetts General Hospital; Boston, MA, 02114, USA;

[9]Institut Hospitalo-Universitaire, Pôle Hépato-digestif; Nouvel Hôpital Civil; Strasbourg, 67000; France.

[10]Lead Contact

Correspondence to:

Georg M. Lauer, Gastrointestinal Unit, Massachusetts General Hospital and Harvard Medical School, 55 Fruit Street, Boston, MA 02114

glauer@mgh.harvard.edu

Keywords

Hepatitis C Virus, CD8 T cells, CD4 T cell help, T cell dysfunction, metabolism, nucleosome, adaptive immunity, viral escape, network analysis, transcriptional regulation

Highlights

- Transcriptional differences in T cells are associated with outcome and viral escape
- T cells from different outcomes share a core of co-regulated T cell identity genes
- Metabolic, nucleosome, and immune genes are dysregulated early in chronic infection
- T cell dysregulation correlates with sex, age, and availability of CD4 T cell help

Summary

Distinct molecular pathways govern the differentiation of CD8 effector T cells into memory or exhausted T cells in acute and chronic viral infection and cancer. Utilizing an integrative network and differential expression-based systems approach, we investigated early transcriptional events that direct the early CD8 T cell response in dichotomous outcomes of human hepatitis C virus infection. We identify the core of a common T cell identity, but also highly exclusive regulatory interaction networks highlighting dysregulation of crucial metabolic functions early on during persistent infection, together with changes in expression of genes related to nucleosomal regulation of transcription, T cell differentiation, and the inflammatory response, with associations to subject age, sex and levels of available CD4 T cell help. These data identify critical pathways of T cell regulation and provide a framework for investigating immune responses in human subjects.

Introduction

Over the last two decades we have gained important insights into the defining features of T cell responses in the context of controlled and chronic viral infections. These advances, most notably the differentiation between effective T cell memory and functionally exhausted T cells (Wherry and Kurachi, 2015) have largely been driven by work performed in animal models such as lymphocytic choriomeningitis virus (LCMV) infection in mice, and have had a major impact on our understanding of T cell immunology beyond the scope of viral infections (Pardoll, 2012). The key concepts from these studies have been successfully translated in many human infections, including those with human immunodeficiency virus (HIV), hepatitis B virus (HBV), and HCV (Kahan et al., 2015). Nevertheless, our understanding of how different molecular mechanisms integrate into a concerted program leading to an effective or failing T cell response remains incomplete. This is especially true in the context of human infections, where genetic diversity and variability, differences in age and comorbidities, as well as environmental factors influence both the immune response and the outcome of infection significantly (Brodin and Davis, 2016). Recent advances in sensitivity and resolution of available molecular and immunological assays now allows for comprehensive investigation of fundamental research questions directly in the human immune system.

Hepatitis C virus infection presents an exceptional opportunity to study regulation of immune responses, as it is unique among human infections in that it is spontaneously and fully resolved about 20% of subjects within 6-9 months of infection, even after exposure a viral inoculum that will result in persistent infection in other subjects (Major et al., 2004). Data from humans as well as from the chimpanzee model of infection have demonstrated that the presence of adaptive immune responses by both CD4 and CD8 T cells, while indispensable to resolution of infection (Grakoui, 2003; Shoukry et al., 2003), is not sufficient, as they are also detected during the early phase in subjects developing

chronic infection (Cox et al., 2005; Schulze zur Wiesch et al., 2012). In addition to T cells, neutralizing antibodies have been shown to contribute to control of the virus during the acute phase of infection, where their induction is correlated with viral clearance (Osburn et al., 2014; Pestka et al., 2007). A strong host component to viral control, evident also in associations between HLA expression or sex with infection outcome (Bakr et al., 2006; Kuniholm et al., 2010), separates HCV from LCMV, the classic mouse model of acute and chronic viral infection in inbred mouse strains, where different courses of viral replication are only observed when animals are infected with different strains of the virus. The analysis of the early anti-HCV T cell response in humans with different clinical outcomes can therefore add additional insights and lend a unique perspective into the complexity of immune response regulation in genetically diverse hosts.

Here, we define the molecular components of a successful CD8 T cell response to HCV infection and contrast it with transcriptional events that govern HCV-specific CD8 T cells in persisting HCV infection. We isolated HCV-specific HLA-multimer positive CD8 T cells from 43 subjects with different infection outcomes at multiple time points during the initial 36 weeks of infection and analyzed their transcriptional profiles by microarray.

Taking advantage of two important features of HCV infection, its dichotomous outcome, with chronic viremia or complete clearance of the virus, and the occurrence of HCV viral sequence variation leading to viral escape from the CD8 T cell response, we were able not only directly compare T cell responses that control viremia to those that do not, but also differentiate between changes in T cell phenotype and function mediated by prolonged T cell receptor (TCR) stimulation versus those mostly induced by a chronic inflammatory environment.

Our results reveal a core T cell identity as well as unique outcome associated traits indicating early dysregulation of HCV-specific CD8 T cell responses. Specifically, we identify major differences in regulation of metabolic processes during early HCV infection together with differential expression

patterns of genes involved in regulation of apoptosis, T cell differentiation and the response to inflammation.

By identifying a core of partially conserved transcriptional programs related to T cell immune function, T cell metabolism and histone regulation, and contrasting them with programs that differentiate T cells in three discrete immunological states, we gain important insights into critical diversions in the regulation of the primary CD8 T cell response to viral infection and establish a reference framework for more detailed mechanistic studies into T cell mediated viral control and T cell failure.

Results

Multivariate analysis of adaptive immunity during early HCV infection

To identify pivotal regulatory processes controlling the CD8 response during early infection, we isolated HCV-specific CD8 T cells (Figure 1A) from 43 subjects at multiple time points within the first 36 weeks of infection (Figure 1B and Table S1) and analyzed their transcriptional profiles by microarray. To detect potential effects of other branches of the adaptive immune system on CD8 T cell gene regulation, we assessed levels of available CD4 help and neutralizing antibody titers in a subset of these samples (Figure 1B and Table S1, STAR Methods).

For analysis, we split subjects and samples into three groups of distinct immunological states based on disease outcome and conservation of the viral epitope recognized by the T cell receptor (TCR): 1) Chronic (persisting infection, preserved targeted epitope), 2) Escape (persisting infection, mutated targeted epitope with known diminished signal) and 3) Resolver (resolving infection, preserved targeted epitope), that we refer to as C (Chronic), E (Escape), and R (Resolver) hereafter.

Virus-specific CD8 T cells display distinct transcriptional profiles of resolution, inflammation and persistent antigen exposure

To identify clear outcome-associated differences in gene expression we analyzed CD8 T cell transcriptional profiles of C and R groups and found 258 genes that were significantly differentially expressed ($|\text{fold change}| > 1.5$, FDR < 0.05, Table S2) between C and R during either early (<18 weeks) or late (>18 weeks) phase of infection or between early and late phase of infection in either C or R (Figure 2A). Despite not being incorporated for detection of differentially expressed genes (DEGs), we observed that E samples clearly helped to separate genes into distinct expression patterns for each group

We found about half of all DEGs to be expressed at similar levels between C and R within each phase of infection (Figures A2 and 2B), with higher and lower overall expression levels dominating the early and late phase, respectively. Among these genes were markers of T cell activation, such as *CD74* and *HLA-DRB1*, and T cell homing and proliferation, like *ELF4*, which exhibited much lower expression levels in the later phase compared to the early phase. This apparent dampening of the T cell response, irrespective of outcome, is consistent with the natural course of persistent HCV infection, where inflammation is much less pronounced in the later phase of infection when compared to the early acute phase (Bowen and Walker, 2005).

Another group of genes with similar expression levels in C and R included the cytokines *TNF* and *TGFB1*, their respective downstream signaling components (*NKFB1/JUNB* and *KLF10/SMAD7*) as well as the chemokine receptors *CXCR4* and *CCR7*. Interestingly, these highly functionally related genes were all down-regulated in early C and R samples, but up-regulated in E samples throughout both early and late phase, indicating that abrogation of TCR stimulation evoked a distinct and stably maintained transcriptional profile in these cells.

While many genes shared expression levels between C and R groups both in the early and late phase, we also found significant differences between these two groups. Throughout the observation period, C samples were characterized by higher expression levels for important regulators of T cell immune function, proliferation, and survival, such as *TBK1*, *SIRT1*, *BCOR*, and *BCL2L11*, while R samples were marked by higher expression for regulators of T cell differentiation and memory, e.g. TCF7 and its transcriptional target *LEF1*. Interestingly, E samples exhibited a mixed expression profile for most of these genes, either sharing expression levels with R (*TCF7*) or with C (*LEF1*) throughout the infection, or sharing features of C early and R later (*BCL2L11*) or vice versa (*SIRT1*), suggesting that persistent TCR stimulation and chronic inflammation each drive different aspects of the observed divergent transcriptional programs in CD8 T cells during the acute phase of HCV infection.

Modules of tightly co-regulated genes give rise to distinct patterns of transcriptional regulation in different infection outcomes

To better address the complexity of the regulatory processes that govern the CD8 T cell responses in different immunological states we applied a weighted gene co-expression network analysis (WGCNA) approach (Langfelder and Horvath, 2008) combining early and late samples for each group and constructed weighted correlation networks for them (Table S4, STAR Methods).

By means of hierarchical clustering, we identified 9, 8, and 8 modules of tightly co-expressed genes (Figure 3A) for C, E, and R, respectively. When examining overall network topology (Figure 3B), we observed that some genes were not only correlated with other genes in the same module, but also exhibited correlations with genes in other modules, supporting a second tier of interconnectedness within groups at the module level.

We next assessed preservation of modules between groups by analyzing the overlap in gene content between individual group-pairs (Figures 3C and 3D) and defined the significance of overlap between a module and another module as its core score and the overlap between a module in one group and uncorrelated genes in another group (grey module) as its isolation score (STAR Methods). We observed distinct patterns of co-regulation, with most modules in C and R either dominated by genes that shared co-regulation between the groups (Figure 3C, high core score, broad blue connections) or by genes that were exclusively co-regulated in each respective group (high isolation score, broad red connections).

Many genes accounting for the overlap between modules that shared co-regulation between C and R, like *JUNB*, *TNF*, and *KLF10* in modules c1-r5 (Table S4), also exhibited similar differential expression patterns in C and R (but not E, Figure 2A), supporting their preserved roles in early T cell responses that receive TCR-mediated signals.

Other genes within preserved modules, however, were part of the differential expression signature that distinguished C from R, such as *IFNGR1* and *SIRT1* in c2-r5, emphasizing that shared co-regulation does not imply similar directionality of expression or connectivity between modules across groups.

E modules exhibited an overall weaker pattern of co-regulation on the gene and module correlation levels (Figures 3A and 3B), indicating less concerted regulation with abrogation of TCR stimulation. Nonetheless, we identified several modules with significant preservation between E and C and/or R, most notably c7-e7-r8, which shared co-regulation of genes including *CD14*, *TLR2*, *CXCL2*, and *CXCL8*, indicating a core of T cell processes that might operate independent of TCR signaling.

To formally identify patterns of interconnection between modules within and across groups, we combined intra-group module correlations (Figures 3B and Figure 3E, left) and inter-group module overlap (Figure 3C and Figure 3E, middle), creating a module network that allowed us to systematically detect module community structures (Figure 3E, right, STAR Methods). We identified three core-centric (c7-e7-r8, c2-r3-r4, and c1-e4-e5-r5) and one isolation-centric module community (c3-c5-c6-r1-r2), as well as one with a more complex connectivity pattern (c4-c8-c9-e2-r6-r7), more concisely defining both core elements T cell identity and unique regulatory features of different infection outcomes.

Differential expression of network modules is preserved across cohorts of acute HCV infection

To ensure that our observations represented valid and reproducible biological phenomena and to confirm robustness of the identified network modules across different experimental setups, we validated the results in an independent transcriptional data set of HCV-specific CD8 T cells from 10 subjects with acute and chronic courses of infection sampled during the early acute phase of infection ($\leq$ 21 weeks, Table S5). As it was not feasible to generate a second, sufficiently large data set from the

rare cases of acute HCV infection to perform WGCNA, we chose to perform validation by testing the results of differential expression analysis between C and R for enrichment of the identified network modules (Figure 3) using CAMERA (Wu and Smyth, 2012) (STAR Methods). We expected that robust modules that displayed a clear directionality in gene expression between Chronic and Resolver groups, should be enriched to a similar degree and in the same direction during early infection in both the original and the validation data. Analogously, modules that did not show a clear overall directionality of expression between groups, should not be enriched in either the old or the new set. Indeed, we observed strong enrichments for several modules, such as r2, r5, and r6, in both the new (Figure 4B) and the early original data set (Figure 4A, left), and fewer shared enrichment patterns with late samples of the original data set (r5 and r6). Other modules, like c5, were not enriched in any of the data sets. These results support the robustness of our findings and suggest their reproducibility in other cohorts of acute and chronic HCV infection.

Outcome-associated clinical traits impact co-regulated modules representing different cellular processes and immune pathways

Next, we tested modules for correlations with clinical traits, i.e. disease and immune parameters of HCV infection (Figure 5A, STAR Methods). To further link them to biological function we tested them for enrichment of: 1) differential expression signatures of CD8 T cells in different disease models (HCV (from Figure 2), HIV (Gaiha et al., 2014), LCMV (Doering et al., 2012), and cancer (Singer et al., 2016)) or T cell memory states (Subramanian et al., 2005), 2) module gene signatures of antigen-specific CD8 T cells in chronic vs acute LCMV infection (Doering et al., 2012), and 3) functional gene sets related to immune pathways (Langfelder and Horvath, 2008) and gene ontology and KEGG pathway databases (Ashburner et al., 2000; Kanehisa, 2000) (Figures 5B, 5C, and 5D, Tables S3 and S7, STAR Methods).

To allow for easier interpretation of functional enrichments in the context of module communities (Figure 3E, right) and immunological states, we grouped enriched terms into larger clusters of processes related to immune/T cell regulation (Figure 5D, grey panel, red dots), nucleosome associated regulation of transcription (grey panel, blue dots) and metabolism (grey panel, yellow dots), based on their functional annotation and co-occurrence in modules across different groups.

When relating modules to the traits defining these states, we observed that about half of all modules were significantly correlated with at least one clinical trait (Figure 5A), with ALT, sex, and age showing the most correlations, suggesting a strong impact of liver inflammation, but also of demographic features in a heterogeneous human cohort. The only two modules, c3 and c5 (Figure 5A), that were (negatively) correlated with time after infection (decreasing expression over time), also the exhibited the highest isolation scores (Figure 3C and 3D) and were enriched for metabolic pathways (Figure 5D), indicating unique dynamics of metabolic regulation in CD8 T cells during early chronic infection. Higher expression levels of genes in c3 and c5 also correlated with female sex and younger age (negative correlation), both of which are predictors of favorable disease outcome, while another module that was enriched for metabolic pathways and apoptosis, c1, exhibited an inverse correlation (Figure 5A), with higher expression levels correlating with higher age and male sex.

Interestingly, c5 was also enriched for a signature associated with long-term viral control in HIV (Gaiha et al., 2014) and correlated with levels of CD4 help. Module c8 (Figure 5A), displayed an even stronger association with CD4 help and was enriched for multiple processes related to the regulation of immune response, cell adhesion and homing, and nucleosome associated regulation of transcription (Figure 5D), identifying a direct impact of sustained T cell help on specific cellular programs governing the CD8 response. No correlation was found with neutralizing antibodies as barely any nAb responses were detected in this cohort during the observation period.

Evaluation of differential expression signature enrichments (Figure 5B) revealed that several HCV signatures were enriched across multiple modules, substantiating our hypothesis that complex regulatory interactions give rise to the divergent expression profiles observed for different immunological states (Figure 2).

We observed little enrichment of differential expression signatures from acute versus chronic LCMV infection (Doering et al., 2012) or cancer (Singer et al., 2016), but found significant overlap between module signatures from acute vs chronic LCMV infection (Figure 5C) and our modules, particularly between immune related module signatures and modules from the core-centric community of c7-e7-r8, highlighting the advantage employing a co-regulation based network analysis approach.

While being highly preserved across immunological states and infection models, these core modules exhibited distinct functional enrichments for immune pathways (Figure 5D), suggesting that subtle changes in connectivity can result in differential functional output from these modules.

Functional networks related to immune regulation, nucleosome associated immune regulation and metabolism define both preserved and exclusive transcriptional features of T cells from different infection outcomes

To further delineate the commonalities and differences in T cell regulation between C, E and R groups, we created functional cluster networks (STAR Methods) from the original gene correlation networks of each group, using the genes that were annotated in the immune, nucleosome, and metabolism clusters (Figure 5D, grey panel, colored dots) and examined them for patterns of shared and exclusive regulation at the individual gene-level. As can be expected, we observed shared components between all three or any combination of two groups in each of the three clusters, but also group-exclusive components containing genes that were co-regulated in one outcome only. A core component of co-

regulated genes shared between all three groups was most extensive in the immune and nucleosome networks (Figure S2, Table S8). These two networks were further characterized by wide overlap between C and R samples, indicating that the abrogation of TCR signaling in E samples also disrupts co-regulation of gene networks otherwise conserved in CD8 T cells irrespective of viral control. Especially noteworthy in this context, is that this shared C-R component contained more than half of all histone genes annotated in the nucleosome cluster network (Figure S2D-F, Tables S4 and S8).

The metabolism network was marked by large components that were only regulated in C (Figures 6A and S1, yellow component) or C and E samples (pink component) and that contained many genes from c3 and c5, modules for which we had identified strong associations with age, sex, CD4 help, and time from infection (Figure 5A). To assess whether individual components of the network were associated with specific metabolic pathways, we performed a second KEGG pathway enrichment analysis (STAR Methods), which revealed a strong enrichment of genes involved in oxidative phosphorylation in the C-exclusive component (Figure 6B, Table S9).

Interestingly, Bengsch et al. recently reported oxidative phosphorylation (OXPHOS) to also be one of the key processes involved in metabolic dysregulation of exhausted T cells in persisting clone 13 LCMV infection (Bengsch et al., 2016). When we compared genes driving the enrichment of OXPHOS in the C-exclusive component of the metabolism cluster network to the leading edge signature driving the signature of metabolic dysregulation in LCMV, we found not only that they overlapped highly (12/17 genes, Figure 6C), but also that this overlap was mostly accounted for by modules c3 and c5 (and c6), with genes in these modules exhibiting expression kinetics similar to those observed in chronic LCMV infection, where an early surge in expression was followed by rapid downregulation (Figure 6D). This similarity between HCV and LCMV-specific CD8 T cells, however, seemed to be largely limited to enrichment and expression kinetics of OXPHOS-related genes, as enrichment of other metabolic processes found in HCV (Figure 6B), such as biosynthesis of amino

acids in the R-exclusive component and cysteine and methionine metabolism in the chronic-exclusive component, were not observed in LCMV and vice versa. While R-exclusive enrichment of amino acid biosynthesis and carbon metabolism might indicate improved regulation of glycolysis-fueled anabolic processes in CD8 T cells from resolving infection, the genes driving this enrichment were different from those driving enrichment of fatty acid metabolism and glycolysis in acute LCMV (Figures 6A, 6B and S1, Table S9).

Together, these results strongly suggest that early dysregulation of metabolic processes, particularly of pathways related to cellular respiration, might play a central role in the making of an exhausted T cell response that is unable to control viral replication. At the same time, our data indicate that specific features of metabolic dysregulation might be highly dependent on infection- and cellular context.

Distinct regulatory interactions link dysregulation of metabolic, nucleosomal, and immune processes in CD8 T cells from early chronic HCV infection

Since the observed dynamics of CD8 T cell gene expression in chronic subjects were both CD4 help- and time-dependent as well as highly consistent across multiple functionally related modules (Figure 6D), we hypothesized that these changes are subject to active transcriptional regulation and that the regulators effecting these changes are likely to share expression patterns with their targets, and should therefore be annotated in the same module.

To test this hypothesis, we assembled a large interaction network, consisting of ~2.9 million unique regulatory interactions between 1319 known transcriptional regulators (TR) and their targets, from a variety of publicly available databases, network repositories and published CD8- and lymphocyte-specific regulatory networks (STAR Methods), and intersected it with the correlation networks we constructed (Figure 3) to determine the number of interactions between TRs and targets within their respective modules (TR-target coverage, Table S10, STAR Methods).

When we compared the calculated target coverage for each TR to its intramodular connectivity to identify the most important TRs for each module, we observed a positive trend of increasing intramodular connectivity (k_{Within}) with increasing target coverage (Figures 7A, S3A, and S3B), indicating that genes with high k_{Within}, so-called hub genes, are likely to be of high functional importance.

To identify the TRs that were likely to be causal to the dysregulation of metabolic processes we had identified (Figure 6), we next constructed a compact regulatory network based on the top scoring TRs in c3, c5 and c6, (*STAT5A*, *KDM5B*, *RFX5*, *NELFE*, *CBX3*, *STAT1*, and *TP53*, Figure 7A, Table S10). To allow for the possibility that the observed changes were not caused by active regulation, but by the lack thereof, we chose to include the TRs *CREB1*, *IRF3* and *FLI1* from r2, a module from the same community (Figure 3E) which also contained *STAT1* and *TP53* (Figure S3A).

The results of this analysis revealed a compact regulatory network (Figure 7B), that not only mapped many of the metabolic dysregulation signature genes (Figures 6A and 6C, Table S8) to known regulatory interactions for the identified transcriptional regulators, but also contained regulatory interactions for several histone subunits, integrins, class II MHC molecules, chemokines and chemokine receptors (Figure 7B, Table S8) and was only partly preserved in Escape and Resolver groups.

Specifically, we identified regulatory interactions between *STAT5A*, *KDM5B*, and *RFX5* and genes of the metabolism cluster (Table S8), that were regulated exclusively in C (Figure S4C, yellow nodes) and C/E groups (pink nodes), and which included the hub genes for modules c3, c5, and c6 (*TYMS*, *CMAS*, and *B4GALT3*), but also important genes annotated to the nucleosome (e.g. multiple histone subunits and integrins, Figure 7B) and immune clusters (e.g. chemokine receptors *CCR5* and *CX3CR1*, and chemokines *CCL4*, and *CCL5*).

Furthermore, genes in the Chronic regulatory network were marked by distinct expression kinetics in the form of rapid downregulation (Figures 7C and S3C) following high initial levels of expression, suggesting that the identified transcriptional regulators might indeed mediate early transcriptional dysregulation that has widespread effects on CD8 T cell metabolism, transcription and replication, and immune function, making them prime candidates for further investigation of CD8 T cell regulation in acute and chronic infections.

Discussion

Despite two decades of study, the molecular programs that initiate the divergence of effector T cells into either memory or exhausted T cells in the face of viral infection remain incompletely understood. Here we employed a stepwise, integrative systems immunology approach to identify key transcriptional commonalities and differences between virus-specific CD8 T from subjects with persistent and spontaneously resolving hepatitis C virus infection cells during the critical acute phase. Analyzing basic mechanisms of cellular regulation in human disease in this manner has only recently become feasible through technological advances in generation and analysis of large data sets from small clinical samples. While the inter-individual heterogeneity of human data sets presents challenges for their analysis and interpretation, our work underlines the importance of studying human populations that fully reflect the differences in genetic backgrounds, age, sex, and environmental influences, by adding important insights and offering a unique and partly contrasting perspective to knowledge gained primarily from disease models in inbred laboratory animals.

To account for this diversity in our study and to create a robust data set we generated what is, to our knowledge, the largest transcriptional data set of human primary virus-specific CD8 T cells to date, with 78 distinct T cell populations from 43 patients. Moreover, by comparing cells from three, rather than two distinct immunological states, we simultaneously increase the precision and accuracy of our analysis, since links between multiple groups are less likely occur simply by chance and since we can distinguish between antigenic and inflammatory influences on adaptive immunity, respectively.

To further ensure the validity of our results beyond our original cohort of HCV infection, we also performed a constrained validation analysis in a separate gene expression data set from a second group of patients with acute HCV infection, which shows that our findings will be reproducible in other

cohorts of acute and chronic HCV infection, and are therefore likely to represent meaningful biological differences in the regulation of T cell responses between acute and chronic infection.

The main approaches used, supervised differential expression analysis and weighted gene co-expression network analysis, complement each other in that they interrogate two separate features of cellular process regulation: gene expression levels and patterns of co-regulation. In both analyses, we find a strong core of genes that are regulated similarly in both Chronic and Resolver samples as well as significant differences between the groups that manifest during the earliest stages of infection, indicating that differential gene-regulatory programs are initiated in these T cells well before differences in the quality of the T cell response and the level of viral control become more apparent.

Our most striking finding was a highly distinct co-expression signature of genes related to metabolic processes that were regulated exclusively in Chronic samples and in a markedly temporal manner, with high initial expression levels followed by rapid downregulation. Parts of this metabolic dysregulation signature are shared by a signature recently described for CD8 T cells in persistent LCMV infection with clone 13 (Bengsch et al., 2016), indicating that proper regulation of metabolic processes is likely to present a truly universal feature of a successful immune response. This is further substantiated by the fact that one of the driving modules behind the metabolic signature we observed, was also strongly enriched for genes identified in HIV-specific CD8 T cells from patients that maintain long-term control of viral replication (Gaiha et al., 2014).

Differences in the individual metabolic pathways enriched in signatures from different viruses, however, also suggest that regulation of T cell metabolism is likely highly context-specific. Indeed, our analysis further revealed strong correlations between expression changes in driving modules of this metabolic signature and with subject age, sex, and the presence of CD4 T help, three traits that present the strongest predictors of HCV infection outcome. This work thus identifies new prospects for investigation, as the impact of sex and age on the immune response, while generally accepted (Giefing

Kröll et al., 2015), are not well understood mechanistically, especially in the context of metabolic regulation of immune cells.

Delving deeper into the regulatory interactions that might drive this dysregulation by cross-referencing identified modules with known database-derived regulatory interactions, we find that most dysregulation signature genes are regulated by a handful of transcription factors that are highly connected within in their respective modules, but also annotated for interactions with many genes related to immune function and regulation of transcription in closely connected modules, demonstrating that the dysregulation of metabolism is not isolated but unfolds in tandem with other transcriptional changes.

The transcription factors that represent central drivers of these early changes in T cell regulation include *CREB1*, *FLI1*, *KDM5B*, *RFX5*, *STAT1*, *STAT5A*, and *TP53*. While *CREB1* and *RFX5*, through activation of MHC class II promoters (Lochamy et al., 2007), *FLI1*, through its role in autoimmunity, *STAT1* and *STAT5A*, through mediation of IFN responses and T cell memory formation (O'Shea and Plenge, 2012), are key regulators of immune function and development, their involvement in metabolic regulation has not so far been elucidated. Conversely, while the role of *TP53* in metabolism is well known (Berkers et al., 2013), its part in regulation of immune responses has only recently gained increasing attention (Muñoz-Fontela et al., 2016).

The described regulatory network and its differential expression and connectivity across individual immunological states highlight a unique combinatorial role of these transcription factors in the early dysregulation of CD8 T cell responses in persistent viral infection. Similar differences in the connectivity of transcriptional network hubs in the context of different infection outcomes have been described in LCMV (Doering et al., 2012), albeit for other transcription factors and without distinction between TCR- and inflammation-mediated effects.

The opportunity to make this distinction and analyze three distinct T cell populations led to another set of valuable insights. Escape samples did not share the same signature of metabolism and immune dysfunction that seems to drive exhaustion in Chronic samples, indicating that this process is driven by protracted TCR signaling. Indeed, there is strong data supporting some recovery of escaped CD8 responses in chronic HCV infection towards T cell memory, as these cells respond better to a therapeutic vaccine (Swadling et al., 2014), upregulate CD127 and downregulate PD-1 (Kasprowicz et al., 2010). On the other hand, E samples lacked distinct co-regulation of most histones, compared to C and R, and were the only cells expressing *TNF* and *TGFB1* and downstream signals at constant high levels, suggesting that the abrupt abrogation of TCR signal in a chronic inflammatory environment does not result in immediate memory differentiation. Whether this is a result mainly of prolonged exposure to type I interferons (Stelekati et al., 2014), or other inflammatory pathways, warrants further investigation.

Together, our results identify critical early changes in HCV-specific CD8 T cells that precede the establishment of T cell exhaustion in chronic viral infection, with metabolic function at the center of a highly dysregulated transcriptional program that seems to operate under partial TCR control and which is linked to factors of human heterogeneity, like age and sex of the patient as well as to the presence of CD4 T help. In addition to these specific findings, the extensive human data set of virus-specific CD8 T cells from different infection outcomes and with varying levels of viral control presented here constitutes an unprecedented resource the wider scientific community that will enable and inspire further inquiry into the regulatory mechanisms that govern successful adaptive immunity in response to viral infection.

Author Contributions

Conceptualization, D.W. and G.M.L.; Methodology, D.W. and G.M.L.; Formal Analysis, D.W.; Investigation, D.W., P.K.F., D.C., C.F., A.W., S.I., M.T.W, and D.C.T.; Resources, L.L.L.X., A.K., T.M.A., R.T.C., J.T., W.N.H., T.F.B., and G.M.L.; Data curation, D.W., J.A., A.K., and G.M.L.; Writing- Original Draft, D.W. and G.M.L.; Writing – Review & Editing, D.W., P.T., A.T.C., A.K., T.F.B., and G.M.L.; Supervision, W.N.H., T.F.B., and G.M.L.; Project Administration, G.M.L.; Funding Acquisition, L.L.L.X., A.K., R.T.C., W.N.H, T.F.B., and G.M.L.;

Acknowledgments

We thank Drs. Brad Rosenberg, Naglaa Shoukry, Paul Klenerman, and Kate Jeffrey for constructive discussions. This work was funded by the NIH through U19AI066345, U19AI082630, U01AI13131401, and R01AI105035, as well as by the European Union.

References

Alexa, A., Rahnenfuhrer, J., and Lengauer, T. (2006). Improved scoring of functional groups from gene expression data by decorrelating GO graph structure. Bioinformatics *22*, 1600–1607.

Ashburner, M., Ball, C.A., Blake, J.A., Botstein, D., Butler, H., Cherry, J.M., Davis, A.P., Dolinski, K., Dwight, S.S., Eppig, J.T., et al. (2000). Gene Ontology: tool for the unification of biology. Nat Genet *25*, 25–29.

Bakr, I., Rekacewicz, C., Hosseiny, El, M., Ismail, S., Daly, El, M., El-Kafrawy, S., Esmat, G., Hamid, M.A., Mohamed, M.K., and Fontanet, A. (2006). Higher clearance of hepatitis C virus infection in females compared with males. Gut *55*, 1183–1187.

Barabási, A.-L., and Oltvai, Z.N. (2004). Network biology: understanding the cell's functional organization. Nature Reviews Genetics *5*, 101–113.

Bengsch, B., Johnson, A.L., Kurachi, M., Odorizzi, P.M., Pauken, K.E., Attanasio, J., Stelekati, E., McLane, L.M., Paley, M.A., Delgoffe, G.M., et al. (2016). Bioenergetic Insufficiencies Due to Metabolic Alterations Regulated by the Inhibitory Receptor PD-1 Are an Early Driver of CD8+ T Cell Exhaustion. Immunity *45*, 358–373.

Berkers, C.R., Maddocks, O.D.K., Cheung, E.C., Mor, I., and Vousden, K.H. (2013). Metabolic Regulation by p53 Family Members. Cell Metabolism *18*, 617–633.

Blondel, V.D., Guillaume, J.-L., Lambiotte, R., and Lefebvre, E. (2008). Fast unfolding of communities in large networks. J. Stat. Mech. *2008*, P10008.

Bowen, D.G., and Walker, C.M. (2005). Adaptive immune responses in acute and chronic hepatitis C virus infection. Nature *436*, 946–952.

Brodin, P., and Davis, M.M. (2016). Human immune system variation. Nat Rev Immunol *17*, 21–29.

Cox, A.L., Mosbruger, T., Lauer, G.M., Pardoll, D., Thomas, D.L., and Ray, S.C. (2005). Comprehensive analyses of CD8+ T cell responses during longitudinal study of acute human hepatitis C. Hepatology *42*, 104–112.

Csardi, G., and Nepusz, T. (2006). The igraph software package for complex network research. InterJournal Complex Systems *1695*, 1695.

Dai, M. (2005). Evolving gene/transcript definitions significantly alter the interpretation of GeneChip data. Nucl. Acids Res. *33*, e175–e175.

Doering, T.A., Crawford, A., Angelosanto, J.M., Paley, M.A., Ziegler, C.G., and Wherry, E.J. (2012). Network Analysis Reveals Centrally Connected Genes and Pathways Involved in CD8+ T Cell Exhaustion versus Memory. Immunity *37*, 1130–1144.

Dunham, I., Kundaje, A., Aldred, S.F., Collins, P.J., Davis, C.A., Doyle, F., Epstein, C.B., Frietze, S., Kaul, R., Khatun, J., et al. (2012). An integrated encyclopedia of DNA elements in the human

genome. Nature *489*, 57–74.

Durinck, S., Spellman, P.T., Birney, E., and Huber, W. (2009). Mapping identifiers for the integration of genomic datasets with the R/Bioconductor package biomaRt. Nat Protoc *4*, 1184–1191.

Erickson, A.L., Kimura, Y., Igarashi, S., Eichelberger, J., Houghton, M., Sidney, J., McKinney, D., Sette, A., Hughes, A.L., and Walker, C.M. (2001). The Outcome of Hepatitis C Virus Infection Is Predicted by Escape Mutations in Epitopes Targeted by Cytotoxic T Lymphocytes. Immunity *15*, 883–895.

Fafi-Kremer, S., Fofana, I., Soulier, E., Carolla, P., Meuleman, P., Leroux-Roels, G., Patel, A.H., Cosset, F.L., Pessaux, P., Doffoël, M., et al. (2010). Viral entry and escape from antibody-mediated neutralization influence hepatitis C virus reinfection in liver transplantation. J. Exp. Med. *207*, 2019–2031.

Fofana, I., Krieger, S.E., Grunert, F., Glauben, S., Xiao, F., Fafi-Kremer, S., Soulier, E., Royer, C., Thumann, C., Mee, C.J., et al. (2010). Monoclonal Anti-Claudin 1 Antibodies Prevent Hepatitis C Virus Infection of Primary Human Hepatocytes. Gastroenterology *139*, 953–964.e954.

Gaiha, G.D., McKim, K.J., Woods, M., Pertel, T., Rohrbach, J., Barteneva, N., Chin, C.R., Liu, D., Soghoian, D.Z., Cesa, K., et al. (2014). Dysfunctional HIV-Specific CD8+ T Cell Proliferation Is Associated with Increased Caspase-8 Activity and Mediated by Necroptosis. Immunity *41*, 1001–1012.

Gautier, L., Cope, L., Bolstad, B.M., and Irizarry, R.A. (2004). affy--analysis of Affymetrix GeneChip data at the probe level. Bioinformatics *20*, 307–315.

Giefing Kröll, C., Berger, P., Lepperdinger, G., and Grubeck-Loebenstein, B. (2015). How sex and age affect immune responses, susceptibility to infections, and response to vaccination. Aging Cell *14*, 309–321.

Grakoui, A. (2003). HCV Persistence and Immune Evasion in the Absence of Memory T Cell Help. Science *302*, 659–662.

Han, H., Shim, H., Shin, D., Shim, J.E., Ko, Y., Shin, J., Kim, H., Cho, A., Kim, E., Lee, T., et al. (2015). TRRUST: a reference database of human transcriptional regulatory interactions. Sci. Rep. *5*, 11432.

Kahan, S.M., Wherry, E.J., and Zajac, A.J. (2015). T cell exhaustion during persistent viral infections. Virology *479-480*, 180–193.

Kanehisa, M. (2000). KEGG: Kyoto Encyclopedia of Genes and Genomes. Nucl. Acids Res. *28*, 27–30.

Kasprowicz, V., Kang, Y.H., Lucas, M., Schulze zur Wiesch, J., Kuntzen, T., Fleming, V., Nolan, B.E., Longworth, S., Berical, A., Bengsch, B., et al. (2010). Hepatitis C Virus (HCV) Sequence Variation Induces an HCV-Specific T-Cell Phenotype Analogous to Spontaneous Resolution. J. Virol. *84*, 1656–1663.

Kato, M., Hata, N., Banerjee, N., Futcher, B., and Zhang, M.Q. (2004). Identifying combinatorial regulation of transcription factors and binding motifs. Genome Biol *5*, R56.

Kauffmann, A., Gentleman, R., and Huber, W. (2009). arrayQualityMetrics--a bioconductor package for quality assessment of microarray data. Bioinformatics *25*, 415–416.

Kuniholm, M.H., Kovacs, A., Gao, X., Xue, X., Marti, D., Thio, C.L., Peters, M.G., Terrault, N.A., Greenblatt, R.M., Goedert, J.J., et al. (2010). Specific human leukocyte antigen class I and II alleles associated with hepatitis C virus viremia. Hepatology *51*, 1514–1522.

Langfelder, P., and Horvath, S. (2008). WGCNA: an R package for weighted correlation network analysis. BMC Bioinformatics *9*, 559.

Leek, J.T., and Storey, J.D. (2007). Capturing Heterogeneity in Gene Expression Studies by Surrogate Variable Analysis. PLoS Genet *3*, e161.

Liu, Z.-P., Wu, C., Miao, H., and Wu, H. (2015). RegNetwork: an integrated database of transcriptional and post-transcriptional regulatory networks in human and mouse. Database *2015*, bav095.

Lochamy, J., Rogers, E.M., and Boss, J.M. (2007). CREB and phospho-CREB interact with RFX5 and CIITA to regulate MHC class II genes. Molecular Immunology *44*, 837–847.

Major, M.E., Dahari, H., Mihalik, K., Puig, M., Rice, C.M., Neumann, A.U., and Feinstone, S.M. (2004). Hepatitis C virus kinetics and host responses associated with disease and outcome of infection in chimpanzees. Hepatology *39*, 1709–1720.

Marbach, D., Lamparter, D., Quon, G., Kellis, M., Kutalik, Z., and Bergmann, S. (2016). Tissue-specific regulatory circuits reveal variable modular perturbations across complex diseases. Nature Methods *13*, 366–370.

Mathelier, A., Zhao, X., Zhang, A.W., Parcy, F., Worsley-Hunt, R., Arenillas, D.J., Buchman, S., Chen, C.-Y., Chou, A., Ienasescu, H., et al. (2014). JASPAR 2014: an extensively expanded and updated open-access database of transcription factor binding profiles. Nucl. Acids Res. *42*, D142–D147.

Matys, V. (2006). TRANSFAC(R) and its module TRANSCompel(R): transcriptional gene regulation in eukaryotes. Nucl. Acids Res. *34*, D108–D110.

Muñoz-Fontela, C., Mandinova, A., Aaronson, S.A., and Lee, S.W. (2016). Emerging roles of p53 and other tumour-suppressor genes in immune regulation. Nat Rev Immunol *16*, 741–750.

Osburn, W.O., Snider, A.E., Wells, B.L., Latanich, R., Bailey, J.R., Thomas, D.L., Cox, A.L., and Ray, S.C. (2014). Clearance of hepatitis C infection is associated with the early appearance of broad neutralizing antibody responses. Hepatology *59*, 2140–2151.

Oytam, Y., Sobhanmanesh, F., Duesing, K., Bowden, J.C., Osmond-McLeod, M., and Ross, J. (2016). Risk-conscious correction of batch effects: maximising information extraction from high-throughput genomic datasets. BMC Bioinformatics *17*, 733.

O'Shea, J.J., and Plenge, R. (2012). JAK and STAT Signaling Molecules in Immunoregulation and Immune-Mediated Disease. Immunity *36*, 542–550.

Pardoll, D.M. (2012). The blockade of immune checkpoints in cancer immunotherapy. Nat Rev Cancer *12*, 252–264.

Pestka, J.M., Zeisel, M.B., Blaser, E., Schurmann, P., Bartosch, B., Cosset, F.L., Patel, A.H., Meisel, H., Baumert, J., Viazov, S., et al. (2007). Rapid induction of virus-neutralizing antibodies and viral clearance in a single-source outbreak of hepatitis C. Proc Natl Acad Sci USA *104*, 6025–6030.

Ravasi, T., Suzuki, H., Cannistraci, C.V., Katayama, S., Bajic, V.B., Tan, K., Akalin, A., Schmeier, S., Kanamori-Katayama, M., Bertin, N., et al. (2010). An atlas of combinatorial transcriptional regulation in mouse and man. Cell *140*, 744–752.

Reményi, A., Schöler, H.R., and Wilmanns, M. (2004). Combinatorial control of gene expression. Nat. Struct. Mol. Biol. *11*, 812–815.

Ritchie, M.E., Phipson, B., Wu, D., Hu, Y., Law, C.W., Shi, W., and Smyth, G.K. (2015). limma powers differential expression analyses for RNA-sequencing and microarray studies. Nucl. Acids Res. *43*, e47–e47.

Rouillard, A.D., Gundersen, G.W., Fernandez, N.F., Wang, Z., Monteiro, C.D., McDermott, M.G., and Ma'ayan, A. (2016). The harmonizome: a collection of processed datasets gathered to serve and mine knowledge about genes and proteins. Database *2016*, baw100.

Schulze zur Wiesch, J., Ciuffreda, D., Lewis-Ximenez, L., Kasprowicz, V., Nolan, B.E., Streeck, H., Aneja, J., Reyor, L.L., Allen, T.M., Lohse, A.W., et al. (2012). Broadly directed virus-specific CD4 +T cell responses are primed during acute hepatitis C infection, but rapidly disappear from human blood with viral persistence. J. Exp. Med. *209*, 61–75.

Shoukry, N.H., Grakoui, A., Houghton, M., Chien, D.Y., Ghrayeb, J., Reimann, K.A., and Walker, C.M. (2003). Memory CD8 +T Cells Are Required for Protection from Persistent Hepatitis C Virus Infection. J. Exp. Med. *197*, 1645–1655.

Singer, M., Wang, C., Cong, L., Marjanovic, N.D., Kowalczyk, M.S., Zhang, H., Nyman, J., Sakuishi, K., Kurtulus, S., Gennert, D., et al. (2016). A Distinct Gene Module for Dysfunction Uncoupled from Activation in Tumor-Infiltrating T Cells. Cell *166*, 1500–1511.e1509.

Stelekati, E., Shin, H., Doering, T.A., Dolfi, D.V., Ziegler, C.G., Beiting, D.P., Dawson, L., Liboon, J., Wolski, D., Ali, M.-A.A., et al. (2014). Bystander Chronic Infection Negatively Impacts Development of CD8+ T Cell Memory. Immunity *40*, 801–813.

Subramanian, A., Tamayo, P., Mootha, V.K., Mukherjee, S., Ebert, B.L., Gillette, M.A., Paulovich, A., Pomeroy, S.L., Golub, T.R., Lander, E.S., et al. (2005). Gene set enrichment analysis: A knowledge-based approach for interpreting genome-wide expression profiles. Proc Natl Acad Sci USA *102*, 15545–15550.

Swadling, L., Capone, S., Antrobus, R.D., Brown, A., Richardson, R., Newell, E.W., Halliday, J., Kelly, C., Bowen, D., Fergusson, J., et al. (2014). A human vaccine strategy based on chimpanzee

adenoviral and MVA vectors that primes, boosts, and sustains functional HCV-specific T cell memory. Science Translational Medicine *6*, 261ra153–261ra153.

Teng, L., He, B., Gao, P., Gao, L., and Tan, K. (2013). Discover context-specific combinatorial transcription factor interactions by integrating diverse ChIP-Seq data sets. Nucl. Acids Res. *42*, gkt1105–e24.

Timm, J., Lauer, G.M., Kavanagh, D.G., Sheridan, I., Kim, A.Y., Lucas, M., Pillay, T., Ouchi, K., Reyor, L.L., Wiesch, zur, J.S., et al. (2004). CD8 Epitope Escape and Reversion in Acute HCV Infection. J. Exp. Med. *200*, 1593–1604.

Wherry, E.J., and Kurachi, M. (2015). Molecular and cellular insights into T cell exhaustion. Nat Rev Immunol *15*, 486–499.

Wu, D., and Smyth, G.K. (2012). Camera: a competitive gene set test accounting for inter-gene correlation. Nucl. Acids Res. *40*, e133–e133.

Zhang, H.M., Liu, T., Liu, C.J., Song, S., Zhang, X., Liu, W., Jia, H., Xue, Y., and Guo, A.Y. (2015). AnimalTFDB 2.0: a resource for expression, prediction and functional study of animal transcription factors. Nucl. Acids Res. *43*, D76–D81.

Figure Legends

Figure 1. Multivariate analysis of adaptive immunity during early HCV infection

(A) Gating strategy for sorting of HCV-specific CD8 T cells. Cells of interest were defined as CD8 and peptide-MHC multimer positive lymphocytes negative for CD4, CD14, CD19, CD16, CD56, Annexin V, and LiveDead viability stain.

(B) Sampling and assay overview. HCV-specific CD8 T cells from 43 subjects with different outcomes and varying levels of antigen recognition (Chronic (C), Escape (E), and Resolver (R)) were sampled at multiple time points (dots) within the first 36 weeks of infection (n_{total} = 78, STAR Methods). Status of CD4 T cell help (magnitude of HCV-specific CD4 T cells response measured by multi-color flow cytometry, dot color) and neutralizing antibodies (titers from HCV pseudoparticle neutralization assay, white bars) were assessed for a subset of these samples (n_{help} = 37 and $n_{neutralization}$=32).

See also Table S1.

Figure 2. Virus-specific CD8 T cells display distinct transcriptional profiles of resolution, inflammation and persistent antigen exposure

(A) Heatmap of 258 differentially expressed genes across C, E, and R groups during early and late acute phase of HCV infection (<18 and >18 weeks post infection). Transcriptional profiles of HCV-specific CD8 T cells were analyzed using microarrays. Differential expression was assessed between C and R in early or late acute infection or between early and late infection within C or R. Expression levels for E samples were not used for detection of differentially expressed genes but are also displayed. Shown are means of scaled expression levels (expression scores) by group.

(B) Venn diagrams of distinct transcriptional signatures defined by patterns of shared differential expression between C, E, and R groups and in early and late acute phase of infection.

See also Tables S1, S2, and S3.

Figure 3. Modules of tightly co-regulated genes give rise to distinct patterns of transcriptional regulation in different infection outcomes

(A) Detection of gene co-expression modules in C, E, and R groups. Weighted gene co-expression networks were constructed using WGCNA and modules of highly correlated genes were detected by hierarchical clustering. Colored bars indicate detected modules and their relative size, similar colors across groups do not imply overlap.

(B) Heatmap of scaled topological overlap matrices for isolated network modules from C, E, and R groups. Lighter colors indicate stronger positive correlation between genes within and across modules.

(C and D) Chord diagrams of gene module correspondence between C, E, and R groups. Diagrams show significance of gene overlap between two modules (core score, blue connection) or a module and unconnected genes (isolation score, red connections) for individual group pairs of (C) C/R or (D) C/E and E/R. Shown are scores that passed a significance threshold of FDR <0.01.

(E) Correlation, overlap and community networks for modules detected in C, E, and R groups. Correlation and overlap networks were constructed using within-group correlation significance (FDR <0.01) and across-group overlap significance (FDR <0.01) and merged for detection of module communities (indicated by color) (STAR Methods). Significance of correlation and overlap were used for network layout and shown as width of the edges connecting modules within networks.

See also Table S4.

Figure 4. Differential expression of network modules is preserved across cohorts of acute HCV infection

(A and B) Barcode plots of network module signature enrichments for (A) HCV-specific CD8 T cells from C and R patients during the early and late phase of acute infection as well for (B) HCV-specific CD8 T cells from a separate validation cohort of chronic and resolving patients sampled during the early acute phase of infection (≤21 weeks post infection).

Ranked lists of $\log_2$ fold changes from analysis of differential expression between C and R groups were tested for enrichment of network modules (STAR Methods). Shown are representative examples of significantly (FDR < 0.05) enriched (r2, r6 and r5) and universally non-enriched modules (c5).

See also Tables S4, S5, and S6.

Figure 5. Correlation and enrichment maps link gene co-expression modules from different immunological states to clinical traits, immune signatures and biological function

(A) Trait correlation map for C, E and R groups in acute HCV infection. Eigengenes (first principal components) of network modules were correlated with clinical traits (colors indicate r value and sign of correlations (red = positive, blue = negative). Shown are correlations with FDR < 0.1.

(B and C) Enrichment maps for C, E, and R groups, showing enrichments scores for all significant enrichments (FDR < 0.05). (B) Modules were tested for enrichment of CD8 T cell differential expression signatures from HCV (Figure 2), HIV (Gaiha et al., 2014), and mouse models of T cell memory and exhaustion (Doering et al., 2012; Singer et al., 2016; Subramanian et al., 2005) (C) Modules were tested for enrichment of CD8 T cell WGCNA module signatures from acute (AM) and chronic (CM) LCMV infection (Doering et al., 2012).

(D) Functional enrichment maps for C, E, and R groups. Detected modules were tested for enrichment of immune pathways (Langfelder and Horvath, 2008), GO terms, and KEGG pathways. Shown are enrichment scores for top-scoring immune pathways (5 most enriched pathways per group per module by enrichment score and number of genes driving the enrichment) with FDR <0.05 and

KEGG pathway/GO term enrichments below a significance threshold of FDR <1e-10. Enriched processes and contained genes were grouped into clusters of functionally related and co-regulated terms related to metabolism, immune, and nucleosome clusters as indicated by colored dots in grey panels to the right of enrichment maps.

See also Tables S3, S7 and S8.

Figure 6. A distinct temporal pattern of metabolic regulation marks chronic HCV infection

(A) Metabolism Cluster Network for C, E, and R, groups. Module networks for each group were subset to genes annotated to the metabolism cluster and visualized as networks with components of genes grouped by exclusive or shared regulation between groups (colored bubbles). Nodes are sized by intramodular connectivity and colored by group expression score during the early phase of infection.

(B) KEGG pathway enrichment in metabolism cluster network. Individual components from (A) were tested for enrichment of KEGG pathways. All pathways that were significantly enriched (FDR <0.05) in at least one component are shown.

(C) Chronic-exclusively regulated genes annotated for OXPHOS. Genes (shown as nodes), colored by their module membership in the C group. Genes that overlap with a leading-edge signature of metabolic processes associated with T cell exhaustion (Bengsch et al., 2016) are encircled by a dashed line (12/17 genes).

(D) Expression kinetics of hub genes for modules c3, c5, c6. Log_2-transformed gene expression levels for the most highly connected genes from modules c3, c5, and c6 are plotted for each group over time (dots represent individual time point samples, color indicates module membership). Longitudinal trends in expression are visualized using a local regression based (LOESS) smoother (grey shading indicates 95% confidence intervals of the local regression).

See also Figures S1 and S2, and Tables S4, S8, and S9.

Figure 7. Distinct regulatory interactions link dysregulation of metabolic, nucleosomal, and immune processes in CD8 T cells from early chronic HCV infection

(A) Transcriptional regulator (TR) target coverage for CD8 T cells in chronic HCV infection. A large network of regulatory interactions was assembled from the literature (STAR Methods) and subset to TR-target interactions with matching module assignments. TRs are plotted by number (left) or percentage (right) of within-module regulatory interactions and intramodular connectivity. Transcription factors with intramodular connectivity > 0.5 and/or target coverage count > 20 or percentage >5% are labeled with their respective gene symbols. TR module membership is indicated by color.

(B) Regulatory networks for select TRs from modules c3, c5, c6, and r2. Weighted gene correlation networks were restricted to strong interactions (weight > 0.025) between selected TRs and known targets (kWithin >0.25). For transcription co-factors and chromatin remodeling genes, only interactions targeting transcription factors are shown. TRs and targets are both labeled with gene symbols and colored by their regulatory function or their annotation in metabolism, nucleosome, or immune cluster networks. Interaction types are indicated by color of edges connecting TRs and targets.

(C) Representative expression kinetics for genes from the Chronic regulatory network. Shown are log2-transformed expression levels (dots represent individual samples) of genes annotated for regulation of transcription (Histones, RNA & DNA polymerases), metabolism (ATP Synthase, NADH dehydrogenase, Cytochrome C oxidase, and Oxidoreductase activity), and T cell function and homing (T cell maintenance & activation, Cell adhesion & migration), which illustrate highly time-dependent expression dynamics. Module membership for C samples is indicated by color and module

number. Longitudinal trends in expression are visualized using a local regression based (LOESS) smoother (grey shading indicates 95% confidence intervals of the local regression). See also Figures S3 and S4, and Tables S8 and S10.

Supplemental Figure Legends

Figure S1. Metabolism cluster networks in HCV-specific CD8 T cells visualized by gene expression levels and module color, Related to Figures 5 and 6

Metabolism Cluster Networks (STAR Methods) derived from functional enrichments (Figure 5) in Chronic (C), Escape (E), and Resolver (R) groups colored by (A) mean gene expression levels per group during the late phase of infection and (B) module membership of genes within each group. Analogous to Figure 6A, module networks for each group were subset to genes annotated to the metabolism cluster and visualized as networks with genes grouped by exclusive or shared regulation between groups. Colored bubbles highlight components comprised of groups of genes undergoing shared or exclusive regulation between groups. Nodes are sized by scaled intramodular connectivity.

Figure S2. Immune and Nucleosome cluster networks in HCV-specific CD8 T cells visualized by gene expression levels and module color, Related to Figures 5 and 6

(A, B, and C) Immune Cluster Networks and (D, E, and F) Nucleosome Cluster Networks derived from functional enrichments (Figure 5) in Chronic (C), Escape (E), and Resolver (R) groups and colored by mean gene expression levels per group during the (A and F) early or (B and E) late phase of infection or by (C and F) module membership of genes within each group. Analogous to Figure 6A, module networks for each group were subset to genes annotated to the immune (panels A, B, and C) or nucleosome (panels D, E, and F) clusters and visualized as networks with genes grouped by exclusive or shared regulation between groups. Colored bubbles highlight components comprised of groups of genes undergoing shared or exclusive regulation between groups. Nodes are sized by scaled intramodular connectivity.

Figure S3. Diverging patterns of transcription factor target coverage in WGCNA network modules of CD8 T cells in Escape and Resolver samples, Related to Figure 7

(A and B) Transcription factor target coverage by module for (A) Resolver and (B) Escape groups. Analogous to Figure 7A, regulated transcription factors and their within-module targets were identified and plotted by intramodular connectivity and number/percentage of targeted genes (STAR Methods). Transcription factors with intramodular connectivity >0.5 and/or target coverage count >20 or percentage >5% are labeled with their respective gene symbols. Module membership for each transcription factor is indicated by its respective color.

(C) Expression kinetics for genes from the Chronic regulatory network. Shown are representative genes that illustrate highly time-dependent gene expression levels. Log2-transformed gene expression levels are plotted over time (dots represent individual samples) and colored by module membership. Longitudinal trends in expression are visualized using a local regression based (LOESS) smoother (grey shading indicates 95% confidence intervals of the local regression).

Figure S4. Regulatory circuitry in HCV-specific CD8 T cells displays profound differences across different infection outcomes and levels of viral control, Related to Figure 7

Regulatory networks for transcriptional regulators selected from Chronic modules c3, c5, c6, and Resolver module r2, as shown in Figure 7B. Module networks were restricted to known regulator-target interactions for selected transcription factors, transcription co-factors and chromatin remodeling genes from a regulatory network of TF-target interactions assembled from the literature (STAR Methods). The resulting regulatory networks were subset to edges with weight >0.025 and target nodes with intramodular connectivity >0.25. For transcription co-factors and chromatin remodeling genes, only interactions targeting transcription factors are shown. Nodes are labeled with gene symbols and colored by mean gene expression levels per group during the (A) early or (B) late

phase of infection or by (C) components of shared and exclusive regulation between groups or (D) module membership of genes within each group. Colors of directed edges connecting transcription factors and their targets indicate the interaction type.

Supplemental Tables

Table S1. Clinical information for subjects and samples of the original data set, Related to Figures 1 and 2

Table S2. Differentially expressed genes with log2 fold changes and FDR values, Related to Figure 2

Table S3. Custom signatures used in differential expression signature, module signature enrichment analyses in CD8 T cell network modules, Related to Figures 2 and 5

Table S4. Gene-Module assignments and intramodular connectivities for Chronic, Escape, and Resolver co-expression networks, Related to Figures 3 and 4

Table S5. Clinical information for subjects and samples of the validation data set, Related to Figure 4

Table S6. Full results for CAMERA validation enrichment analysis in differential expression gene lists ranked by fold change between Chronic and Resolver groups, Related to Figure 4

Table S7. Full results for differential expression signature, module signature, and functional enrichment analyses in CD8 T cell network modules from Chronic, Escape, and Resolver groups, Related to Figure 5

Table S8. Genes included in Metabolism, Immune, and Nucleosome Cluster Networks by components of shared or exclusive regulation, Related to Figures 6 and 7

Table S9. Results of KEGG pathway enrichments in Metabolism Cluster Network, Related to Figure 6

Table S10. Coverage for transcriptional regulators annotated in CD8 T cell network modules from Chronic, Escape, and Resolver groups, Related to Figure 7

STAR Methods

CONTACT FOR REAGENT AND RESOURCE SHARING

All requests for reagents and resources can be directed at Georg M. Lauer (glauer@mgh.harvard.edu)

EXPERIMENTAL MODELS AND SUBJECT DETAILS

Human subjects and samples

We collected blood samples from 41 patients at multiple time points during the early and late acute phase (0 to 36 weeks) of infection with hepatitis C virus and extracted PBMC and plasma by Ficoll-Paque (GE Healthcare Life Sciences) density gradient centrifugation. To reduce the impact of sources of variability or bias, we excluded subjects that had tested positive for co-infections such as HIV or HBV as well as subjects that had previously been treated for HCV infection or resolved a previous infection on their own. Furthermore, we excluded subjects with resolving infection for which recognized epitopes bore known escape mutations, and subjects for whom the natural course of infection could not be determined accurately, due to lack of follow-up or treatment within the acute phase of infection. Informed consent was given by all subjects under two protocols approved by the Partners Healthcare Human Research Committee and the IRB of the Oswaldo Cruz Institute in Rio de Janeiro, Brazil.

To capture both cross-sectional and longitudinal changes, we sampled subjects during the entire phase of acute infection, capturing 1-3 time points per patient, for a total of 78 samples, 41 from chronic and 37 from resolving patients. For analysis purposes, we distinguished between CD8 T cells from chronic infection targeting conserved vs escaped viral epitopes as determined by viral sequencing, resulting in three groups of samples that we refer to as Chronic (C, chronic with conserved epitope,

nchronic = 27), Escape (E, chronic with escaped epitope, nescape = 14), and Resolver (R, resolver with conserved epitope, nresolver = 37) (Figure 1B, Table S1).

For the validation cohort (Table S5), we sampled 7 chronic (C) and 3 resolving (R) patients at the earliest time point each (≤21 weeks) using the same criteria as outlined above.

METHOD DETAILS

Flow Cytometry and Cell Sorting

We detected, quantified, and sorted HCV-specific CD8+ T cells from human PBMC by multi-color flow cytometry and fluorescence assisted cell sorting using class I MHC multimers (Figure 1A). Multimers were matched to each subject's human leukocyte antigen type and individual peptide response profile, which had been mapped by IFN-gamma secretion assay prior to the study. HCV-specific CD8 T cells were defined as cells positive for CD3/CD8/pMHC-multimer (inclusion of specific CD8 T cells) and negative for CD4/CD14/CD19/CD16/CD56 (exclusion of CD4 T cells, natural killer T cells, natural killer cells, monocytes, and B cells) as well as negative for Live/Dead viability dye and Annexin V (exclusion of dead and apoptotic cells). All steps were performed at 4˚C, unless specified otherwise by the manufacturer. In brief, cells were thawed to a temperature of 4˚C washed in FBS (1x) and R10 (1x), and resuspended in PBS for LiveDead viability staining (Thermo Fisher Scientific) at room temperature for 30min. Cells were washed in FACS buffer, stained for TCR using peptide-MHC multimers and washed again (FACS buffer, 1x) prior to surface antigen staining (KEY RESOURCES TABLE). Following surface antigen staining, cells were washed (FACS buffer, 2x) and stained for Annexin V (Thermo Fisher Scientific) per manufacturer instructions and cells were sorted into phosphate buffered saline (PBS) on ice (4°C) using a BD FACSARIA (BD Biosciences), subsequently pelleted by centrifugation, and resuspended in cold TRIzol (Invitrogen). Samples were

then stored at -80°C until further processing. Details on used antibodies and reagents are listed in the KEY RESOURCES TABLE.

Data on Other Adaptive Immune Effectors

Magnitude of CD4 T cell response

In a subset of the samples used for CD8 gene expression analysis we measured the magnitude of the HCV-specific CD4 T cell response by multi-color flow cytometry using MHC class II multimers in the same approach as described above to be used as a basic indicator of the amount of CD4 help available to CD8 T cells (n=37/78, Figure 1, Table S1). CD4 help was categorized as follows: Samples with no detectable CD4 T cells (≤0.001% of total T cells (CD3+)) at the time point in question or within 2 weeks of it and which had detectable CD4 T cells at other time points (including time points outside of this study) were classified as no help (none), samples with detectable CD4 T cells (>0.001% and < 0.01% of CD3+) at the time point in question or within 2 weeks of it were classified as low help (low), and samples with detectable CD4 T cells (≥0.01% of CD3+) at the time point in question or within 2 weeks of it were classified as high help. Furthermore, samples from subjects with high CD4 help at a later time point (> 2 weeks) were classified as "high" and samples from subjects with no CD4 help at an earlier time point (> 2 weeks) were classified as "none".

Neutralizing antibodies

HCV-specific neutralizing antibodies were quantified in serum of a subset of patients (n=32/78, Figure 1B, Table S1) using a neutralization assay based on the infection of Huh7 cells with retroviral pseudoparticles (HCVpp) that express genotype-specific HCV envelope glycoproteins E1 and E2. Neutralizing antibodies were quantified using endpoint titration, as described in detail in (Fafi-Kremer

et al., 2010; Fofana et al., 2010; Pestka et al., 2007). For analysis purposes, titers were classified as non-neutralizing (<1:100) and neutralizing (1:100). Neutralizing antibodies could not be used for trait correlations with module genes (Figure 5A), since only 4 subjects, distributed over all three groups, displayed significant levels of neutralization.

Viral Genome Sequencing

We sequenced the Hepatitis C viral genome on a per patient and time point basis for samples where a sufficiently high viral load was detectable. We surveyed the relevant viral epitopes used in the flow cytometry and cell-sorting step for sequence conservation and stratified samples by levels of epitope recognition and processing based on published data (Erickson et al., 2001; Grakoui, 2003; Timm et al., 2004). For our study, we excluded all samples from resolving patients where evidence suggested a severe lack of recognition or processing of the viral epitope. Samples from chronic patients were classified as escape samples based on the same criteria, resulting in the three groups we investigate here, namely Chronic, Escape and Resolver.

RNA Processing

We extracted total RNA from samples with >500 sorted cells using the RNAdvance Tissue Isolation Kit (Agencourt), reverse transcribed RNA into cDNA and amplified it using the WT-Ovation Pico Amplification System (Nugen). Following that, we tested for cDNA yield by Nanodrop (Thermo Fisher Scientific) and purity by 2100 Bioanalyzer (Agilent Technologies). We then hybridized concentration-adjusted amounts of cDNA to GeneChip HG U133A 2.0 (Affymetrix) microarrays to measure gene expression. Details on used reagents are listed in the KEY RESOURCES TABLE.

QUANTIFICATION AND STATISTICAL ANALYSIS

Microarray Data Preprocessing

Raw CEL files, containing probe level expression data, were imported into R using affy (Gautier et al., 2004), background-corrected, normalized, summarized to probe set level, and finally log transformed by robust multi-array average (RMA) using a custom HGU133A2_Hs_ENTREZG v20.0.0 chip definition file (CDF) file obtained from http://brainarray.mbni.med.umich.edu (Dai, 2005). Prior to correction for known technical batch effects (sample source and array batch), we ensured that variables of interest (disease outcome, viral escape) had a reasonably balanced distribution among batches and estimated the number of latent variables by sva (Leek and Storey, 2007). Probe set level data were batch effect corrected using the risk-conscious PCA-based adjustment method Harman (Oytam et al., 2016), while controlling for variables of interest. We reran sva to confirm successful batch correction and confirm that no significant latent variables remained in the data.

To remove lowly expressed genes and reduce the impact of noise on analysis of the data, probe sets were filtered based on mean expression and variance, keeping only those with a mean log2 expression value >4.25 and a variance >0.3 across all samples. Finally, probe sets were collapsed to the gene level using genefilter (Kauffmann et al., 2009), removing duplicate entries and manufacturer quality control probe sets, resulting in a set of 5246 genes.

Data were split into three sample sets by disease outcome and status of viral escape. Obvious outlier samples were identified by hierarchical clustering and excluded from further analysis.

To improve speed and sensitivity of our analysis pipeline we calculated the nearest neighbor connectivity for each of the 5246 genes (per group) using WGCNA (Langfelder and Horvath, 2008) by set (nneighbors=50) and kept only the union of the top 45% most connected genes from each group, resulting in a final set of 3850 genes used for all downstream analysis.

For the validation experiment (Figure 4, Tables S5 and S6), we processed data in the same manner as outlined above using a custom CDF file (HTHGU133A_Hs_ENTREZG v20.0.0) and used the same subset of genes that were used in the original data set for subsequent analysis.

Differential Expression Analysis

To improve group homology for detection of differentially expressed genes, sample groups were split into early (≤18 weeks post infection) and late (>18 and <36 weeks post infection) subgroups (Figure 1B). We assessed differential gene expression between early (≤18 weeks post infection) and late (>18 and <36 weeks post infection) Chronic and Resolver samples (Figure 2A, Table S2), using an empirical Bayes moderated ANOVA after fitting an observation level mean-variance model to data subsets to adjust for heteroscedasticity as implemented in limma (Ritchie et al., 2015), returning an F test statistic and p value analogous to those of regular ANOVA. P-values were corrected for multiple hypothesis testing by controlling the false discovery rate (FDR). Genes were called differentially expressed with an FDR <0.05 and an absolute fold change > 1.5, corresponding to a 50% difference in expression between Chronic and Resolver groups during early or late acute phase of infection or between early and late phase of acute infection in Chronic or Resolver groups, resulting in a set 4 contrasts between groups and timeframes across which we detected 258 differentially expressed genes (Figure 2, Table S2). We expressly based detection of differentially expressed genes on Chronic and Resolver samples only, as the differences between these samples were the focus of this study, but also plotted the mean scaled expression scores for the early and late Escape samples (Figure 2A), to identify whether Escape samples shared part of their transcriptional signature with Chronic or Resolver groups.

Based on shared expression profiles of differentially expressed genes between Chronic, Escape and Resolver groups (Figure 2A) we defined a set of 8 gene expression signatures for both the early and late acute phase of infection (Figure 2B, Table S3). Each set was defined as 7 signatures of upregulated

genes (Resolver, Escape/Resolver, Chronic/Resolver, Escape, Chronic/Escape, Chronic, and All) and one signature of downregulated genes (All).

The same parameters as described above were used for differential expression analysis in the validation cohort (Figure 4, Tables S5 and S6)

Network Construction and Module Detection

We used WGCNA (Langfelder and Horvath, 2008) to construct a weighted gene co-expression network for each sample set. WGCNA assumes that co-expression of genes, measured by their correlation across samples within an experimental group also implies their co-regulation. In this semi-supervised way, WGCNA allows for detection of modules of highly correlated and often functionally related genes that can be tested for their degree of preservation and difference in connectivity between individual networks. By applying weights to correlations by raising them to a power beta, giving preference to strong correlations over weak ones, WGCNA achieves both a reduction of noise in the data and a scale-free network topology. This scale-freeness is considered to reflect an intrinsic and desirable property of most biological networks, as it is strongly correlated with a network's robustness to random perturbation (e.g. random mutation) (Barabási and Oltvai, 2004). Accordingly, a signed network adjacency matrix was calculated from the biweight midcorrelation between all gene pairs of each group (Chronic, Escape, and Resolver) using soft thresholding powers (see WGCNA parameter table). Network adjacencies were then transformed into topological overlap dissimilarity measures and subjected to average distance hierarchical clustering. The resulting clustering dendrograms (Figure 3A), that visualize distances between genes in terms of their co-expression profiles, with lower hanging branches indicating clusters of highly correlated genes, were then used to isolate 9 Chronic, 8 Escape, and 8 Resolver gene modules using a dynamic tree cutting algorithm (Langfelder and Horvath, 2008).

Highly similar modules were merged based on a minimum dissimilarity threshold. Since WGCNA allows a host of different parameter choices, and to ease reproduction of our results, we have itemized details of parameter choices below.

Parameter choices for construction of weighted gene co-expression networks

Category	Function	Parameter	Value
Network Construction	adjacency	corFnc	"bicor"
		corOptions	"use = 'p', maxPOutliers = 0.05"
		type	"signed hybrid"
		power	4/7/3 (Chronic/Escape/Resolver)
	TOMsimilarity	TOMType	"signed"
		TOMDenom	"min"
	TOM scaling[a] (scale TOM matrices for comparability)	percentile	0.95
		sample size	1/(1- percentile) * 1000
		reference set	"Resolver"
	Gene clustering[a] (cluster genes based on scaled TOM)	dist	1-scaledTOM
		clustering method	"average"
Module Detection	cutreeDynamic	method	"hybrid"
		minClusterSize	60
		maxCoreScatter	0.75
		minGap	(1- maxCoreScatter)*3/4
		pamStage	FALSE
	mergeCloseModules	useAbs	TRUE
		cutHeight	0.25

Identification of Module Communities

We calculated pairwise biweight midcorrelations between first principal components of individual modules (module eigengenes) within groups and determined correlation significance using Fisher's exact test. We also determined overlap in gene content between modules between different groups and calculated the significance of this overlap using a one-tailed Fisher's exact test. Both correlation and overlap p-values were corrected for multiple comparisons by control of FDR. Furthermore, for Figures 3C and 3D we defined the significance of each overlap as its core or isolation score, depending on whether the overlap was between two modules in two groups (core score) or a module and unconnected genes (grey pseudo module) (isolation score). Next, we created correlation and overlap module networks (Figure 3E, left and middle), where module correlations or overlaps with FDR <0.01 were defined as connections between individual modules. We then used the strength, defined as –log10(FDR), and number of these connections to identify communities of related modules (Figure 3E) in a merged network of correlations and overlaps (Figure 3E, right). Modules communities were detected using a multi-level algorithm (Blondel et al., 2008) as implemented in igraph (Csardi and Nepusz, 2006).

Trait Correlations

To correlate identified modules with clinical traits, we calculated the first principal component (eigengene) of each module and correlated it with several clinical and immunological traits (Figure 5A), including HCV viral load (log2 tranformed), alanine aminotransferase (log2 transformed), time from infection (weeks), subject sex and age, as well as status of CD4 help (measured as number of detectable HCV-specific CD4 T cells, see above) or neutralizing antibody status (measured as titer threshold, see above). Biweight midcorrelation was used for all continuous variables (age, viral load, ALT, time from infection) and Pearson correlation was used for all ordinal variables (sex, CD4 help).

Ordinal variables were coded as follows: sex, female = 1, male = 2; CD4 help, none = 0, low = 1, high = 2.

Gene Set Enrichment Analysis

Assembly of external gene signatures

We assembled a set 6 of HIV-specific CD8 T cell signatures from based on genes that were differentially expressed (FDR $\leq$ 0.05, $|\log2(\text{fold change})| \geq 1.5$) in HIV-specific CD8 T cells from elite/viremic controllers and chronic progressors (Gaiha et al., 2014) based on comparisons between peptide-stimulated controllers and progressors and between stimulated and unstimulated cells in controller and progressor groups (Table S3).

For mouse signatures of T cell dysfunction vs activation, we used a set of 4 signatures (Table S3) recently published by Singer et al., that define genes related to T cell dysfunction, T cell activation, T cell activation/dysfunction and naïve/memory like T cells based on their correlation with the first two principal components that separate tumor-infiltrating lymphocytes according to their functionality and activation status based on expression of inhibitory receptors Tim-3 and PD-1 and deficiency of metallothioneins MT1 and MT2 (Singer et al., 2016).

We assembled other mouse signatures of naïve, memory and exhausted T cells from the literature as detailed by Singer et al. (Singer et al., 2016), to ensure direct comparability with the novel signatures of T cell dysfunction and activation they describe. In brief, we compiled consensus signatures of naïve and memory T cells from multiple MSigDB v5.0 gene signatures (Subramanian et al., 2005) (naïve: 28 genes upregulated in > 10/26 , memory: 23 genes upregulated in > 6 out of 13 signatures, Table S3). Furthermore, we compiled a T cell exhaustion signature from genes that were differentially expressed (FDR < 0.05 and $|\text{fold change}| \geq 2$) in LCMV-specific CD8 T cells between chronic and acute disease on day 15 and 30 of LCMV infection (Doering et al., 2012) (73 genes, Table S3). In addition to the

late exhaustion signature, we also assembled an early exhaustion signature (31 genes) based on differential expression (FDR < 0.05 and |fold change| ≥ 2) at day 8 of LCMV infection as well as resolution signatures at day 8 (4 genes, Table S3) and day 15/30 (7 genes, Table S3).

For external module signatures, we used WGCNA based gene modules from CD8 T cells in chronic and acute LCMV infection (Doering et al., 2012).

To account for mismatches in gene annotation between organisms, we transformed all mouse signature into human signatures by mapping from MGI symbols to ENSEMBL identifiers and from ENSEMBL identifiers back to HGNC symbols using biomaRt (Durinck et al., 2009).

HCV module signature enrichments for module validation

For validation of detected network modules we used CAMERA (Wu and Smyth, 2012) to test both the original data set (Table S1) and a separate data set of microarray data from HCV-specific CD8 T cells from patients with persisting and resolving infection within 20 weeks of infection ("validation" set, Table S5) for enrichment of the modules we derived from the original data set.

Similar to GSEA (Subramanian et al., 2005), CAMERA allows ranked list of genes as input (here, we rank genes by differential expression between Chronic and Resolver within the different data sets).

Furthermore, CAMERA allows specification of inter gene correlations to adjust significance of detected enrichments, based on the assumption that sets of correlated genes often lead to inflated p-values. Since we wanted to test sets of genes that were defined by their high degree of correlation, we set the inter gene correlation to be at a low, fixed level of 0.01, deliberately allowing our module gene sets to achieve high enrichment scores, which were then corrected for multiple hypothesis testing within each data set (early, late, and validation) by FDR control. Figure 4 shows examples of enrichment plots for modules r2, r5, r6, and c5 for both the early and late group of the original data set (Figure 4A) and the validation data set (Figure 4B). Full enrichment results are listed in Table S6.

Differential Expression and Module Signature Enrichments

We performed a variety of gene set enrichment analyses per module per experimental group (Chronic, Escape, Resolver). For the differential expression signature enrichment analysis (Figure 5B), we used 30 CD8 T cell gene expression signatures related to different T cell states, including the 16 gene signatures defined from differential expression profiles in our data set of HCV-specific CD8 T cells (Figure 2, Tables S2 and S3) as well as 14 gene sets assembled from the literature which were related to CD8 T cell dysfunction, exhaustion and memory state in murine models (Doering et al., 2012; Singer et al., 2016; Subramanian et al., 2005) or derived from peptide stimulated CD8 T cells in subjects with controlled or progressing HIV infection (Gaiha et al., 2014) (Table S3).

For a module signature enrichment analysis (Figure 5C), we used 19 CD8 T cell co-expression module signatures that were identified using WGCNA in longitudinally sampled, antigen-specific CD8 T cells isolated from mice infected with acute (13 modules) or chronically persisting (6 modules) strains of lymphocytic choriomeningitis virus (LCMV) (Doering et al., 2012) (Table S3). Details for the assembly of the used gene signatures are explained earlier in STAR Methods.

Both expression and module signature enrichments (Figures 5B and 5C) were calculated using a standard hypergeometric test as implemented in WGCNA using the entire set of 3850 genes included in the analysis as background. Gene signature enrichment scores in the form of p-values were corrected for multiple hypothesis testing within experimental groups and modules by control of FDR. All enrichments with FDR <0.05 are shown in Figures 4B and 4C. A comprehensive list of signature enrichment results for all groups and modules can be found in Table S7.

Functional Enrichments

For the Immune Pathway enrichment (Figure 5D, top) we used a manually curated list of 54 immune pathways as contained in the WGCNA package (assembled from Ingenuity, WikiPathways, and literature (Langfelder and Horvath, 2008) (Table S3). Immune pathway enrichments were calculated using a standard hypergeometric test as implemented in WGCNA. Enrichment scores in the form of p-values were corrected for multiple hypothesis testing within experimental groups and modules by control of FDR. The top 5 enrichments (by score and size of overlap) per group and modules that were also enriched above a significance threshold of FDR < 0.05 are shown in Figure 5D.

For the functional database enrichment (Figure 5D, bottom) we used the publicly available gene ontology and KEGG pathway databases (Ashburner et al., 2000; Kanehisa, 2000). We used topGO (Alexa et al., 2006) to test the identified network modules for enrichment of gene ontology terms related to biological processes, cellular components and molecular function with scoring based on topGO's mixed elimination and weight algorithm and Fisher's exact test. For analysis of KEGG pathway enrichments (Figures 5D) we used the corresponding function implemented in limma (Ritchie et al., 2015). Rather than controlling the FDR, we opted to impose a more stringent cutoff for significance thresholding of GO and KEGG enrichment analyses ($p < 1e\text{-}10$), since these generally produced very strong p-values. Furthermore, topGO utilizes the underlying graph structure of the GO topology to return enrichment scores which can be considered to not be affected by multiple testing. A comprehensive list of functional enrichment results for all groups and modules can be found in Table S7.

For the KEGG enrichment analyses of the metabolism cluster network (Figure 6B, Table S8) we corrected enrichment scores (p-values) for multiple hypothesis testing by controlling the FDR. For this enrichment, all significant enrichments with ≥4 genes and FDR <0.05 are shown.

All functional enrichments were calculated using the entire set of 3850 genes included in the analysis as background.

Identification and visualization of cluster networks

Based on detected module communities (Figure 3E, right) and results from enrichment analysis of gene ontologies, pathways and gene signatures performed (Figure 5) we selected gene sets of common functional annotation to construct networks of co-regulated gene clusters related to metabolism, nucleosome and immune signaling (Table S8). We visualized these networks with igraph (Csardi and Nepusz, 2006) using a fixed network structure to allow for easy identification of functionally preserved components and connections within subnetworks (Figures 6A, S1 and S2).

Regulatory Network Analysis

Regulatory interaction network assembly

We integrated information on experimentally confirmed and predicted interactions of regulatory genes and their targets from multiple publicly available repositories to create a large regulatory interaction network, consisting of 1319 regulators and ~2.9 million unique regulatory interactions. We combined data from CHEA, ENCODE (Dunham et al., 2012), TRANSFAC (Matys, 2006), and JASPAR (Mathelier et al., 2014) data sets obtained from the Harmonizome (Rouillard et al., 2016) repository and combined it with information on interactions from the TRRUST (Han et al., 2015) and RegNetwork (Liu et al., 2015) repositories, which also included information on interaction type and confidence. Links to the individual resources are given in the KEY RESOURCES TABLE.

Furthermore, we included interactions from two weighted, cell type-specific regulatory networks for CD8 T cells and lymphocytes inferred recently published by Marbach et al. (Marbach et al., 2016). For

purposes of this study, only interactions with an interaction weight >0.005 were included from these two networks.

Regulatory molecules were annotated for their class (transcription factor, transcription co-factor, and chromatin remodeling gene) in accordance with their annotation in the animal transcription factor database (Zhang et al., 2015).

Identification of High Confidence Transcriptional Regulators

We intersected the assembled regulatory interaction network with the constructed gene co-expression networks for Chronic, Escape, and Resolver groups that were pruned to exclude weak interactions (only interactions with weight >0.025 were included), resulting in networks of high-confidence regulatory interactions present in the HCV data.

To identify the most important within-module regulatory interactions for each regulator annotated for a module, we counted the number of regulatory interactions between the regulator and its targets within the same module and compared it to its intramodular connectivity (Figures 7A and S3, Table S10). To account for varying module sizes we assessed regulatory target coverage both by total number of connections and number of connections relative to module size (percentage).

Construction of HCV-specific CD8 T cell regulatory networks

To identify and highlight high-confidence regulatory interactions between important transcriptional regulators (Figure 7A) and genes of interest from the functional cluster networks (Figures 6A, S1, and S2), we subset regulatory interaction networks for Chronic, Escape, and Resolver groups to important transcriptional regulators of interest (Figures 7A and S3, Table S10) and genes with intramodular connectivity >0.25 contained in metabolism, immune, and immune/nucleosome cluster networks. We allowed for connections of regulatory genes to targets across modules that had been omitted in the

transcription factor identification step, since the existence of such connections is likely to better reflect the underlying biology as investigated modules are highly co-regulated. In contrast, their inclusion in the identification step would have inevitably lead to overestimation of the importance of individual transcription factors (as some TFs are annotated for >20,000 interactions) and likely obscure the highly combinatorial design, by which transcriptional regulation is organized (Kato et al., 2004; Ravasi et al., 2010; Reményi et al., 2004; Teng et al., 2013).

We created regulatory networks based on the interactions of the transcriptional regulators *STAT5A, KDM5B, CBX3, RFX5, NELFE, STAT1, TP53, FLI1, IRF3, CREB1* within Chronic, Escape and Resolver groups in our data set and visualized them by functional annotation (Figure 7B) as well early and late gene expression levels (see Figure 2), module color (see Figure 3) and shared co-regulation among groups (see Figures 6A, S1 and S2) using igraph (FigureS4). To reduce visual redundancies, regulatory interactions for annotated as transcription co-factors and chromatin remodeling genes were subset to those targeting transcription factors.

DATA AND SOFTWARE AVAILABILITY

Data Resources

The raw and processed microarray data generated for this study are deposited in the gene expression omnibus (GEO) and can be found under the accession numbers GSE93712 for the original data set and GSE93711 for the validation data set.

Figure 1

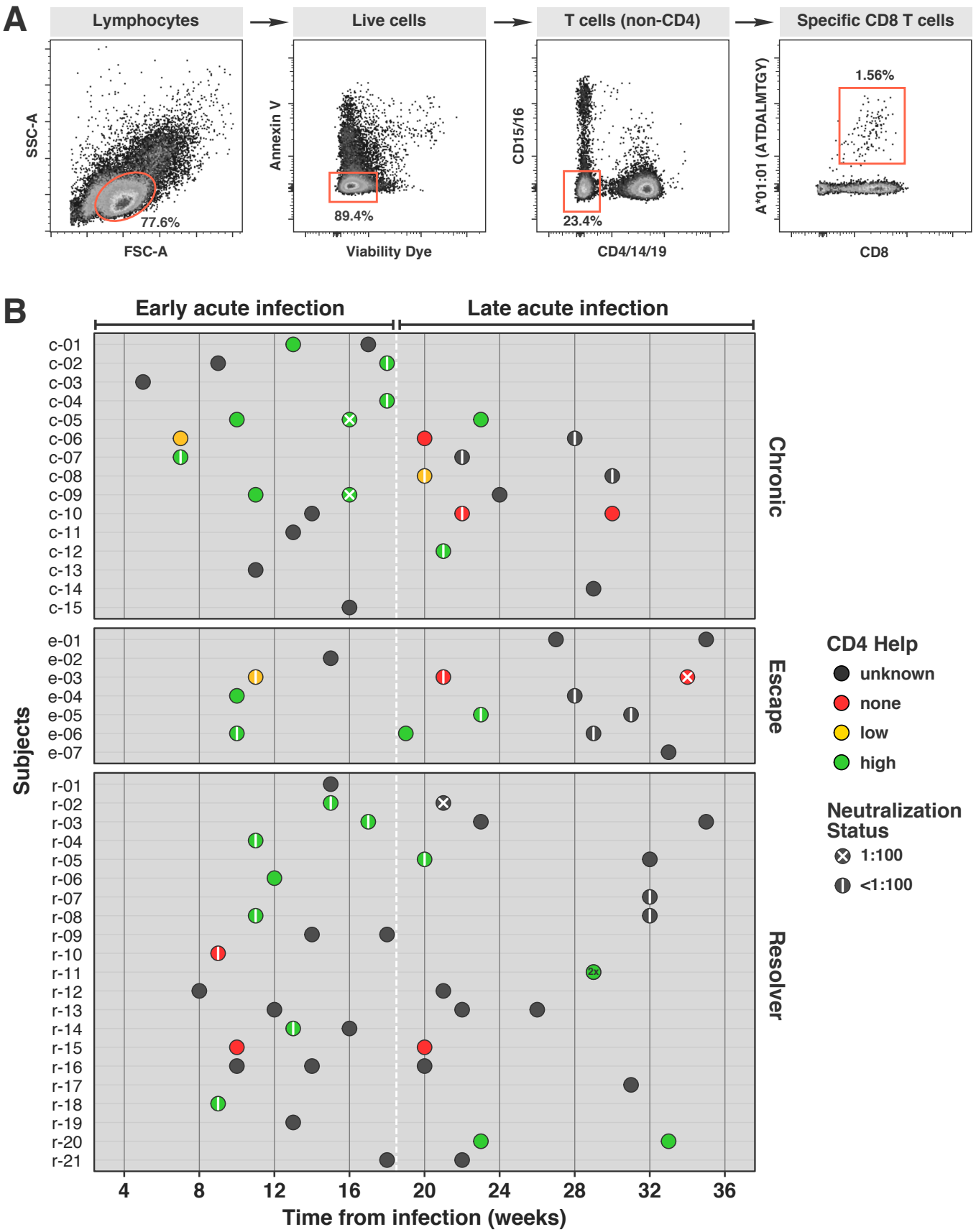
A
Lymphocytes
Live cells
T cells (non-CD4)
Specific CD8 T cells
SSC-A
FSC-A
77.6%
Annexin V
Viability Dye
89.4%
CD15/16
CD4/14/19
23.4%
A*01:01 (ATDALMTGY)
CD8
1.56%
B
Early acute infection
Late acute infection
Chronic
Escape
Resolver
Subjects
Time from infection (weeks)
CD4 Help
unknown
none
low
high
Neutralization Status
1:100
<1:100

Figure 2

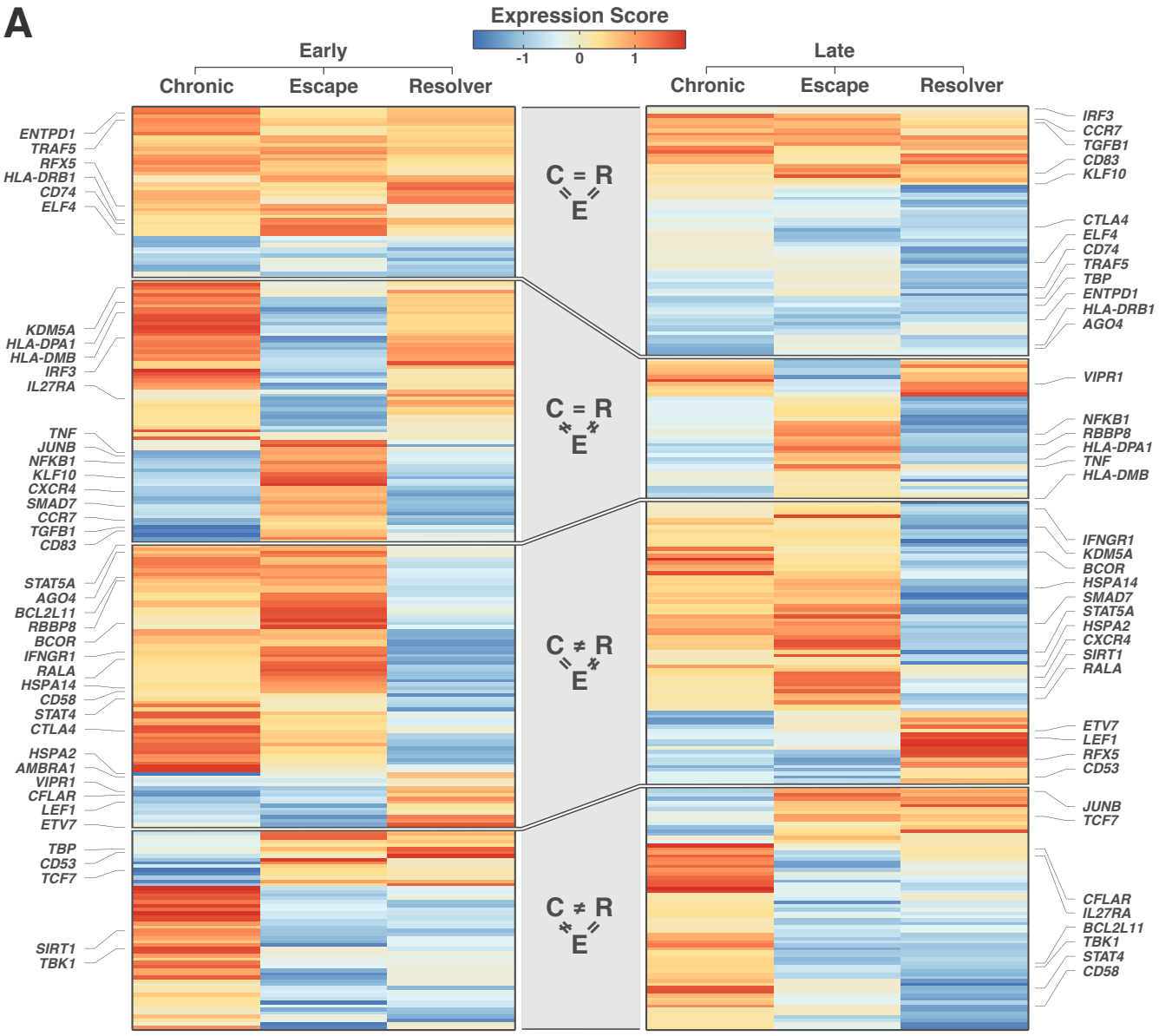
A
Expression Score
-1
0
1
Early
Chronic
Escape
Resolver
Late
Chronic
Escape
Resolver
ENTPD1
TRAF5
RFX5
HLA-DRB1
CD74
ELF4
KDM5A
HLA-DPA1
HLA-DMB
IRF3
IL27RA
TNF
JUNB
NFKB1
KLF10
CXCR4
SMAD7
CCR7
TGFB1
CD83
STAT5A
AGO4
BCL2L11
RBBP8
BCOR
IFNGR1
RALA
HSPA14
CD58
STAT4
CTLA4
HSPA2
AMBRA1
VIPR1
CFLAR
LEF1
ETV7
TBP
CD53
TCF7
SIRT1
TBK1
C = R
E
C = R
E
C ≠ R
E
C ≠ R
E
IRF3
CCR7
TGFB1
CD83
KLF10
CTLA4
ELF4
CD74
TRAF5
TBP
ENTPD1
HLA-DRB1
AGO4
VIPR1
NFKB1
RBBP8
HLA-DPA1
TNF
HLA-DMB
IFNGR1
KDM5A
BCOR
HSPA14
SMAD7
STAT5A
HSPA2
CXCR4
SIRT1
RALA
ETV7
LEF1
RFX5
CD53
JUNB
TCF7
CFLAR
IL27RA
BCL2L11
TBK1
STAT4
CD58

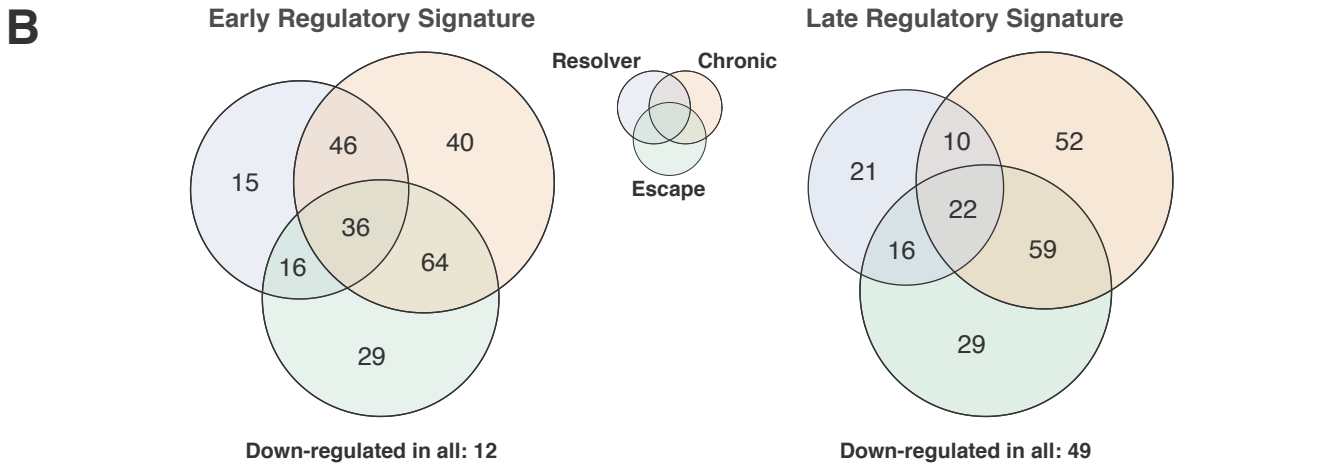
B
Early Regulatory Signature
Resolver
Chronic
Escape
15
46
40
36
16
64
29
Down-regulated in all: 12
Late Regulatory Signature
21
10
52
22
16
59
29
Down-regulated in all: 49

Figure 3

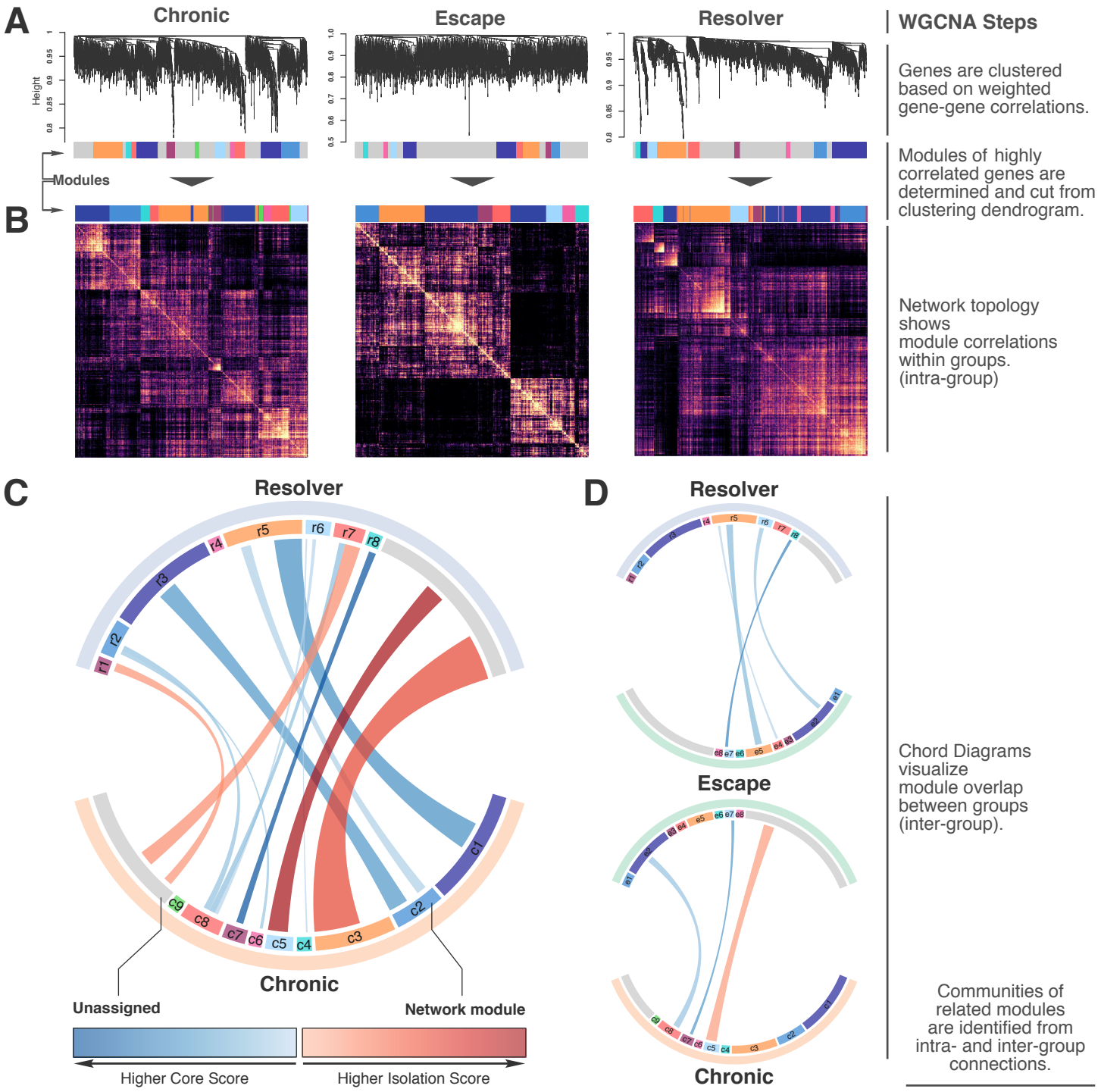
A
Chronic
Escape
Resolver
Height
Modules
B
C
Resolver
Chronic
Unassigned
Network module
Higher Core Score
Higher Isolation Score
D
Resolver
Escape
Chronic
WGCNA Steps
Genes are clustered based on weighted gene-gene correlations.
Modules of highly correlated genes are determined and cut from clustering dendrogram.
Network topology shows module correlations within groups. (intra-group)
Chord Diagrams visualize module overlap between groups (inter-group).
Communities of related modules are identified from intra- and inter-group connections.

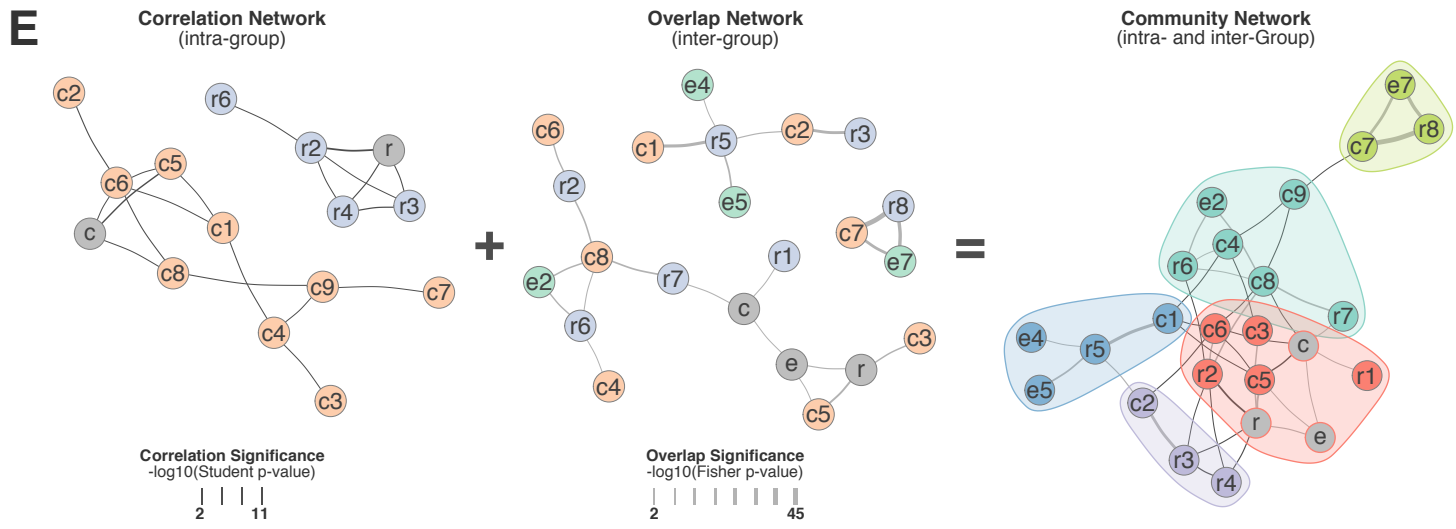
E
Correlation Network
(intra-group)
Overlap Network
(inter-group)
Community Network
(intra- and inter-Group)
Correlation Significance
-log10(Student p-value)
2
11
Overlap Significance
-log10(Fisher p-value)
2
45

Figure 4

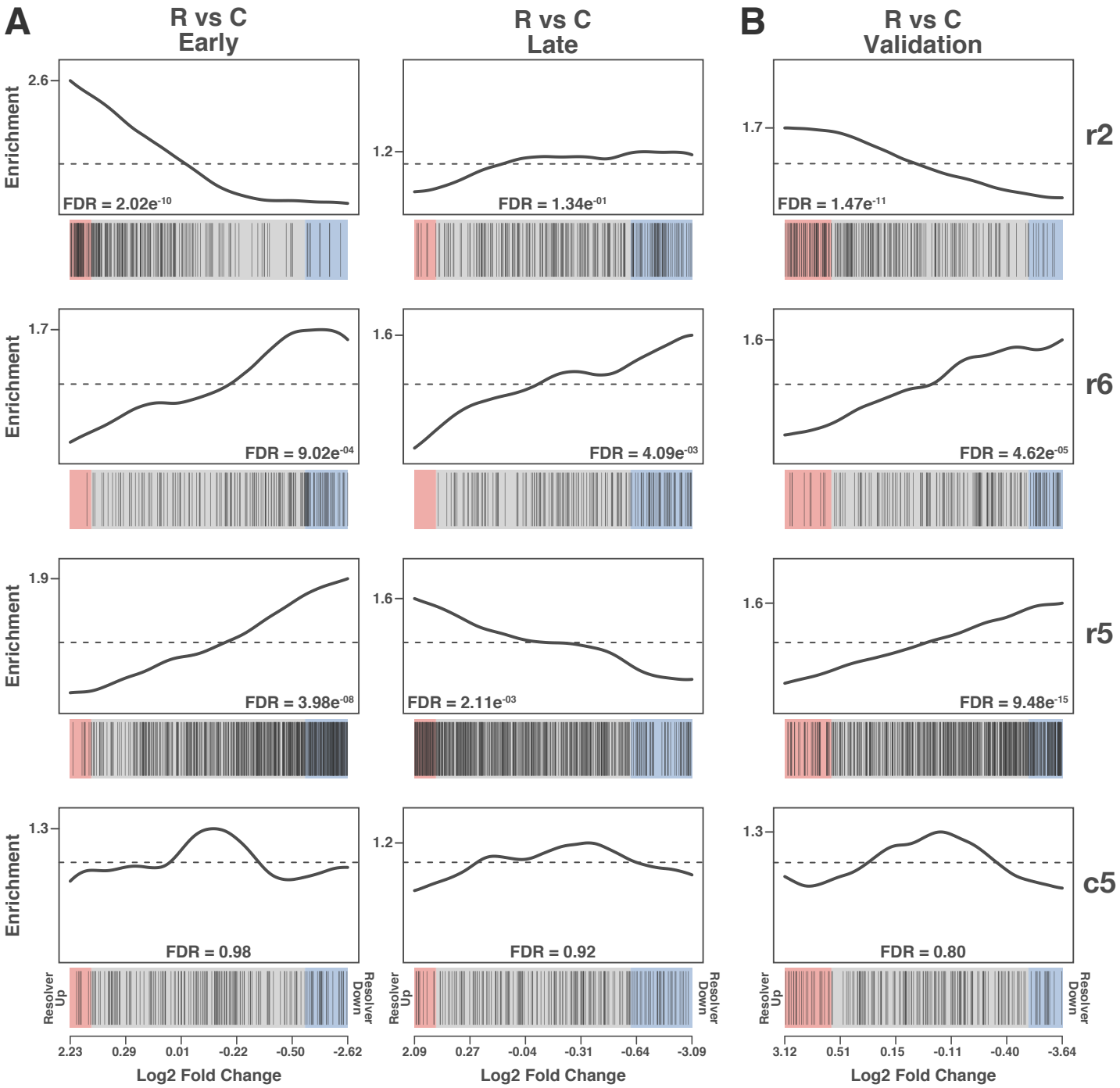
A
R vs C
Early
R vs C
Late
B
R vs C
Validation
Enrichment
2.6
1.2
1.7
r2
FDR = 2.02e-10
FDR = 1.34e-01
FDR = 1.47e-11
1.7
1.6
1.6
r6
FDR = 9.02e-04
FDR = 4.09e-03
FDR = 4.62e-05
1.9
1.6
1.6
r5
FDR = 3.98e-08
FDR = 2.11e-03
FDR = 9.48e-15
1.3
1.2
1.3
c5
FDR = 0.98
FDR = 0.92
FDR = 0.80
Resolver Up
Resolver Down
2.23 0.29 0.01 -0.22 -0.50 -2.62
2.09 0.27 -0.04 -0.31 -0.64 -3.09
3.12 0.51 0.15 -0.11 -0.40 -3.64
Log2 Fold Change

Figure 5

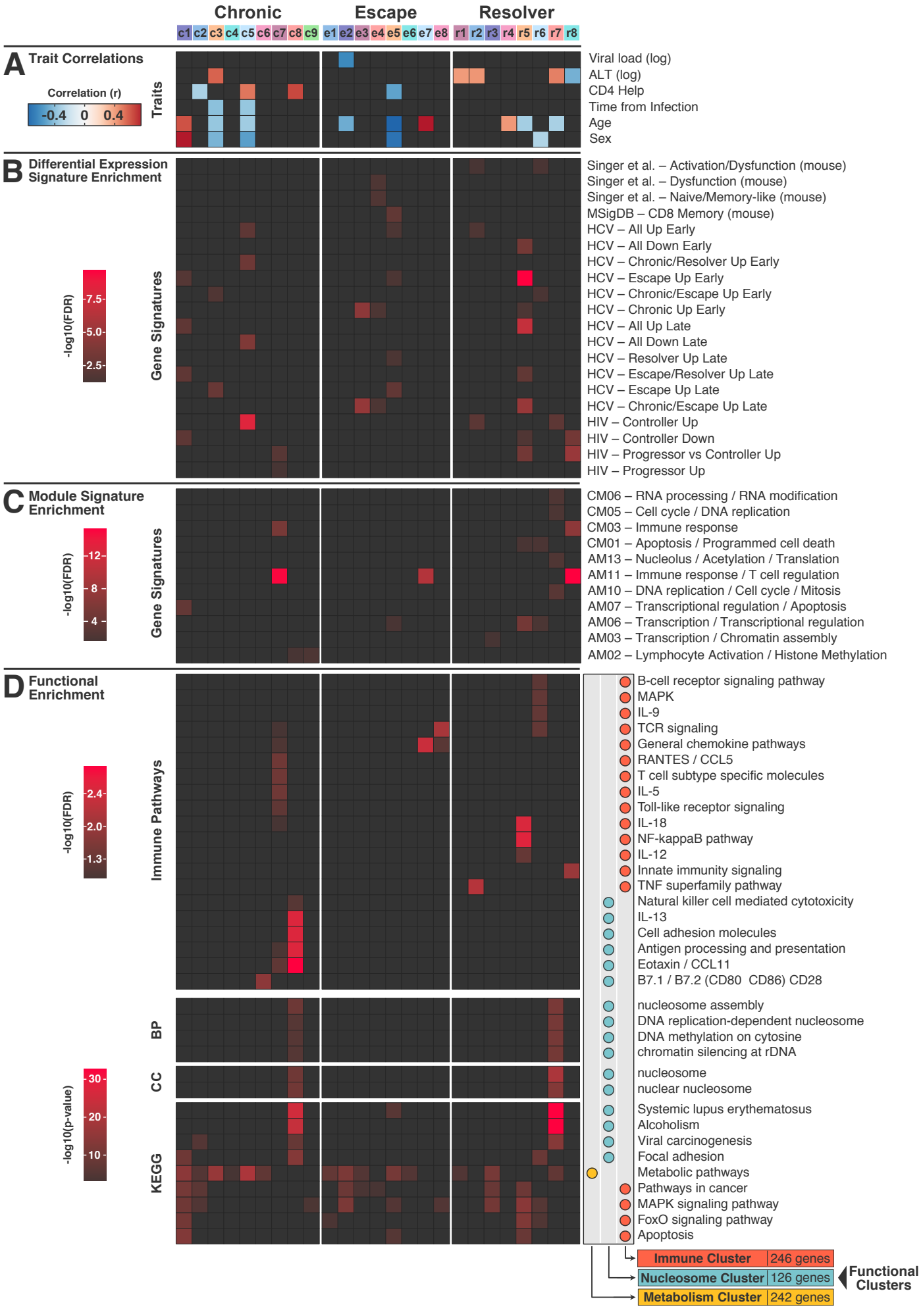
Chronic
Escape
Resolver
c1 c2 c3 c4 c5 c6 c7 c8 c9 e1 e2 e3 e4 e5 e6 e7 e8 r1 r2 r3 r4 r5 r6 r7 r8
A Trait Correlations
Correlation (r)
-0.4 0 0.4
Traits
Viral load (log)
ALT (log)
CD4 Help
Time from Infection
Age
Sex
B Differential Expression Signature Enrichment
-log10(FDR)
7.5
5.0
2.5
Gene Signatures
Singer et al. – Activation/Dysfunction (mouse)
Singer et al. – Dysfunction (mouse)
Singer et al. – Naive/Memory-like (mouse)
MSigDB – CD8 Memory (mouse)
HCV – All Up Early
HCV – All Down Early
HCV – Chronic/Resolver Up Early
HCV – Escape Up Early
HCV – Chronic/Escape Up Early
HCV – Chronic Up Early
HCV – All Up Late
HCV – All Down Late
HCV – Resolver Up Late
HCV – Escape/Resolver Up Late
HCV – Escape Up Late
HCV – Chronic/Escape Up Late
HIV – Controller Up
HIV – Controller Down
HIV – Progressor vs Controller Up
HIV – Progressor Up
C Module Signature Enrichment
-log10(FDR)
12
8
4
Gene Signatures
CM06 – RNA processing / RNA modification
CM05 – Cell cycle / DNA replication
CM03 – Immune response
CM01 – Apoptosis / Programmed cell death
AM13 – Nucleolus / Acetylation / Translation
AM11 – Immune response / T cell regulation
AM10 – DNA replication / Cell cycle / Mitosis
AM07 – Transcriptional regulation / Apoptosis
AM06 – Transcription / Transcriptional regulation
AM03 – Transcription / Chromatin assembly
AM02 – Lymphocyte Activation / Histone Methylation
D Functional Enrichment
-log10(FDR)
2.4
2.0
1.3
Immune Pathways
B-cell receptor signaling pathway
MAPK
IL-9
TCR signaling
General chemokine pathways
RANTES / CCL5
T cell subtype specific molecules
IL-5
Toll-like receptor signaling
IL-18
NF-kappaB pathway
IL-12
Innate immunity signaling
TNF superfamily pathway
Natural killer cell mediated cytotoxicity
IL-13
Cell adhesion molecules
Antigen processing and presentation
Eotaxin / CCL11
B7.1 / B7.2 (CD80 CD86) CD28
-log10(p-value)
30
20
10
BP
nucleosome assembly
DNA replication-dependent nucleosome
DNA methylation on cytosine
chromatin silencing at rDNA
CC
nucleosome
nuclear nucleosome
KEGG
Systemic lupus erythematosus
Alcoholism
Viral carcinogenesis
Focal adhesion
Metabolic pathways
Pathways in cancer
MAPK signaling pathway
FoxO signaling pathway
Apoptosis
Immune Cluster 246 genes
Nucleosome Cluster 126 genes
Metabolism Cluster 242 genes
Functional Clusters

Figure 6

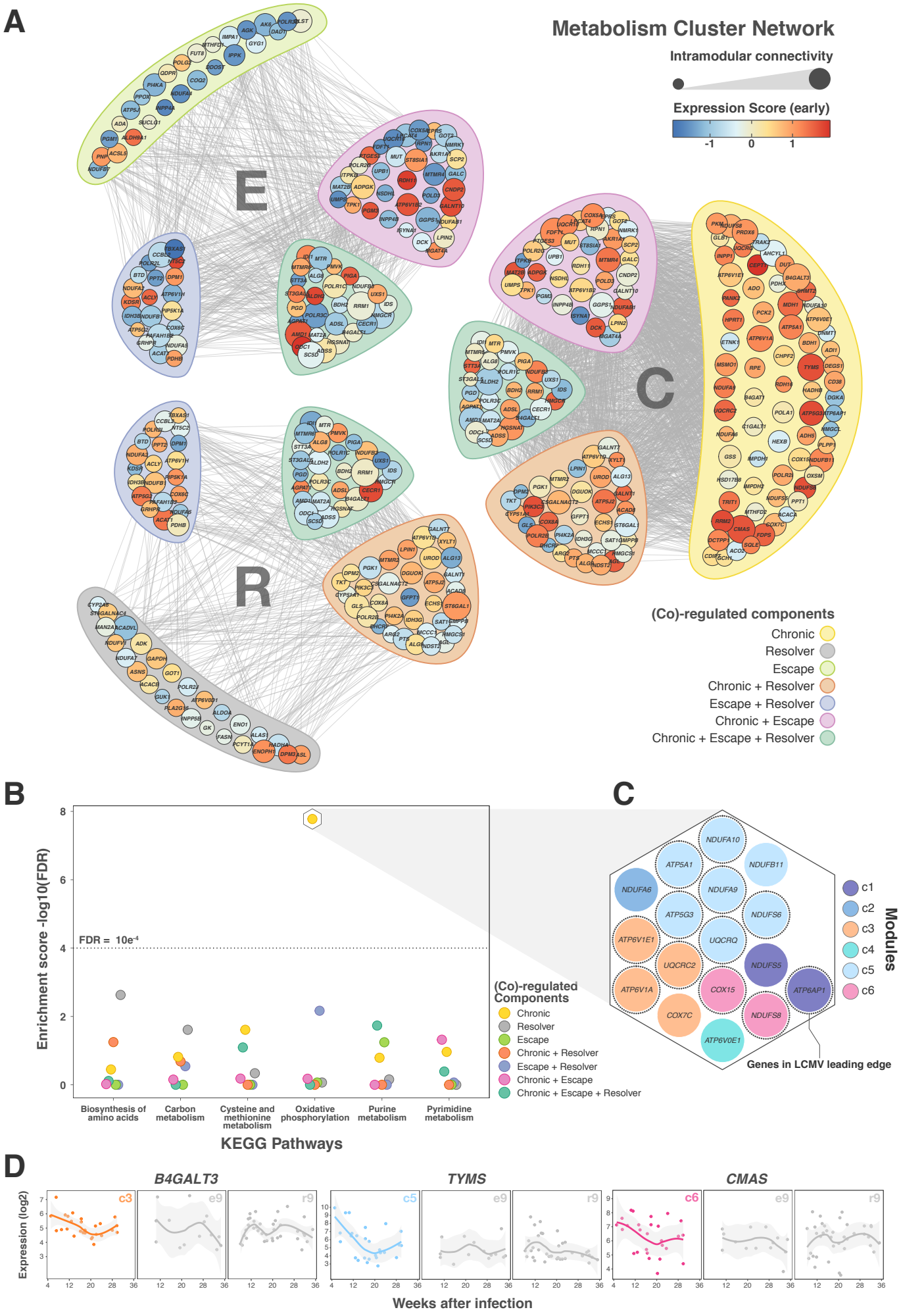
A
Metabolism Cluster Network
Intramodular connectivity
Expression Score (early)
-1
0
1
E
C
R
(Co)-regulated components
Chronic
Resolver
Escape
Chronic + Resolver
Escape + Resolver
Chronic + Escape
Chronic + Escape + Resolver
B
Enrichment score -log10(FDR)
FDR = 10e-4
Biosynthesis of amino acids
Carbon metabolism
Cysteine and methionine metabolism
Oxidative phosphorylation
Purine metabolism
Pyrimidine metabolism
KEGG Pathways
(Co)-regulated Components
Chronic
Resolver
Escape
Chronic + Resolver
Escape + Resolver
Chronic + Escape
Chronic + Escape + Resolver
C
NDUFA10
ATP5A1
NDUFB11
NDUFA6
NDUFA9
ATP5G3
NDUFS6
ATP6V1E1
UQCRQ
UQCRC2
NDUFS5
ATP6V1A
COX15
ATP6AP1
COX7C
NDUFS8
ATP6V0E1
Genes in LCMV leading edge
c1
c2
c3
c4
c5
c6
Modules
D
B4GALT3
TYMS
CMAS
Expression (log2)
c3
e9
r9
c5
e9
r9
c6
e9
r9
Weeks after infection

Figure 7

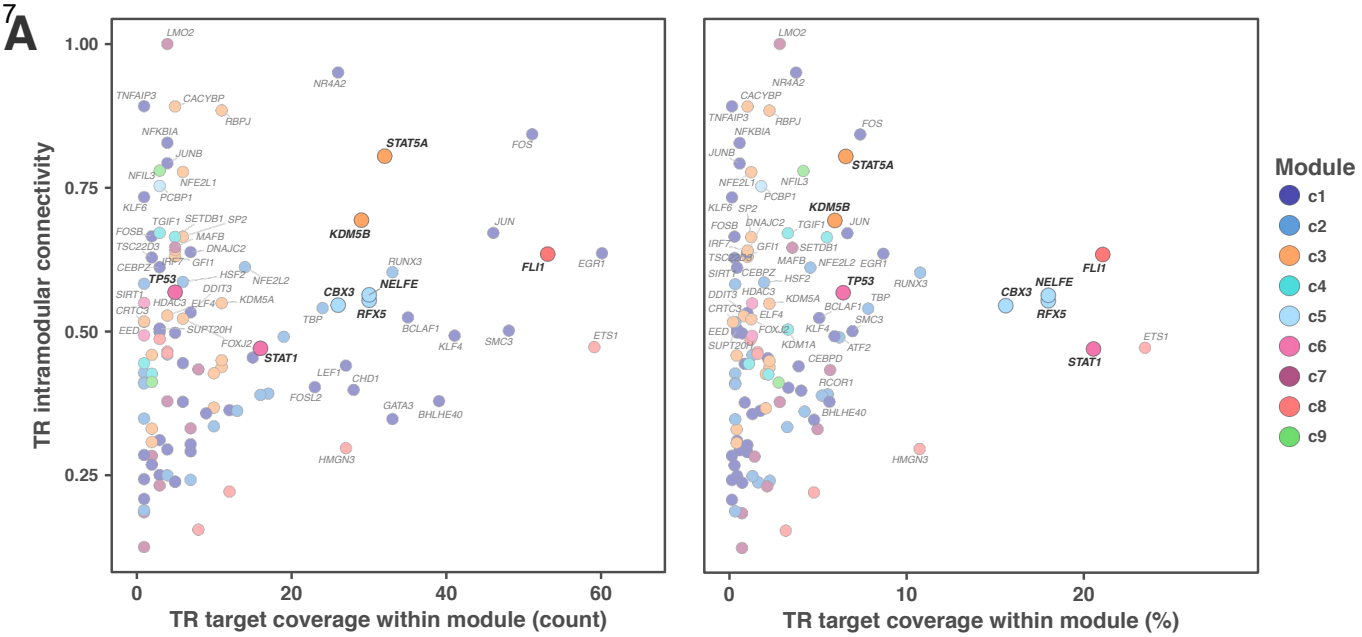
A
TR intramodular connectivity
1.00
0.75
0.50
0.25
0
20
40
60
TR target coverage within module (count)
0
10
20
TR target coverage within module (%)
Module
c1
c2
c3
c4
c5
c6
c7
c8
c9

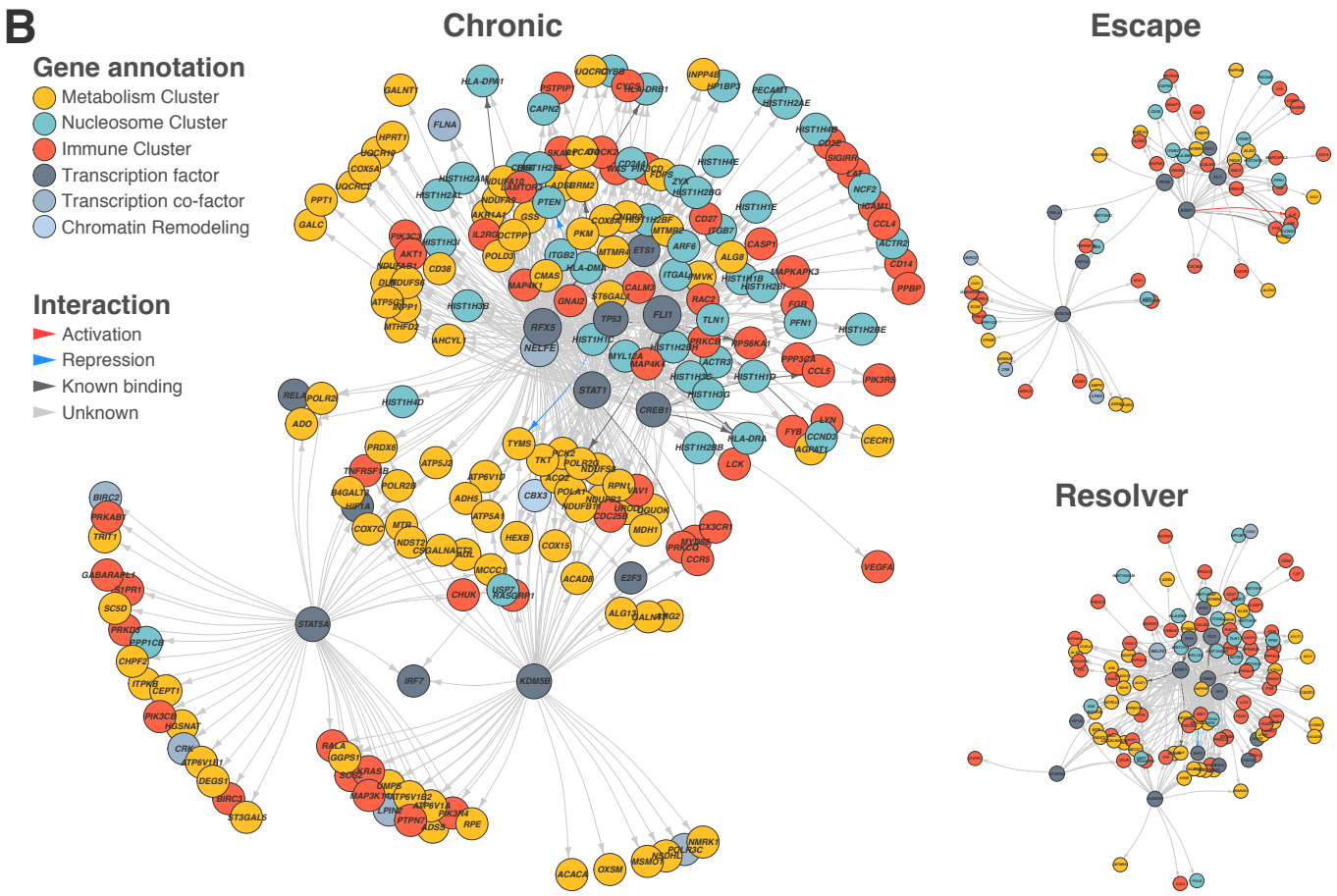
B
Chronic
Escape
Resolver
Gene annotation
Metabolism Cluster
Nucleosome Cluster
Immune Cluster
Transcription factor
Transcription co-factor
Chromatin Remodeling
Interaction
Activation
Repression
Known binding
Unknown

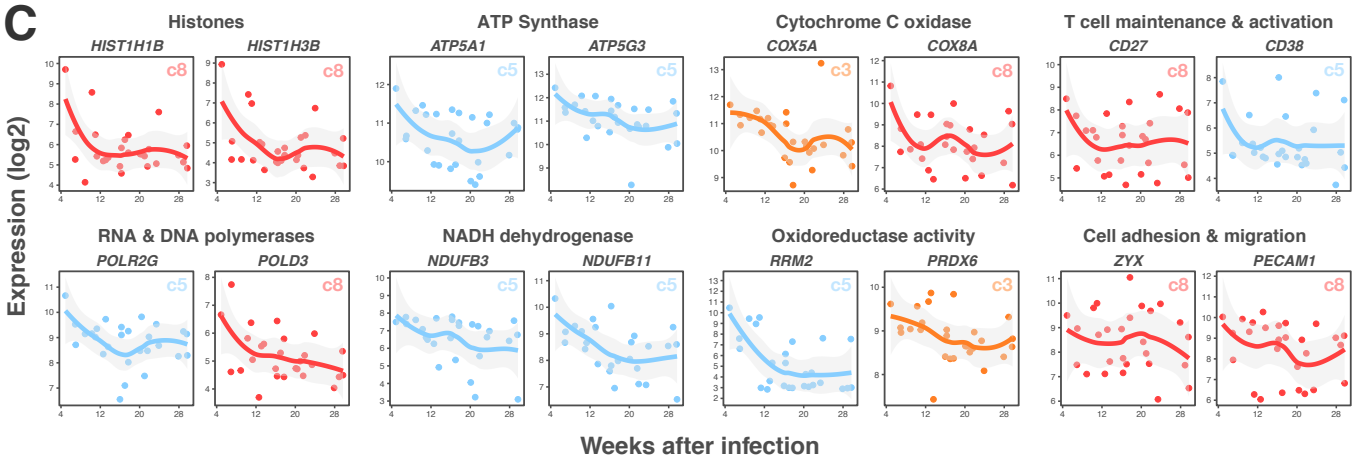
C
Histones
HIST1H1B
HIST1H3B
ATP Synthase
ATP5A1
ATP5G3
Cytochrome C oxidase
COX5A
COX8A
T cell maintenance & activation
CD27
CD38
RNA & DNA polymerases
POLR2G
POLD3
NADH dehydrogenase
NDUFB3
NDUFB11
Oxidoreductase activity
RRM2
PRDX6
Cell adhesion & migration
ZYX
PECAM1
Expression (log2)
Weeks after infection

Figure S1

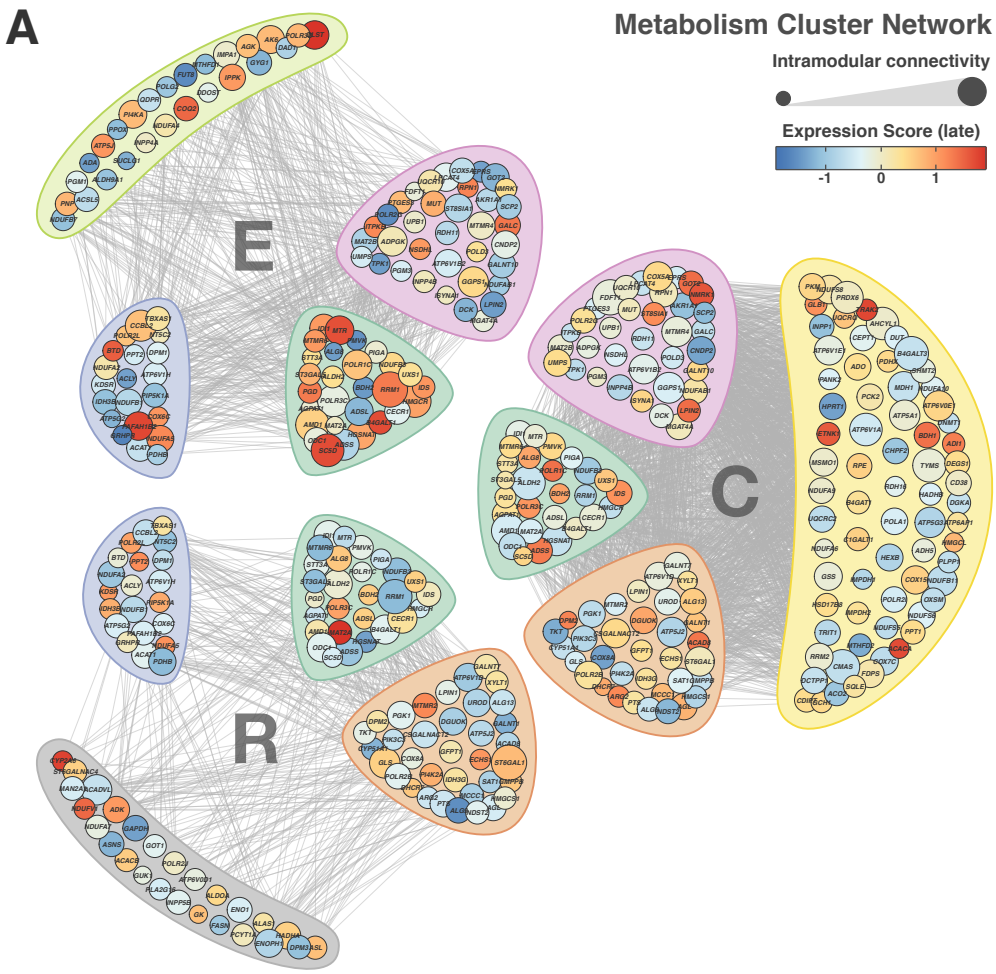
A
Metabolism Cluster Network
Intramodular connectivity
Expression Score (late)
-1
0
1
E
R
C

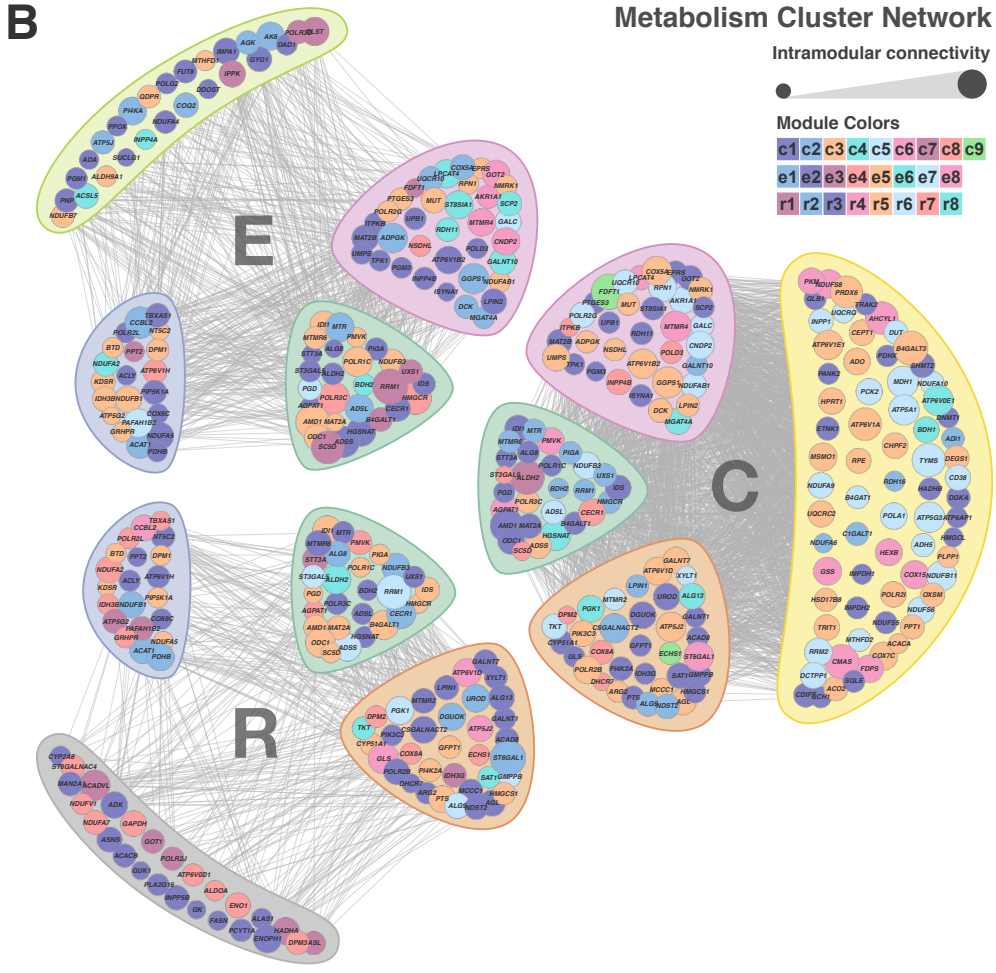
B
Metabolism Cluster Network
Intramodular connectivity
Module Colors
c1 c2 c3 c4 c5 c6 c7 c8 c9
e1 e2 e3 e4 e5 e6 e7 e8
r1 r2 r3 r4 r5 r6 r7 r8
E
R
C

Figure S2

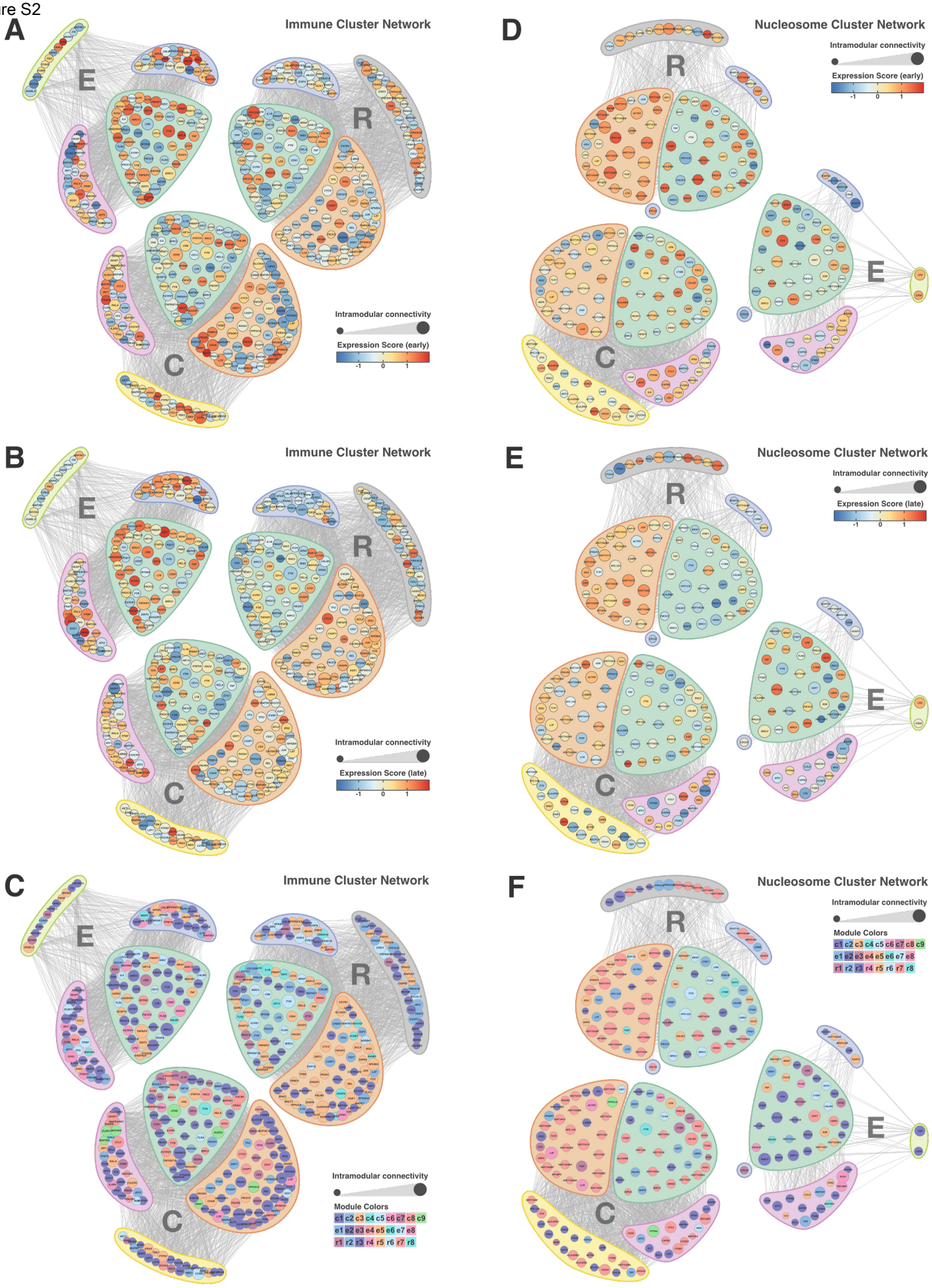
A
Immune Cluster Network
E
R
C
Intramodular connectivity
Expression Score (early)
-1
0
1
D
Nucleosome Cluster Network
Intramodular connectivity
Expression Score (early)
-1
0
1
R
E
C
B
Immune Cluster Network
E
R
C
Intramodular connectivity
Expression Score (late)
-1
0
1
E
Nucleosome Cluster Network
Intramodular connectivity
Expression Score (late)
-1
0
1
R
E
C
C
Immune Cluster Network
E
R
C
Intramodular connectivity
Module Colors
c1 c2 c3 c4 c5 c6 c7 c8 c9
e1 e2 e3 e4 e5 e6 e7 e8
r1 r2 r3 r4 r5 r6 r7 r8
F
Nucleosome Cluster Network
Intramodular connectivity
Module Colors
c1 c2 c3 c4 c5 c6 c7 c8 c9
e1 e2 e3 e4 e5 e6 e7 e8
r1 r2 r3 r4 r5 r6 r7 r8
R
E
C

Figure S3

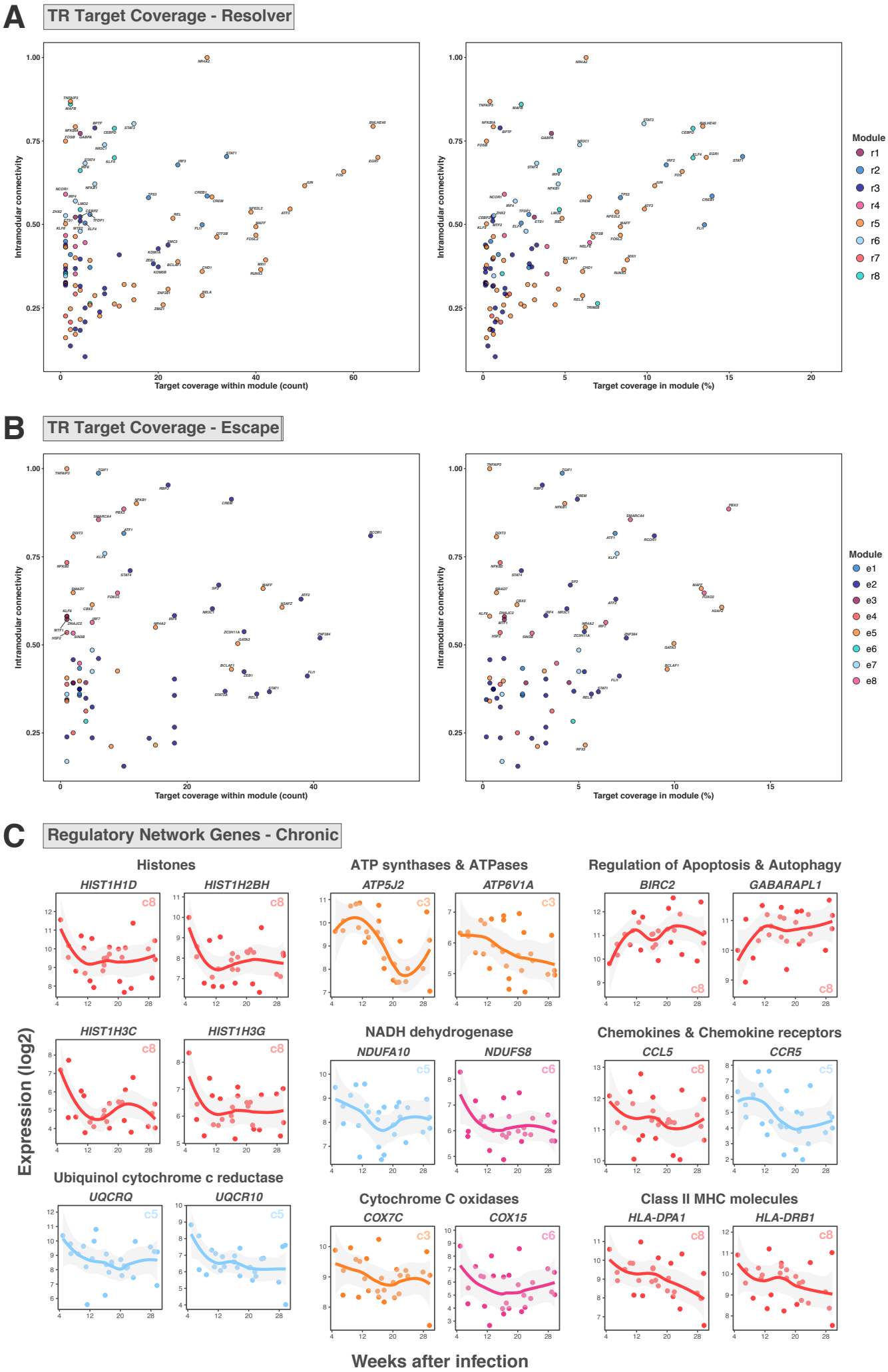
A
TR Target Coverage - Resolver
Intramodular connectivity
Target coverage within module (count)
Target coverage in module (%)
Module
r1
r2
r3
r4
r5
r6
r7
r8
B
TR Target Coverage - Escape
Intramodular connectivity
Target coverage within module (count)
Target coverage in module (%)
Module
e1
e2
e3
e4
e5
e6
e7
e8
C
Regulatory Network Genes - Chronic
Histones
HIST1H1D
HIST1H2BH
HIST1H3C
HIST1H3G
ATP synthases & ATPases
ATP5J2
ATP6V1A
Regulation of Apoptosis & Autophagy
BIRC2
GABARAPL1
NADH dehydrogenase
NDUFA10
NDUFS8
Chemokines & Chemokine receptors
CCL5
CCR5
Ubiquinol cytochrome c reductase
UQCRQ
UQCR10
Cytochrome C oxidases
COX7C
COX15
Class II MHC molecules
HLA-DPA1
HLA-DRB1
Expression (log2)
Weeks after infection

Figure S4

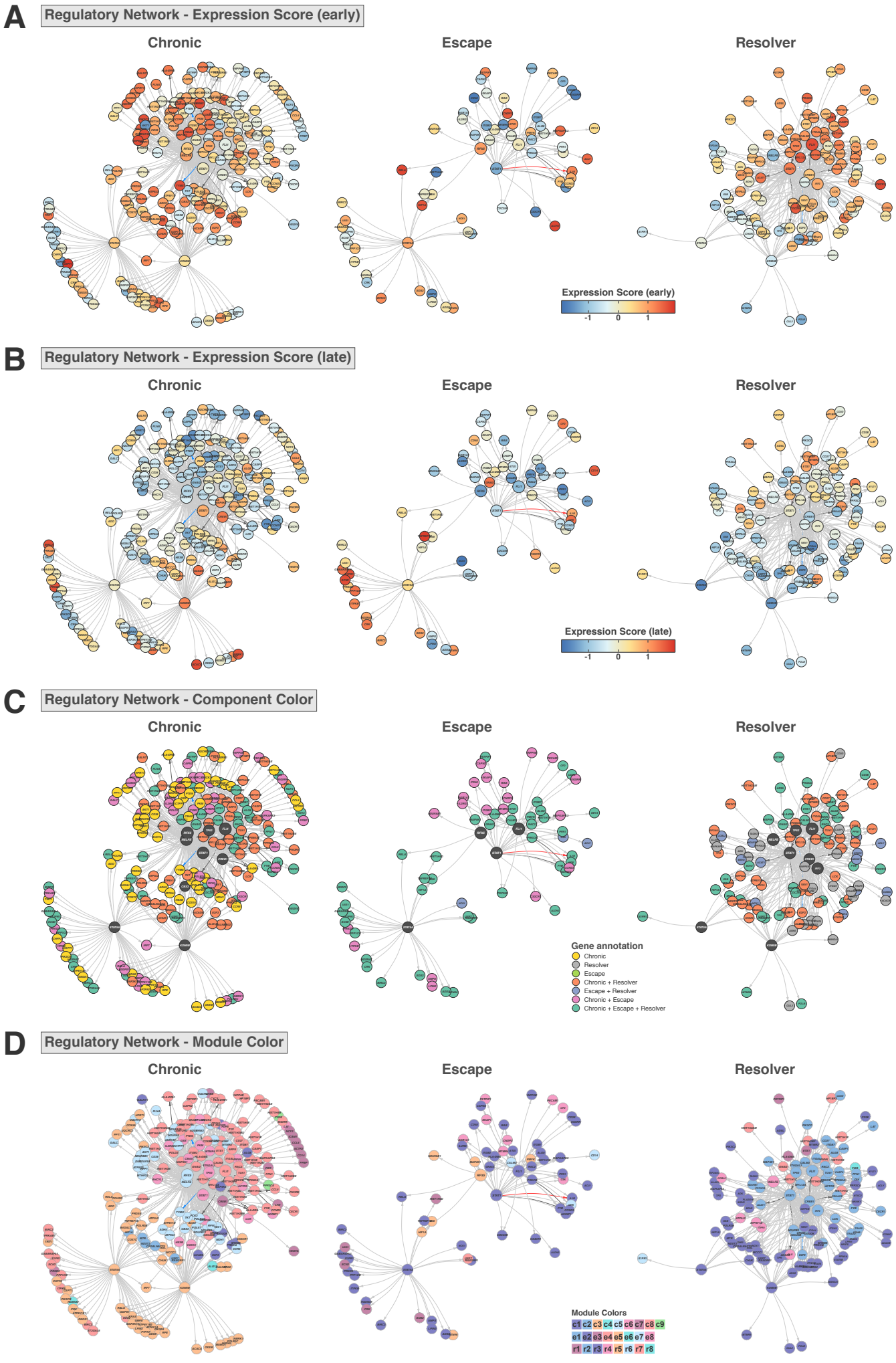
A
Regulatory Network - Expression Score (early)
Chronic
Escape
Resolver
Expression Score (early)
-1
0
1
B
Regulatory Network - Expression Score (late)
Chronic
Escape
Resolver
Expression Score (late)
-1
0
1
C
Regulatory Network - Component Color
Chronic
Escape
Resolver
Gene annotation
Chronic
Resolver
Escape
Chronic + Resolver
Escape + Resolver
Chronic + Escape
Chronic + Escape + Resolver
D
Regulatory Network - Module Color
Chronic
Escape
Resolver
Module Colors
c1 c2 c3 c4 c5 c6 c7 c8 c9
e1 e2 e3 e4 e5 e6 e7 e8
r1 r2 r3 r4 r5 r6 r7 r8

Part 2: CD39 Expression Identifies Terminally Exhausted CD8 + T Cells

Prakash K. Gupta*, Jernej Godec*, **David Wolski***, Emily Adland, Kathleen Yates, Kristen E. Pauken, Cormac Cosgrove, Carola Ledderose, Wolfgang G. Junger, Simon C. Robson, E. John Wherry, Galit Alter, Philip J. R. Goulder, Paul Klenerman, Arlene H. Sharpe, Georg M. Lauer, W. Nicholas Haining

* These authors contributed equally to this work.

PLoS Pathogens, 2015 vol. 11 (10) p. e1005177.

Introduction

The goal for this part of my thesis was a proof-of-concept experiment in a pilot cohort of 30 subjects with resolving or persistent HCV infection during the acute phase of infection to demonstrate that we could obtain high quality gene expression data using RNA extracted from small numbers of cells (on the order ~1000) of extremely rare HCV-specific CD8 T cells to identify potential gene candidates involved in T cell functionality and determination of disease outcome. The work described here was performed prior to the work outlined in Part 1 of this thesis and was the basis for its experimental design.

An unsupervised analysis of the data from the successful trial experiment (unpublished) revealed separation of cells between clinical outcomes that was associated with several different genes. In our validation efforts using a multi-color flow cytometry approach, we observed that one of the target genes, ectonucleoside triphosphate diphosphohydrolase-1 (*ENTPD1*) or CD39, was indeed expressed at higher levels in patients with persistent infection. Furthermore we showed that the enzyme, which hydrolyses nucleoside tri- and diphosphates ((A/U)TP and (A/U)DP) to monophosphates ((A/U)MP), is

catalytically active on the surface of HCV-specific CD8 T cells. CD39 expression had previously only been shown in CD4 T regulatory cells, where its enzymatic function of turning over immune-stimulatory molecules in purinergic signaling pathways is hypothesized to contribute to the inhibitory effector function in these cells (Deaglio et al., 2007).

Our follow-up experiments showed that elevated CD39 expression was also observed in chronically progressing versus controlled HIV infection, albeit less pronounced, with CD8 T cells from controlling patients expressing less CD39. We also measured CD39 expression levels targeting other chronic human viruses in control subjects (non-HIV and non-HCV), and found that both the total CD8 population as well as specific CD8 T cells for the chronically-controlled human cytomegalovirus (HCMV) and Epstein-Barr-Virus (EBV) expressed very low levels of CD39. An increasing gradient of expression along the axis of viral control, which was also correlated with HCV/HIV viral load expression levels of the co-inhibitory receptor programmed cell death protein 1 (PD-1), suggested a potential involvement of CD39 in T cell activation and dysfunction. This hypothesis is supported by the fact, that we could replicate these results in a mouse model of chronic viral infection (LCMV), where CD39 was highly expressed in exhausted CD8 T cells and correlated with a loss of effector function. Together, these data both implicate CD39 as a key player in T cell exhaustion and highlight the importance of metabolic regulation for T cell function. My contribution to the work in this publication was the initial evaluation of potential markers of T cell exhaustion by multi-color flow cytometry and all experiments that were performed on samples from HCV-infected individuals.

Results

Publication No. 1

PLOS | PATHOGENS

RESEARCH ARTICLE

CD39 Expression Identifies Terminally Exhausted CD8$^+$ T Cells

Prakash K. Gupta[1,2☯], Jernej Godec[1,3☯], David Wolski[4☯], Emily Adland[2], Kathleen Yates[1], Kristen E. Pauken[5], Cormac Cosgrove[6], Carola Ledderose[7], Wolfgang G. Junger[7], Simon C. Robson[8], E. John Wherry[5], Galit Alter[6], Philip J. R. Goulder[2], Paul Klenerman[2], Arlene H. Sharpe[3,9], Georg M. Lauer[4], W. Nicholas Haining[1,9,10]*

1 Department of Pediatric Oncology, Dana-Farber Cancer Institute, Boston, Massachusetts, United States of America, **2** Peter Medawar Building for Pathogen Research, University of Oxford, Oxford, United Kingdom, **3** Department of Microbiology and Immunobiology and Evergrande Center for Immunologic Diseases, Harvard Medical School and Brigham and Women's Hospital, Boston, Massachusetts, United States of America, **4** Gastrointestinal Unit, Massachusetts General Hospital and Harvard Medical School, Massachusetts, United States of America, **5** Department of Microbiology and Institute for Immunology, University of Pennsylvania Perelman School Medicine, Philadelphia, Pennsylvania, United States of America, **6** Ragon Institute of Massachusetts General Hospital, Harvard University and Massachusetts Institute of Technology, Cambridge, Massachusetts, United States of America, **7** Department of Surgery, Beth Israel Deaconess Medical Center, Harvard Medical School, Boston, Massachusetts, United States of America, **8** Division of Gastroenterology, Department of Medicine, Beth Israel Deaconess Medical Center, Harvard University, Boston, Massachusetts, United States of America, **9** Broad Institute of MIT and Harvard, Cambridge, Massachusetts, United States of America, **10** Division of Hematology/Oncology, Children's Hospital, Harvard Medical School, Boston, Massachusetts, United States of America

☯ These authors contributed equally to this work.
* Nicholas_Haining@dfci.harvard.edu

OPEN ACCESS

Citation: Gupta PK, Godec J, Wolski D, Adland E, Yates K, Pauken KE, et al. (2015) CD39 Expression Identifies Terminally Exhausted CD8$^+$ T Cells. PLoS Pathog 11(10): e1005177. doi:10.1371/journal.ppat.1005177

Editor: Daniel C. Douek, Vaccine Research Center, UNITED STATES

Received: June 15, 2015

Accepted: August 30, 2015

Published: October 20, 2015

Data Availability Statement: All relevant data are within the paper and its Supporting Information files. Raw microarray files are publicly available at http://www.ncbi.nlm.nih.gov/geo/query/acc.cgi?acc=GSE72752.

Funding: The author(s) received no specific funding for this work.

Competing Interests: The authors have declared that no competing interests exist.

Abstract

Exhausted T cells express multiple co-inhibitory molecules that impair their function and limit immunity to chronic viral infection. Defining novel markers of exhaustion is important both for identifying and potentially reversing T cell exhaustion. Herein, we show that the ectonucleotidse CD39 is a marker of exhausted CD8$^+$ T cells. CD8$^+$ T cells specific for HCV or HIV express high levels of CD39, but those specific for EBV and CMV do not. CD39 expressed by CD8$^+$ T cells in chronic infection is enzymatically active, co-expressed with PD-1, marks cells with a transcriptional signature of T cell exhaustion and correlates with viral load in HIV and HCV. In the mouse model of chronic Lymphocytic Choriomeningitis Virus infection, virus-specific CD8$^+$ T cells contain a population of CD39^{high} CD8$^+$ T cells that is absent in functional memory cells elicited by acute infection. This CD39^{high} CD8$^+$ T cell population is enriched for cells with the phenotypic and functional profile of terminal exhaustion. These findings provide a new marker of T cell exhaustion, and implicate the purinergic pathway in the regulation of T cell exhaustion.

Author Summary

Chronic viral infection induces an acquired state of T cell dysfunction known as exhaustion. Discovering surface markers of exhausted T cells is important for both to identify

exhausted T cells as well as to develop potential therapies. We report that the ectonucleotidase CD39 is expressed by T cells specific for chronic viral infections in humans and a mouse model, but is rare in T cells following clearance of acute infections. In the mouse model of chronic viral infection, CD39 demarcates a subpopulation of dysfunctional, exhausted CD8$^+$ T cells with the phenotype of irreversible exhaustion. CD39 expression therefore identifies terminal CD8$^+$ T cell exhaustion in mice and humans, and implicates the purinergic pathway in the regulation of exhaustion.

Introduction

In acute infections, antigen-specific T cells differentiate into activated effector cells and then into memory T cells which rapidly gain effector functions and re-expand on subsequent encounter with the same pathogen [1]. In contrast, during chronic infections, pathogen-specific T cells gradually lose effector functions, fail to expand, and can eventually become physically deleted [2]. These traits are collectively termed T cell exhaustion, and have been described both in animal models of chronic viral infection as well as in human infections with hepatitis C virus (HCV) and human immunodeficiency virus (HIV) [2–4]. Identifying reversible mechanisms of T cell exhaustion is therefore a major goal in medicine.

Prolonged or high-level expression of multiple inhibitory receptors such as PD-1, Lag3, and CD244 (2B4) is a cardinal feature of exhausted T cells in both animal models and human disease [5–7]. Expression of PD-1 appears to be a particularly important feature of exhausted CD8$^+$ T cells, as the majority of exhausted cells in mouse models of chronic infection express this receptor, and blockade of the PD-1:PD-L1 axis can restore the function of exhausted CD8$^+$ T cells in humans and mouse models [2,6]. However, in humans, many inhibitory receptors also can be expressed by a large fraction of fully functional memory CD8$^+$ T cells. PD-1, for instance, can be expressed by up to 60% of memory CD8$^+$ T cells in healthy individuals, making it challenging to use PD-1 to identify exhausted CD8$^+$ T cells in humans, particularly when the antigen-specificity of potentially exhausted CD8$^+$ T cells is not known [8].

Studies in mice and humans suggest that exhausted CD8$^+$ T cells are not a homogeneous population, but instead include at least two subpopulations of T cells that differentially express the transcription factors T-bet and Eomesodermin (Eomes) [9–11]. T-bet^{high} CD8$^+$ T cells represent a progenitor subset with proliferative potential that give rise to Eomes^{high} CD8$^+$ T cells, which are terminally differentiated and can no longer proliferate in response to antigen or be rescued by PD-1 blockade [9,12]. Both populations express PD-1, but Eomes^{high} exhausted cells express the highest levels of PD-1. However, no specific cell-surface markers of this terminally differentiated population of exhausted cells have thus far been identified.

CD39 (*ENTPD1*) is an ectonucleotidase originally identified as an activation marker on human lymphocytes and as the vascular ecto-ADPase [13], but has subsequently been shown to be a hallmark feature of regulatory T cells [14–16]. CD39 hydrolyzes extracellular ATP and ADP into adenosine monophosphate, which is then processed into adenosine by CD73, an ecto-5'-nucleotidase [17]. Adenosine is a potent immunoregulator that binds to A2A receptors expressed by lymphocytes causing accumulation of intracellular cAMP, preventing T cell activation and NK cytotoxicity [18–20]. Loss of CD39 in Tregs markedly impairs their ability to suppress T cell activation, suggesting that the juxtacrine activity of CD39 serves to negatively regulate T cell function [15]. However, blood CD8$^+$ T cells have generally been reported to be CD39$^-$ [14,21–23], and the expression of this marker on exhausted T cells has not been examined.

In this study, we demonstrate that, in contrast to CD8$^+$ T cells from healthy donors, antigen-specific CD8$^+$ T cells responding to chronic viral infection in humans and a mouse model express high levels of biochemically active CD39. CD39$^+$ CD8$^+$ T cells co-express PD-1 and are enriched for a gene signature of T cell exhaustion. In the mouse model of chronic LCMV infection, high levels of CD39 expression demarcate terminally differentiated virus-specific CD8$^+$ T cells within the pool of exhausted CD8$^+$ T cells. Thus, CD39 provides a specific, pathological marker of exhausted CD8$^+$ T cells in chronic viral infection in humans and mouse models of chronic viral infection.

Results

CD39 is expressed by CD8$^+$ T cells responding to chronic infection

We surveyed the expression of CD39 by CD8$^+$ T cells from healthy adult subjects without chronic viral infection. Consistent with previous reports we found that only a small fraction (mean 6%) of CD8$^+$ T cells in healthy individuals expressed CD39 (Fig 1A and 1B) [14,21–23]. This small population of CD39$^+$ CD8$^+$ T cells in healthy donors was primarily found in the central and effector memory compartments while virtually no naive CD8$^+$ T cells expressed CD39 (S1 Fig). We next focused on CD39 expression by antigen-specific CD8$^+$ T cells specific for latent viruses in healthy subjects and found that only a very small fraction of CMV- or EBV-specific CD8$^+$ T cells expressed CD39 (Fig 1A and 1B) (mean 3% and 7% respectively).

We next measured CD39 expression by T cells specific for the chronic viral pathogens HCV and HIV. We measured CD39 expression in 57 subjects with acute HCV infections (23 with acute resolving infection and 34 with chronically evolving infection), and in 40 subjects with HIV infection (28 chronic progressors and 12 controllers; clinical characteristics of the subjects are summarized in S1 Table). We found a mean of 51% of HCV-specific CD8$^+$ T cells and 31% of HIV-specific CD8$^+$ T cells expressed CD39, a number significantly higher than CD8$^+$ T cells specific for EBV or CMV, or in total CD8$^+$ T cell populations from healthy individuals (Fig 1A and 1B). A slightly greater fraction of virus-specific CD8$^+$ T cells from HCV-infected subjects expressed CD39 than did those from HIV-infected subjects.

In subjects with chronic infection, the frequency of CD39-expressing cells in the virus-specific (tetramer$^+$) CD8$^+$ T cell population was significantly higher than in the total CD8$^+$ T cell population (Fig 1C and 1D). However the fraction of total CD8$^+$ T cells expressing CD39 in the CD8$^+$ T cell compartment of individuals with HCV or HIV infection was slightly increased compared to healthy controls (Fig 1E), consistent with the presence of other, unmeasured virus-specific CD8$^+$ T cells that were also CD39$^+$ in the tetramer$^-$fraction of CD8$^+$ T cells. Thus CD39 is expressed infrequently by CD8$^+$ T cells in healthy donors, but marks a large fraction of pathogen-specific cells CD8$^+$ T cells in patients with chronic infection.

CD39 expressed by CD8$^+$ T cells hydrolyzes ATP

CD39 expressed by regulatory T cells catalyzes the hydrolysis of ADP to 5'-AMP [14–16] but its enzymatic activity can be regulated by a range of post-transcriptional mechanisms [PMID. We therefore tested CD39 expressed by CD8$^+$ T cells from patients infected with chronic HCV was functional using ATP hydrolysis as a surrogate marker of CD39 activity [24–26]. We sorted CD39$^-$ and CD39$^+$ CD8$^+$ T cells from six HCV-infected individuals (four with chronic infection and two with resolved infection) and incubated equal numbers of cells in the presence of extracellular ATP (eATP). Remaining levels of eATP were measured in the supernatant by HPLC. As a control, we assessed ATP hydrolysis by CD4$^+$ CD25$^+$ CD39$^+$ regulatory T cells (Tregs) sorted from the same individuals (Fig 2A).

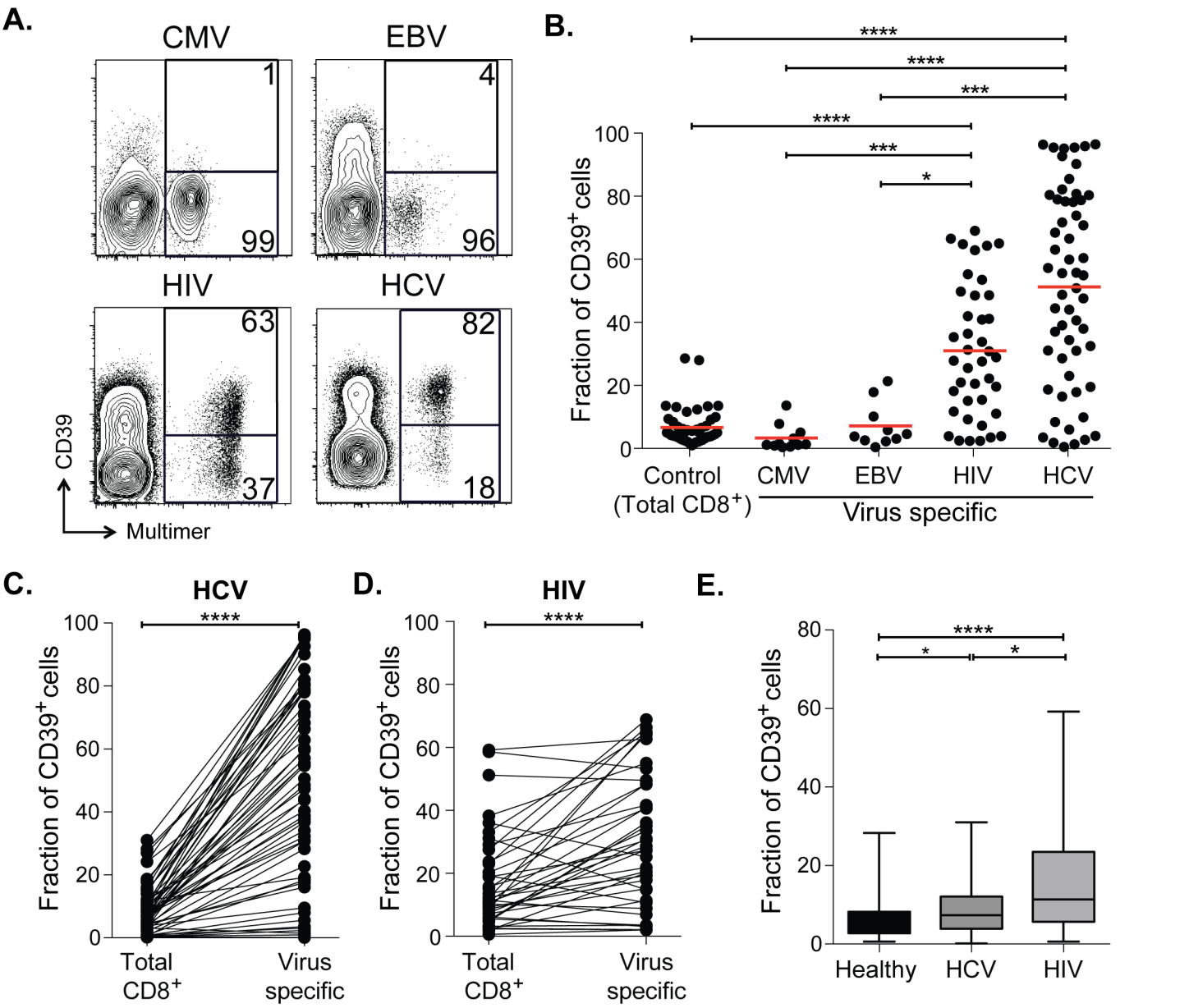

Fig 1. CD39 is highly expressed by virus-specific CD8+ T cells in chronic viral infection. (A) Expression of CD39 by virus-specific CD8+ T cells. Plots are gated on CD8+. **(B)** Fraction of total or antigen-specific CD8+ T cells expressing CD39. **(C, D)** Comparison of CD39 expression by total CD8+ T cells with virus-specific CD8+ T cells from patients with HCV (C) and HIV (D) infections. **(E)** Fraction of total CD8+ T cells expressing CD39 in healthy, HIV or HCV infected donors. Error bars represent SEM. Statistical significance was assessed by Kruskal-Wallis test (B, E), or Wilcoxon test (C, D). **P* <0.05, ****P* <0.001, *****P* <0.0001.

doi:10.1371/journal.ppat.1005177.g001

Within the CD39+ CD8+ T cell population the level of CD39 expression was lower than in Tregs (Fig 2B). Consistent with reduced CD39 expression relative to Tregs, ATP hydrolysis by CD39+ CD8+ T cells was less than that by Tregs (Fig 2C). However ATP hydrolysis by CD39+ CD8+ T cells was significantly greater than that of CD39− cells (Fig 2C). Thus CD39 expressed by CD8+ T cells in HCV infection is enzymatically active and capable of hydrolyzing ATP.

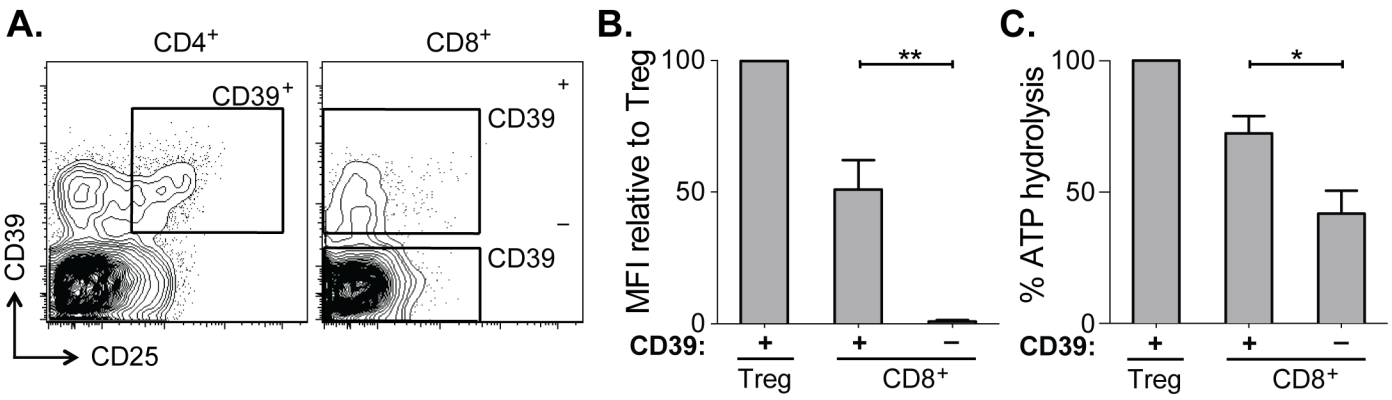

Fig 2. CD39 expressed by CD8+ T cells in HCV infection is enzymatically active. (A) Flow cytometry sorting gates of CD39+ and CD39− CD8+ T cells and CD39+ CD25+ CD4+ Tregs used for rpHPLC analysis of CD39 activity. **(B)** Summary of CD39 expression level relative to Tregs in the same subjects. **(C)** ATP hydrolysis by CD8+ T cell populations relative to Tregs. Data represent 6 patients with chronic HCV infection. Error bars represent SEM. Statistical significance was assessed by paired Student's t-test (B, C). *P <0.05, **P <0.01.

doi:10.1371/journal.ppat.1005177.g002

CD39 is co-expressed with PD-1 on virus-specific CD8+ T cells and correlates with viral load in both HCV and HIV infection

CD8+ T cells specific for chronic viruses such as HCV and HIV express increased levels of PD-1 [3,27]. We therefore examined the relationship between CD39 and PD-1 expression by virus-specific CD8+ T cells in 54 patients with HCV (23 chronically infected and 31 resolvers) and 40 patients infected with HIV (28 chronic progressors, 7 viremic controllers and 5 elite controllers). In both diseases we found a significant association between the level of expression (mean fluorescence intensity, MFI) of CD39 and PD-1 on antigen-specific CD8+ T cells in subjects with HCV and with HIV ($r = 0.70$, $P < 0.0001$ and $r = 0.54$, $P < 0.05$, respectively) (Fig 3A and 3B).

We next examined the relationship between CD39 and PD-1 expression and viral load in HCV and HIV infection. We found that in both the HCV and HIV infection there was a modest but significant correlation between viral load and the level of CD39 expression on virus-specific CD8+ T cells measured by MFI (Fig 3C). The fraction of CD39+, virus-specific CD8+ T cells was significantly higher in HIV progressors compared with those from HIV controllers (S2 Fig). A similar, but non-significant, trend was seen comparing CD39 expression in HCV-specific CD8+ T cells in patients with chronic versus resolved disease. However, in HCV, a significantly higher fraction of virus-specific CD8+ T cells co-expressed both CD39 and PD-1 in patients with chronic versus resolved disease (S2 Fig). Consistent with these findings, there was a significant correlation between viral load and the fraction of virus-specific CD8+ T cells that were CD39+ PD-1+ double positive in both HCV and HIV infection (S2 Fig). PD-1 expression was also modestly correlated with the viral load in HCV and in HIV-infected patients (Fig 3D) [3,27]. Thus CD39 expression by virus-specific CD8+ T cells is greatest in setting of high antigen burden.

Transcriptional analysis of CD39+ CD8+ T cells in HCV infection

In order to characterize more broadly the phenotype of CD39+ CD8+ T cells from individuals with chronic infection, we compared the global gene expression profiles of sorted CD39+ and CD39− CD8+ T cells from 8 HCV-infected subjects (3 with acute resolving infection and 5 with chronically evolving infection; S4 Table). Limited numbers of cells precluded the comparison of CD39+ and CD39− CD8+ T cells within HCV-specific cells, leading us to focus on the total

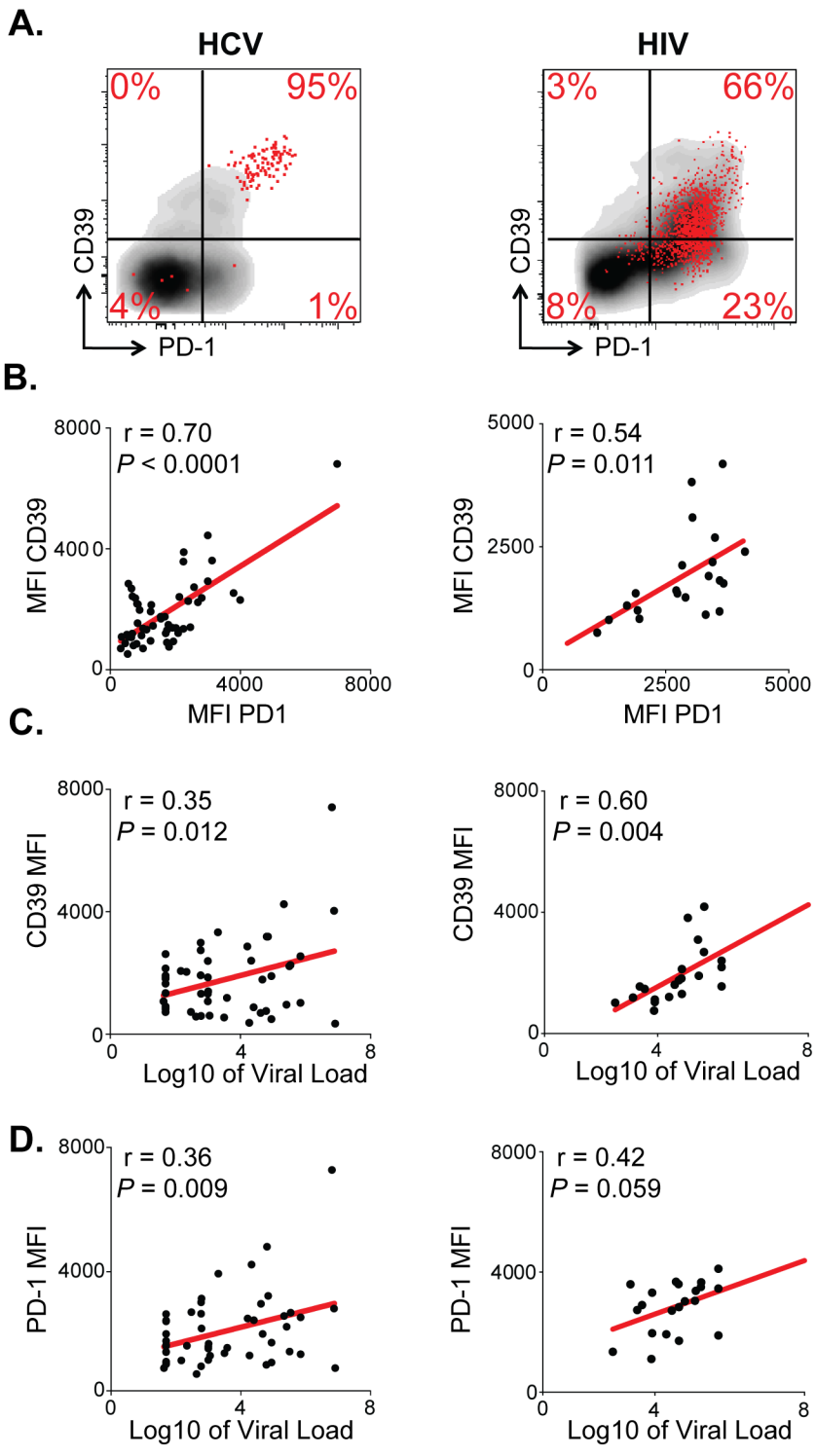

Fig 3. CD39 expression correlates with PD-1 expression and viral load in chronic viral infection. (A) CD39 and PD-1 expression in chronic HCV (left) or HIV infection (right). Representative plots demonstrate total (gray) and virus-specific (red) $CD8^+$ T cells. **(B)** Correlation between CD39 and PD-1 expression by HCV- (left) and HIV-specific (right) $CD8^+$ T cells. **(C)** Correlation between CD39 expression by virus-specific $CD8^+$ T cells and viral load count in HCV (left) or HIV (right) infection. **(D)** Correlation between PD-1 expression by virus-specific $CD8^+$ T cells and viral load in HCV (left) or HIV (right) infection. Correlation was assessed by Pearson correlation coefficient (B, C, D). MFI; mean fluorescence intensity.

doi:10.1371/journal.ppat.1005177.g003

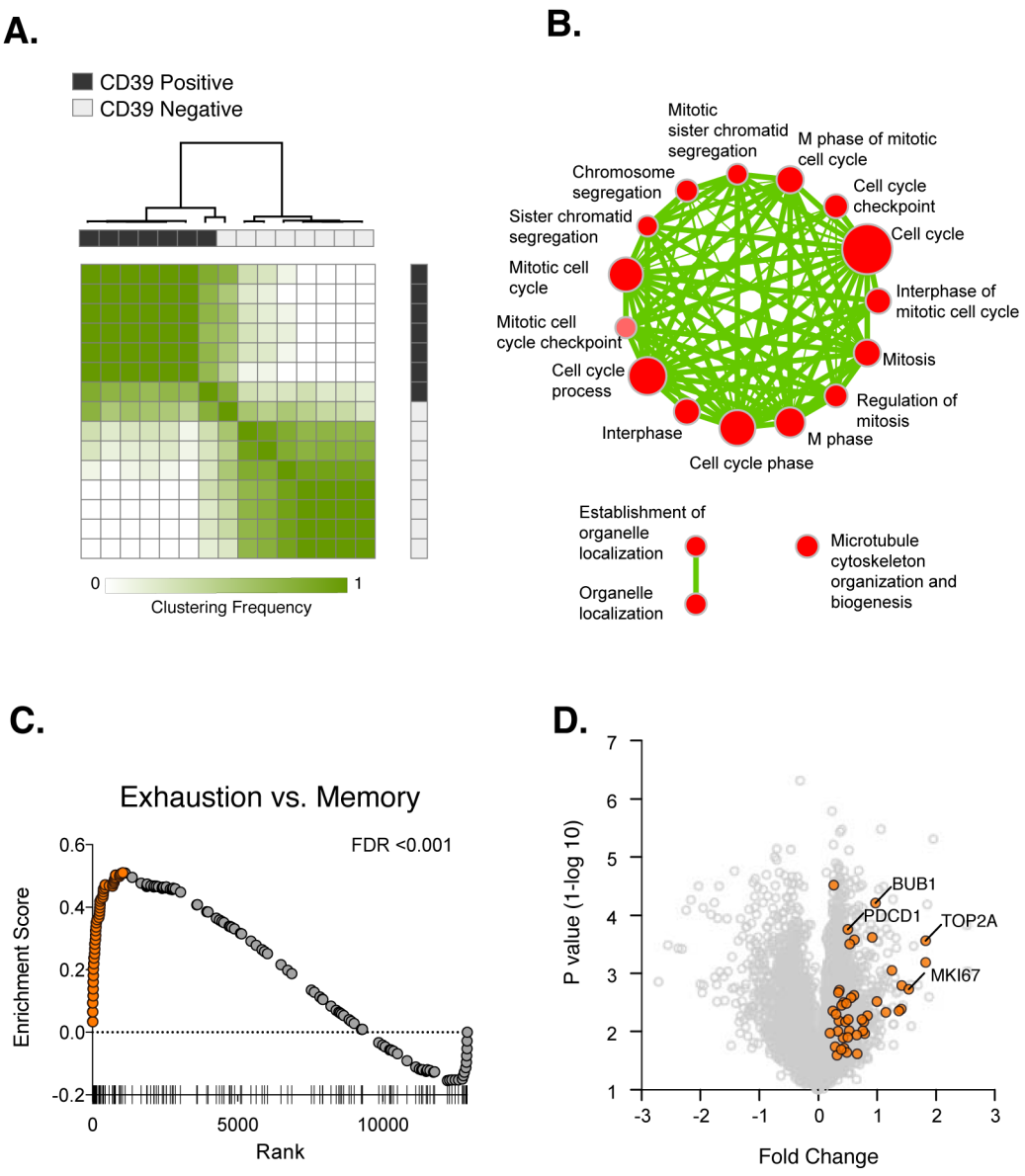

Fig 4. Transcriptional analysis of CD39$^+$ and CD39$^-$ CD8$^+$ T cells in HCV infection. (A) Consensus hierarchical clustering of expression profiles from CD39$^+$ (black) and CD39$^-$ (grey) CD8$^+$ T cells from 8 HCV infected patients. Clustering is based on the top 10% of genes by variance across the dataset. Sample similarity (1-Pearson correlation coefficient) is annotated with color from low (white) to high (green). **(B)** Gene set enrichment map displaying Gene Ontology gene sets enriched (FDR < 0.1) in CD39$^+$ CD8$^+$ T cells from (A). Nodes (in red) are sized in proportion to gene set size; connecting line thickness represents extent of gene member overlap between gene sets. **(C)** Gene set enrichment analysis of a signature of 200 genes up-regulated in exhausted CD8$^+$ T cells from the mouse model of chronic viral infection versus acute infection (day 30 post infection) in the ranked list of genes differentially expressed by CD39$^+$ vs. CD39$^-$ CD8$^+$ T cells. Leading edge genes are indicated by orange symbols. **(D)** Volcano plot of all genes (grey) or exhausted leading edge genes (orange) from (C).

doi:10.1371/journal.ppat.1005177.g004

CD8$^+$ population of antigen-experienced CD8$^+$ T cells (S4 Table). Because naive CD8$^+$ T cells express little CD39 (S1 Fig), we excluded this population from the sorted cells (S3 Fig) to enable direct comparison of antigen-experienced CD39$^+$ and CD39$^-$ CD8$^+$ T cells.

We first used unbiased clustering approaches to identify whether CD39$^+$ and CD39$^-$ CD8$^+$ T cells showed distinct patterns of gene expression. Analysis of gene expression profiles using consensus hierarchical clustering (Fig 4A) showed two distinct clusters of samples that

corresponded almost exactly to CD39$^+$ and CD39$^-$ populations, suggesting that that in both acute and chronic infection, CD39 expression demarcates two types of CD8$^+$ T cells with markedly different patterns of gene expression. Supervised analysis of differential gene expression identified 619 genes differentially expressed (FDR<0.15) between CD39$^+$ and CD39$^-$ CD8$^+$ T cells (S4 Table). Inspection of the list of differentially expressed genes revealed many with known roles in CD8$^+$ T cell biology including increased expression of the inhibitory receptors PD-1 and CTLA-4 in CD39$^+$ CD8$^+$ T cells.

To identify biological processes that were differentially active in CD39$^+$ vs. CD39$^-$ cells, we performed gene set enrichment analysis using the Gene Ontology collection of gene sets [28]. We found no significant enrichment of GO terms in the CD39$^-$ CD8$^+$ subset. In contrast, 21 gene sets significantly enriched (FDR<0.1) in CD39$^+$ population, almost all of which were related to mitosis and cell-cycle associated genes or cytoskeleton organization (Fig 4B). This suggests that CD39$^+$ CD8$^+$ T cells in chronic viral infection show coordinate up-regulation of genes related to proliferation.

The expression of CD39 by CD8$^+$ T cells in chronic but not acute/latent infection, suggests that it may be a marker of T cell exhaustion. We therefore tested whether the profile of CD39$^+$ CD8$^+$ T cells was enriched for genes expressed by exhausted CD8$^+$ cells. Previous studies of gene expression in CD8$^+$ T cells in the mouse model of chronic viral infection with the Clone 13 strain of LCMV have identified signatures of T cell exhaustion that are also enriched in exhausted CD8$^+$ T cells in humans [29–31]. We therefore curated a signature of 200 genes up-regulated by exhausted CD8$^+$ T cells responding to chronic infection relative to functional memory CD8$^+$ T cells generated by acute infection (LCMV Armstrong strain). We found that the exhausted CD8$^+$ T cell signature from LCMV model was significantly enriched in CD39$^+$ vs. CD39$^-$ CD8$^+$ T cells in subjects with HCV infection (Fig 4C). We focused on the "leading edge" genes contributing most to the enrichment [32], which correspond to genes up-regulated both in the mouse exhausted signature and in the human CD39$^+$ profile. As expected, the leading edge genes included PD-1 (*PDCD1*), a feature of both human CD39$^+$ CD8$^+$ T cells and of exhausted CD8$^+$ T cells in the mouse model (Fig 4D). In addition we found that up-regulation of many genes associated with proliferation including *BUB1*, *TOP2A* and *MKI67* was common to mouse exhausted CD8$^+$ T cells and human CD39$^+$ CD8$^+$ T cells. Thus CD39$^+$ CD8$^+$ T cells in HCV infection and exhausted CD8$^+$ T cells in a mouse model of chronic infection share transcriptional features that include genes related to proliferation.

CD39 is increased in exhausted CD8$^+$ T cells in the mouse model of chronic LCMV infection

Because the mouse signature of CD8$^+$ T cell exhaustion was significantly enriched in the transcriptional profile of CD39$^+$ CD8$^+$ T cells in HCV-infected patients, we next asked if CD39 was up-regulated by CD8$^+$ T cells in the mouse model of chronic viral infection. To address this question we compared two well-described mouse models of viral infection using two strains of LCMV: LCMV Armstrong that causes an acute infection that is resolved in up to 8 days; and LCMV Clone 13 that persists in mice for up to 3 months and leads to T cell exhaustion [5,6].

We measured CD39 expression and compared it to PD-1 expression in CD8$^+$ T cells responding to each infection. While naive CD8$^+$ T cells expressed neither CD39 nor PD-1 (Fig 5A), both were rapidly and coordinately up-regulated by antigen-experienced cells following either infection (day 7 post infection [d7 p.i.], Fig 5B). However, in acute infection, the fraction of CD39 bright PD-1$^+$ population decreased with time. In contrast, high expression of CD39 and PD-1 was maintained in Clone 13 infection. The accumulation of CD39 bright PD-1$^+$ cells

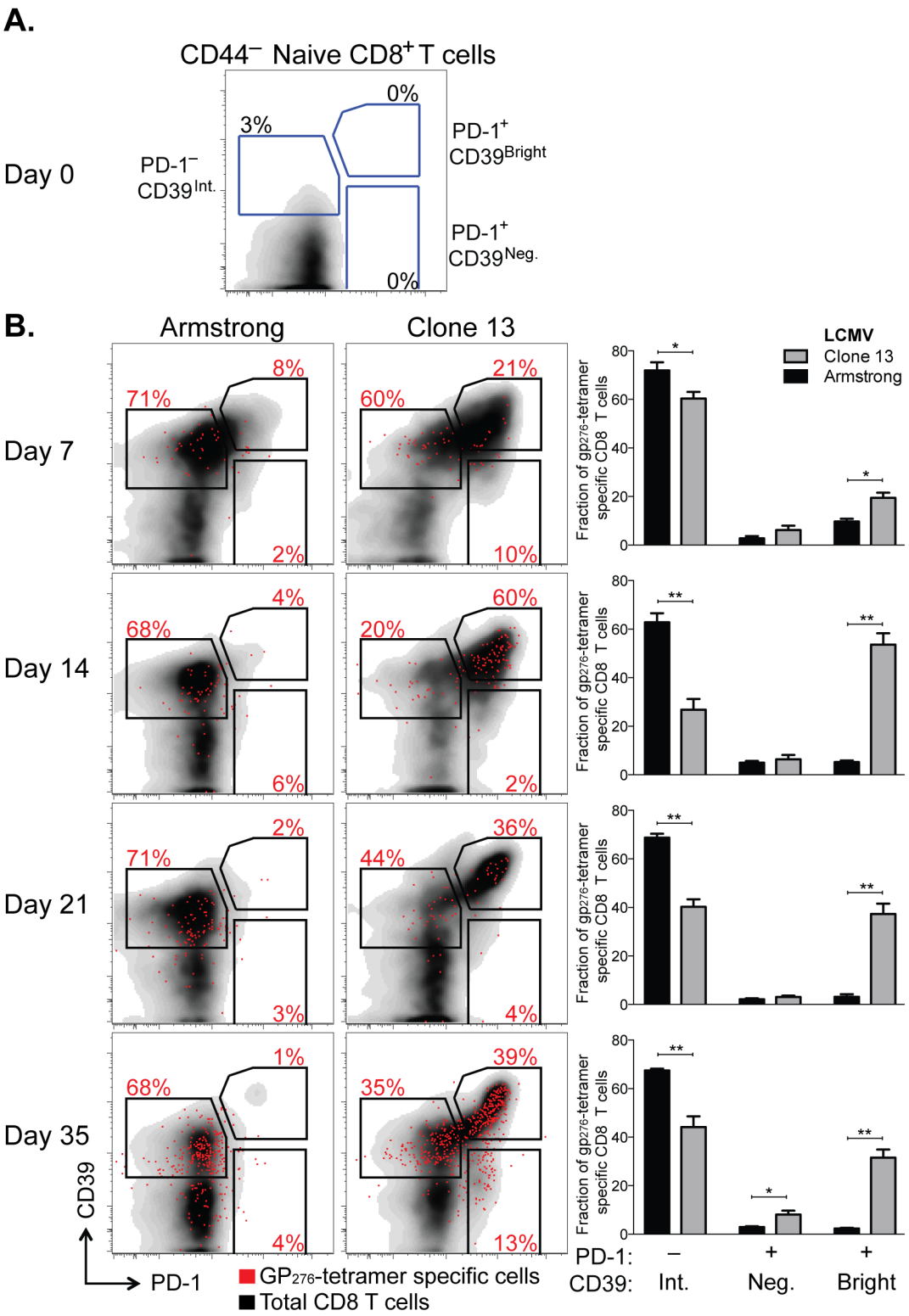

Fig 5. CD39 is highly up-regulated by exhausted CD8+ T cells in a mouse model of chronic infection. (**A, B**) Expression of CD39 and PD-1 by CD44− naive mouse CD8+ T cells (A) and in CD8+ T cells at indicated times following LCMV Armstrong (acute) or Clone 13 (chronic) infection (B). Representative plots show total (black) and H-2Db $GP_{276-286}$ tetramer-specific CD8+ T cells (red). Summary of results in 5 mice per group is shown in bar-graphs on the right. Statistical significance was assessed with Mann-Whitney test. *$P < 0.5$, **$P < 0.01$.

doi:10.1371/journal.ppat.1005177.g005

among the total CD8$^+$ population was most apparent in the H-2D^b GP$_{276-286}$ tetramer-specific CD8$^+$ T cells (Fig 5B).

Thus after chronic viral infection, antigen-specific CD8$^+$ T cells can be identified by high expression of both CD39 and PD-1. This difference in expression of both markers between chronic and acute infection is noticeable as early as d7 p.i. but becomes more pronounced with time after infection.

CD39 expression correlates with a terminally exhausted phenotype in virus-specific CD8$^+$ T cells in chronic infection

Having determined that high, persistent expression of CD39 is a feature of LCMV-specific CD8$^+$ T cells during chronic LCMV infection, we next sought to further characterize the phenotype of CD39$^+$ CD8$^+$ T cells during Clone 13 infection. We analyzed CD39 expression in antigen-experienced, CD44$^+$ CD8$^+$ T cells and found that mice infected with Clone 13 developed a population of cells with particularly high expression of CD39 (CD39^{high}). This population was entirely absent in mice infected with the acute LCMV Armstrong strain at d35 p.i., which only exhibited the presence of intermediate levels of CD39 staining (CD39^{int}) (Fig 6A). Further characterization of the two sub-populations in Clone 13 infected mice revealed that the CD39^{high} cells showed more down-regulation of CD127 (Fig 6B) and higher expression of PD-1 (Fig 6C) than did the CD39^{int} population.

Because the highest levels of PD-1 are characteristic of terminally exhausted CD8$^+$ T cells in chronic infection [12,33], we tested whether CD39^{high} T cells in chronic infection showed other phenotypic characteristics of terminal exhaustion. Analysis of expression of two additional co-inhibitory receptors, CD244 (2B4) and Lag3, showed that a significantly higher fraction of CD39^{high} cells co-expressed multiple receptors, consistent with terminal exhaustion. In contrast, CD39^{int} CD8$^+$ T cells were generally negative for all three receptors analyzed (Fig 6D and 6E). We next examined the expression of the transcription factors T-bet and Eomes. We found that the CD39^{high} subset of CD8$^+$ T cells was comprised primarily of Eomes^{high} T-bet^{low} terminally exhausted phenotype, while the CD39^{int} CD8$^+$ T cells showed a comparable distribution of both (Fig 6F). Similarly, we found that in CD8$^+$ T cells from subjects with either HCV or HIV infection, the CD39$^+$ CD8$^+$ T cell compartment contained a significantly higher ratio of Eomes^{high} T-bet^{low}: Eomes^{low} T-bet^{high} relative to CD39$^-$ CD8$^+$ T cells (S4 Fig). Thus in both humans and mice with chronic viral infection, CD39$^+$ CD8$^+$ T cells show a phenotype consistent with previous descriptions of terminal exhaustion [9].

CD39 correlates with reduced functionality in virus-specific CD8$^+$ T cells in chronic infection

We next examined the functional properties of CD39^{high} and CD39^{int} CD8$^+$ T cells from mice with chronic LCMV infection. Co-production of cytokines IFN-γ and TNFα is a feature of virus-specific T cells responding to acute infection and in the early stages of chronic infection but is progressively lost as exhaustion evolves [2]. To compare the functionality of CD39^{high} and CD39^{int} virus-specific CD8$^+$ T cells, we isolated CD8$^+$ T cells from mice with chronic infection at d35 post-infection and stained for IFN-γ and TNFα following in vitro stimulation with GP$_{33-41}$ peptide. We found a significantly smaller fraction of antigen-specific coproduced IFN-γ and TNFα in CD39^{high} CD8$^+$ T cells compared to CD39^{int} CD8$^+$ T cells (Fig 7A and 7B).

To confirm this finding, we analyzed the function of transferred P14 CD8$^+$ T cells in chronic infection. The P14 TCR transgene recognizes the GP$_{33-41}$ peptide of LCMV presented on H-2D^b. We found that both the frequency of IFN-γ-producing and IFN-γ/TNFα co-producing

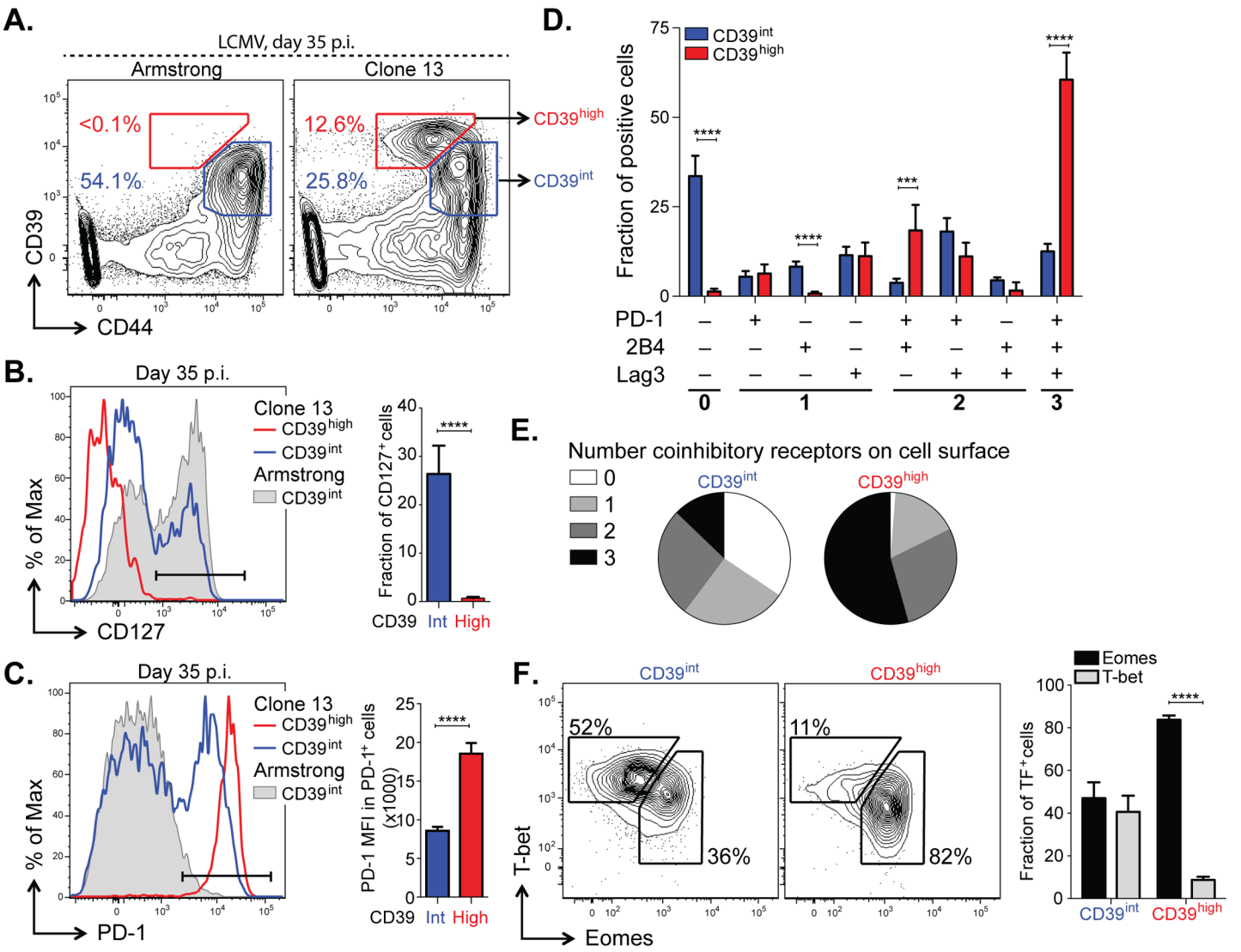

Fig 6. CD39 identifies terminally exhausted CD8+ T cells in mice with chronic LCMV infection. (**A**) Expression of CD39 and CD44+ by mouse CD8+ T cells 30–35 days following LCMV Armstrong (left) or Clone 13 (right) infection. (**B**, **C**) Representative histograms (left) of CD127 (B) and PD-1 (C) expression by CD39^{high} and CD39^{int} CD8+ T cells from Clone 13 (red and blue, respectively) and CD39^{int} from Armstrong (filled gray) infected mice on d35 p.i. (left). Fraction of CD127+ (B) and MFI of PD-1 in PD-1+ cells (C) is shown on the right. Results are from 5 mice. (**D**) Fraction of CD39^{high} and CD39^{int} CD44+ CD8+ T cells expressing different combinations of co-inhibitory receptors PD-1, 2B4, and Lag3. (**E**) Average number of co-inhibitory receptors expressed by CD39^{int} (left) or CD39^{high} (right) CD8+ T cells at d35 p.i. following LCMV Clone 13 infection. (**F**) Representative plots of T-bet and Eomes expression in CD39^{int} (left) and CD39^{high} (right) cells as in (A). Summary of results is shown on the right. Data are representative of three experiments of 5 mice per group. Statistical significance was assessed with Student's t-test (B, C, F) with Holm-Sidak multiple comparison correction (D). $^{**}P < 0.01$, $^{****}P < 0.0001$.

doi:10.1371/journal.ppat.1005177.g006

P14 T cells was significantly lower in CD39^{high} CD8+ T cells compared to CD39^{int} CD8+ T cells (Fig 7C and 7D). The defect in cytokine secretion was not only observed in terms of the frequency of cytokine-secreting cells, but also in the amount of cytokine detected per cell. Even among cells that did secrete IFN-γ, we found the MFI of expression to be significantly lower in CD39^{high} CD8+ T cells compared to CD39^{int} CD8+ T cells (Fig 7E and 7F). Thus high levels of CD39 expression demarcate a population of exhausted cells with the poorest function in chronic infection.

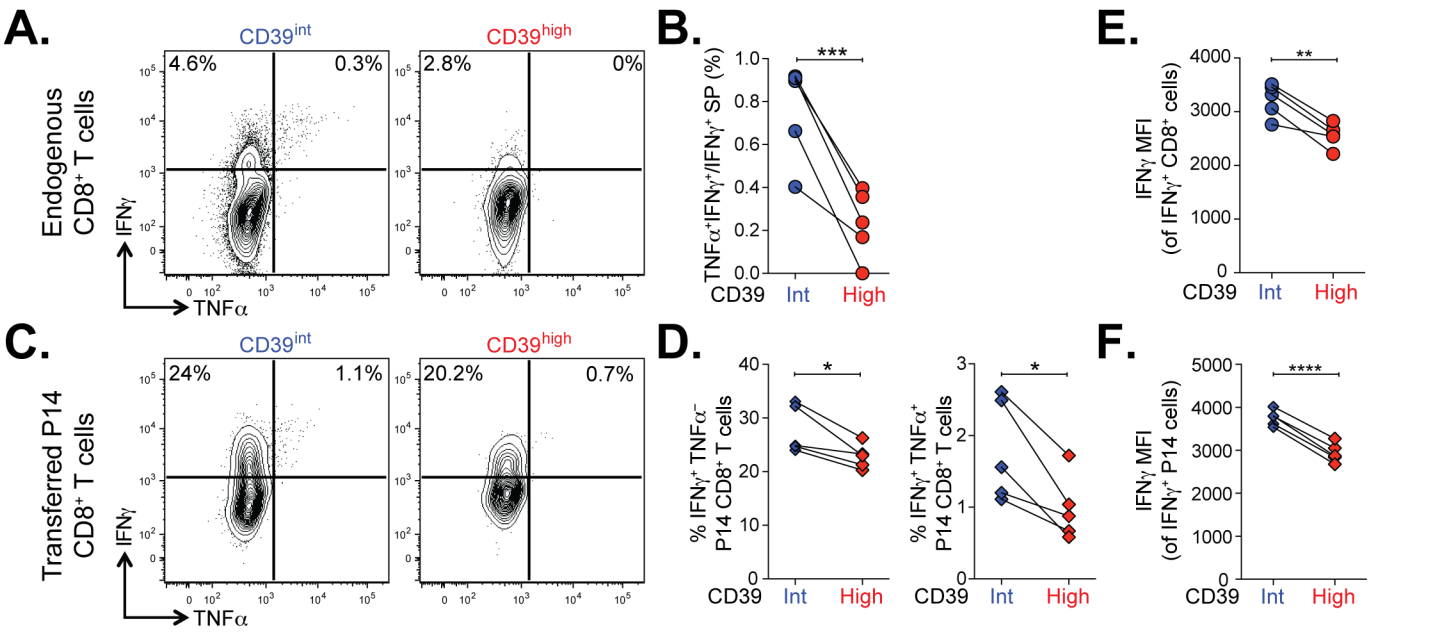

Fig 7. Terminally exhausted CD8+ T cells marked by high levels of CD39 are most impaired in their effector function. (**A**) Representative plots showing the production of IFN-γ and TNFα in CD39^{int} or CD39^{high} CD8+ T cells 36 days following LCMV Clone 13 infection. (**B**) Quantification of cells in (A) that produce both TNFα and IFN-γ relative to IFN-γ only. (**C, D**) Cytokine production by P14 cells (C) gated from an infection as in (A) and summary of IFN-γ and TNFα producing cells. (**E, F**) Mean fluorescence intensity (MFI) of IFN-γ in IFN-γ positive endogenous (E) and transferred P14 cells (F). Statistical significance was assessed with paired Student's t-test. *$P < 0.05$, **$P < 0.01$, ***$P < 0.001$, ****$P < 0.0001$.

doi:10.1371/journal.ppat.1005177.g007

Discussion

The state of CD8+ T cell exhaustion is characterized by widespread changes in gene expression relative to functional memory CD8+ T cells [5]. However, in humans, identification of specific T cell exhaustion markers that are not shared by more functional CD8+ T cell populations has been challenging [8]. We show that high-level expression of the ectonucleotidase CD39 is characteristic of CD8+ T cells specific for chronic viral infections in humans and mice, but is otherwise rare in the CD8+ T cell compartment of healthy donors. Persistent, high-level expression is also seen in the LCMV mouse model of chronic viral infection, suggesting that CD39 expression is a phenotypic marker of CD8+ T cell exhaustion. Moreover, within the exhausted population in the mouse model, CD39^{high} CD8+ T cells express the highest levels of PD-1, co-express multiple inhibitory receptors and have profoundly impaired function. We found that in both mice and humans, CD39 is expressed preferentially by CD8+ T cells that are T-bet^{low}/Eomes^{high}. These data suggest that CD39 expression by CD8+ T cells is a pathological finding and demarcates the population of CD8+ T cells previously identify as being terminally exhausted [9].

The fact that peripheral blood CD8+ T cells in humans can express CD39 is surprising. Previous data have shown that CD39 expression is restricted to CD4+ regulatory T cells, Th17 cells, and small populations of regulatory-like CD8+ T cells [14,21–23]. Indeed, we find that in the bulk population of CD8+ T cells in healthy donors only a small minority of CD8+ T cells expresses CD39. However, CD39 is abundantly expressed by virus-specific CD8+ T cells in two human chronic infections (HIV and HCV). This helps explain why CD39+ CD8+ T cells have not been appreciated in earlier studies that have focused on healthy individuals, and suggests that, in steady-state conditions, the expression of CD39 by CD8+ T cells is a pathological occurrence that is related to the development of T cell exhaustion. Whether the small fraction of

CD8$^+$ T cells expressing CD39 in healthy donors represents acutely activated CD8$^+$ T cells, or those exhausted by asymptomatic chronic pathogens or inflammatory signals is an important question for future studies.

Several features of CD39-expressing CD8$^+$ T cells suggest that CD39 is a diagnostically valuable marker of T cell exhaustion. First, in both human and mouse CD8$^+$ T cells responding to chronic infection, CD39 is co-expressed with PD-1, an inhibitory receptor expressed by the majority of exhausted T cells [5,6]. Second, CD39 expression correlates with viral load in subjects with HIV and HCV infection suggesting that the conditions of high levels of inflammation and antigen load that lead to exhaustion also increase CD39 expression in the virus-specific pool of CD8$^+$ T cells, as has been observed for PD-1 [3,34]. Third, gene signatures characteristic of exhausted mouse CD8$^+$ T cells are enriched in CD39$^+$ cells relative to CD39$^-$ CD8$^+$ T cells in subjects with HCV infection, underscoring the association between CD39 expression and T cell exhaustion. Finally, chronic LCMV infection in the mouse model increases CD39 expression by exhausted virus-specific CD8$^+$ T cells, and elicits a population of CD39^{high} cells that are absent in functional memory cells. Previous studies show that CD39, like PD-1, is transiently up-regulated by acute T cell activation [14,35]. Additional studies will therefore be required to determine the extent to which T cell activation (rather than exhaustion *per se*) contributes to the up-regulation of CD39 and PD-1 in chronic infection. However, the strong association between CD39 expression and the hallmark phenotypic features of T cell exhaustion in humans and a mouse model suggests that it can serve as a valuable marker of the exhausted T cells state.

The expression of molecules, such as PD-1, that inhibit T cell function has been used to identify exhausted CD8$^+$ T cells in several studies of human chronic infection and cancer [2]. However, there are important distinctions between the pattern of CD39 expression and that of inhibitory receptors. Many inhibitory receptors, such as PD-1 [3,8,36] and CD244 [37,38] are also expressed by a substantial fraction of CD8$^+$ T cells in healthy donors that are not exhausted. In contrast, CD39 expression is found in only a very small minority of CD8$^+$ T cells from healthy donors. This expression pattern suggests that CD39 expression, particularly in combination with PD-1, may be useful as a more specific phenotype of exhausted CD8$^+$ T cells, at least in HCV and HIV infection. In addition, CD39 may provide a useful marker to isolate exhausted CD8$^+$ T cells in settings such as tumor-specific responses where very few reagents are available to identify antigen-specific T cells. Importantly, while CD39 is rare in the CD8$^+$ compartment in healthy donors, it is expressed by CD4$^+$ Tregs–as is PD-1 –making it difficult to distinguish between exhausted CD4$^+$ T cells and Tregs by CD39 expression alone.

Analysis of global expression profiles of CD39$^+$ *versus* CD39$^-$ CD8$^+$ T cells in HCV-infected subjects showed that the CD39$^+$ fraction was strongly enriched for genes related to proliferation. This may at first seem counterintuitive, given the functional defects that have been described in exhausted CD8$^+$ T cells [2,5]. However, data from the mouse model of chronic infection suggest that, unlike memory CD8$^+$ T cells, exhausted CD8$^+$ T cells are dependent on continuous exposure to viral antigen to ensure their survival and undergo extensive cell division at a rate higher than that seen in physiological homeostatic proliferation of the memory CD8$^+$ T cell pool [39]. Exhausted CD8$^+$ T cells therefore have a paradoxical increase in their proliferation *in vivo* despite reduced proliferative potential *in vitro* [40], explaining the increased expression of proliferation-associated genes in CD39$^+$ CD8$^+$ T cells in HCV infection and in mouse exhausted CD8$^+$ T cells [9,41].

Recent studies of exhausted CD8$^+$ T cells have revealed that two distinct states of virus-specific CD8$^+$ T cells exist in chronically infected mice and humans [9,10]. Differential expression of the T-box transcription factors T-bet and Eomes characterize two populations, which form a progenitor-progeny relationship. T-bet^{high} cells display low intrinsic turnover but are capable

of proliferation in response to persisting antigen, giving rise to Eomes^{high} terminal progeny. In contrast, Eomes^{high} CD8$^+$ T cells responding to chronic infection had reduced capacity to undergo additional proliferation *in vivo*. The T-bet^{low} /Eomes^{high} exhausted subset of CD8$^+$ T cells correspond to the PD-1 bright population that has also been shown to be unresponsive to PD-1:PD-L1 blockade. These data suggest that the differential expression of these transcription factors identifies subpopulations of exhausted CD8$^+$ T cells with fundamentally different fates and functional profiles. Our data show that in the LCMV mouse model of chronic infection and in HIV infection, the CD39^{high} subset of CD8$^+$ T cells demarcates T-bet^{low} /Eomes^{high} cells. Consistent with this, CD39$^+$ CD8$^+$ T cells in the mouse model express the highest levels of PD-1, co-express multiple inhibitory receptors and show marked functional defects. These findings suggest that CD39 may be a marker not only of the exhausted state, but specifically of the most terminally exhausted cells, at least in the mouse model. Additional studies of the fate of transferred CD39$^+$ vs. CD39$^-$ exhausted CD8$^+$ T cells in the mouse model, and broader surveys of CD39 expression in human chronic infections will be required to determine whether this marker can be used as a surrogate for terminal exhaustion. However, the strong association between CD39 expression and the key features of terminal exhaustion suggests that it may prove a useful marker to help distinguish between "reversible" and "irreversible" T cell exhaustion. Moroever, the fact that isolating CD39$^+$ cells does not require intracellular staining (as is required for T-bet and Eomes) makes this marker useful for studying the function of this terminally exhausted cells *ex vivo*.

The fact that CD39 is expressed by a slightly larger fraction of HCV-specific CD8$^+$ T cells than HIV-specific CD8$^+$ T cells may be related to differences in the timing of blood sampling during the course of infection, or may be due to differences in the extent of antigen-load and inflammation in the two infections. Alternatively, it may be consistent with a model in which HCV-specific CD8$^+$ T cells are in a more “terminal” state of exhaustion than CD8$^+$ T cells specific for HIV. This possibility is supported by profound loss of HCV-specific CD8$^+$ T cells over the course of chronic infection [42] that is not seen in the HIV-specific CD8$^+$ T cell pool, consistent with the clonal deletion seen in mouse models of extreme CD8$^+$ T cell exhaustion [43,44]

It is tempting to speculate that expression of CD39 contributes to the dysfunction of exhausted T cells [45]. For instance, the expression of CD39 might enable CD8$^+$ T cells to provide negative regulation in an autocrine or juxtacrine fashion via adenosine [18–20] in the same manner as Tregs [15,35]. The fact that CD39 requires both a substrate (ATP) and a downstream enzyme (CD73) to generate adenosine could provide a mechanism to ensure that this negative signaling occurred only in certain contexts such as in inflamed, damaged tissues where the extracellular concentrations of ATP are high and CD73-expressing cells are present [46]. Moreover, CD39-expressing CD8$^+$ T cells may contribute to the general inhibitory milieu by contributing to the inhibition of activated T cells that express the adenosine receptor but are not yet exhausted. It will therefore be important to determine whether inhibition of CD39 activity could provide an additional therapeutic strategy to rescue the function of exhausted T cells.

Materials and Methods

Human Subjects

Healthy human donors were recruited at the Kraft family Blood Donor Center, Dana-Farber Cancer Institute. All human subjects with HCV infection were recruited at the Gastrointestinal Unit and the Department of Surgery of the Massachusetts General Hospital (Boston, MA) (S1 Table).

Individuals with chronic HCV infection (n = 82) were defined by positive anti-HCV antibody and detectable viral load. Patients with spontaneous clearance of HCV, termed resolvers (n = 30), were defined by positive anti-HCV antibody but an undetectable viral load for at least 6 months. The estimated time of infection was calculated either using the exposure date or the time of onset of symptoms and peak ALT (which are assumed to be 7 weeks post infection). All HCV patients were treatment naive and studied at 5.9 and 219.7 weeks post infection. HCV RNA levels were determined using the VERSANT HCV RNA 3.0 (bDNA 3.0) assay (Bayer Diagnostics).

All HIV infected subjects (n = 40) were recruited at the Ragon Institute at the Massachusetts General Hospital (Boston, USA) or the Peter Medawar Building for Pathogen Research (Oxford, UK) (S2 Table). HIV controllers included elite controllers (n = 5) defined as having HIV RNA below the level of detection (<75 viral copies per ml) and viremic controllers (n = 7) with HIV RNA levels < 2,000 viral copies per ml. HIV chronic progressors (n = 28) were defined as having > 2,000 viral copies per ml. All subjects were off therapy. Viral load during chronic infection was measured using the Roche Amplicor version 1.5 assay.

MHC Class I Tetramers

Major histocompatibility complex (MHC) class I HIV Gag-specific tetramers were produced as previously described [47] or obtained from Proimmune. CMV- and EBV-specific MHC class I dextramers conjugated with FITC and APC were purchased from Immudex. Mouse MHC class I tetramers of H-2D^b complexed with LCMV GP$_{276-286}$ were produced as previously described [48,49]. Biotinylated complexes were tetramerized using allophycocyanin-conjugated streptavidin (Molecular Probes). The complete list of multimers can be found in supplemental materials (S3 Table).

Antibodies and flow cytometry

The following anti-human (hu) and anti-mouse (m) fluorochrome-conjugated antibodies were used for flow cytometry: huCD8α (RPA-T8), huCD4 (OKT4), huCD3 (OKT3), huCD39 (A1), huPD-1 (EG12.2H7), huCD25 (BC96), huCCR7 (G043H7), huCD45RA (HI100), huT-bet (4B10), mCD8α (53–6.7), mCD4 (GK1.5), mCD3 (145-2C11), mCD244.2 (m2B4 (B6)458.1), mPD-1 (RMP1-30), mLag3 (C9B7W), mCD44 (IM7), mCD127 (A7R34), mTNFα (MP6X T22) (all from Biolegend), mT-bet (04–46; BD Pharmingen), mCD39 (24DMS1), mIFN-γ (XMG1.2), huEomes (WD1928) and mEomes (Dan11mag) (eBioscience). Intracellular staining was performed following surface staining and fixed and permeabilized using the FoxP3/Transcription Factor Staining Buffer Set (eBioscience). Cells were sorted by BD FACS ARIA II and all other analyses were performed on BD LSR II and BD LSR Fortessa flow cytometers equipped with FACSDiva v6.1. Gates were set using Full Minus One (FMO) controls. Data were analyzed using FlowJo software v9.8 (Treestar).

For intracellular cytokine analysis of mouse T cells, 2x10^6 splenocytes were cultured in the presence of GP$_{33-41}$ peptide (0.2 μg/ml) (sequence KAVYNFATM), brefeldin A (BD), and monensin (BD) for 4.5 hours at 37°C. Following staining for surface antigens, cells were permeabilized and stained for intracellular cytokines with the Cytofix/Cytoperm kit according to manufacturer's instructions (BD Biosciences).

Mice and infections

Wild-type C57BL/6J mice were purchased from The Jackson Laboratory. Female mice (6–8 weeks old) were infected with 2 x 10^5 plaque forming units (p.f.u.) of LCMV-Armstrong intraperitoneally or 4 x 10^6 p.f.u. of LCMV-Clone 13 intravenously and analyzed at indicated time

points by homogenizing the spleen into a single-cell suspension, Ammonium-Chloride-Potassium lysis of red blood cells, followed by antibody staining. For experiments involving P14 cell transfers, Ly5.1+ P14s were isolated from peripheral blood, and 500 P14 cells were transferred i.v. into 5–6 week old wild-type female mice one day prior to infection. Viruses were propagated as described previously [48–50].

HPLC analysis of ATP levels

The concentration of ATP hydrolyzed by $CD8^+$ T cells from subjects with HCV infection (n = 6) was assessed by high performance liquid chromatography (HPLC) as previously described [51]. Briefly, 10,000 $CD39^+$ $CD8^+$ T cells were sorted and placed on ice to minimize ATP production by cells. 20 μM of ATP was added and incubated for 1 h at 37°C in 5% CO_2 to allow for cellular activity to increase and CD39-mediated ATP hydrolysis to occur. Samples were then placed in an ice bath for 10 min to halt enzymatic activity, collected, and centrifuged for 10 min at 380 x g and 0°C. Cells were discarded and supernatant centrifuged again to remove remaining cells (2350 x g, 5 min, 0°C). The resulting RPMI samples (160 μl) were treated with 10 μl of an 8 M perchloric acid solution (Sigma-Aldrich) and centrifuged at 15,900 x g for 10 min at 0°C to precipitate proteins. In order to neutralize the pH of the resulting solutions and to remove lipids, supernatants (80 μl) were treated with 4 M K_2HPO_4 (8 μl) and tri-N-octylamine (50 μl). These samples were mixed with 50 μl of 1,1,2-trichloro-trifluoroethane and centrifuged (15,900 x g, 10 min, 0°C) and this last lipid extraction step was repeated once. The resulting supernatants were subjected to the following procedure to generate fluorescent etheno-adenine products: 150 μl supernatant (or nucleotide standard solution) was incubated at 72°C for 30 min with 250 mM Na_2HPO_4 (20 μl) and 1 M chloroacetaldehyde (30 μl; Sigma-Aldrich) in a final reaction volume of 200 μl, resulting in the formation of 1, N6-etheno derivatives as previously described [51]. Samples were placed on ice, alkalinized with 0.5 M NH_4HCO_3 (50 μl), filtered with a 1 ml syringe and 0.45 μM filter and analyzed using a Waters HPLC system and Supelcosil 3 μM LC-18T reverse phase column (Sigma), consisting of a gradient system described previously, a Waters autosampler, and a Waters 474 fluorescence detector [52]. Empower2 software was used for the analysis of data and all samples were compared with water and ATP standard controls as well as a sample with no cells to determine background degradation of ATP.

Microarray data acquisition

$CD8^+$ T cells from subjects with HCV infection were sorted and pelleted and re-suspended in TRIzol (Invitrogen). RNA extraction was performed using the RNAdvance Tissue Isolation kit (Agencourt). Concentrations of total RNA were determined with a Nanodrop spectrophotometer or Ribogreen RNA quantification kits (Molecular Probes/Invitrogen). RNA purity was determined by Bioanalyzer 2100 traces (Agilent Technologies). Total RNA was amplified with the WT-Ovation Pico RNA Amplification system (NuGEN) according to the manufacturer's instructions. After fragmentation and biotinylation, cDNA was hybridized to HG-U133A 2.0 microarrays (Affymetrix). Data have been deposited in Gene Expression Omnibus with accession code GSE72752.

Statistics

Prior to analysis, microarray data were pre-processed and normalized using robust multichip averaging, as previously described [53]. Differentially gene expression and consensus clustering [54] were performed using Gene-E software (www.broadinstitute.org/cancer/software/GENE-E/), and gene set enrichment analysis was performed as described previously using gene sets from MSigDB [55] or published resources [29,32].

Consensus hierarchical clustering was performed using the top 10% of genes that varied across the dataset, without reference to sample identity. Consensus cluster assesses the "stability" of the clusters discovered using unbiased methods such as hierarchical clustering i.e. the robustness of the putative clusters to sampling variability. The basic assumption is that if the data represent a sample of items drawn from distinct sub-populations, a different sample drawn from the same sub-populations, would result in cluster composition and number should not be radically different. Therefore, the more the attained clusters are robust to sampling variability, the greater the likelihood that the observed clusters represent real structure. The result of consensus clustering is a matrix that shows, for each pair of samples, the proportion of clustering runs on sub-sampled data in which those two items cluster together (shown on a scale of 0 to 1).

Enrichment Map analysis of GSEA results was performed as described [56]. The gene signature of exhaustion was generated by identifying the top 200 genes upregulated in CD8$^+$ T cells responding to chronic vs. acute LCMV infection in microarray data from a previously published study [29].

Ethics statement

All human subjects were recruited with recruited with written informed consent in accordance with Dana-Farber Cancer Institute IRB approval DFCI 00–159, Partners IRB approvals 2010P002121, 2010P002463, 1999P004983, and Oxford Research Ethics Committee approval 06/Q1604/12. The mouse work was performed under a protocol 01214 approved by the HMA Institutional Animal Care and Use Committee (IACUC), in strict accordance with the recommendations in the Guide for the care and use of Laboratory Animals of the National Institutes of Health. The Harvard Medical School animal management program is accredited by the Association for the Assessment and Accreditation of Laboratory Animal Care International (AAALAC).

Supporting Information

S1 Fig. CD39 is expressed by few CD8$^+$ T cells in health donors. Fraction of CD39$^+$ cells in naïve CD8$^+$ T and central memory (CM), effector memory (EM) and effector memory RA$^+$ (EMRA) subpopulations of CD8$^+$ T cells based on CD45RA and CCR7 staining from 18 healthy human donors. Error bars represent SEM. Statistical significance was assessed by Friedman test. $^{**}P < 0.01$, $^{***}P < 0.001$.
(TIF)

S2 Fig. CD39 and PD-1 co-expression in HCV and HIV. (A, B) Fraction of HCV-specific (A) and HIV-specific (B) CD8$^+$ T cells expressing PD-1, CD39, or both in patients with persistent high viral load (black) or patients controlling the disease (grey). Correlation of the fraction of PD-1 and CD39 double positive virus specific CD8$^+$ T cells with the viral load in the blood in HCV (C) and HIV (D) infected patients. Statistical significance was assessed by Mann-Whitney test with Bonferroni correction (A, B). $^{*}P < 0.05$. Correlation was assessed by Pearson correlation coefficient (C, D). MFI; mean fluorescence intensity.
(TIF)

S3 Fig. Cell sorting strategy for microarray analysis. Gating strategy for CD39$^+$ and CD39$^-$ live non-naive CD8$^+$ T cells from HCV-infected patients.
(TIF)

S4 Fig. Comparison of T-bet and Eomes expression by CD39$^+$ and CD39$^-$ CD8$^+$ T cells in patients with chronic viral infection. (**A, D**) Expression of CD39 in CD8$^+$ T cells in patients

infected with HCV (A) and HIV (D). (**B, E**) Expression of transcription factors T-bet and Eomes on CD39$^-$ and CD39$^+$ populations identified in (A) and (D). (**C, F**) Summary of the ratio of terminally exhausted Eomes^{high}/T-bet^{low} CD8$^+$ T cells in CD39$^-$ and CD39$^+$ subsets in HCV (C) and HIV (F) infection. Statistical significance was assessed with paired Student's t-test. $^*P < 0.05$, $^{***}P < 0.001$.
(TIF)

S1 Table. Clinical characteristics of the subjects with HCV infection.
(XLSX)

S2 Table. Clinical characteristics of the subjects with HIV infection.
(XLSX)

S3 Table. The complete list of MHC-peptide multimers used in the study.
(XLSX)

S4 Table. List of genes differentially expressed in CD39$^+$ vs CD39$^-$ CD8$^+$ T cells in HCV infected subjects (FDR<0.15).
(XLSX)

Author Contributions

Conceived and designed the experiments: PKG JG DW EJW GML PK AHS WNH. Performed the experiments: PKG JG DW KY KEP CC EA CL. Analyzed the data: PKG JG DW KY KEP EA. Contributed reagents/materials/analysis tools: WGJ SCR GA PJRG. Wrote the paper: PKG JG DW PK AHS GML WNH.

References

1. Kaech SM, Cui W (2012) Transcriptional control of effector and memory CD8+ T cell differentiation. Nat Rev Immunol 12: 749–761. doi: 10.1038/nri3307 PMID: 23080391
2. Wherry EJ (2011) T cell exhaustion. Nat Immunol 12: 492–499. PMID: 21739672
3. Day CL, Kaufmann DE, Kiepiela P, Brown JA, Moodley ES, et al. (2006) PD-1 expression on HIV-specific T cells is associated with T-cell exhaustion and disease progression. Nature 443: 350–354. PMID: 16921384
4. Lechner F, Wong DK, Dunbar PR, Chapman R, Chung RT, et al. (2000) Analysis of successful immune responses in persons infected with hepatitis C virus. J Exp Med 191: 1499–1512. PMID: 10790425
5. Wherry EJ, Ha SJ, Kaech SM, Haining WN, Sarkar S, et al. (2007) Molecular signature of CD8+ T cell exhaustion during chronic viral infection. Immunity 27: 670–684. PMID: 17950003
6. Barber DL, Wherry EJ, Masopust D, Zhu B, Allison JP, et al. (2006) Restoring function in exhausted CD8 T cells during chronic viral infection. Nature 439: 682–687. PMID: 16382236
7. Kroy DC, Ciuffreda D, Cooperrider JH, Tomlinson M, Hauck GD, et al. (2014) Liver environment and HCV replication affect human T-cell phenotype and expression of inhibitory receptors. Gastroenterology 146: 550–561. doi: 10.1053/j.gastro.2013.10.022 PMID: 24148617
8. Duraiswamy J, Ibegbu CC, Masopust D, Miller JD, Araki K, et al. (2011) Phenotype, function, and gene expression profiles of programmed death-1(hi) CD8 T cells in healthy human adults. J Immunol 186: 4200–4212. doi: 10.4049/jimmunol.1001783 PMID: 21383243
9. Paley MA, Kroy DC, Odorizzi PM, Johnnidis JB, Dolfi DV, et al. (2012) Progenitor and terminal subsets of CD8+ T cells cooperate to contain chronic viral infection. Science 338: 1220–1225. doi: 10.1126/science.1229620 PMID: 23197535
10. Buggert M, Tauriainen J, Yamamoto T, Frederiksen J, Ivarsson MA, et al. (2014) T-bet and Eomes are differentially linked to the exhausted phenotype of CD8+ T cells in HIV infection. PLoS Pathog 10: e1004251. doi: 10.1371/journal.ppat.1004251 PMID: 25032686
11. Kurktschiev PD, Raziorrouh B, Schraut W, Backmund M, Wachtler M, et al. (2014) Dysfunctional CD8+ T cells in hepatitis B and C are characterized by a lack of antigen-specific T-bet induction. J Exp Med 211: 2047–2059. doi: 10.1084/jem.20131333 PMID: 25225458

12. Blackburn SD, Shin H, Freeman GJ, Wherry EJ (2008) Selective expansion of a subset of exhausted CD8 T cells by alphaPD-L1 blockade. Proc Natl Acad Sci U S A 105: 15016–15021. doi: 10.1073/pnas.0801497105 PMID: 18809920

13. Kaczmarek E, Koziak K, Sevigny J, Siegel JB, Anrather J, et al. (1996) Identification and characterization of CD39/vascular ATP diphosphohydrolase. J Biol Chem 271: 33116–33122. PMID: 8955160

14. Kansas GS, Wood GS, Tedder TF (1991) Expression, distribution, and biochemistry of human CD39. Role in activation-associated homotypic adhesion of lymphocytes. J Immunol 146: 2235–2244. PMID: 1672348

15. Deaglio S, Dwyer KM, Gao W, Friedman D, Usheva A, et al. (2007) Adenosine generation catalyzed by CD39 and CD73 expressed on regulatory T cells mediates immune suppression. J Exp Med 204: 1257–1265. PMID: 17502665

16. Borsellino G, Kleinewietfeld M, Di Mitri D, Sternjak A, Diamantini A, et al. (2007) Expression of ectonucleotidase CD39 by Foxp3+ Treg cells: hydrolysis of extracellular ATP and immune suppression. Blood 110: 1225–1232. PMID: 17449799

17. Junger WG (2011) Immune cell regulation by autocrine purinergic signalling. Nature Publishing Group: Nature Publishing Group. pp. 201–212. doi: 10.1038/nri2938 PMID: 21331080

18. Zarek PE, Huang CT, Lutz ER, Kowalski J, Horton MR, et al. (2008) A2A receptor signaling promotes peripheral tolerance by inducing T-cell anergy and the generation of adaptive regulatory T cells. Blood 111: 251–259. PMID: 17909080

19. Huang S, Apasov S, Koshiba M, Sitkovsky M (1997) Role of A2a extracellular adenosine receptor-mediated signaling in adenosine-mediated inhibition of T-cell activation and expansion. Blood 90: 1600–1610. PMID: 9269779

20. Lokshin A, Raskovalova T, Huang X, Zacharia LC, Jackson EK, et al. (2006) Adenosine-mediated inhibition of the cytotoxic activity and cytokine production by activated natural killer cells. Cancer Res 66: 7758–7765. PMID: 16885379

21. Moncrieffe H, Nistala K, Kamhieh Y, Evans J, Eddaoudi A, et al. (2010) High Expression of the Ectonucleotidase CD39 on T Cells from the Inflamed Site Identifies Two Distinct Populations, One Regulatory and One Memory T Cell Population. The Journal of Immunology. pp. 134–143. doi: 10.4049/jimmunol.0803474 PMID: 20498355

22. Pulte D, Furman RR, Broekman MJ, Drosopoulos JH, Ballard HS, et al. (2011) CD39 expression on T lymphocytes correlates with severity of disease in patients with chronic lymphocytic leukemia. Clin Lymphoma Myeloma Leuk 11: 367–372. doi: 10.1016/j.clml.2011.06.005 PMID: 21816376

23. Boer MC, van Meijgaarden KE, Bastid J, Ottenhoff TH, Joosten SA (2013) CD39 is involved in mediating suppression by Mycobacterium bovis BCG-activated human CD8(+) CD39(+) regulatory T cells. Eur J Immunol 43: 1925–1932. doi: 10.1002/eji.201243286 PMID: 23606272

24. Robson SC, Kaczmarek E, Siegel JB, Candinas D, Koziak K, et al. (1997) Loss of ATP diphosphohydrolase activity with endothelial cell activation. J Exp Med 185: 153–163. PMID: 8996251

25. Papanikolaou A, Papafotika A, Murphy C, Papamarcaki T, Tsolas O, et al. (2005) Cholesterol-dependent lipid assemblies regulate the activity of the ecto-nucleotidase CD39. J Biol Chem 280: 26406–26414. PMID: 15890655

26. Wu Y, Sun X, Kaczmarek E, Dwyer KM, Bianchi E, et al. (2006) RanBPM associates with CD39 and modulates ecto-nucleotidase activity. Biochem J 396: 23–30. PMID: 16478441

27. Kasprowicz V, Schulze Zur Wiesch J, Kuntzen T, Nolan BE, Longworth S, et al. (2008) High level of PD-1 expression on hepatitis C virus (HCV)-specific CD8+ and CD4+ T cells during acute HCV infection, irrespective of clinical outcome. J Virol 82: 3154–3160. PMID: 18160439

28. Ashburner M, Ball CA, Blake JA, Botstein D, Butler H, et al. (2000) Gene ontology: tool for the unification of biology. The Gene Ontology Consortium. Nat Genet 25: 25–29. PMID: 10802651

29. Doering TA, Crawford A, Angelosanto JM, Paley MA, Ziegler CG, et al. (2012) Network analysis reveals centrally connected genes and pathways involved in CD8+ T cell exhaustion versus memory. Immunity 37: 1130–1144. doi: 10.1016/j.immuni.2012.08.021 PMID: 23159438

30. Quigley M, Pereyra F, Nilsson B, Porichis F, Fonseca C, et al. (2010) Transcriptional analysis of HIV-specific CD8+ T cells shows that PD-1 inhibits T cell function by upregulating BATF. Nat Med 16: 1147–1151. doi: 10.1038/nm.2232 PMID: 20890291

31. Baitsch L, Baumgaertner P, Devevre E, Raghav SK, Legat A, et al. (2011) Exhaustion of tumor-specific CD8(+) T cells in metastases from melanoma patients. J Clin Invest 121: 2350–2360. doi: 10.1172/JCI46102 PMID: 21555851

32. Subramanian A, Tamayo P, Mootha VK, Mukherjee S, Ebert BL, et al. (2005) Gene set enrichment analysis: a knowledge-based approach for interpreting genome-wide expression profiles. Proc Natl Acad Sci U S A 102: 15545–15550. PMID: 16199517

33. Blackburn SD, Shin H, Haining WN, Zou T, Workman CJ, et al. (2009) Coregulation of CD8+ T cell exhaustion by multiple inhibitory receptors during chronic viral infection. Nat Immunol 10: 29–37. doi: 10.1038/ni.1679 PMID: 19043418

34. Trautmann L, Janbazian L, Chomont N, Said EA, Gimmig S, et al. (2006) Upregulation of PD-1 expression on HIV-specific CD8+ T cells leads to reversible immune dysfunction. Nat Med 12: 1198–1202. PMID: 16917489

35. Jenabian MA, Seddiki N, Yatim A, Carriere M, Hulin A, et al. (2013) Regulatory T cells negatively affect IL-2 production of effector T cells through CD39/adenosine pathway in HIV infection. PLoS Pathog 9: e1003319. doi: 10.1371/journal.ppat.1003319 PMID: 23658513

36. Petrovas C, Casazza JP, Brenchley JM, Price DA, Gostick E, et al. (2006) PD-1 is a regulator of virus-specific CD8+ T cell survival in HIV infection. J Exp Med 203: 2281–2292. PMID: 16954372

37. Pita-Lopez ML, Gayoso I, DelaRosa O, Casado JG, Alonso C, et al. (2009) Effect of ageing on CMV-specific CD8 T cells from CMV seropositive healthy donors. Immun Ageing 6: 11. doi: 10.1186/1742-4933-6-11 PMID: 19715573

38. Rey J, Giustiniani J, Mallet F, Schiavon V, Boumsell L, et al. (2006) The co-expression of 2B4 (CD244) and CD160 delineates a subpopulation of human CD8+ T cells with a potent CD160-mediated cytolytic effector function. Eur J Immunol 36: 2359–2366. PMID: 16917959

39. Shin H, Blackburn SD, Intlekofer AM, Kao C, Angelosanto JM, et al. (2009) A role for the transcriptional repressor Blimp-1 in CD8(+) T cell exhaustion during chronic viral infection. Immunity 31: 309–320. doi: 10.1016/j.immuni.2009.06.019 PMID: 19664943

40. Migueles SA, Laborico AC, Shupert WL, Sabbaghian MS, Rabin R, et al. (2002) HIV-specific CD8+ T cell proliferation is coupled to perforin expression and is maintained in nonprogressors. Nat Immunol 3: 1061–1068. PMID: 12368910

41. Shin H, Blackburn SD, Blattman JN, Wherry EJ (2007) Viral antigen and extensive division maintain virus-specific CD8 T cells during chronic infection. J Exp Med 204: 941–949. PMID: 17420267

42. Cox AL, Mosbruger T, Lauer GM, Pardoll D, Thomas DL, et al. (2005) Comprehensive analyses of CD8 + T cell responses during longitudinal study of acute human hepatitis C. Hepatology 42: 104–112. PMID: 15962289

43. Zajac AJ, Blattman JN, Murali-Krishna K, Sourdive DJ, Suresh M, et al. (1998) Viral immune evasion due to persistence of activated T cells without effector function. J Exp Med 188: 2205–2213. PMID: 9858507

44. Moskophidis D, Lechner F, Pircher H, Zinkernagel RM (1993) Virus persistence in acutely infected immunocompetent mice by exhaustion of antiviral cytotoxic effector T cells. Nature 362: 758–761. PMID: 8469287

45. Seddiki N, Brezar V, Draenert R (2014) Cell exhaustion in HIV-1 infection: role of suppressor cells. Curr Opin HIV AIDS 9: 452–458. doi: 10.1097/COH.0000000000000087 PMID: 25010895

46. Toth I, Le AQ, Hartjen P, Thomssen A, Matzat V, et al. (2013) Decreased frequency of CD73+CD8+ T cells of HIV-infected patients correlates with immune activation and T cell exhaustion. J Leukoc Biol 94: 551–561. doi: 10.1189/jlb.0113018 PMID: 23709688

47. Leisner C, Loeth N, Lamberth K, Justesen S, Sylvester-Hvid C, et al. (2008) One-pot, mix-and-read peptide-MHC tetramers. PLoS One 3: e1678. doi: 10.1371/journal.pone.0001678 PMID: 18301755

48. Wherry EJ, Blattman JN, Murali-Krishna K, van der Most R, Ahmed R (2003) Viral persistence alters CD8 T-cell immunodominance and tissue distribution and results in distinct stages of functional impairment. J Virol 77: 4911–4927. PMID: 12663797

49. Murali-Krishna K, Altman JD, Suresh M, Sourdive DJ, Zajac AJ, et al. (1998) Counting antigen-specific CD8 T cells: a reevaluation of bystander activation during viral infection. Immunity 8: 177–187. PMID: 9491999

50. Ahmed R, Salmi A, Butler LD, Chiller JM, Oldstone MB (1984) Selection of genetic variants of lymphocytic choriomeningitis virus in spleens of persistently infected mice. Role in suppression of cytotoxic T lymphocyte response and viral persistence. J Exp Med 160: 521–540. PMID: 6332167

51. Lazarowski ER, Tarran R, Grubb BR, van Heusden CA, Okada S, et al. (2004) Nucleotide release provides a mechanism for airway surface liquid homeostasis. J Biol Chem 279: 36855–36864. PMID: 15210701

52. Chen Y, Corriden R, Inoue Y, Yip L, Hashiguchi N, et al. (2006) ATP release guides neutrophil chemotaxis via P2Y2 and A3 receptors. Science 314: 1792–1795. PMID: 17170310

53. Haining WN, Ebert BL, Subrmanian A, Wherry EJ, Eichbaum Q, et al. (2008) Identification of an evolutionarily conserved transcriptional signature of CD8 memory differentiation that is shared by T and B cells. J Immunol 181: 1859–1868. PMID: 18641323

54. Monti S TP, Mesirov J, Golub T (2003) Consensus Clustering: A Resampling-Based Method for Class Discovery and Visualization of Gene Expression Microarray Data. Machine Learning 52: 91–118.

55. Liberzon A (2014) A description of the Molecular Signatures Database (MSigDB) Web site. Methods Mol Biol 1150: 153–160. doi: 10.1007/978-1-4939-0512-6_9 PMID: 24743996

56. Merico D, Isserlin R, Stueker O, Emili A, Bader GD (2010) Enrichment map: a network-based method for gene-set enrichment visualization and interpretation. PLoS One 5: e13984. doi: 10.1371/journal.pone.0013984 PMID: 21085593

Supplemental Material

PLOS Pathogens | DOI:10.1371/journal.ppat.1005177

October 20, 2015

CD39 expression identifies terminally exhausted $CD8^+$ T cells

Prakash K. Gupta*, Jernej Godec*, David Wolski*, Emily Adland, Kathleen Yates, Cormac Cosgrove, Carola Ledderose, Wolfgang G. Junger, Simon C. Robson, E. John Wherry, Galit Alter, Philip J. R. Goulder, Paul Klenerman, Arlene H. Sharpe, Georg M. Lauer, W. Nicholas Haining.

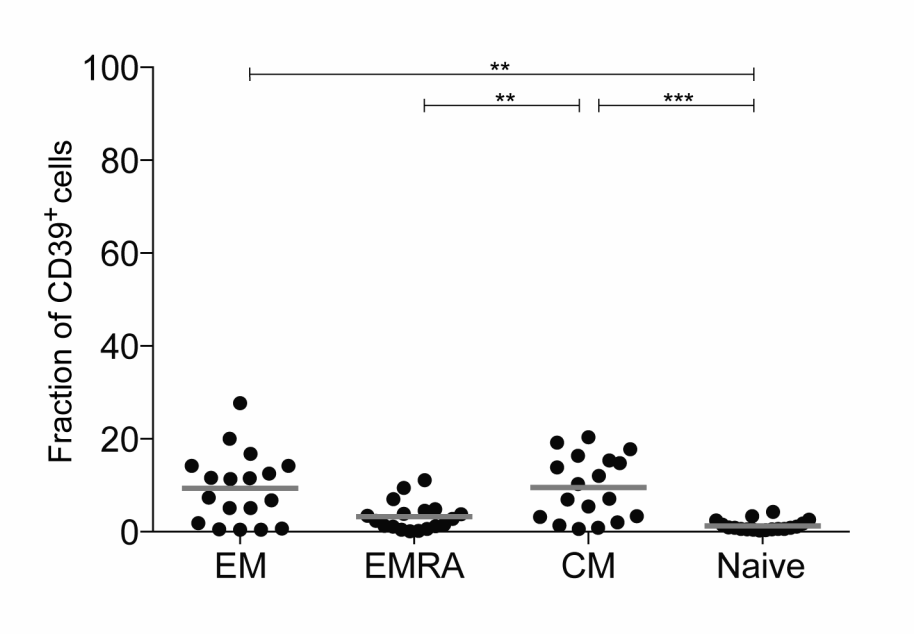

Supplemental Figure 1. CD39 is expressed by few CD8$^+$ T cells in health donors.

Fraction of CD39$^+$ cells in naïve CD8$^+$ T and central memory (CM), effector memory (EM) and effector memory RA$^+$ (EMRA) subpopulations of CD8$^+$ T cells based on CD45RA and CCR7 staining from 18 healthy human donors. Error bars represent SEM. Statistical significance was assessed by one-way ANOVA. ***P* <0.01, ****P* <0.001.

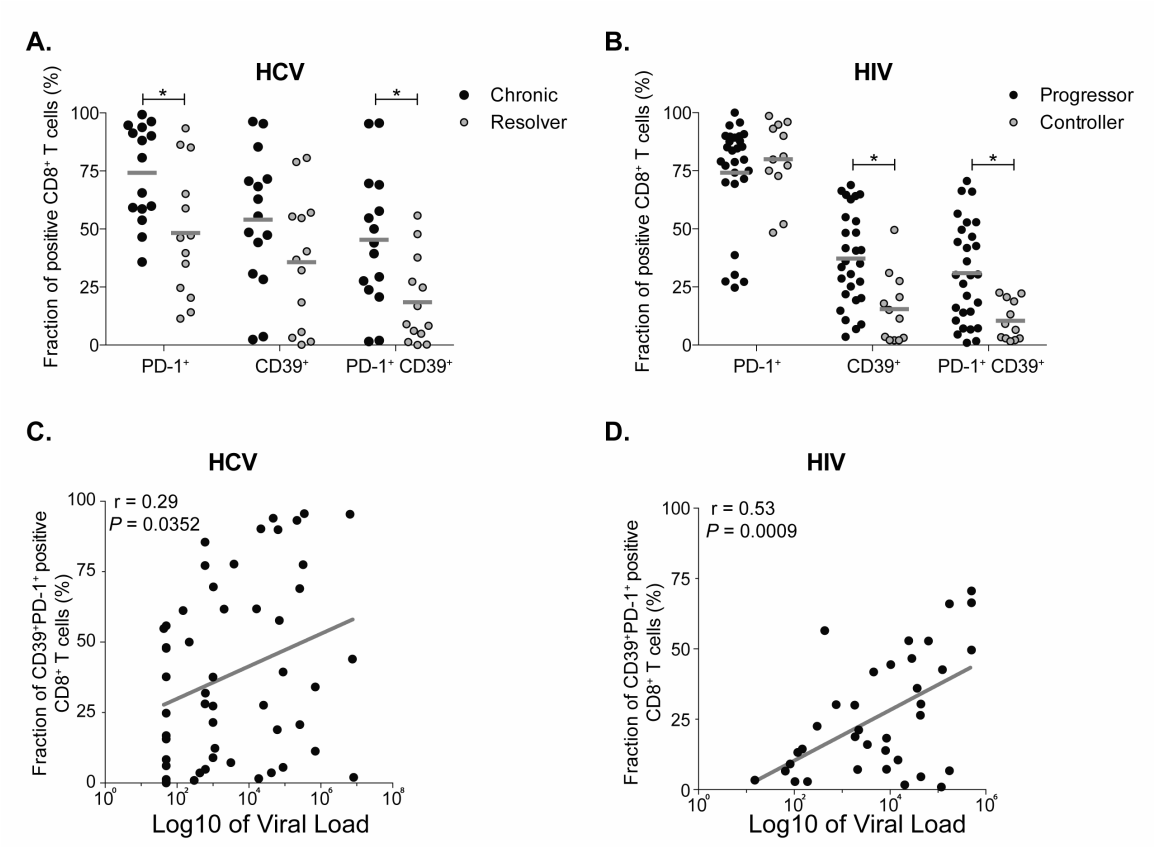

Supplemental Figure 2. CD39 and PD-1 co-expression in HCV and HIV. Fraction of HIV-specific CD8+ T cells expressing PD-1, CD39, or both in progressors (black) or controllers (grey). Statistical significance was assessed by one-way ANOVA. *P <0.05.

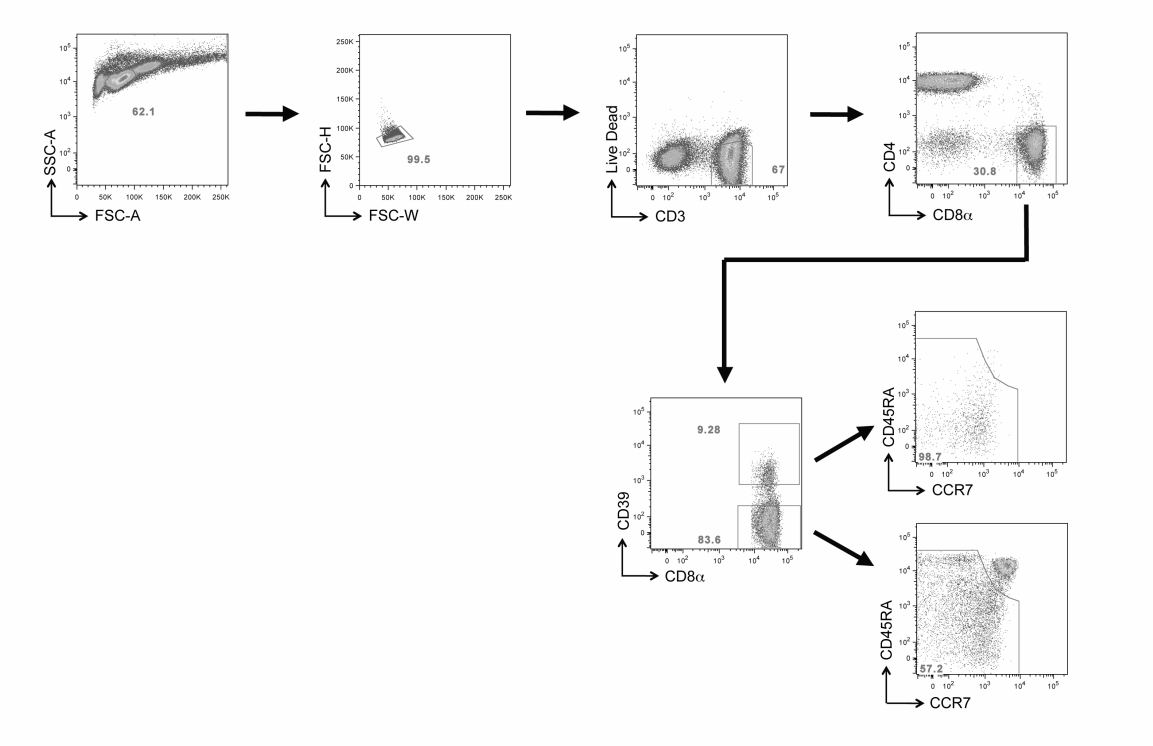

Supplemental Figure 3. Cell sorting strategy for microarray analysis. Gating strategy for $CD39^{+}$ and $CD39^{-}$ live non-naive $CD8^{+}$ T cells from HCV-infected patients.

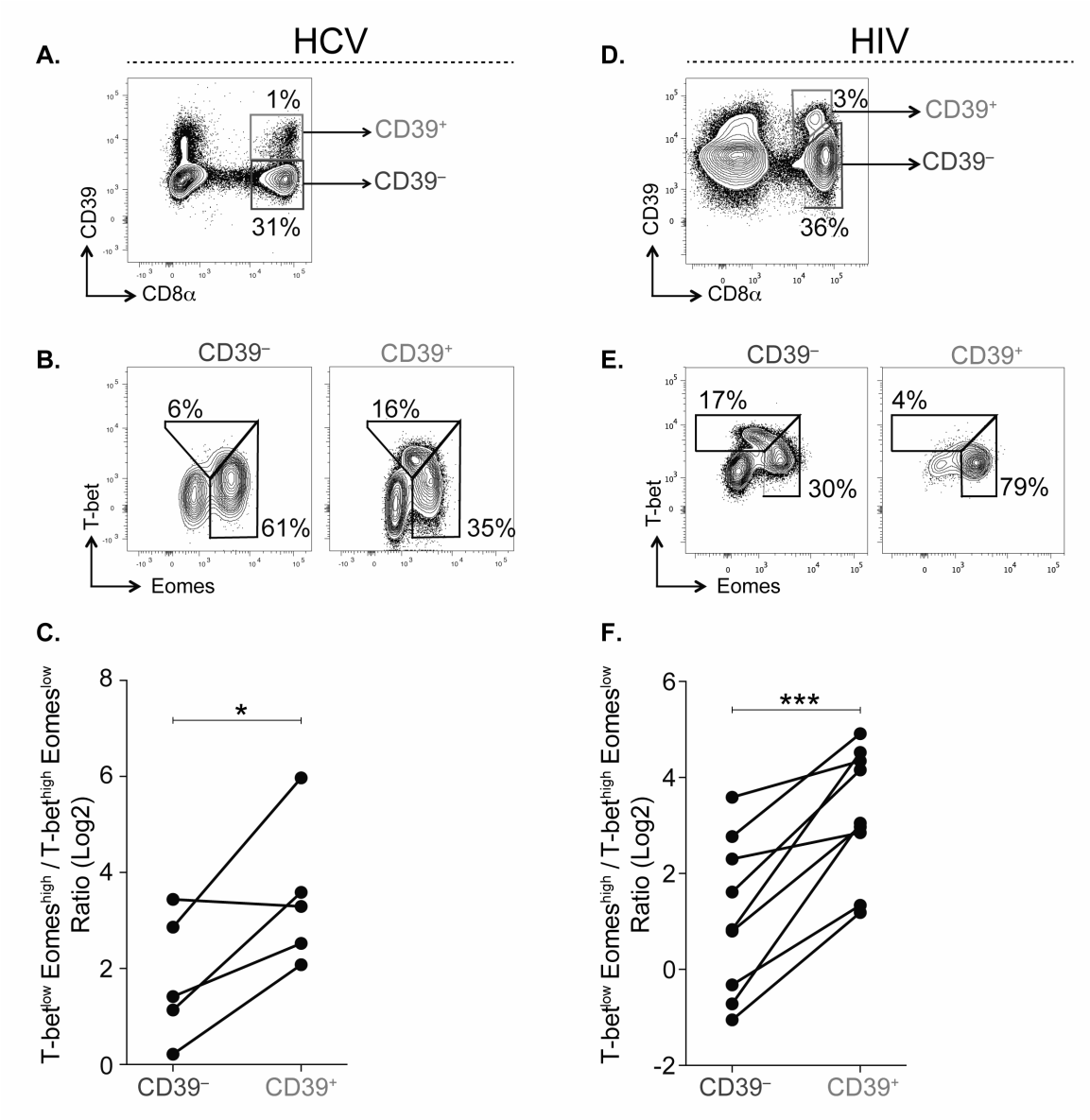

Supplemental Figure 4. Comparison of T-bet and Eomes expression by CD39$^+$ and CD39$^-$ CD8$^+$ T cells in HIV infection. (**A**) Expression of CD39 in CD8$^+$ T cells in patients infected with HIV. (**B**) Expression of transcription factors T-bet and Eomes on CD39$^-$ and CD39$^+$ populations identified in (A). (**C**) Summary of the frequency of Eomes^{hi}/T-bet^{lo} T cells in CD39$^-$ and CD39$^+$ CD8$^+$ T cells in HIV infection. Statistical significance was assessed with paired Student's t-test. *P < 0.05.

Supplemental Table 1. Clinical characteristics of the subjects with HCV infection.

00-010	M	Resolver	P16		40	Undetected	IU/ml	Undetected	39
00-023	F	Chronic	P11	27	14	300	IU/ml	Type 1	18
01-00E	F	Resolver	P5		36		IU/ml	Undetected	
02-003	F	Chronic	P2	80.9	22	18700	IU/ml	Type 1	123
02-00Z	M	Resolver	P4		50		IU/ml	No test/unknown	NA
05-00Y	F	Resolver	P2	23	21	Undetected	IU/ml	Undetected	14
05-013	M	Chronic	P7	69.1	20	170000	IU/ml	Type 1	140
06-003	M	Chronic	P12	284.4	20	369000	IU/ml	Type 1	590
06-00H	M	Chronic	P11	281	21	520000	IU/ml	Type 1	19
06-00K	F	Resolver	P3	48	22	600	IU/ml	Type 1	124
06-00K	F	Resolver	P6	68.6	22	Undetected	IU/ml	Type 1	NA
06-00L	M	Resolver	P7	18.4	29	Undetected	IU/ml	Type 3	82
06-042	M	Chronic	P5	44.9	39	615	IU/ml	Type 1	NA
07-00I	M	Chronic	P3	16	41	1162	IU/ml	Type 4	34
07-00P	M	Chronic	P4	27.4	34		IU/ml	Type 1	1379
07-00S	F	Resolver	P4	20.1	32	615	IU/ml	No test/unknown	212
07-00Z	F	Resolver	P2	12.3	21		IU/ml	No test/unknown	375
07-032	M	Chronic	P2	34.7	27		IU/ml	Type 2	565
07-032	M	Chronic	P5	49.4	27	89200	IU/ml	Type 2	263
07-039	M	Chronic	P18	144.4	31	1170	IU/ml	Type 1	33
07-052	F	Chronic	P6	47.3	35	219	IU/ml	Type 1	NA
07-080	F	Resolver	P2	13.4	22	21500	IU/ml	No test/unknown	316
07-082	F	Chronic	P8	129	27	261000	IU/ml	Type 1	NA
08-024	F	Chronic	P1	20.7	33	7.00E+05	IU/ml	Type 1	411
08-024	F	Chronic	P14	109.6	33	43	IU/ml	Type 1	11
08-024	F	Chronic	P4	25.9	33	7540000	IU/ml	Type 1	259
08-024	F	Chronic	P5	31.9	33	600	IU/ml	Type 1	35
08-024	F	Chronic	P6	33.9	33	Undetected	IU/ml	Type 1	11
08-027	M	Chronic	P1	10.4	22	3838	IU/ml	No test/unknown	58
08-027	M	Chronic	P5	28.4	22	1021	IU/ml	No test/unknown	75
09-00B	M	Chronic	P1	7	54	217000	IU/ml	Type 1	354
09-031	M	Chronic	P5	68	20	4490000	IU/ml	Type 1	148
09-033	F	Resolver	P1	6.7	41	7.00E+05	IU/ml	Type 1	2299
09-033	F	Resolver	P5	40.9	41	Undetected	IU/ml		
09-037	M	Chronic	P3	17.7	19	600	IU/ml	Type 1	32
10-00H	F	Chronic	P1	19.1	47	704	IU/ml	Type 1	107
10-00M	F	Resolver	P3	11	42		IU/ml	No test/unknown	NA
10-034	M	Chronic	P2	33.3	39		IU/ml	Type 3	58
10-048	F	Chronic	P2	11	30	321000	IU/ml	Type 1	179
10-054	F	Chronic	P1	14	23	1130	IU/ml	Type 1	209
10-062	F	Chronic	P1	11.4	30	2587650	IU/ml	Type 3	109
10-078	M	Resolver	P1	7.1	19	89200	IU/ml	Type 3	875
10-094	M	Chronic	P4	19.3	20	822000	IU/ml	Type 3	146
10-106	F	Resolver	P1	7	21	19347	IU/ml	No test/unknown	217
11-00M	M	Chronic	P1	15.3	27	8150000	IU/ml	Type 1	371
11-014	M	Resolver	P1	8.7	28	3150	IU/ml	Type 2	129
11-017	F	Chronic	P4	22.6	23	25431	IU/ml	Type 1	481
12-043	M	Resolver	P2	33.9	22	61602	IU/ml	No test/unknown	692
12-055	M	Resolver	P1	17.1	30	2311	IU/ml	Type 1	47
12-088	F	Chronic	P2	10.4	24		IU/ml	Type 1	NA
12-103	F	Chronic	P1	8.4	25	432	IU/ml	Type 3	44
12-108	M	Chronic	P1	28	67	42000	IU/ml	Type 1	81
12-181	F	Chronic	P1		29	346000	IU/ml	Type 3	657
13-022	M	Chronic	P1		46	2260000	IU/ml	Type 2	587
13-024	M	Chronic	P1	6	40	241	IU/ml	Type 1	205
13-066	F	Chronic	P1		20	43	IU/ml	No test/unknown	118
14-134	M	Chronic	P2		NA	258000	IU/ml	No test/unknown	198
14-140	M	Chronic	P1		NA		IU/ml	Type 1	NA
99-021	M	Resolver	P3		40		IU/ml	No test/unknown	NA
BR-1036	F	Resolver	P13	56.9	50	1000	copies/ml	Type 1	NA
BR-1036	F	Resolver	P9	31.7	50	1000	copies/ml	Type 1	4
BR-1144	F	Resolver	P10	67	47	1000	copies/ml	Type 1	29
BR-1144	F	Resolver	P5	38.9	47	1000	copies/ml	Type 1	2
BR-277	F	Resolver	P19	80	52	Undetected	IU/ml	Type 1	13
BR-3000	M	Resolver	P12	40.1	41	Undetected	IU/ml	Type 1	24
BR-3000	M	Resolver	P2	10	41	47272	IU/ml	Type 1	36
BR-3012	M	Resolver	P10	101.7	45	Undetected	IU/ml	Type 1	NA
BR-3497	M	Chronic	P15	43.4	72	381000	IU/ml	Type 1	112
BR-3497	M	Chronic	P2	8.3	72		IU/ml	Type 1	67
BR-3821	F	Resolver	P20	90	38	Undetected	IU/ml	Type 1	NA
BR-54	F	Chronic	P2	5.9	29		IU/ml	Type 1	237
BR-54	F	Chronic	P3	15.3	29		IU/ml	Type 1	103
BR-554	F	Chronic	P13	47.6	34	2038	copies/ml	Type 1	9
BR-554	F	Chronic	P17	82.4	34	6463017	copies/ml	Type 1	45
BR-554	F	Chronic	P4	13.6	34	64497	copies/ml	Type 1	112
BR-599	F	Resolver	P19	107.3	59	1000	copies/ml	Type 1	16
BR-84	M	Resolver	P6	62.7	61	Undetected	IU/ml	Undetected	12
BR-903	M	Chronic	P12	118.1	43	2551871	copies/ml	Type 3	176
BR-903	M	Chronic	P3	32.6	43	3341	copies/ml	Type 3	45
BR-903	M	Chronic	P7	58.4	43	1168427	copies/ml	Type 3	160
BR-949	F	Chronic	P5	48.9	37	70047	copies/ml	Type 1	36
BR-994	M	Chronic	P13	66.6	44		IU/ml	Type 1	102

Supplemental Table 2. Clinical characteristics of the subjects with HIV infection.

254567	M	Chronic	OFF	1823	606
350103	F	Chronic	OFF	431	625
350534	M	Chronic	OFF	24500	154
359260	M	Chronic	OFF	10322	541
384682	M	Chronic	ON	147	510
387879	M	Chronic	OFF	14600	677
403998	F	Chronic	OFF	2100	877
128019	M	Viraemic Controllers	OFF	unknown	unknown
186089	M	Viraemic Controllers	OFF	82	740
237983	F	Viraemic Controllers	OFF	189	1232
270245	M	Viraemic Controllers	OFF	15	unknown
302225	M	Viraemic Controllers	OFF	65	484
711950	M	Viraemic Controllers	OFF	300	700
732751	M	Viraemic Controllers	OFF	1860	1550
255675	M	Elite Controllers	OFF	103	963
269198	M	Elite Controllers	OFF	unknown	unknown
285297	F	Elite Controllers	OFF	118	1246
321797	M	Elite Controllers	OFF	unknown	unknown
831969	F	Elite Controllers	OFF	unknown	unknown
R060	M	Chronic	OFF	117934	480
R086	M	Chronic	OFF	172886	410
R089	M	Chronic	OFF	44000	680
R046	M	Chronic	OFF	28445	910
R050	M	Chronic	OFF	20210	440
R041	M	Chronic	OFF	8435	320
R017	M	Chronic	OFF	172886	410
N034	M	Chronic	OFF	44000	680
R134	M	Chronic	OFF	500000	430
N012	M	Chronic	OFF	36695	?
N090	F	Chronic	OFF	3362	490
N104	M	Chronic	OFF	4533	390
OX019	F	Chronic	OFF	42912	740
R051	M	Chronic	OFF	500000	560
R069	M	Chronic	OFF	63257	450
N004	M	Chronic	OFF	500000	430
N093	F	Chronic	OFF	2216	700
OX034	M	Chronic	OFF	124153	430
H005	M	Chronic	OFF	747	640
H033	M	Chronic	OFF	8036	430
R103	F	Chronic	OFF	8435	320

Supplemental Table 3. The complete list of MHC-peptide multimers used in the study.

Virus	Multimer type	MHC	Peptide used	Antigen derived from	Supplier
HCV	Pentamer	A*02:01	GIDPNIRTGV	HCV NS3 1273-1082	Proimmune
HCV	Pentamer	A*02:01	KLVALGINAV	HCV NS3 1406-1415	Proimmune
HCV	Pentamer	A*01:01	ATDALMTGY	HCV NS3 1435-1443	Proimmune
HCV	Pentamer	B*40:01	REISVPAEIL	HCV NS5a 2266-2275	Proimmune
HCV	Pentamer	B*07:02	GPRLGVRAT	HCV core 41-49	Proimmune
HCV	Pentamer	A*02:01	VLSDFKTWL	HCV NS5a 1987-1995	Proimmune
HCV	Pentamer	A*02:01	YPYRLWHYPC	HCV E2 610-619	Proimmune
HCV	Pentamer	B*27:01	ARMILMTHF	HCV core 470-478	Proimmune
HCV	Pentamer	A*02:01	CINGVCWTV	HCV NS3 1073-1081	Proimmune
CMV	Dextramer	A*02:01	NLVPMVATC	HCMV pp65	Immudex
EBV	Dextramer	A*02:01	GLCTLVAML	EBV BMLF-1	Immudex
HIV	Tetramer	A*24:02	RYPLTFGW	Nef RW8	Custom made
HIV	Tetramer	B*57:01	KAFSPEVIPMF	Gag KF11	Custom made
HIV	Tetramer	B*14:02	DRFYKTLRA	Gag DA9	Custom made
HIV	Tetramer	B*35:01	HPVHAGPIA	Gag HA9	Custom made
HIV	Tetramer	B*14:02	DRFYKTLRA	Gag DA9	Custom made
HIV	Dextramer	A*02:01	SLYNTVATL	Gag SL9	Immudex
HIV	Pentamer	B*07:02	TPQDLNTML	Gag TL9	Proimmune
HIV	Dextramer	A*02:01	SLYNTVATL	Gag SL9	Immudex
HIV	Dextramer	B*57:01	KAFSPEVIPMF	Gag KF11	Immudex
HIV	Tetramer	B*08:01	EIYKRWII	Gag EI8	Custom made
HIV	Tetramer	B*35:01	VPLRPMTY	Nef VY8	Beckman
HIV	Dextramer	B*07:02	GPGHKARVL	Gag GL9	Immudex
LCMV	Tetramer	H-2Db	SGVENPGGYCL	GP276-286	Dr. E. John Wherry

Conclusions and Perspectives

Recent advances in the development of direct-acting antivirals have rung in a new age of HCV treatment, with increasingly potent drugs and combination therapies that can cure over 90% of treated subjects. However, the large number of people infected worldwide, especially in resource poor settings, and continued transmission and re-infections in high risk populations will undoubtedly assure that chronic hepatitis C and its clinical consequences will remain a challenge for the foreseeable future. Developing a protective vaccine, the cornerstones of which will most likely be the induction of a highly functional T cell response in concert with potent neutralizing antibodies (Baumert et al., 2014), therefore remains a high priority. Such a vaccine could either prevent infection completely or, in a second line of defense, control viral infection effectively and swiftly before viral adaptations and T cell exhaustion can turn the tide towards persisting infection.

Aim of this thesis was to both gain a better understanding of how the CD8 T cell response is regulated on the transcriptional level during early acute infection and to identify patterns of regulation that are associated with either protective immunity or emerging dysregulation leading to T cell exhaustion in the context of presence or absence of other components of the adaptive immune response. Our findings are supposed to inform vaccine design and to set a framework for immune monitoring during future clinical trials of HCV vaccines.

In the work that constitutes the second part of the thesis we describe a novel marker of T cell exhaustion, by demonstrating that the ectonucleotidase CD39 is catalytically active and expressed at higher levels in CD8 T cells in persisting HCV infection as well as chronically progressing HIV infection. Furthermore, CD39 expression is correlated with viral load and PD-1 expression in these subjects. The LCMV mouse model of T cell exhaustion confirmed that exhausted T cells in persisting infection expressed high levels of CD39 and that CD39+ T cells represented the most profoundly dysfunctional

cell population. As part of the purinergic signaling pathway, CD39 converts immune-stimulatory ATP and ADP to AMP. Catalytic activity of CD39 is involved in the inhibitory function of CD4 T regulatory cells, where it provides the substrate for CD73, another ectonucleotidase, that hydrolyzes AMP to immune-inhibitory adenosine (Cekic & Linden, 2016; Junger, 2011). An important future question to address will be whether CD39 expression is just a correlate marker of T cell exhaustion or whether its catalytic function of removing immune-stimulatory ATP from the cellular environment is by itself an immediate driver of T cell exhaustion.

In the second part of the thesis, we identify critical early transcriptional events in HCV-specific CD8 T cell that precede the establishment of T cell exhaustion in chronic viral infection, with metabolic function at the center of a highly dysregulated transcriptional program that seems to operate under partial TCR control and which is linked to factors of human heterogeneity like age and sex of the patient as well as to the presence of CD4 T help, all of which are strong predictors of disease outcome in HCV infection.

While the impact of sex and age on the immune response are generally accepted and increasingly well documented concepts (Giefing Kröll, Berger, Lepperdinger, & Grubeck-Loebenstein, 2015; Klein & Flanagan, 2016; Shaw, Goldstein, & Montgomery, 2013), the underlying processes are not well understood, especially in the context of metabolic regulation of immune cells. The strong associations we observe between metabolic dysregulation and patient sex and age thus provide us with new prospects for avenues of investigation into these mechanics, while simultaneously highlighting the importance of human research in real-world cohorts, as such information is usually lost in animal models of viral infection, such as LCMV, where all animals are usually identical in age and sex.

By performing a transcriptional profiling experiment in a large and well defined cohort of longitudinally sampled human subjects with persisting and resolving infection in which we differentiate

between CD8 T cell responses from chronically infected subjects that targeted conserved and escaped variants of the circulating virus, we were able to not only appropriately capture human demographic heterogeneity, but also to distinguish transcriptional events associated with T cell exhaustion based on TCR stimulation from those that are related to non-specific effects of the inflammatory environment in chronic HCV infection.

We found that T cells from chronically infected patients targeting escaped viral epitopes did not share the same signature of metabolic and immune dysfunction that seemed to drive exhaustion in T cells with persistent antigen exposure, indicating that this process might be driven by protracted TCR signaling. This notion is supported by strong evidence showing that escaped CD8 T cell responses in chronic HCV infection recover towards T cell memory phenotype, as these cells upregulate CD127, downregulate PD-1, and are more responsive to a therapeutic vaccine (Kasprowicz et al., 2010; Swadling et al., 2014).

However, our results also indicate that these cells lack distinct co-regulation of most histones and sustain high expression levels of both *TNF* and *TGFB1* as well as some of their downstream signaling components, when compared to T cells targeting conserved epitopes from both chronic and resolving patients. This suggests that the abrupt abrogation of TCR signal in the context of a chronic inflammatory environment does not result in complete and immediate memory differentiation, but effects a shift towards a cytokine-focused transcriptional program atypical of these cells. Whether this switch is mainly dependent on prolonged exposure to type I interferons (Stelekati et al., 2014), or involves other inflammatory pathways, warrants further investigation.

Apart from measuring the transcriptional profiles of CD8 T cells, we also quantified HCV-specific CD4 T cell responses and neutralizing antibodies in these subjects to identify potential patterns

of association and co-regulation between these responses and CD8 T cell gene regulation. The presence or absence of HCV-specific CD4 T cells is thought to directly affect the quality of the CD8 T cell response and associations between CD8 T cell gene regulation and neutralizing antibodies might help to answer the question of whether a) a synergistic response by both arms of the adaptive response is required for viral clearance, and b) the presence of HCV nAbs, and their potential effect on viremia, has an impact on CD8 transcriptional profiles.

Indeed, our data revealed strong correlations between expression changes in driving modules of the observed metabolic dysregulation signature and the presence of CD4 T cells, indicating that proper CD4 T cell help is crucial to maintaining a functional and capable CD8 T cell response to HCV infection. While the absence of strong neutralizing antibody responses in almost all patients impeded our ability to detect meaningful correlations with CD8 T cell gene regulation, it gives us reason to believe that any differences in disease outcome can, in fact, be traced back to differences in the quality of the CD8 T cell response. To this end, our results also serve as an example of how integrating information from multiple levels of primary data and different immune cell subsets, can serve as a tool to better evaluate to which extent the different components of the adaptive immune response might contribute to viral resolution both in individual patients and in general.

Besides the strong correlations with clinical and immunological traits, our most striking finding was that the genes of the observed co-expression signature, which did not only include genes related to metabolic processes, but also featured important modulators of immune function and transcriptional regulation, were regulated in a markedly temporal manner, with high initial expression levels followed by rapid downregulation. The fact that these drastic changes manifested during the earliest stages of infection, i.e. within the first 12 weeks, indicates that these T cells initiate differential gene-regulatory

programs well before differences in the quality of the T cell response and the level of viral control become more apparent and therefore suggests that these changes might be causal, rather than consequential to T cell exhaustion.

Parts of the metabolic dysregulation signature we describe are shared by a signature recently described for CD8 T cells in persistent LCMV infection with clone 13 (Bengsch et al., 2016), indicating that proper maintenance of cell metabolic function is likely to present a truly universal feature of a successful immune response. This is further substantiated by the fact that one of the driving modules behind this signature was also strongly enriched for genes identified in HIV-specific CD8 T cells from patients that maintain long-term control of viral replication (Gaiha et al., 2014). There were, however, also marked differences in the individual metabolic pathways enriched in signatures from different viruses, suggesting that regulation of T cell metabolism is likely highly context-specific.

Delving deeper into the regulatory interactions that might drive this dysregulation by cross-referencing identified modules with known database-derived regulatory interactions, we found that most genes with metabolic function were regulated by a handful of transcription factors that were not just highly connected within in their respective modules, but also annotated for interactions with many genes related to immune function and regulation of transcription in closely connected modules, demonstrating that metabolic dysregulation is not isolated but unfolds in tandem with other transcriptional changes.

While most transcription factors that constitute the central drivers of the early changes of CD8 T cell regulation in response to HCV infection, such as *CREB1*, *RFX5*, *FLI1, STAT1,* and *STAT5A,* are known regulators of immune function and development (Gil, Salomon, Louten, & Biron, 2006; Lochamy, Rogers, & Boss, 2007; O'Shea & Plenge, 2012; Ravasi et al., 2010; Tripathi et al., 2010; Villard et al., 2000), their involvement in metabolic regulation has not so far been elucidated, and, conversely,

while the role of *TP53* in metabolism is well established (Berkers, Maddocks, Cheung, Mor, & Vousden, 2013), its part in regulation of immune responses has only recently gained increasing attention (Muñoz-Fontela, Mandinova, Aaronson, & Lee, 2016). The described regulatory network and its differential expression and connectivity across individual immunological states therefore highlight a unique previously unknown combinatorial role of these transcription factors in the early dysregulation of CD8 T cell responses in persistent viral infection.

Similar differences in the connectivity of transcriptional network hubs in the context of different infection outcomes have been described in LCMV (Doering et al., 2012), albeit for other transcription factors and without distinction between TCR- and inflammation-mediated effects, demonstrating that the differences in metabolic regulation observed between different viruses are also reflected at the level of implicated transcriptional regulators. Further investigation into the differences and similarities of transcriptional profiles of CD8 T cells specific to different viruses with varying host species and cellular tropism would be highly informative towards better classification of species-, tissue- and virus-specific regulatory programs and would thus allow for further dissemination of what truly differentiates a successful from a failing T cell response.

In summary, the work presented in this thesis demonstrates that transcriptional events in HCV-specific CD8 T cells during the critical acute phase of HCV infection are marked by changes in regulation of base metabolic functions, pro-inflammatory signaling pathways and processes related to nucleosome assembly and chromatin silencing. These highly time-dependent changes track with levels of increasing T cell dysfunction and partly with availability of CD4 T cell help and loss of antigen recognition, suggesting that disruption of basic cellular metabolic functions may lead to dysregulation of transcriptional processes, which in turn is likely to result in T cell exhaustion and failure of the CD8 T

cell response in the acute phase of HCV infection. Future work should be aimed at functional models that can deliver more insight into the regulation of T cell metabolism and how it controls the functional and transcriptional integrity of T cells in the high stress environments of infection sites as well as at a deeper understanding of the role that epigenetic modifications of DNA and histones play in the regulation of T cell immunity. By combining information on transcriptional regulators with information on associated regulation of metabolic processes and immunological function and linking it to regulation of histones and histone modifying enzymes, this work highlights the merit of integrating quantitative information from multiple sources and fields of expertise to gain a better understanding of the complex biological interactions and bears the potential to serve as a blueprint for more targeted and concise follow-up studies into the dynamics of immune cell regulation in response to viral infection.

References

Aderem, A., Adkins, J. N., Ansong, C., Galagan, J., Kaiser, S., Korth, M. J., et al. (2010). A Systems Biology Approach to Infectious Disease Research: Innovating the Pathogen-Host Research Paradigm. *mBio*, *2*, e00325–10–e00325–10.

Albert, R., Jeong, H., & Barabási, A.-L. (2000). Error and attack tolerance of complex networks. *Nature*, *406*, 378–382.

Alexa, A., Rahnenfuhrer, J., & Lengauer, T. (2006). Improved scoring of functional groups from gene expression data by decorrelating GO graph structure. *Bioinformatics*, *22*, 1600–1607.

Alter, H. J., Holland, P. V., Morrow, A. G., Purcell, R. H., Feinstone, S. M., & Moritsugu, Y. (1975). Clinical and serological analysis of transfusion-associated hepatitis. *The Lancet*, *2*, 838–841.

Angelosanto, J. M., Blackburn, S. D., Crawford, A., & Wherry, E. J. (2012). Progressive Loss of Memory T Cell Potential and Commitment to Exhaustion during Chronic Viral Infection. *Journal of Virology*, *86*, 8161–8170.

Arnaud, N., Dabo, S., Akazawa, D., Fukasawa, M., Shinkai-Ouchi, F., Hugon, J., et al. (2011). Hepatitis C Virus Reveals a Novel Early Control in Acute Immune Response. *PLoS Pathogens*, *7*, e1002289.

Ashburner, M., Ball, C. A., Blake, J. A., Botstein, D., Butler, H., Cherry, J. M., et al. (2000). Gene Ontology: tool for the unification of biology. *Nature Genetics*, *25*, 25–29.

Barabási, A.-L., & Albert, R. (1999). Emergence of Scaling in Random Networks. *Science*, *286*, 509–512.

Barabási, A.-L., & Oltvai, Z. N. (2004). Network biology: understanding the cell's functional organization. *Nature Reviews Genetics*, *5*, 101–113.

Barber, D. L., Wherry, E. J., Masopust, D., Zhu, B., Allison, J. P., Sharpe, A. H., et al. (2005). Restoring function in exhausted CD8 T cells during chronic viral infection. *Nature*, *439*, 682–687.

Bartenschlager, R., Lohmann, V., & Penin, F. (2013). The molecular and structural basis of advanced antiviral therapy for hepatitis C virus infection. *Nature Reviews Microbiology*, *11*, 482–496.

Bartenschlager, R., Penin, F., Lohmann, V., & André, P. (2011). Assembly of infectious hepatitis C virus particles. *Trends in Microbiology*, *19*, 95–103.

Baumert, T. F., Fauvelle, C., Chen, D. Y., & Lauer, G. M. (2014). A prophylactic hepatitis C virus vaccine: A distant peak still worth climbing. *Journal of Hepatology*, *61*, S34–S44.

Beebe, D. J., Mensing, G. A., & Walker, G. M. (2002). Physics and Applications of Microfluidics in Biology. *Annual Review of Biomedical Engineering*, *4*, 261–286.

Belkaid, Y. (2007). Regulatory T cells and infection: a dangerous necessity. *Nature Reviews Immunology*, *7*, 875–888.

Bellecave, P., Sarasin-Filipowicz, M., Donzé, O., Kennel, A., Gouttenoire, J., Meylan, E., et al. (2009). Cleavage of mitochondrial antiviral signaling protein in the liver of patients with chronic hepatitis C correlates with a reduced activation of the endogenous interferon system. *Hepatology (Baltimore, Md.)*, *51*, 1127–1136.

Bender, S., Reuter, A., Eberle, F., Einhorn, E., Binder, M., & Bartenschlager, R. (2015). Activation of Type I and III Interferon Response by Mitochondrial and Peroxisomal MAVS and Inhibition by Hepatitis C Virus. *PLoS Pathogens*, *11*, e1005264.

Bengsch, B., Johnson, A. L., Kurachi, M., Odorizzi, P. M., Pauken, K. E., Attanasio, J., et al. (2016). Bioenergetic Insufficiencies Due to Metabolic Alterations Regulated by the Inhibitory Receptor PD-1 Are an Early Driver of CD8(+) T Cell Exhaustion. *Immunity*, *45*, 358–373.

Berkers, C. R., Maddocks, O. D. K., Cheung, E. C., Mor, I., & Vousden, K. H. (2013). Metabolic Regulation by p53 Family Members. *Cell Metabolism*, *18*, 617–633.

Blackburn, S. D., Shin, H., Haining, W. N., Zou, T., Workman, C. J., Polley, A., et al. (2008). Coregulation of CD8+ T cell exhaustion by multiple inhibitory receptors during chronic viral infection. *Nature Immunology*, *10*, 29–37.

Blankley, S., Graham, C. M., Howes, A., Bloom, C. I., Berry, M. P. R., Chaussabel, D., et al. (2014). Identification of the Key Differential Transcriptional Responses of Human Whole Blood Following TLR2 or TLR4 Ligation In-Vitro. *PLoS ONE*, *9*, e97702.

Boettler, T., Spangenberg, H. C., Neumann-Haefelin, C., Panther, E., Urbani, S., Ferrari, C., et al. (2005). T Cells with a CD4+CD25+ Regulatory Phenotype Suppress In Vitro Proliferation of Virus-Specific CD8+ T Cells during Chronic Hepatitis C Virus Infection. *Journal of Virology*, *79*, 7860–7867.

Bowen, D. G., & Walker, C. M. (2005). Adaptive immune responses in acute and chronic hepatitis C virus infection. *Nature*, *436*, 946–952.

Brimacombe, C. L., Grove, J., Meredith, L. W., Hu, K., Syder, A. J., Flores, M. V., et al. (2010). Neutralizing Antibody-Resistant Hepatitis C Virus Cell-to-Cell Transmission. *Journal of Virology*, *85*, 596–605.

Bumgarner, R. (2001). Overview of DNA Microarrays: Types, Applications, and Their Future. Hoboken, NJ, USA: John Wiley & Sons, Inc. doi:10.1002/0471142727.mb2201s101

Cabrera, R., Tu, Z., Xu, Y., Firpi, R. J., Rosen, H. R., Liu, C., & Nelson, D. R. (2004). An immunomodulatory role for CD4+CD25+ regulatory T lymphocytes in hepatitis C virus infection. *Hepatology (Baltimore, Md.)*, *40*, 1062–1071.

Cekic, C., & Linden, J. (2016). Purinergic regulation of the immune system. *Nature Reviews Immunology*, *16*, 177–192.

Chandler, D. E., Penin, F., Schulten, K., & Chipot, C. (2012). The p7 Protein of Hepatitis C Virus Forms Structurally Plastic, Minimalist Ion Channels. *PLoS Computational Biology*, *8*, e1002702.

Chaussabel, D., & Baldwin, N. (2014). Democratizing systems immunology with modular transcriptional repertoire analyses. *Nature Reviews Immunology*, *14*, 271–280.

Chen, E. Y., Tan, C. M., Kou, Y., Duan, Q., Wang, Z., Meirelles, G., et al. (2013). Enrichr: interactive and collaborative HTML5 gene list enrichment analysis tool. *BMC Bioinformatics*, *14*, 128.

Choo, Q., Kuo, G., Weiner, A., Overby, L., Bradley, D., & Houghton, M. (1989). Isolation of a cDNA clone derived from a blood-borne non-A, non-B viral hepatitis genome. *Science*, *244*, 359–362.

Chung, R. T., & Baumert, T. F. (2014). Curing Chronic Hepatitis C — The Arc of a Medical Triumph. *New England Journal of Medicine*, *370*, 1576–1578.

Cox, A. L., Mosbruger, T., Lauer, G. M., Pardoll, D., Thomas, D. L., & Ray, S. C. (2005a). Comprehensive analyses of CD8+ T cell responses during longitudinal study of acute human hepatitis C. *Hepatology (Baltimore, Md.)*, *42*, 104–112.

Cox, A. L., Mosbruger, T., Lauer, G. M., Pardoll, D., Thomas, D. L., & Ray, S. C. (2005b). Comprehensive analyses of CD8+ T cell responses during longitudinal study of acute human hepatitis C. *Hepatology (Baltimore, Md.)*, *42*, 104–112.

Cox, A. L., Mosbruger, T., Mao, Q., Liu, Z., Wang, X.-H., Yang, H.-C., et al. (2005c). Cellular immune selection with hepatitis C virus persistence in humans. *The Journal of Experimental Medicine*, *201*, 1741–1752.

Day, C. L., Lauer, G. M., Robbins, G. K., McGovern, B., Wurcel, A. G., Gandhi, R. T., et al. (2002). Broad Specificity of Virus-Specific CD4+ T-Helper-Cell Responses in Resolved Hepatitis C Virus Infection. *Journal of Virology*, *76*, 12584–12595.

Deaglio, S., Dwyer, K. M., Gao, W., Friedman, D., Usheva, A., Erat, A., et al. (2007). Adenosine generation catalyzed by CD39 and CD73 expressed on regulatory T cells mediates immune suppression. *The Journal of Experimental Medicine*, *204*, 1257–1265.

Dill, M. T., Duong, F. H. T., Vogt, J. E., Bibert, S., Bochud, P.-Y., Terracciano, L., et al. (2011). Interferon-Induced Gene Expression Is a Stronger Predictor of Treatment Response Than IL28B Genotype in Patients With Hepatitis C. *Gastroenterology*, *140*, 1021–1031.e10.

Doering, T. A., Crawford, A., Angelosanto, J. M., Paley, M. A., Ziegler, C. G., & Wherry, E. J. (2012). Network Analysis Reveals Centrally Connected Genes and Pathways Involved in CD8+ T Cell Exhaustion versus Memory. *Immunity*, *37*, 1130–1144.

Donahue, J. G., Muñoz, A., Ness, P. M., Brown, D. E., Jr., Yawn, D. H., McAllister, H. A., Jr., et al. (1992). The Declining Risk of Post-Transfusion Hepatitis C Virus Infection. *New England Journal of Medicine*, *327*, 369–373.

Dreux, M., Garaigorta, U., Boyd, B., Décembre, E., Chung, J., Whitten-Bauer, C., et al. (2012). Short-Range Exosomal Transfer of Viral RNA from Infected Cells to Plasmacytoid Dendritic Cells Triggers Innate Immunity. *Cell Host & Microbe*, *12*, 558–570.

Edlich, B., Ahlenstiel, G., Zabaleta, A. A., Stoltzfus, J., Noureddin, M., Serti, E., et al. (2011). Early changes in interferon signaling define natural killer cell response and refractoriness to interferon-based therapy of hepatitis C patients. *Hepatology (Baltimore, Md.)*, *55*, 39–48.

Egger, D., Wolk, B., Gosert, R., Bianchi, L., Blum, H. E., Moradpour, D., & Bienz, K. (2002). Expression of Hepatitis C Virus Proteins Induces Distinct Membrane Alterations Including a Candidate Viral Replication Complex. *Journal of Virology*, *76*, 5974–5984.

Erickson, A. L., Kimura, Y., Igarashi, S., Eichelberger, J., Houghton, M., Sidney, J., et al. (2001). The Outcome of Hepatitis C Virus Infection Is Predicted by Escape Mutations in Epitopes Targeted by Cytotoxic T Lymphocytes. *Immunity*, *15*, 883–895.

Fabregat, A., Sidiropoulos, K., Garapati, P., Gillespie, M., Hausmann, K., Haw, R., et al. (2016). The Reactome pathway Knowledgebase. *Nucleic Acids Research*, *44*, D481–D487.

Gaiha, G. D., McKim, K. J., Woods, M., Pertel, T., Rohrbach, J., Barteneva, N., et al. (2014). Dysfunctional HIV-Specific CD8+ T Cell Proliferation Is Associated with Increased Caspase-8 Activity and Mediated by Necroptosis. *Immunity*, *41*, 1001–1012.

Germain, R. N., Meier-Schellersheim, M., Nita-Lazar, A., & Fraser, I. D. C. (2011). Systems Biology in Immunology: A Computational Modeling Perspective *. *Annual Review of Immunology*, *29*, 527–585.

Giefing Kröll, C., Berger, P., Lepperdinger, G., & Grubeck-Loebenstein, B. (2015). How sex and age affect immune responses, susceptibility to infections, and response to vaccination. *Aging Cell*, *14*, 309–321.

Gil, M. P., Salomon, R., Louten, J., & Biron, C. A. (2006). Modulation of STAT1 protein levels: a mechanism shaping CD8 T-cell responses in vivo. *Blood*, *107*, 987–993.

Golden Mason, L., Cox, A. L., Randall, J. A., Cheng, L., & Rosen, H. R. (2010). Increased natural killer cell cytotoxicity and NKp30 expression protects against hepatitis C virus infection in high-risk individuals and inhibits replication in vitro. *Hepatology (Baltimore, Md.)*, *52*, 1581–1589.

Gould, E. A. (1999). ENCEPHALITIS VIRUSES (FLAVIVIRIDAE) | Tick-Borne Encephalitis And Wesselsbron Viruses. *Encyclopedia of Virology* (Second Edition, pp. 430–437).

Grakoui, A. (2003). HCV Persistence and Immune Evasion in the Absence of Memory T Cell Help. *Science*, *302*, 659–662.

Guerra, J., Garenne, M., Mohamed, M. K., & Fontanet, A. (2012). HCV burden of infection in Egypt: results from a nationwide survey. *Journal of Viral Hepatitis*, *19*, 560–567.

Gupta, P. K., Godec, J., Wolski, D., Adland, E., Yates, K., Pauken, K. E., et al. (2015). CD39 Expression Identifies Terminally Exhausted CD8+ T Cells. *PLoS Pathogens*, *11*, e1005177.

Hajarizadeh, B., Grebely, J., & Dore, G. J. (2013). Epidemiology and natural history of HCV infection. *Nature Reviews Gastroenterology & Hepatology*, *10*, 553–562.

Harris, A. M., Iqbal, K., Schillie, S., Britton, J., Kainer, M. A., Tressler, S., & Vellozzi, C. (2016). Increases in Acute Hepatitis B Virus Infections — Kentucky, Tennessee, and West Virginia, 2006–2013. *MMWR. Morbidity and Mortality Weekly Report*, *65*, 47–50.

Heim, M. H. (2013). 25 years of interferon-based treatment of chronic hepatitis C: an epoch coming to an end. *Nature Reviews Immunology*, *13*, 535–542.

Herrmann, H., & Bucksch, H. (2014). biostrat(igraph)ic unit. In *Dictionary Geotechnical Engineering/Wörterbuch GeoTechnik* (pp. 127–127). Berlin, Heidelberg: Springer Berlin Heidelberg.

Hiet, M.-S., Bauhofer, O., Zayas, M., Roth, H., Tanaka, Y., Schirmacher, P., et al. (2015). Control of temporal activation of hepatitis C virus-induced interferon response by domain 2 of nonstructural protein 5A. *Journal of Hepatology*, *63*, 829–837.

Hill, A., & Cooke, G. (2014). Hepatitis C can be cured globally, but at what cost? *Science*, *345*, 141–142.

Hill, A., Khoo, S., Fortunak, J., Simmons, B., & Ford, N. (2014). Minimum Costs for Producing Hepatitis C Direct-Acting Antivirals for Use in Large-Scale Treatment Access Programs in Developing Countries. *Clinical Infectious Diseases*, *58*, 928–936.

Hill, C. (2016). SciPy. In *Learning Scientific Programming with Python* (pp. 333–401). Cambridge: Cambridge University Press.

Hoffman, B., & Liu, Q. (2011). Hepatitis C viral protein translation: mechanisms and implications in developing antivirals. *Liver International*, *31*, 1449–1467.

Huang, D. W., Sherman, B. T., & Lempicki, R. A. (2008). Systematic and integrative analysis of large gene lists using DAVID bioinformatics resources. *Nature Protocols*, *4*, 44–57.

Huber, W., Carey, V. J., Gentleman, R., Anders, S., Carlson, M., Carvalho, B. S., et al. (2015). Orchestrating high-throughput genomic analysis with Bioconductor. *Nature Methods*, *12*, 115–121.

Ihaka, R., & Gentleman, R. (1996). R: A Language for Data Analysis and Graphics. *Journal of Computational and Graphical Statistics*, *5*, 299.

Jang, Y.-S., Kang, W., Chang, D.-Y., Sung, P. S., Park, B.-C., Yoo, S. H., et al. (2013). CD27 engagement by a soluble CD70 protein enhances non-cytolytic antiviral activity of CD56bright natural killer cells by IFN-γ secretion. *Clinical Immunology*, *149*, 379–387.

Jangra, R. K., Yi, M., & Lemon, S. M. (2010). Regulation of Hepatitis C Virus Translation and Infectious Virus Production by the MicroRNA miR-122. *Journal of Virology*, *84*, 6615–6625.

Jayasekera, C. R., Barry, M., Roberts, L. R., & Nguyen, M. H. (2014). Treating Hepatitis C in Lower-Income Countries. *New England Journal of Medicine*, *370*, 1869–1871.

Jones, D. M., Patel, A. H., Targett-Adams, P., & McLauchlan, J. (2009). The Hepatitis C Virus NS4B Protein Can trans-Complement Viral RNA Replication and Modulates Production of Infectious Virus. *Journal of Virology*, *83*, 2163–2177.

Junger, W. G. (2011). Immune cell regulation by autocrine purinergic signalling. *Nature Reviews Immunology*, *11*, 201–212.

Kanehisa, M. (2000). KEGG: Kyoto Encyclopedia of Genes and Genomes. *Nucleic Acids Research*, *28*, 27–30.

Kasprowicz, V., Kang, Y. H., Lucas, M., Schulze zur Wiesch, J., Kuntzen, T., Fleming, V., et al. (2010). Hepatitis C Virus (HCV) Sequence Variation Induces an HCV-Specific T-Cell Phenotype Analogous to Spontaneous Resolution. *Journal of Virology*, *84*, 1656–1663.

Kasprowicz, V., Schulze zur Wiesch, J., Kuntzen, T., Nolan, B. E., Longworth, S., Berical, A., et al. (2008). High Level of PD-1 Expression on Hepatitis C Virus (HCV)-Specific CD8+ and CD4+ T Cells during Acute HCV Infection, Irrespective of Clinical Outcome. *Journal of Virology*, *82*, 3154–3160.

Kim, A. Y., Onofrey, S., & Church, D. R. (2013). An Epidemiologic Update on Hepatitis C Infection in Persons Living With or at Risk of HIV Infection. *Journal of Infectious Diseases*, *207*, S1–S6.

Kitano, H. (2002). Computational systems biology. *Nature*, *420*, 206–210.

Klein, S. L., & Flanagan, K. L. (2016). Sex differences in immune responses. *Nature Reviews Immunology*, *16*, 626–638.

Kroy, D. C., Ciuffreda, D., Cooperrider, J. H., Tomlinson, M., Hauck, G. D., Aneja, J., et al. (2014). Liver Environment and HCV Replication Affect Human T-Cell Phenotype and Expression of Inhibitory Receptors. *Gastroenterology*, *146*, 550–561.

Kuntzen, T., Timm, J., Berical, A., Lewis-Ximenez, L. L., Jones, A., Nolan, B., et al. (2007). Viral Sequence Evolution in Acute Hepatitis C Virus Infection. *Journal of Virology*, *81*, 11658–11668.

Langfelder, P., & Horvath, S. (2007). Eigengene networks for studying the relationships between co-expression modules. *BMC Systems Biology*, *1*, 54.

Langfelder, P., & Horvath, S. (2008). WGCNA: an R package for weighted correlation network analysis. *BMC Bioinformatics*, *9*, 559.

Langfelder, P., Mischel, P. S., & Horvath, S. (2013). When Is Hub Gene Selection Better than Standard Meta-Analysis? *PLoS ONE*, *8*, e61505.

Langfelder, P., Zhang, B., & Horvath, S. (2008). Defining clusters from a hierarchical cluster tree: the Dynamic Tree Cut package for R. *Bioinformatics*, *24*, 719–720.

Lauer, G. M. (2013). Immune Responses to Hepatitis C Virus (HCV) Infection and the Prospects for an Effective HCV Vaccine or Immunotherapies. *Journal of Infectious Diseases*, *207*, S7–S12.

Lauer, G. M., & Walker, B. D. (2001). Hepatitis C Virus Infection. *New England Journal of Medicine*, *345*, 41–52.

Lauer, G. M., Lucas, M., Timm, J., Ouchi, K., Kim, A. Y., Day, C. L., et al. (2005). Full-Breadth Analysis of CD8+ T-Cell Responses in Acute Hepatitis C Virus Infection and Early Therapy. *Journal of Virology*, *79*, 12979–12988.

Li, K., Li, N. L., Wei, D., Pfeffer, S. R., Fan, M., & Pfeffer, L. M. (2012). Activation of chemokine and inflammatory cytokine response in hepatitis C virus-infected hepatocytes depends on toll-like receptor 3 sensing of hepatitis C virus double-stranded RNA intermediates. *Hepatology (Baltimore, Md.)*, *55*, 666–675.

Lochamy, J., Rogers, E. M., & Boss, J. M. (2007). CREB and phospho-CREB interact with RFX5 and CIITA to regulate MHC class II genes. *Molecular Immunology*, *44*, 837–847.

Logvinoff, C., Major, M. E., Oldach, D., Heyward, S., Talal, A., Balfe, P., et al. (2004). Neutralizing antibody response during acute and chronic hepatitis C virus infection. *Proceedings of the National Academy of Sciences*, *101*, 10149–10154.

Lohmann, V. (2013). Hepatitis C Virus RNA Replication. In *Hepatitis C Virus: From Molecular Virology to Antiviral Therapy* (Vol. 369, pp. 167–198). Berlin, Heidelberg: Springer Berlin Heidelberg.

Lorenz, I. C., Marcotrigiano, J., Dentzer, T. G., & Rice, C. M. (2006). Structure of the catalytic domain of the hepatitis C virus NS2-3 protease. *Nature*, *442*, 831–835.

Luik, P., Chew, C., Aittoniemi, J., Chang, J., Wentworth, P., Dwek, R. A., et al. (2009). The 3-dimensional structure of a hepatitis C virus p7 ion channel by electron microscopy. *Proceedings of the National Academy of Sciences*, *106*, 12712–12716.

Luo, W., Friedman, M. S., Shedden, K., Hankenson, K. D., & Woolf, P. J. (2009). GAGE: generally applicable gene set enrichment for pathway analysis. *BMC Bioinformatics*, *10*, 161.

Miyagi, T., Takehara, T., Nishio, K., Shimizu, S., Kohga, K., Li, W., et al. (2010). Altered interferon-α-signaling in natural killer cells from patients with chronic hepatitis C virus infection. *Journal of Hepatology*, *53*, 424–430.

Morikawa, K., Lange, C. M., Gouttenoire, J., Meylan, E., Brass, V., Penin, F., & Moradpour, D. (2011). Nonstructural protein 3-4A: the Swiss army knife of hepatitis C virus. *Journal of Viral Hepatitis*, *18*, 305–315.

Muñoz-Fontela, C., Mandinova, A., Aaronson, S. A., & Lee, S. W. (2016). Emerging roles of p53 and other tumour-suppressor genes in immune regulation. *Nature Reviews Immunology*, *16*, 741–750.

Negash, A. A., Ramos, H. J., Crochet, N., Lau, D. T. Y., Doehle, B., Papic, N., et al. (2013). IL-1β Production through the NLRP3 Inflammasome by Hepatic Macrophages Links Hepatitis C Virus Infection with Liver Inflammation and Disease. *PLoS Pathogens*, *9*, e1003330.

O'Garra, A., & Vieira, P. (2004). Regulatory T cells and mechanisms of immune system control. *Nature Medicine*, *10*, 801–805.

Osburn, W. O., Fisher, B. E., Dowd, K. A., Urban, G., Liu, L., Ray, S. C., et al. (2010). Spontaneous Control of Primary Hepatitis C Virus Infection and Immunity Against Persistent Reinfection. *Gastroenterology*, *138*, 315–324.

Osburn, W. O., Snider, A. E., Wells, B. L., Latanich, R., Bailey, J. R., Thomas, D. L., et al. (2014). Clearance of hepatitis C infection is associated with the early appearance of broad neutralizing antibody responses. *Hepatology (Baltimore, Md.)*, *59*, 2140–2151.

O'Shea, J. J., & Plenge, R. (2012). JAK and STAT Signaling Molecules in Immunoregulation and Immune-Mediated Disease. *Immunity*, *36*, 542–550.

Pestka, J. M., Zeisel, M. B., Blaser, E., Schurmann, P., Bartosch, B., Cosset, F. L., et al. (2007). Rapid induction of virus-neutralizing antibodies and viral clearance in a single-source outbreak of hepatitis C. *Proceedings of the National Academy of Sciences*, *104*, 6025–6030.

Phan, T., Kohlway, A., Dimberu, P., Pyle, A. M., & Lindenbach, B. D. (2011). The Acidic Domain of Hepatitis C Virus NS4A Contributes to RNA Replication and Virus Particle Assembly. *Journal of Virology*, *85*, 1193–1204.

Poynard, T., Bedossa, P., & Opolon, P. (1997). Natural history of liver fibrosis progression in patients with chronic hepatitis C. *The Lancet*, *349*, 825–832.

Qu, K., Garamszegi, S., Wu, F., Thorvaldsdóttir, H., Liefeld, T., Ocana, M., et al. (2016). Integrative genomic analysis by interoperation of bioinformatics tools in GenomeSpace. *Nature Methods*, *13*, 245–247.

Raghuraman, S., Park, H., Osburn, W. O., Winkelstein, E., Edlin, B. R., & Rehermann, B. (2012). Spontaneous Clearance of Chronic Hepatitis C Virus Infection Is Associated With Appearance of Neutralizing Antibodies and Reversal of T-Cell Exhaustion. *Journal of Infectious Diseases*, *205*, 763–771.

Randall, G., Chen, L., Panis, M., Fischer, A. K., Lindenbach, B. D., Sun, J., et al. (2006). Silencing of USP18 Potentiates the Antiviral Activity of Interferon Against Hepatitis C Virus Infection. *Gastroenterology*, *131*, 1584–1591.

Ravasi, T., Suzuki, H., Cannistraci, C. V., Katayama, S., Bajic, V. B., Tan, K., et al. (2010). An atlas of combinatorial transcriptional regulation in mouse and man. *Cell*, *140*, 744–752.

Ray, S. C., & Thomas, D. L. (2015). 156 Hepatitis C. *Mandell, Douglas, and Bennett's Principles and Practice of Infectious Diseases* (Eighth Edition, pp. 1904–1927.e9).

Rehermann, B. (2009). Hepatitis C virus versus innate and adaptive immune responses: a tale of coevolution and coexistence. *Journal of Clinical Investigation*, *119*, 1745–1754.

Reich, M., Liefeld, T., Gould, J., Lerner, J., Tamayo, P., & Mesirov, J. P. (2006). GenePattern 2.0. *Nature Genetics*, *38*, 500–501.

Ritchie, M. D., Holzinger, E. R., Li, R., Pendergrass, S. A., & Kim, D. (2015). Methods of integrating data to uncover genotype-phenotype interactions. *Nature Reviews Genetics*, *16*, 85–97.

Rushbrook, S. M., Ward, S. M., Unitt, E., Vowler, S. L., Lucas, M., Klenerman, P., & Alexander, G. J. M. (2005). Regulatory T Cells Suppress In Vitro Proliferation of Virus-Specific CD8+ T Cells during Persistent Hepatitis C Virus Infection. *Journal of Virology*, *79*, 7852–7859.

Rutebemberwa, A., Ray, S. C., Astemborski, J., Levine, J., Liu, L., Dowd, K. A., et al. (2008). High-Programmed Death-1 Levels on Hepatitis C Virus-Specific T Cells during Acute Infection Are Associated with Viral Persistence and Require Preservation of Cognate Antigen during Chronic Infection. *The Journal of Immunology*, *181*, 8215–8225.

Sakaguchi, S., Yamaguchi, T., Nomura, T., & Ono, M. (2008). Regulatory T Cells and Immune Tolerance. *Cell*, *133*, 775–787.

Sarrazin, C., Hézode, C., Zeuzem, S., & Pawlotsky, J.-M. (2012). Antiviral strategies in hepatitis C virus infection. *Journal of Hepatology*, *56*, S88–S100.

Scheel, T. K. H., & Rice, C. M. (2013). Understanding the hepatitis C virus life cycle paves the way for highly effective therapies. *Nature Medicine*, *19*, 837–849.

Schena, M., Shalon, D., Davis, R. W., & Brown, P. O. (1995). Quantitative Monitoring of Gene Expression Patterns with a Complementary DNA Microarray. *Science*, *270*, 467–470.

Schmidhuber, J. (2015). Deep learning in neural networks: An overview. *Neural Networks*, *61*, 85–117.

Schoggins, J. W., Wilson, S. J., Panis, M., Murphy, M. Y., Jones, C. T., Bieniasz, P., & Rice, C. M. (2011). A diverse range of gene products are effectors of the type I interferon antiviral response. *Nature*, *472*, 481–485.

Schulze zur Wiesch, J., Ciuffreda, D., Lewis-Ximenez, L., Kasprowicz, V., Nolan, B. E., Streeck, H., et al. (2012). Broadly directed virus-specific CD4+ T cell responses are primed during acute hepatitis C infection, but rapidly disappear from human blood with viral persistence. *The Journal of Experimental Medicine*, *209*, 61–75.

Schulze zur Wiesch, J., Lauer, G. M., Day, C. L., Kim, A. Y., Ouchi, K., Duncan, J. E., et al. (2005). Broad Repertoire of the CD4+ Th Cell Response in Spontaneously Controlled Hepatitis C Virus Infection Includes Dominant and Highly Promiscuous Epitopes. *The Journal of Immunology*, *175*, 3603–3613.

Seeff, L. B. (2002). Natural history of chronic hepatitis C. *Hepatology (Baltimore, Md.)*, *36*, s35–s46.

Shannon, P. (2003). Cytoscape: A Software Environment for Integrated Models of Biomolecular Interaction Networks. *Genome Research*, *13*, 2498–2504.

Shaw, A. C., Goldstein, D. R., & Montgomery, R. R. (2013). Age-dependent dysregulation of innate immunity. *Nature Reviews Immunology*, *13*, 875–887.

Shay, T., & Kang, J. (2013). Immunological Genome Project and systems immunology. *Trends in Immunology*, *34*, 602–609.

Shin, E.-C., Sung, P. S., & Park, S.-H. (2016). Immune responses and immunopathology in acute and chronic viral hepatitis. *Nature Reviews Immunology*, *16*, 509–523.

Shoukry, N. H., Grakoui, A., Houghton, M., Chien, D. Y., Ghrayeb, J., Reimann, K. A., & Walker, C. M. (2003). Memory CD8 +T Cells Are Required for Protection from Persistent Hepatitis C Virus Infection. *The Journal of Experimental Medicine*, *197*, 1645–1655.

Simmonds, P., Bukh, J., Combet, C., Deléage, G., Enomoto, N., Feinstone, S., et al. (2005). Consensus proposals for a unified system of nomenclature of hepatitis C virus genotypes. *Hepatology (Baltimore, Md.)*, *42*, 962–973.

Smith, D. B., Bukh, J., Kuiken, C., Muerhoff, A. S., Rice, C. M., Stapleton, J. T., & Simmonds, P. (2013). Expanded classification of hepatitis C virus into 7 genotypes and 67 subtypes: Updated criteria and genotype assignment web resource. *Hepatology (Baltimore, Md.)*, *59*, 318–327.

Smyk-Pearson, S., Golden Mason, L., Klarquist, J., Burton, J. R., Tester, I. A., Wang, C. C., et al. (2008). Functional suppression by FoxP3+CD4+CD25(high) regulatory T cells during acute hepatitis C virus infection. *Journal of Infectious Diseases*, *197*, 46–57.

Subramanian, A., Tamayo, P., Mootha, V. K., Mukherjee, S., Ebert, B. L., Gillette, M. A., et al. (2005). Gene set enrichment analysis: A knowledge-based approach for interpreting genome-wide expression profiles. *Proceedings of the National Academy of Sciences*, *102*, 15545–15550.

Sugden, P. B., Cameron, B., Mina, M., & Lloyd, A. R. (2014). Protection against hepatitis C infection via NK cells in highly-exposed uninfected injecting drug users. *Journal of Hepatology*, *61*, 738–745.

Sulkowski, M. S. (2003). Hepatitis C in the HIV-Infected Person. *Annals of Internal Medicine*, *138*, 197.

Sung, P. S., Cheon, H., Cho, C. H., Hong, S.-H., Park, D. Y., Seo, H.-I., et al. (2015). Roles of unphosphorylated ISGF3 in HCV infection and interferon responsiveness. *Proceedings of the National Academy of Sciences*, *112*, 10443–10448.

Swadling, L., Capone, S., Antrobus, R. D., Brown, A., Richardson, R., Newell, E. W., et al. (2014). A human vaccine strategy based on chimpanzee adenoviral and MVA vectors that primes, boosts, and sustains functional HCV-specific T cell memory. *Science Translational Medicine*, *6*, 261ra153–261ra153.

Teschke, R. (2015). Hepatology Highlights. *Annals of Hepatology*, *14*, 772–773.

The Gene Ontology Consortium. (2015). Gene Ontology Consortium: going forward. *Nucleic Acids Research*, *43*, D1049–D1056.

Timm, J., Lauer, G. M., Kavanagh, D. G., Sheridan, I., Kim, A. Y., Lucas, M., et al. (2004). CD8 Epitope Escape and Reversion in Acute HCV Infection. *The Journal of Experimental Medicine*, *200*, 1593–1604.

Tripathi, P., Kurtulus, S., Wojciechowski, S., Sholl, A., Hoebe, K., Morris, S. C., et al. (2010). STAT5 Is Critical To Maintain Effector CD8+ T Cell Responses. *The Journal of Immunology*, *185*, 2116–2124.

UNODC. (2013). World Drug Report 2013. United Nations Office on Drugs and Crime. doi:10.18356/d30739c2-en

Villard, J., Peretti, M., Masternak, K., Barras, E., Caretti, G., Mantovani, R., & Reith, W. (2000). A functionally essential domain of RFX5 mediates activation of major histocompatibility complex class II promoters by promoting cooperative binding between RFX and NF-Y. *Molecular and Cellular Biology*, *20*, 3364–3376.

Wherry, E. J. (2011). T cell exhaustion. *Nature Immunology*, *131*, 492–499.

Wherry, E. J., & Kurachi, M. (2015). Molecular and cellular insights into T cell exhaustion. *Nature Reviews Immunology*, *15*, 486–499.

Wozniak, A. L., Griffin, S., Rowlands, D., Harris, M., Yi, M., Lemon, S. M., & Weinman, S. A. (2010). Intracellular Proton Conductance of the Hepatitis C Virus p7 Protein and Its Contribution to Infectious Virus Production. *PLoS Pathogens*, *6*, e1001087.

Wu, D., & Smyth, G. K. (2012). Camera: a competitive gene set test accounting for inter-gene correlation. *Nucleic Acids Research*, *40*, e133–e133.

Wu, D., Lim, E., Vaillant, F., Asselin-Labat, M. L., Visvader, J. E., & Smyth, G. K. (2010). ROAST: rotation gene set tests for complex microarray experiments. *Bioinformatics*, *26*, 2176–2182.

Xiao, F., Fofana, I., Heydmann, L., Barth, H., Soulier, E., Habersetzer, F., et al. (2014). Hepatitis C Virus Cell-Cell Transmission and Resistance to Direct-Acting Antiviral Agents. *PLoS Pathogens*, *10*, e1004128.

Yip, A. M., & Horvath, S. (2007). Gene network interconnectedness and the generalized topological overlap measure. *BMC Bioinformatics*, *8*, 22.

Zhang, B., & Horvath, S. (2005). A general framework for weighted gene co-expression network analysis., *4*, Article17.

Zhang, X., Bogunovic, D., Payelle-Brogard, B., Francois-Newton, V., Speer, S. D., Yuan, C., et al. (2014). Human intracellular ISG15 prevents interferon-α/β over-amplification and auto-inflammation. *Nature*, *517*, 89–93.

Page intentionally left blank

Appendix

Appendix A: Bystander Chronic Infection Negatively Impacts Development of CD8+ T Cell Memory.

Erietta Stelekati, Haina Shin, Travis A Doering, Douglas V Dolfi, Carly G Ziegler, Daniel P Beiting, Lucas Dawson, Jennifer Liboon, David Wolski, Mohammed-Alkhatim A Ali, Peter D Katsikis, Hao Shen, David S Roos, W Nicholas Haining, Georg M Lauer, and E John Wherry.

Immunity, 2014 vol. 40 (5) pp. 801-813.

Summary

This work examines bystander effects of chronic viral infection on immune responses targeted at unrelated pathogens. By flow-cytometric and gene expression analysis of CD8 T cell responses in both human HCV infection and a mouse LCMV model, it demonstrates impaired memory development in these cells that is associated with signatures of chronic inflammation. Validation of results from gene expression analysis of T cell responses in an adoptive transfer mouse experiment reveal that transcription factors T-bet and Blimp-1 are involved in the impairment of memory development in these cells. Showing that inflammation related to chronic viral infection has a negative effect on memory formation in cells unrelated to the primary infection, the results from this study have important implications for our understanding of immune responses in the context of long-term persisting infection, co-infections and vaccinations.

Immunity
Article

Bystander Chronic Infection Negatively Impacts Development of CD8$^+$ T Cell Memory

Erietta Stelekati,[1,2] Haina Shin,[1,2] Travis A. Doering,[1,2] Douglas V. Dolfi,[1,2] Carly G. Ziegler,[1,2] Daniel P. Beiting,[3] Lucas Dawson,[1,2] Jennifer Liboon,[1] David Wolski,[4] Mohammed-Alkhatim A. Ali,[1,2] Peter D. Katsikis,[5] Hao Shen,[1] David S. Roos,[3] W. Nicholas Haining,[6] Georg M. Lauer,[4] and E. John Wherry[1,2,*]
[1]Department of Microbiology
[2]Institute for Immunology
University of Pennsylvania Perelman School Medicine, Philadelphia, PA 19104, USA
[3]Department of Biology, University of Pennsylvania, Philadelphia, PA 19104, USA
[4]Gastrointestinal Unit, Massachusetts General Hospital, Harvard Medical School, Boston, MA 02114, USA
[5]Department of Microbiology and Immunology, Drexel University College of Medicine, Philadelphia, PA 19129, USA
[6]Department of Pediatric Oncology, Dana-Farber Cancer Institute and Division of Hematology/Oncology, Children's Hospital, Harvard Medical School, Boston, MA 02115, USA
*Correspondence: wherry@mail.med.upenn.edu
http://dx.doi.org/10.1016/j.immuni.2014.04.010

SUMMARY

Epidemiological evidence suggests that chronic infections impair immune responses to unrelated pathogens and vaccines. The underlying mechanisms, however, are unclear and distinguishing effects on priming versus development of immunological memory has been challenging. We investigated whether bystander chronic infections impact differentiation of memory CD8$^+$ T cells, the hallmark of protective immunity against intracellular pathogens. Chronic bystander infections impaired development of memory CD8$^+$ T cells in several mouse models and humans. These effects were independent of initial priming and were associated with chronic inflammatory signatures. Chronic inflammation negatively impacted the number of bystander CD8$^+$ T cells and their memory development. Distinct underlying mechanisms of altered survival and differentiation were revealed with the latter regulated by the transcription factors T-bet and Blimp-1. Thus, exposure to prolonged bystander inflammation impairs the effector to memory transition. These data have relevance for immunity and vaccination during persisting infections and chronic inflammation.

INTRODUCTION

Chronic infections with persisting pathogens including hepatitis viruses, *Plasmodium*, mycobacteria, or intestinal helminths affect billions of people. In some settings persistent pathogens, such as herpes viruses or GB virus C, can provide intrinsic resistance to unrelated microbes (Barton et al., 2007; Vahidnia et al., 2012). However, accumulating epidemiological evidence suggests that many chronic infections can increase susceptibility and pathology induced by unrelated pathogens. For example, intestinal helminth infections enhance *Mycobacterium tuberculosis* (Mtb)-induced pulmonary pathology (Resende Co et al., 2007) and increase the risk of developing chronic disease upon hepatitis C virus (HCV) infection (Kamal et al., 2001). Mathematical models indicate that malaria actively contributes to the increased rate of infection with HIV (Abu-Raddad et al., 2006), suggesting that dysregulated immunity due to a bystander chronic infection might be responsible for the increased incidence of other infections. Immunity to vaccines is reduced in subjects with chronic infections, suggesting that bystander chronic infections can also negatively impact responses to vaccination (Cooper et al., 2001; Nookala et al., 2004; Elias et al., 2008). Nevertheless, our current understanding of bystander infections and coinfections is based largely on epidemiological data with limited insight into the immunological mechanisms and potential therapeutic strategies to overcome these effects.

Several stages of a developing immune response might be affected by bystander chronic infections (Stelekati and Wherry, 2012). For example, initial entry of microbes or uptake of vaccines might be impacted by an altered mucosal environment due to chronic infections (van Riet et al., 2007). Persisting *Schistosoma* (Bahgat et al., 2010), Mtb (Zhang et al., 1995), or *Plasmodium* (Hawkes et al., 2010) infections can enhance replication of unrelated pathogens, resulting in increased pathogen load in coinfected individuals. Intrinsic defects in innate immune cells, such as natural killer (NK) cells (Morishima et al., 2006) or dendritic cells (DCs) (van Riet et al., 2007) in chronically infected individuals might potentiate defects in early innate immune responses. In addition to early changes in pathogenesis and/or innate immunity, an altered cytokine milieu due to unrelated persisting infections can substantially skew effector T cell differentiation, proliferation, and effector function (Harcourt et al., 2005; van Riet et al., 2007; Moorman et al., 2011).

Altered vaccine-induced immunity in chronically infected individuals suggests that immunological memory might be affected by bystander chronic infections. Indeed, type I interferons (IFN-I) produced by bystander acute viral infections or administration of Toll-like receptor (TLR) agonists, have been implicated in the erosion of preexisting memory CD8$^+$ T cells (McNally et al., 2001; Bahl et al., 2006). However, this attrition of preexisting memory due to subsequent acute infections is not observed in

all settings (Vezys et al., 2009; Odumade et al., 2012) and the role of chronically sustained versus acutely induced IFN-I remains poorly understood. The global impact of different types of bystander chronic coinfections that might or might not induce IFN-I suggests that mechanisms other than IFN-I might also contribute to a dysregulation of memory $CD8^+$ T cell development.

Here, we examined how different bystander chronic infections affect $CD8^+$ T cell memory differentiation and defined common molecular pathways associated with altered development of immunological memory. Chronic bystander infections substantially impaired the development of memory $CD8^+$ T cells, independent of initial priming in several mouse models of persisting viral or parasitic infection, with similar changes in humans chronically infected with HCV. Moreover, these changes in memory $CD8^+$ T cell differentiation were associated with a transcriptional imprint of IFN-I-inducible genes but could occur in the absence of direct signaling through the IFN-α and IFN-β receptor (IFNAR) on $CD8^+$ T cells exposed to bystander chronic infection. Bystander chronic infection and inflammation had a substantial impact on $CD8^+$ T cell survival during the effector to memory transition. In addition, we identified the downstream transcriptional regulators T-box 21 (T-bet) and B lymphocyte induced maturation protein 1 (Blimp-1) as molecular mediators of the effect of bystander inflammation on differentiation, but not survival. These data revealed two distinct mechanisms underlying altered $CD8^+$ T cell memory during coinfection. These results also suggested that, while upregulation of IFN-I-inducible genes is a symptom of this bystander effect, additional transcriptional mechanisms allow redundancy between inflammatory pathways that cause skewing of $CD8^+$ T cell differentiation during bystander chronic infections. Therefore, modulating sustained inflammatory signaling during the crucial phase of effector to memory transitioning might provide therapeutic opportunities to restore optimal vaccine responses in patients with persisting infections or chronic inflammatory conditions.

RESULTS

Chronic Bystander Infections Impair the Transition of $CD8^+$ T Cells from Effector to Memory

To investigate the role of chronic bystander infection in memory $CD8^+$ T cell development, we used persistent lymphocytic choriomeningitis virus (LCMV) clone 13 infection in mice. Naive mice or mice chronically infected with LCMV clone 13 (at day 30 postinfection; d30 p.i.) were infected with *Listeria monocytogenes*-expressing OVA (LM-OVA), and Kb-$OVA_{257–264}$-specific $CD8^+$ T cell responses were examined 30 days later. Although the frequency of Kb-$OVA_{257–264}$-specific $CD8^+$ T cells was higher in LCMV-infected mice compared to controls, the absolute number of Kb-$OVA_{257–264}$-specific $CD8^+$ T cells was not increased (data not shown). However, expression of molecules associated with memory differentiation, such as CD62L, CD27, and CXCR3 was reduced on the OVA-specific $CD8^+$ T cells in LCMV-infected mice compared to controls (see Figure S1 available online). In addition, the proportion of memory precursor cells, defined as $CD127^+KLRG1^-$ cells, was decreased, suggesting altered memory differentiation in the presence of bystander chronic LCMV infection.

To circumvent complications of changes in pathogen replication and/or pathogenesis due to altered innate immunity and/or antigen-presenting cell function during direct coinfection, we used adoptive transfer approaches to specifically examine the impact of bystander chronic infection on the transition of effector $CD8^+$ T cells into the memory pool. CD45.2 TCR-transgenic, $OVA_{257–264}$-specific (OT1) $CD8^+$ T cells were primed in congenic CD45.1 wild-type (WT) C57BL/6 mice with vesicular stomatitis virus-expressing OVA (VSV-OVA). On d8 p.i., equal numbers of these OT1 effector $CD8^+$ T cells were adoptively transferred into recipient CD45.1 mice that were naive (control), infected with the acute strain of LCMV Armstrong (at d8 p.i.), or infected with the persistent strain of LCMV clone 13 (at d8 p.i.). After 30 days, substantially reduced numbers of memory OT1 $CD8^+$ T cells were detected in multiple tissues of recipient mice infected with LCMV clone 13 compared to either naive recipients or the LCMV Armstrong infected recipients (Figure 1A; data not shown). This effect was not due to differences in the "take" after adoptive transfer (Figure S2). In addition, the OT1 $CD8^+$ T cells in mice transitioning to chronic infection had lower expression of the memory-associated molecules CD127, CXCR3, CD27, and CD62L and contained an increased proportion of terminally differentiated $KLRG1^+CD127^-$ cells, as well as fewer cells in the long-lived $CD127^+KLRG1^-$ memory pool (Figure 1B). Moreover, interleukin-2 (IL-2) or tumor necrosis factor alpha (TNF-α) cytokine coproduction with IFN-γ was reduced, although IFN-γ production alone was not dramatically impacted (Figure 1B). Similar results were obtained using a bacterial (LM-OVA) instead of a viral (VSV-OVA) infection for priming of $CD8^+$ T cells (Figure S2). The effect of bystander chronic infection was also observed when the d8 effector OT1 cells were adoptively transferred to chronically infected recipient mice at d30 (Figures S3A and S3B) or at d120 of chronic LCMV infection (Figures S3C and S3D), though the magnitude of the impact of bystander chronic infection on the developing memory $CD8^+$ T cells declined as the severity of infection decreased over time. Thus, chronic bystander viral infection, in striking contrast to acutely resolved viral infection, impairs the efficient transition of $CD8^+$ T cells from effector to memory.

We next examined whether these observations could be extended to other chronic bystander infections that, for example, induce high amounts of IL-12, compared to the IFN-I biased LCMV infection. For this reason, we used the protozoan parasite *Toxoplasma gondii* (*T. gondii*). Effector (d8) OT1 $CD8^+$ T cells adoptively transferred into mice transitioning to a chronic infection with *T. gondii* (at d8 p.i.) exhibited altered memory CD8 T cell development, with reduced numbers of OT1 cells (Figure 2A). Bystander chronic *T. gondii* infection also impaired memory $CD8^+$ T cell differentiation, by reducing the expression of memory-associated molecules, increasing the proportion of terminally differentiated effector cells ($KLRG1^+CD127^-$) and significantly impairing cytokine production (Figure 2B). These data highlight a common effect of bystander chronic viral and parasitic infections and prolonged or chronic inflammation in substantially disrupting memory $CD8^+$ T cell development.

Because both LCMV and *T. gondii* induce sustained T helper 1 (Th1)-type inflammation, we further extended these

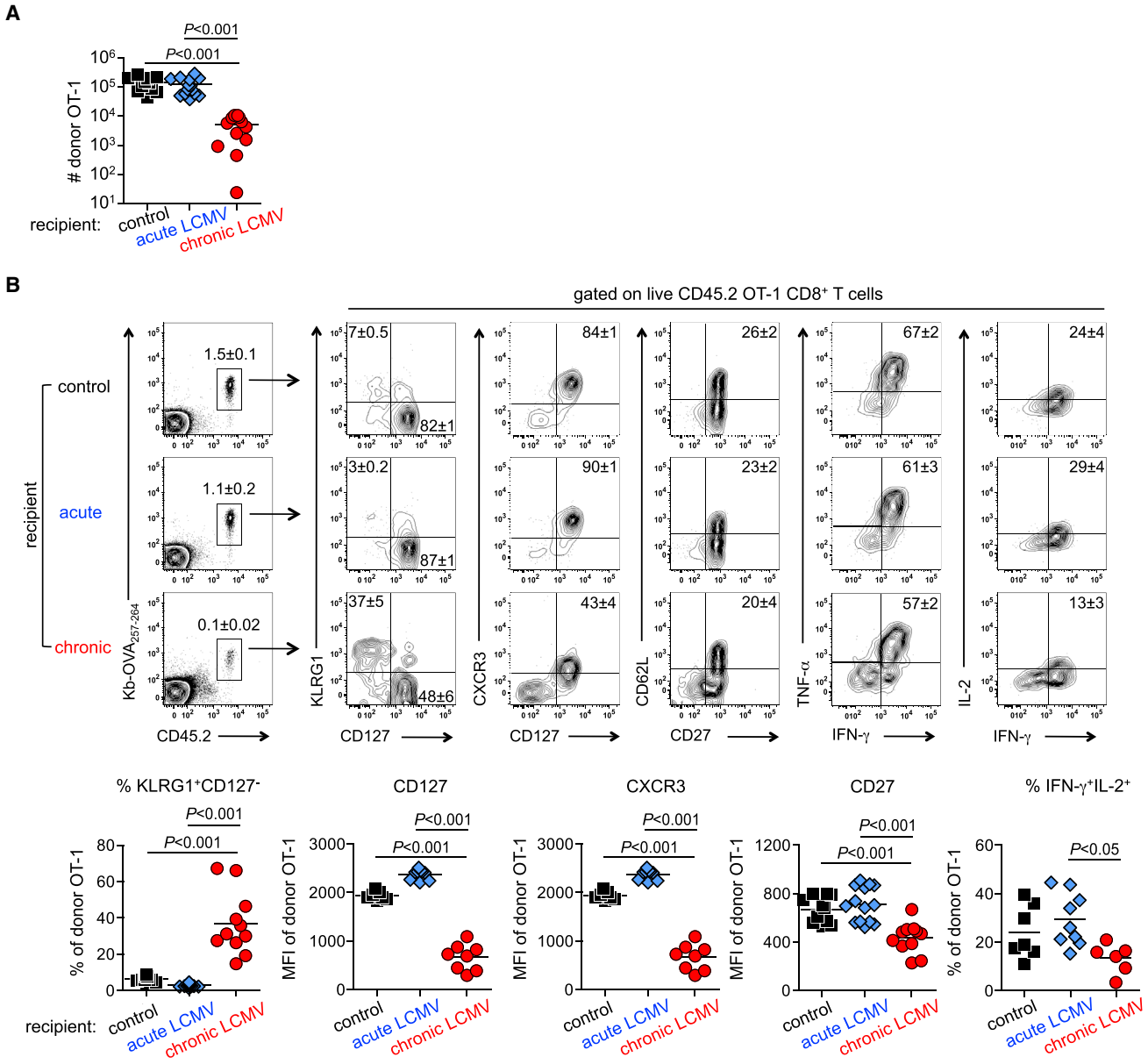

Figure 1. Bystander Chronic Viral Infection Disrupts the Effector to Memory Transition of CD8+ T Cells

CD45.2 OT1 CD8+ T cells were adoptively transferred to congenic CD45.1 mice. Recipients were infected with VSV-OVA. On d8 p.i., splenic CD45.2 OT1 CD8+ T cells were isolated and adoptively transferred to "control" (naive), "acute LCMV" (d8 post-LCMV Armstrong infection), or "chronic LCMV" (d8 post-LCMV clone 13 infection) recipient CD45.1 mice.

(A) OT1 cells were quantified in spleens 30 days posttransfer.

(B) Phenotype and cytokine production of OT1 cells were analyzed 30 days posttransfer in spleens (n > 9). Similar results were obtained from blood, liver, and bone marrow (BM; data not shown). Numbers on FACS plots indicate frequencies of respective populations ± SEM. Statistical significance was calculated with one-way ANOVA for normally distributed samples and Kruskal-Wallis test for nonequally distributed samples.

observations to a chronic helminth infection (*Heligmosomoides polygyrus*; *H. polygyrus*), inducing Th2-type inflammation. After adoptive transfer of effector (d8) OT1 CD8+ T cells, the numbers of memory OT1 cells recovered from mice chronically infected with *H. polygyrus* were reduced compared to control naive recipient mice (Figure S4A). Acquisition of key memory CD8+ T cell differentiation properties was also altered in the presence of bystander *H. polygyrus* infection, though not as dramatically as in the presence of chronic bystander LCMV or *T. gondii* infection (Figure S4B). Together, these data indicated an effect of bystander chronic viral or parasitic infections that induce different inflammatory environments, on the transition of effector CD8+ T cells into the memory pool. Disruption of these key differentiation events resulted in failure to appropriately undergo phenotypic and functional maturation associated with the effector to memory transition.

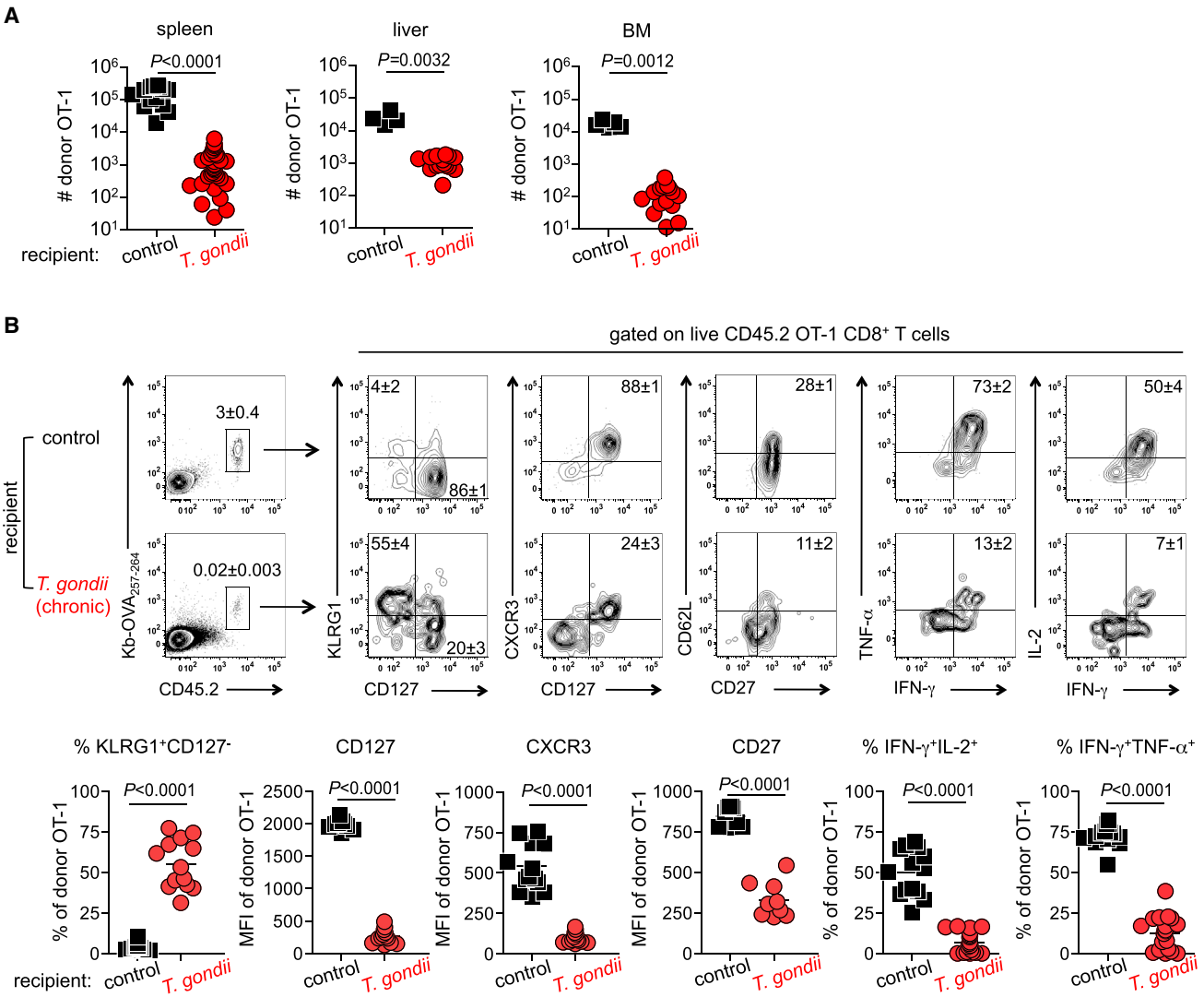

Figure 2. Bystander Chronic Parasitic Infection Disrupts the Effector to Memory Transition of CD8+ T Cells

CD45.2 OT1 CD8+ T cells were adoptively transferred to congenic CD45.1 mice. Recipients were infected with VSV-OVA. On d8 p.i., splenic CD45.2 OT1 CD8+ T cells were isolated and adoptively transferred to "control" (naive) or "*T. gondii*" (d8 post-*T. gondii* infection) recipient CD45.1 mice.

(A) OT1 cells were quantified in spleens, livers, and BM 30 days posttransfer.

(B) Phenotype and cytokine production of OT1 cells were analyzed 30 days posttransfer in spleens (n > 9). Similar results were obtained from blood, liver, and BM (data not shown). Numbers on FACS plots indicate frequencies of respective populations ± SEM. Statistical significance was calculated with two-tailed unpaired t test for normally distributed samples or Mann Whitney test for nonequally distributed samples.

Bystander Infections Impair Secondary Expansion and Protective Immunity of Memory CD8+ T Cells

Changes in the phenotypic markers of memory CD8+ T cell differentiation described above can be symptomatic of broader changes in the memory CD8+ T cell differentiation program. To test this, we examined two fundamental properties of memory CD8+ T cells: rapid recall response and protective immunity. Equal numbers of memory OT1 cells that had been exposed or not to bystander chronic *T. gondii* infection during their effector to memory differentiation (d8 until d40), were adoptively transferred to naive recipient mice that were subsequently challenged with LM-OVA. Upon secondary challenge, expansion of OT1 cells exposed to chronic infection was reduced ~10-fold compared to control OT1 cells (Figure 3A). When recipients were challenged with a higher dose of LM-OVA, control OT1 cells tended to provide better protection than OT1 cells exposed to bystander chronic infection, by increasing the median survival of recipient mice by 4.5 days (from 5.5 to 10 days) (Figure 3B). These results suggested that, in addition to causing attrition of memory CD8+ T cell numbers and skewing memory differentiation, bystander chronic infection impacted the secondary expansion and protective capacity of developing memory CD8+ T cells.

Chronic Bystander Infection Can Affect Preformed Memory CD8+ T Cells

To investigate whether these effects of bystander persisting infections were dependent on the differentiation stage of CD8+ T cells, we asked whether preformed memory CD8+ T cells

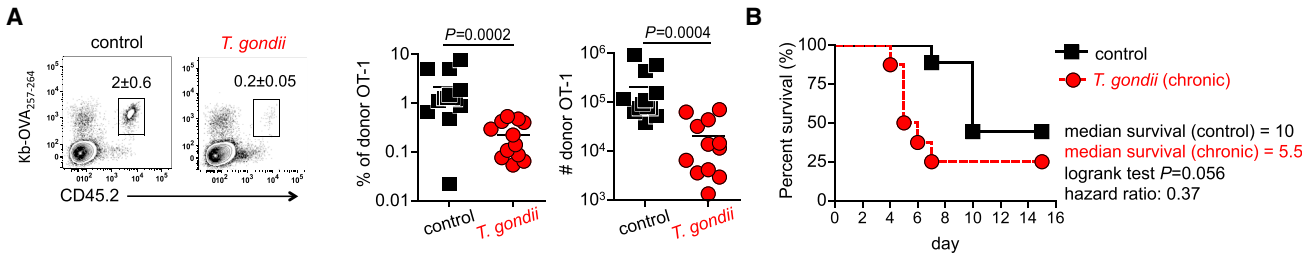

Figure 3. Bystander Chronic Infection Negatively Impacts Secondary Expansion and Protective Immunity of Memory CD8+ T Cells

CD45.2 OT1 CD8+ T cells were adoptively transferred to congenic CD45.1 mice. Recipients were infected with VSV-OVA. On d8 p.i., splenic CD45.2 OT1 CD8+ T cells were isolated and adoptively transferred to "control" (naive) or "*T. gondii*" (d8 post-*T. gondii* infection) recipient CD45.1 mice. Thirty days later, CD8+ T cells were purified and equal numbers (2×10^3) of donor OT1 cells were transferred to naive recipients that were subsequently challenged with LM-OVA. (To ensure equal potential transfer of inflammatory cells and/or mediators from *T. gondii*-infected mice, we mixed "control" cells with splenocytes from *T. gondii*-infected mice that did not contain OT1 cells and "chronic *T. gondii*" cells were mixed with splenocytes from naive mice that did not contain OT1 cells, at 1:1 ratio.)

(A) Expansion of donor OT1 cells was quantified in spleens 5 days after challenge with 8×10^4 LM-OVA (n > 12). Statistical significance was calculated with Mann-Whitney test.

(B) Survival of recipients that were challenged with 8×10^5 LM-OVA (n = 8–9).

would be impacted by bystander chronic infection. Thus, we adoptively transferred effector (d8 p.i.) or fully-formed memory (1 year p.i.) OT1 CD8+ T cells into naive or mice infected with LCMV clone 13 (Figure S5A). Persistence of memory CD8+ T cells was affected in chronically infected recipients (Figure S5B), in agreement with previous reports on the role of LCMV-induced attrition of preformed memory cells (McNally et al., 2001; Kim and Welsh, 2004). However, the effect of bystander chronic infection on the differentiation of preformed memory CD8+ T cells was not as prominent as the effect on transitioning d8 effector CD8+ T cells. For the effector CD8+ T cells transitioning to memory during bystander chronic infection, there was a profound reduction in both amount of CD127 and CXCR3 expressed at the cell surface, as well as the frequency of CD127+KLRG1− cells, as observed above. In contrast, although there was a decrease in the amount of CD127 and CXCR3 expressed per cell for fully-formed memory OT1 cells, the frequency of CD127+KLRG1− memory cells was not affected in the presence of bystander chronic infection (Figure S5C). These results suggest that fully-formed memory CD8+ T cells are less susceptible, though not impervious, to the effects of bystander chronic inflammation. These observations placed emphasis on understanding the particular potent impact of bystander chronic infections specifically during the critical phase of transitioning from effector to memory.

Chronic Bystander Infection Directly Impacts Memory Precursor CD8+ T Cells

Effector CD8+ T cell populations consist of memory precursors and terminally differentiated effector cells (Joshi et al., 2007). The effect of bystander chronic infection on the effector to memory transition could either be due to enhanced survival of terminal effectors or a direct impact on the developmental program of memory precursors. To distinguish between these possibilities, we purified memory precursor (CD127+KLRG1−) OT1 CD8+ T cells at d8 p.i. and adoptively transferred these cells into naive or recipients infected with the persistent strain LCMV clone 13 (Figure 4A). Recovery of OT1 memory CD8+ T cells 30 days later was reduced in mice infected with LCMV clone 13 (Figure 4B). Further, these cells had decreased expression of CD127 and moderately increased KLRG1 expression (Figure 4C). These results indicate a role for bystander chronic infection in directly impacting memory precursor CD8+ T cells in the posteffector phase by decreasing their survival and diverting their differentiation away from long-lived memory CD8+ T cells.

Bystander Infection Affects the Survival of Transitioning Memory CD8+ T Cells during Contraction

To interrogate the mechanism for the reduced recovery of transitioning OT1 memory CD8+ T cells in the presence of bystander persisting infection, we examined the survival of OT1 cells after in vitro culture with or without the T cell survival factor interleukin-7 (IL-7). OT1 cells that had been exposed to bystander chronic LCMV infection, survived less well in vitro with or without IL-7 (Figure S6A). We then examined pathways associated with contraction of effector CD8+ T cells to examine how these might be affected by bystander chronic infection. Contraction of CD127Lo terminal effector CD8+ T cells is mediated by the Bcl-2-interacting mediator of cell death (Bim) (Wojciechowski et al., 2006). We observed substantially increased expression of Bim in terminally differentiated KLRG1+CD127− OT1 cells that had been exposed to bystander chronic infection (Figure S6B), suggesting an increased propensity to die. On the other hand, central memory T cells have been shown to be more sensitive to TNF-α induced apoptosis compared to effector memory cells (Gupta et al., 2006) and TNF signaling through type 2 tumor necrosis factor receptor (TNFR2) was shown to also contribute to the contraction of CD8+ T cells upon influenza infection (Wortzman et al., 2013). We observed a significant increase in TNFR2 expression, specifically in the memory precursor subset (CD127+KLRG1−) of OT1 cells during bystander chronic infection (Figure S6B). Consistent with the results that bystander chronic infection skews the differentiation of memory precursor cells into terminally differentiated cells (see Figure 4), these results suggest a dual role of bystander chronic infection in affecting survival during the transition of effector CD8+ T cells to memory; CD8+ T cells are skewed to a more terminal effector phenotype and survival of both memory precursors and terminally differentiated cells is decreased in the presence of bystander chronic infection.

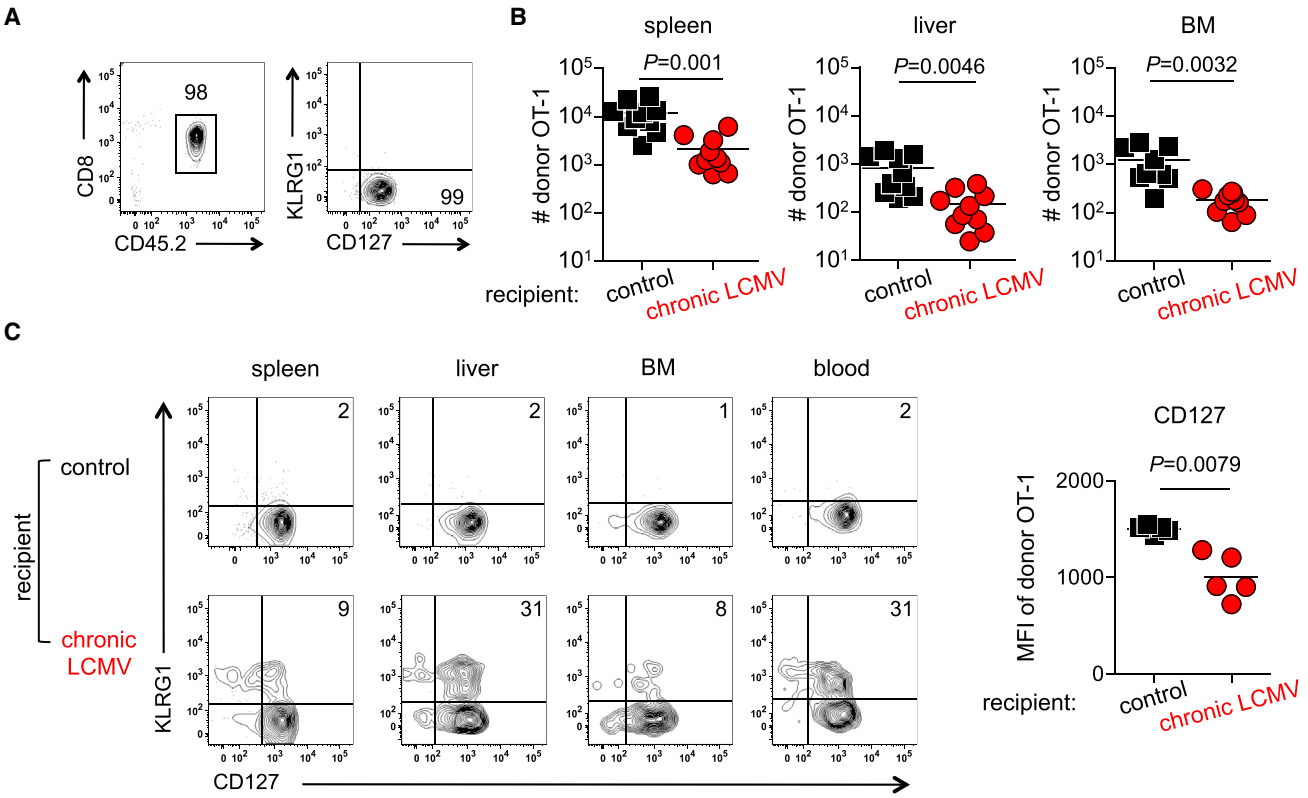

Figure 4. Bystander Chronic Infection Affects Memory Precursor CD8+ T Cells

CD45.1 mice containing CD45.2 OT1 cells were infected with VSV-OVA. On d8 p.i., CD127+KLRG1− CD45.2 OT1 CD8+ T cells were purified by FACS and adoptively transferred to "control" (naive) or "chronic LCMV" (d8 post-LCMV clone 13 infection) recipient CD45.1 mice.

(A) Purity of sorted OT1 cells.

(B) Numbers of OT1 cells were determined on d30 posttransfer (n > 9). Statistical significance was calculated with two-tailed unpaired t test.

(C) Phenotype of OT1 cells on d30 posttransfer (n > 9). FACS plots are gated on live OT1 CD45.2 CD8+ T cells and numbers indicate frequencies of respective populations. Statistical significance was calculated with two-tailed Mann Whitney test.

A Prominent Signature of Inflammatory Pathways in Memory CD8+ T Cells during Bystander Infection

To investigate the molecular mechanisms underlying the impact of bystander infection in skewing memory CD8+ T cell differentiation, we analyzed the gene-expression profiles of OT1 memory cells that had been exposed to bystander chronic LCMV infection during their transition from effector to memory. The transcriptional signature of purified OT1 memory cells exposed to chronic bystander infection was distinct from memory CD8+ T cells that developed in the control mice and revealed prominent upregulation of IFN-I-responsive genes (Figure 5A). By using Gene Set Enrichment Analysis (GSEA; Subramanian et al., 2005) we asked whether previously defined transcriptional signatures of inflammatory pathways or infections showed enrichment toward the transcriptional profile of OT1 cells exposed to bystander chronic infection (from Figure 5A). First, we compared these OT1 transcriptional signatures to previously defined transcriptional signatures of IFN-I and IL-12-regulated genes (Agarwal et al., 2009). The transcriptional signatures of T cells stimulated in vitro with IFN-I or IL-12 showed a robust enrichment toward the OT1 cells exposed to bystander chronic LCMV infection (Figure 5B). Further, inflammatory transcriptional signatures associated with TLR stimulation, such as those induced in dendritic cells by lipopolysaccharide (LPS) or R848 stimulation (Napolitani et al., 2005) and by CpG or Pam3CSK4 stimulation (Amit et al., 2009) also showed a significant enrichment in the transcriptional profile of OT1 cells exposed to bystander chronic LCMV infection (Figures 5C and 5D). Thus, transcriptional profiling of memory CD8+ T cells exposed to bystander persisting LCMV infection during the effector to memory transition suggested a prominent imprint of prolonged microbial stimulation and/or exposure to inflammatory cytokines.

These global gene-expression profiles also allowed us to ask whether the effects of bystander chronic infection extended beyond mouse models. The transcriptional signatures of human peripheral blood mononuclear cells (PBMC) from several viral and microbial infections were significantly enriched in the OT1 cells exposed to chronic LCMV infection (Figure 5E), suggesting that transcriptional changes associated with the bystander effect of CD8+ T cell memory in mice could be found in multiple infections in humans. These results also suggested that although acute inflammation is beneficial during priming, that same inflammatory signature might become detrimental if it is prolonged beyond the priming phase. We extended these human studies by generating the transcriptional signatures of cytomegalovirus (CMV)-specific CD8+ T cells from individuals with

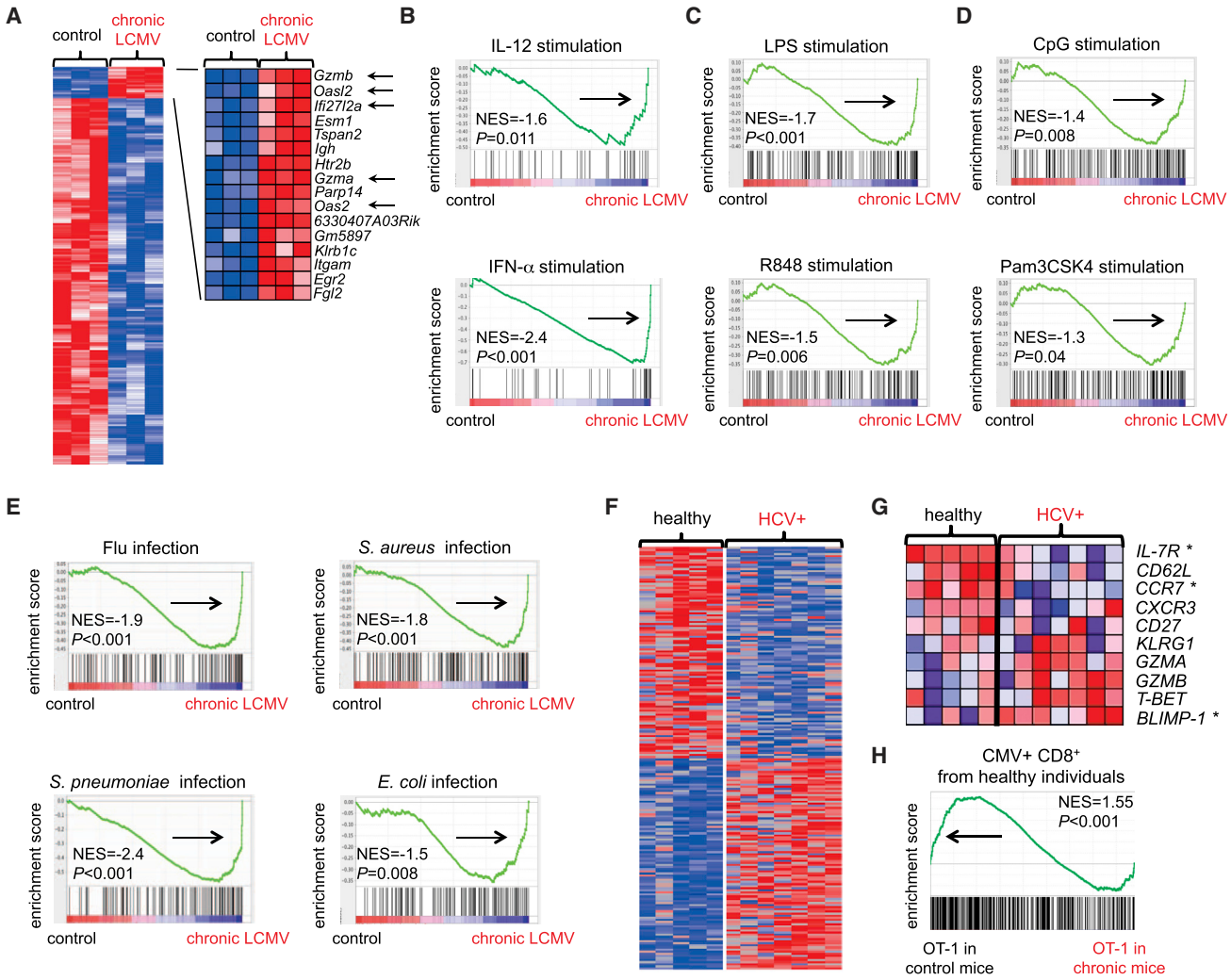

Figure 5. Gene-Expression Profiling Reveals a Prominent Imprint of Inflammatory Pathways in Memory Cells Exposed to Bystander Chronic Infection

(A) CD45.2 OT1 CD8+ T cells were primed in congenic CD45.1 mice following infection with VSV-OVA. On d8 p.i., splenic CD45.2 OT1 CD8+ T cells were isolated and adoptively transferred to "control" (naive) or "chronic LCMV" (d8 post-LCMV-infection) recipient CD45.1 mice. After 30 days, CD45.2 OT1 cells were sorted and microarray analysis was performed (n = 3). Heat map shows differentially expressed genes (>1.2-fold change, $p < 0.05$) in OT1 cells from "control" versus "chronic LCMV" mice. Arrows indicate IFN-I-regulated genes.

(B–E) GSEA was performed to compare: (B) the sets of upregulated genes in T cells during differentiation in vitro in the presence of IL-12 or IFN-I or 48 hr (Agarwal et al., 2009), (C) the sets of upregulated genes in dendritic cells upon stimulation with LPS or R848 for 2 hr (Napolitani et al., 2005), (D) the sets of upregulated genes in dendritic cells upon stimulation with CpG or Pam3CSK4 for 1 hr (Amit et al., 2009), (E) the sets of upregulated genes in human PBMC upon infection (Ramilo et al., 2007) with the transcriptional profile of memory OT1 CD8+ T cells purified from "control" or "chronic LCMV" mice (from Figure 5A). Normalized enrichment scores (NES) with statistical significance (p values), were calculated by GSEA. A negative enrichment score suggests that the transcriptional signature of interest was enriched toward the transcriptional profile of OT1 cells exposed to bystander chronic LCMV infection.

(F–H) Human CMV-specific CD8+ T cells were purified from PBMC obtained from subjects with persistent HCV viremia (infected for >1 year) and from healthy volunteers. (F) Heatmap shows top 50 genes differentially expressed between CMV-specific CD8+ T cells from healthy versus HCV-infected subjects. (G) Gene expression of memory-associated genes in CMV-specific CD8+ T cells from healthy and HCV-infected individuals. *$p < 0.05$. (H) Enrichment plot by GSEA comparing the set of upregulated genes (>2-fold) in CMV-specific CD8+ T cells from healthy individuals with the transcriptional profile of memory OT1 cells purified from "control" or "chronic LCMV" mice (from Figure 5A).

bystander chronic HCV infection and healthy controls (Figure 5F). Human CMV-specific (HLA-A*0201-NLVPMVATV or HLA-B*0702-TPRVTGGGAM tetramer-positive) CD8+ T cells were purified from PBMC of subjects with persistent HCV viremia (infected for >1 year) or from healthy volunteers and transcriptional profiling performed (Table S1). These gene-expression profiles revealed a clear impact of bystander chronic HCV infection on CMV-specific CD8+ T cells, including differential expression of many key CD8+ T cell memory-related genes (Figure 5G). The transcriptional signature of CMV-specific CD8+ T cells from healthy individuals was enriched in the OT1 CD8+ T cells from control, but not from chronically infected mice (Figure 5H),

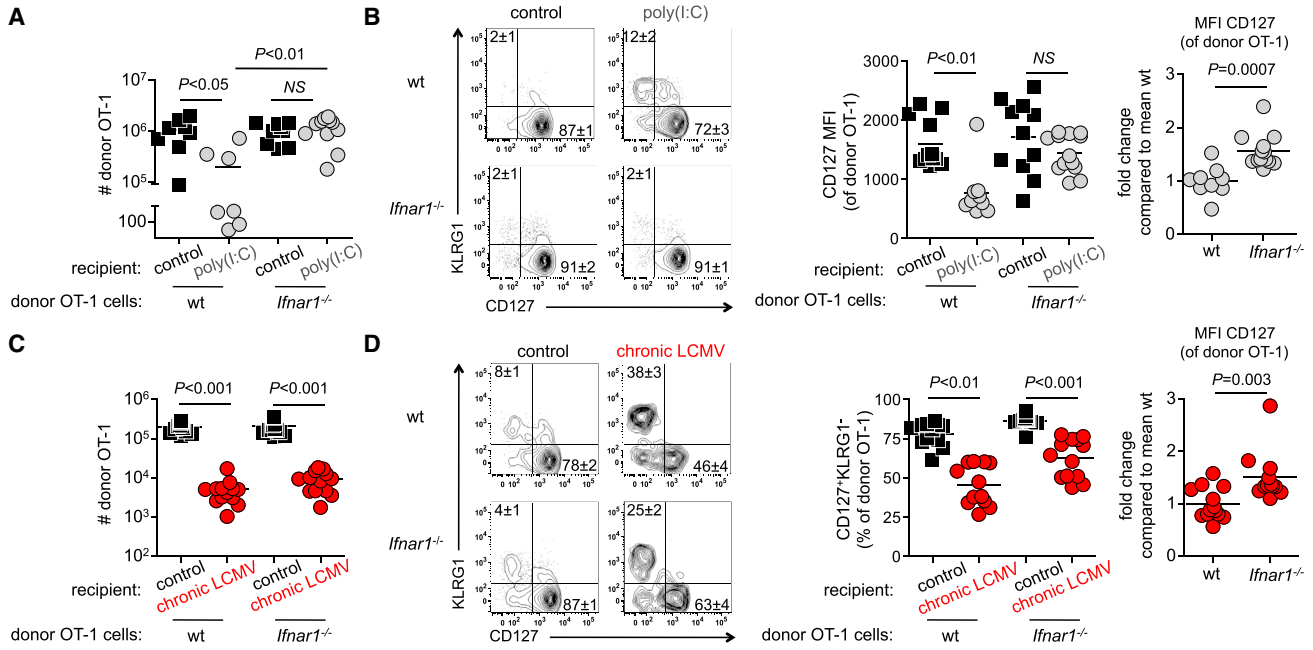

Figure 6. Prolonged IFNAR Signaling Disrupts the Transition of CD8+ T Cells from Effector to Memory

(A and B) WT or *Ifnar1*$^{-/-}$ CD45.2 OT1 CD8+ T cells were primed in recipient CD45.1 mice upon infection with VSV-OVA. Starting on d8 p.i., mice were administered 100 μg poly(I:C) or PBS (control) i.p. every 3 days. (A) Number of OT1 cells was determined in spleens on d40 p.i. (n > 10). Similar results were obtained from livers and BM (data not shown). Statistical significance was calculated with two-tailed Mann Whitney test. (B) Phenotype of OT1 cells was analyzed in spleens on d40 p.i. (n > 10). Similar results were obtained from livers and BM (data not shown). MFI of CD127 on donor OT1 cells in poly(I:C)-treated mice was normalized to the mean measurements of WT OT1 cells in poly(I:C)-treated mice from each experiment. Statistical significance was calculated with two-tailed unpaired t test.

(C and D) CD45.1 mice containing adoptively transferred CD45.2 *Ifnar1*$^{-/-}$ (n = 12) or littermate control WT OT1 CD8+ T cells were infected with VSV-OVA. On d8 p.i., OT1 cells were adoptively transferred to "control" (naive) or "chronic LCMV" (at d8 post-LCMV clone 13 infection) recipient mice. (C) Numbers and (D) phenotype of donor OT1 cells were analyzed in spleens 40 days later. MFI of CD127 on donor OT1 cells in "chronic LCMV" mice was normalized to the mean measurements of WT OT1 cells in "chronic LCMV" mice from each experiment. FACS plots are gated on live OT1 CD45.2 CD8+ T cells and numbers indicate frequencies ± SEM. n.s., not significant.

consistent with the findings that chronic viral and parasitic infections in mouse models skew bystander CD8+ T cells away from normal memory development. These studies revealed a fundamental shared phenomenon of many bystander chronic infections that transcends species and infection type. Moreover, these data implicate chronic exposure to inflammation and downstream inflammation-driven gene expression.

IFN-I Impairs the Transition from Effector to Memory in the Absence of Infection

The robust enrichment of IFN-related genes in CD8+ T cells undergoing memory differentiation in the presence of chronic bystander infections led us to examine the impact of prolonged induction of IFN-I and related inflammatory pathways on memory CD8+ T cell development in the absence of chronic infection. Serial infections can cause attrition of preformed memory CD8+ T cells, an effect attributed to IFN-I (McNally et al., 2001; Kim and Welsh, 2004). However, the impact of chronic IFN-I on effector CD8+ T cells transitioning to memory, as well as the effects on the differentiation program of the resulting memory CD8+ T cells remain poorly understood. To examine this issue, we infected mice containing OT1 cells with VSV-OVA. Starting on d8 p.i., mice were treated every 3 days with poly(I:C), a potent inducer of IFN-I and other inflammatory pathways. Prolonged exposure to poly(I:C) resulted in a progressive loss of OT1 cells (Figure 6A), consistent with the previously described IFN-I-induced attrition (McNally et al., 2001; Kim and Welsh, 2004). However, this treatment also caused a skewed pattern of terminal effector CD8+ T cell differentiation (KLRG1+CD127−) (Figure 6B). These effects were dependent on the expression of IFNAR on CD8+ T cells, because *Ifnar1*$^{-/-}$ OT1 CD8+ T cells developed into CD127+KLRG1− memory cells, even in the presence of poly(I:C)-induced chronic inflammation (Figures 6A and 6B). Similar results were observed following priming with LM-OVA, instead of VSV-OVA (data not shown). Thus, prolonged exposure to poly(I:C)-induced inflammation after clearance of the primary infection recapitulated key aspects of bystander chronic infection, suggesting that chronic inflammatory signals can skew memory development, even in the absence of pathogen.

IFNAR Signaling in CD8+ T Cells Is Crucial during poly(I:C) Treatment but Not Bystander Infection

Although IFN-I is rapidly induced early during many infections, IFN-I production rapidly declines during some chronic infections including LCMV (Zuniga et al., 2008; Ye and Maniatis, 2011), raising the question of whether IFN-I alone could be the signal that caused altered CD8+ T cell memory development during chronic bystander infections. To directly test this possibility,

we examined whether signals through IFNAR were required for the skewed memory CD8+ T cell differentiation during bystander chronic LCMV infection. We adoptively transferred *Ifnar1*$^{-/-}$ OT1 effector CD8+ T cells into control mice or mice infected with persistent LCMV. Absence of IFNAR on OT1 cells did not restore the numerical defects induced by bystander infection (Figure 6C) and led to only a minor impact on the differentiation of OT1 cells during chronic LCMV infection (Figure 6D), despite fully reversing the effect of chronic poly(I:C) administration (Figures 6A and 6B). These results suggested that CD8+ T cell intrinsic IFN-I signaling alone could not fully explain the impact of bystander chronic LCMV infection on memory CD8+ T cell differentiation. Lack of IFN-γR or IL-12R on OT1 cells also did not restore normal memory CD8+ T cell numbers or differentiation during bystander chronic LCMV infection (data not shown). Additionally, by using IFN-γ blocking antibodies in vivo in combination with *Ifnar1*$^{-/-}$ OT1 cells did not improve OT1 memory development (data not shown). Because IFN-α, IFN-β, IFN-γ, and IL-12 can have redundant effects during priming of CD8+ T cells (Haring et al., 2006; Curtsinger and Mescher, 2010), it was possible that different inflammatory pathways had overlapping roles in the detrimental effects of bystander chronic infection. This notion is also consistent with the effects of bystander chronic infection on memory CD8+ T cell development observed during different chronic infections, including the IFN-inducing chronic LCMV, the IL-12-inducing *T. gondii*, and the Th2-type *H. polygyrus* infections.

T-bet and Blimp-1 Regulate Defective Transitioning to Memory during Bystander Chronic Infection

Diverse inflammatory signals can influence T cell differentiation by accessing common transcriptional coordinators of differentiation. Two such transcription factors, T-bet and Blimp-1, are known to have a role in integrating inflammation and antigen signals during priming (reviewed in Kaech and Cui, 2012). However, it is not clear whether these transcription factors have a role in the antigen-independent phase of memory CD8+ T cell differentiation. To test this idea, we used *Prdm1*$^{fl/fl}$ *Gzmb*-Cre mice (in which Blimp-1 was deleted only in CD8+ T cells) or T-bet-heterozygous (*Tbet*$^{+/-}$) effector OT1 CD8+ T cells, generated with VSV-OVA priming. We then adoptively transferred these effector cells into control or mice infected with persistent LCMV and examined the effector to memory transition. The total number of either Blimp-1 or T-bet deficient OT1 CD8+ T cells remained reduced in the mice infected with LCMV clone 13 compared to controls (Figure S7), suggesting that the Bim and TNFR2 effects on the contraction of developing bystander memory CD8+ T cells are independent of these transcription factors. However, Blimp-1 or T-bet deficiency completely abrogated the negative impact of bystander infection on memory CD8+ T cell differentiation, because *Prdm1*$^{fl/fl}$ *Gzmb*-Cre and *Tbet*$^{+/-}$ OT1 cells differentiated into CD127+KLRG1−CXCR3+ memory CD8+ T cells in the presence of bystander infection (Figure 7). Thus, Blimp-1 and T-bet, in addition to transiently integrating antigen and inflammation during the effector T cell expansion (Kaech and Cui, 2012), are also critically involved in sensing prolonged inflammation in the absence of antigen and skewing memory CD8+ T cell differentiation during bystander chronic infections. Together, these data suggest a model where bystander chronic infection and prolonged inflammation impact long-term survival, as well as differentiation of developing memory CD8+ T cells through independent mechanisms.

DISCUSSION

We revealed a pervasive impact of bystander chronic infections and inflammation on immunological memory in multiple settings. Specifically, we found a major unappreciated effect on the transition of optimally primed effector CD8+ T cells into robust memory CD8+ T cell populations. Distinct effects of bystander chronic infection and inflammation on the number of memory CD8+ T cells and on the differentiation program of long-lived memory CD8+ T cells were revealed. The latter effect could be restored by specific CD8+ T cell-intrinsic deficiency of T-bet or Blimp-1. Chronic poly(I:C) treatment recapitulated the known role of IFN-I-associated attrition in viral infections, and a prominent signature of IFN-I-inducible genes pointed to an effect of IFN-I. However, although intrinsic IFNAR deficiency in CD8+ T cells abrogated the effect of chronic poly(I:C) treatment, it did not reverse the effect of bystander chronic LCMV infection. These observations collectively suggest that during actual chronic bystander infection, multiple inflammatory pathways might alter the ability of effector CD8+ T cells to efficiently transition to memory and develop canonical memory CD8+ T cell properties. Our mouse studies are supported by human CMV responses. Although it is not possible to define the timing of CMV versus HCV acquisition or exclude potential changes in the reactivation or viral activity of CMV, the persisting "smoldering" nature of CMV infection suggests that at any given time, some fraction of the CMV-specific CD8+ T cells will be in transition from recent antigen encounter and an "effector" status to resting memory, allowing the imprint of HCV infection on these differentiation events to be detected. It is possible that there might be more CMV replication in the setting of chronic HCV infection, a possibility that might warrant further investigation, but the impact on memory CD8+ T cell differentiation was similar to that observed in the mouse models, suggesting a bystander effect of chronic HCV. It should be noted that while we observed an increase in transcripts encoding memory-associated genes expressed by CMV-specific CD8+ T cells in healthy versus HCV-infected subjects, this does not mean that these cells are more "central memory"-like, because this is only a relative comparison and the CMV-specific CD8 T cells from healthy controls expressed lower amounts of these transcripts compared to naïve T cells. Thus, although the precise pathogenesis of CMV and HCV is different than the mouse pathogens used here, the imprint of bystander chronic infection and prolonged inflammation is conserved between species. Although our studies support a negative impact of different Th1 and Th2-inducing viral and parasitic bystander chronic infections on memory CD8+ T cell development, the effect of other types of infections and/or chronic inflammatory conditions remains to be investigated. Coinfections have long been thought to influence innate immunity, naive to effector T cell differentiation, and skewing of helper T cell lineage (e.g., Th1 versus Th2). These current observations place major emphasis on memory formation and the effector to memory transition as a critical effect of coinfection on long-term immune memory.

Initial priming of CD8+ T cells requires three signals: signal 1 from antigen, signal 2 from costimulation, and signal 3 from

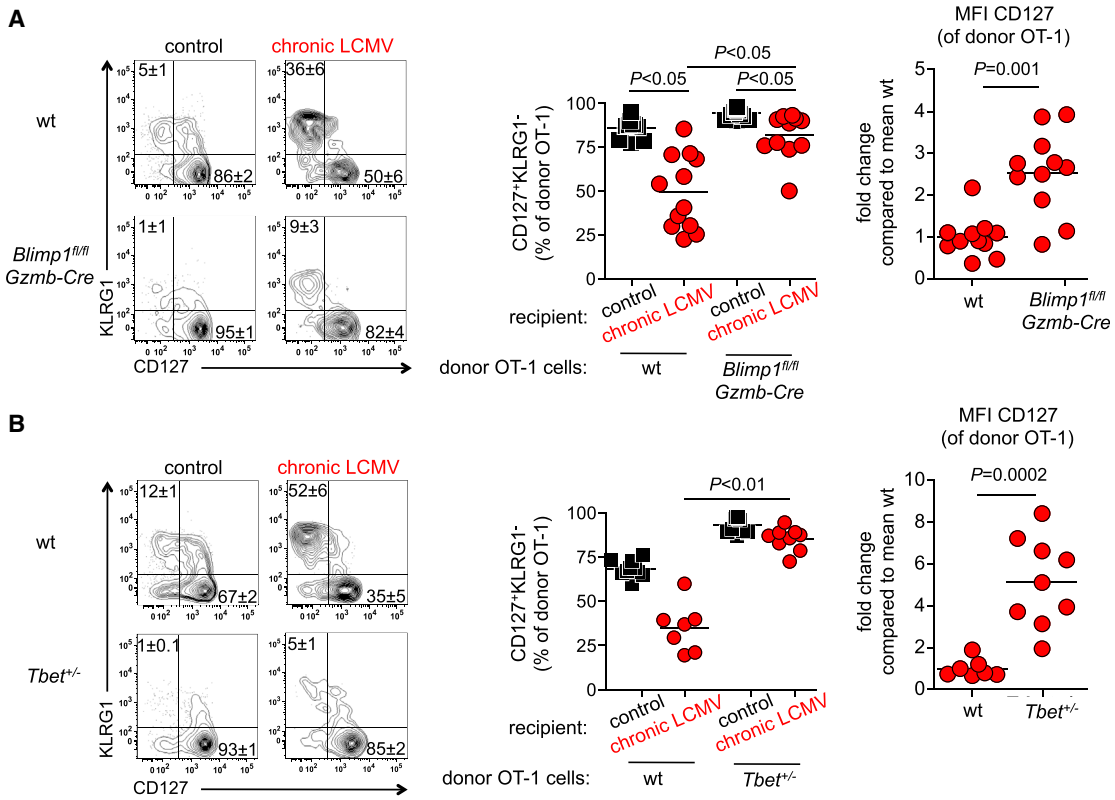

Figure 7. T-bet and Blimp-1 Regulate Memory CD8+ T Cell Development during Chronic Bystander Infection

CD45.1 mice containing adoptively transferred CD45.2 *Prdm1*$^{fl/fl}$ *Gzmb*-Cre (n = 11) (A), *Tbet*$^{+/-}$ (n = 9) (B), or littermate control WT OT1 CD8+ T cells were infected with VSV-OVA. On d8 p.i., OT1 cells were adoptively transferred to "control" (naive) or "chronic LCMV" (at d8 post-LCMV clone 13 infection) recipient mice. Donor OT1 cells were analyzed in spleens 40 days later. FACS plots are gated on live OT1 CD45.2 CD8+ T cells and numbers indicate frequencies ± SEM. MFI of CD127 on donor OT1 cells in "chronic LCMV" mice was normalized to the mean measurements of WT OT1 cells in "chronic LCMV" mice from each experiment.

inflammatory cytokines such as IFN-α and −β, IL-12, IL-1, and IL-33 (Haring et al., 2006; Curtsinger and Mescher 2010; Bonilla et al., 2012). Previous studies have demonstrated that developing effector CD8+ T cells integrate signals from antigen, costimulation, and inflammation to guide the development and differentiation of effector T cells (reviewed in Haring et al., 2006; Curtsinger and Mescher 2010). However, the positive effects of inflammatory signals during priming on the expansion of effector CD8+ T cells can occur at the expense of the quantity and quality of the generated memory CD8+ T cells (Badovinac et al., 2005; Joshi et al., 2007; Pearce and Shen, 2007). Our results further indicate that the effects of inflammation can be uncoupled from antigen stimulation and demonstrate that developing memory CD8+ T cells continue to sense inflammation after antigen clearance. Specifically, this scenario of prolonged antigen-independent sensing of high amounts of inflammation affects the transition of effector CD8+ T cells into robust long-lived memory CD8+ T cells by skewing the pattern of differentiation.

Although there is some evidence from in vitro models that sensing of inflammation changes once TCR signaling has ceased (Schulz et al., 2009), the mechanisms by which inflammation regulates CD8+ T cell memory without concomitant antigen signals in vivo remain poorly understood. Here, we show that the transcription factors T-bet and Blimp-1 integrate inflammatory signals and disrupt the efficient transitioning of effector CD8+ T cells into the memory pool in the absence of ongoing antigen stimulation. Although genetic deletion of Blimp-1 or T-bet led to a dramatic recovery of memory CD8+ T cell differentiation, a numerical defect persisted, suggesting at least two independent effects of bystander chronic infection on establishment of memory CD8+ T cell numbers and differentiation. However, the restoration of memory CD8+ T cell differentiation when Blimp-1 or T-bet were absent or reduced suggests that targeting these transcriptional pathways could potentially improve memory CD8+ T cell development during bystander chronic infection.

Inflammatory signals such as IFN-α, IFN-β, and IFN-γ are crucial in the first few days of infection to initiate a robust antiviral effector CD8+ T cell response (Haring et al., 2006; Curtsinger and Mescher 2010). However, transient IFN-I produced during acute viral infections can inhibit antigen-driven proliferation of preformed bystander memory CD8+ T cells (Marshall et al., 2011). IFN-α, IFN-β, and IFN-γ induced by serial infections has also been implicated in attrition of preformed memory cells in some settings (McNally et al., 2001; Dudani et al., 2008), although attrition of preformed memory CD8+ T cells following repeated acute infections or vaccinations is not always observed (Vezys et al., 2009; Odumade et al., 2012). Thus, the role of IFN pathways in regulating CD8+ T cell memory remains controversial. Despite the persistence of an IFN-I inducible gene signature during chronic infections, sustained IFN-I production is impaired

(Zuniga et al., 2008; Ye and Maniatis, 2011) raising questions about what inflammatory pathways govern this bystander effect during chronic infections. Indeed, removal of IFNAR on CD8+ T cells had only moderate impact on reversing the negative effect of bystander chronic LCMV infection on memory CD8+ T cell development, suggesting involvement of additional pathways. Although other inflammatory pathways could not be individually implicated, preventing the ability to integrate different inflammatory signals via Blimp-1 or T-bet reversed the differentiation defects caused by bystander chronic infection. Thus, our data are consistent with a model where multiple inflammatory pathways act redundantly during chronic infections and cause skewing of the effector to memory transition.

These studies could have implications not only for understanding memory development but also for global health. Some persisting infections confer intrinsic resistance to unrelated infections (Barton et al., 2007; Vahidnia et al., 2012). However, the data presented here suggest that chronic coinfections and inflammation might be a substantial impediment to achieving optimal immunological memory. While IFN-I is clearly antiviral during the early stages of infection, several studies have found a negative association between prolonged IFN-I signaling and the outcome of chronic infections (Antonelli et al., 2010; Berry et al., 2010; Rotger et al., 2011; Fraietta et al., 2013). Moreover, blockade of IFNAR during chronic viral infection has recently been found to paradoxically benefit antiviral adaptive immune responses (Teijaro et al., 2013; Wilson et al., 2013). Several mechanisms might be involved in these settings and it is unclear whether signaling through IFNAR is always required for an IFN-I-inducible gene signature. For example, there is considerable overlap in the genes induced by IL-12 and IFN-I in some settings (Agarwal et al., 2009). However, our data suggest that this IFN-I signature is at least a symptom of the bystander effect and that impaired immunological memory might contribute to negative association of the IFN-I signature and outcome of some chronic infections. Therefore, these observations are relevant for vaccination of patients in developing countries or those with chronic inflammatory diseases, as well as for long-term IFN-I-based treatment of infectious disease. This study suggests opportunities to optimize these vaccination and therapeutic strategies by further understanding the impact of chronic coinfections and prolonged inflammation on immunological memory.

EXPERIMENTAL PROCEDURES

Mice

Four to eight-week-old C57BL/6 Ly5.2CR (CD45.1) mice were purchased from NCI and TCR transgenic OT1 C57BL/6 mice from Jackson Laboratories. IFNAR-deficient (*Ifnar1*$^{-/-}$), IL-12Rβ-deficient (*Il12rb*$^{-/-}$), *Tbx21*-heterozygous (*Tbet*$^{+/-}$), and *Prdm1*$^{flox/flox}$ (Blimp-1) crossed to *Gzmb*-Cre mice were bred with OT1 mice. *Ifngr*$^{-/-}$ CD8+ T cells were provided by Jason Whitmire (University of North Carolina). Animal procedures were performed in accordance with Institutional Animal Care and Use Committee guidelines for the Wistar Institute and University of Pennsylvania.

Viruses and Bacteria

Mice were infected intravenously (i.v.) with 4 × 10^6 PFU LCMV clone 13, intraperitoneally (i.p.) with 2 × 10^5 PFU LCMV Armstrong, i.p. with 250 *T. gondii* tachyzoites (Me49 B7 strain), i.v. with 2 × 10^6 VSV-OVA, or i.p. with 10^4 – 8 × 10^5 cfu LM-OVA, as indicated. LM-OVA was grown and used as described (Pearce and Shen, 2007).

Adoptive Transfer

For the generation of primary OT1 effector cells, 5 × 10^4 CD45.2 CD8+ OT1 cells were adoptively transferred i.v. to WT CD45.1 recipient mice followed by infection with 2 × 10^6 PFU VSV-OVA or with 10^4 cfu LM-OVA. On d8 p.i. splenic CD8+ T cells were purified by negative selection with magnetic beads (Miltenyi Biotec) according to the manufacturer's instructions and 10^7 effector OT1 cells were adoptively transferred i.v. to congenic CD45.1 recipient mice.

Flow Cytometry

Tissues were processed, single cell suspensions obtained, and cells were stained as described (Wherry et al., 2003). Cells were stained with LIVE/DEAD cell stain (Invitrogen), CD8 (Abcam), CD44, CD45.2, CD62L, and CD27 (Biolegend), CD127 (eBiosciences), KLRG1 (Cell Lab), CXCR3 (R&D Systems), TNFR2 (BD PharMingen), Bim (Cell Signaling), and MHC class I/K^b $OVA_{257–264}$ tetramer. Intracellular cytokine staining was performed after 5 hr of ex vivo stimulation with $OVA_{257–264}$ peptide as described (Wherry et al., 2003) and cells stained with IL-2, TNF-α (Biolegend), and IFN-γ (eBioscience). Cells were analyzed with LSRII (BD Biosciences) and FlowJo software (Treestar).

Gene-Expression Profile Analysis

CD8+ T cells were enriched with magnetic beads and CD45.2 OT1 CD8+ T cells were sorted on a FACSAria (BD Biosciences). RNA was isolated with TRIzol (Invitrogen) according to the manufacturer's instructions. RNA was processed, amplified, labeled, and hybridized to Affymetrix GeneChip MoGene 1.0 ST microarrays at the Molecular Profiling Facility of the University of Pennsylvania. Human CMV-specific (HLA-A*0201-NLVPMVATV or HLA-B*0702-TPRVTGGGAM tetramer-positive) CD8+ T cells were purified from PBMC obtained from subjects with persistent HCV viremia (infected for >1 year) or from healthy volunteers who were recruited at Massachusetts General Hospital in Boston (Table S1). The study was approved by the local IRB (Protocol # 1999-P-004983/54; MGH #: 90-7246). RNA was isolated, processed, amplified, labeled, and hybridized to Affymetrix Human Gene 1.0 ST microarrays. Affymetrix Power Tools software was used to process and quantile normalize fluorescent hybridization signals with the Robust Multichip Averaging method (Irizarry et al., 2003). Transcripts were $\log_2$ normalized. Hierarchical Clustering was performed with Gene Pattern (Reich et al., 2006), and Gene Set Enrichment Analysis was performed with GSEA software (Subramanian et al., 2005).

Statistical Analysis

Samples were tested for normal distribution using D'Agostino and Pearson normality test. For equally distributed samples, statistical significance was calculated with unpaired two-tailed t test or one-way ANOVA (with Bonferroni posttest), as indicated. For nonequally distributed samples or samples too small to test for normal distribution, nonparametric Mann-Whitney test or Kruskal-Wallis (with Dunn's posttest) test was performed, as indicated.

SUPPLEMENTAL INFORMATION

Supplemental Information includes seven figures and one table and can be found with this article online at http://dx.doi.org/10.1016/j.immuni.2014.04.010.

ACKNOWLEDGMENTS

We thank the Penn Molecular Profiling Facility at the University of Pennsylvania for conducting the mouse microarray experiment. We thank D. Herbert (UCSF) for the *H. polygyrus* and members of the Wherry laboratory for comments and input. This work was supported by NIH/NIAID grants AI 083022 (to H.S. and E.J.W.) and AI 082630 (to W.N.H., G.M.L., and E.J.W.).

Received: August 19, 2013
Accepted: March 11, 2014
Published: May 15, 2014

REFERENCES

Abu-Raddad, L.J., Patnaik, P., and Kublin, J.G. (2006). Dual infection with HIV and malaria fuels the spread of both diseases in sub-Saharan Africa. Science *314*, 1603–1606.

Agarwal, P., Raghavan, A., Nandiwada, S.L., Curtsinger, J.M., Bohjanen, P.R., Mueller, D.L., and Mescher, M.F. (2009). Gene regulation and chromatin remodeling by IL-12 and type I IFN in programming for CD8 T cell effector function and memory. J. Immunol. *183*, 1695–1704.

Amit, I., Garber, M., Chevrier, N., Leite, A.P., Donner, Y., Eisenhaure, T., Guttman, M., Grenier, J.K., Li, W., Zuk, O., et al. (2009). Unbiased reconstruction of a mammalian transcriptional network mediating pathogen responses. Science *326*, 257–263.

Antonelli, L.R., Gigliotti Rothfuchs, A., Gonçalves, R., Roffê, E., Cheever, A.W., Bafica, A., Salazar, A.M., Feng, C.G., and Sher, A. (2010). Intranasal Poly-IC treatment exacerbates tuberculosis in mice through the pulmonary recruitment of a pathogen-permissive monocyte/macrophage population. J. Clin. Invest. *120*, 1674–1682.

Badovinac, V.P., Messingham, K.A., Jabbari, A., Haring, J.S., and Harty, J.T. (2005). Accelerated CD8+ T-cell memory and prime-boost response after dendritic-cell vaccination. Nat. Med. *11*, 748–756.

Bahgat, M.M., El-Far, M.A., Mesalam, A.A., Ismaeil, A.A., Ibrahim, A.A., Gewaid, H.E., Maghraby, A.S., Ali, M.A., and Abd-Elshafy, D.N. (2010). Schistosoma mansoni soluble egg antigens enhance HCV replication in mammalian cells. J. Infect. Dev. Ctries. *4*, 226–234.

Bahl, K., Kim, S.K., Calcagno, C., Ghersi, D., Puzone, R., Celada, F., Selin, L.K., and Welsh, R.M. (2006). IFN-induced attrition of CD8 T cells in the presence or absence of cognate antigen during the early stages of viral infections. J. Immunol. *176*, 4284–4295.

Barton, E.S., White, D.W., Cathelyn, J.S., Brett-McClellan, K.A., Engle, M., Diamond, M.S., Miller, V.L., and Virgin, H.W., 4th. (2007). Herpesvirus latency confers symbiotic protection from bacterial infection. Nature *447*, 326–329.

Berry, M.P., Graham, C.M., McNab, F.W., Xu, Z., Bloch, S.A., Oni, T., Wilkinson, K.A., Banchereau, R., Skinner, J., Wilkinson, R.J., et al. (2010). An interferon-inducible neutrophil-driven blood transcriptional signature in human tuberculosis. Nature *466*, 973–977.

Bonilla, W.V., Fröhlich, A., Senn, K., Kallert, S., Fernandez, M., Johnson, S., Kreutzfeldt, M., Hegazy, A.N., Schrick, C., Fallon, P.G., et al. (2012). The alarmin interleukin-33 drives protective antiviral CD8+ T cell responses. Science *335*, 984–989.

Cooper, P.J., Chico, M., Sandoval, C., Espinel, I., Guevara, A., Levine, M.M., Griffin, G.E., and Nutman, T.B. (2001). Human infection with Ascaris lumbricoides is associated with suppression of the interleukin-2 response to recombinant cholera toxin B subunit following vaccination with the live oral cholera vaccine CVD 103-HgR. Infect. Immun. *69*, 1574–1580.

Curtsinger, J.M., and Mescher, M.F. (2010). Inflammatory cytokines as a third signal for T cell activation. Curr. Opin. Immunol. *22*, 333–340.

Dudani, R., Murali-Krishna, K., Krishnan, L., and Sad, S. (2008). IFN-gamma induces the erosion of preexisting CD8 T cell memory during infection with a heterologous intracellular bacterium. J. Immunol. *181*, 1700–1709.

Elias, D., Britton, S., Aseffa, A., Engers, H., and Akuffo, H. (2008). Poor immunogenicity of BCG in helminth infected population is associated with increased in vitro TGF-beta production. Vaccine *26*, 3897–3902.

Fraietta, J.A., Mueller, Y.M., Yang, G., Boesteanu, A.C., Gracias, D.T., Do, D.H., Hope, J.L., Kathuria, N., McGettigan, S.E., Lewis, M.G., et al. (2013). Type I interferon upregulates Bak and contributes to T cell loss during human immunodeficiency virus (HIV) infection. PLoS Pathog. *9*, e1003658.

Gupta, S., Su, H., Bi, R., and Gollapudi, S. (2006). Differential sensitivity of naïve and memory subsets of human CD8+ T cells to TNF-alpha-induced apoptosis. J. Clin. Immunol. *26*, 193–203.

Harcourt, G.C., Donfield, S., Gomperts, E., Daar, E.S., Goulder, P., Jr., Phillips, R.E., and Klenerman, P.; Hemophilia Growth and Development Study (HGDS) (2005). Longitudinal analysis of CD8 T-cell responses to HIV and hepatitis C virus in a cohort of co-infected haemophiliacs. AIDS *19*, 1135–1143.

Haring, J.S., Badovinac, V.P., and Harty, J.T. (2006). Inflaming the CD8+ T cell response. Immunity *25*, 19–29.

Hawkes, M., Li, X., Crockett, M., Diassiti, A., Liles, W.C., Liu, J., and Kain, K.C. (2010). Malaria exacerbates experimental mycobacterial infection in vitro and in vivo. Microbes Infect. *12*, 864–874.

Irizarry, R.A., Bolstad, B.M., Collin, F., Cope, L.M., Hobbs, B., and Speed, T.P. (2003). Summaries of Affymetrix GeneChip probe level data. Nucleic Acids Res. *31*, e15.

Joshi, N.S., Cui, W., Chandele, A., Lee, H.K., Urso, D.R., Hagman, J., Gapin, L., and Kaech, S.M. (2007). Inflammation directs memory precursor and short-lived effector CD8(+) T cell fates via the graded expression of T-bet transcription factor. Immunity *27*, 281–295.

Kaech, S.M., and Cui, W. (2012). Transcriptional control of effector and memory CD8+ T cell differentiation. Nat. Rev. Immunol. *12*, 749–761.

Kamal, S.M., Rasenack, J.W., Bianchi, L., Al Tawil, A., El Sayed Khalifa, K., Peter, T., Mansour, H., Ezzat, W., and Koziel, M. (2001). Acute hepatitis C without and with schistosomiasis: correlation with hepatitis C-specific CD4(+) T-cell and cytokine response. Gastroenterology *121*, 646–656.

Kim, S.K., and Welsh, R.M. (2004). Comprehensive early and lasting loss of memory CD8 T cells and functional memory during acute and persistent viral infections. J. Immunol. *172*, 3139–3150.

Marshall, H.D., Urban, S.L., and Welsh, R.M. (2011). Virus-induced transient immune suppression and the inhibition of T cell proliferation by type I interferon. J. Virol. *85*, 5929–5939.

McNally, J.M., Zarozinski, C.C., Lin, M.Y., Brehm, M.A., Chen, H.D., and Welsh, R.M. (2001). Attrition of bystander CD8 T cells during virus-induced T-cell and interferon responses. J. Virol. *75*, 5965–5976.

Moorman, J.P., Zhang, C.L., Ni, L., Ma, C.J., Zhang, Y., Wu, X.Y., Thayer, P., Islam, T.M., Borthwick, T., and Yao, Z.Q. (2011). Impaired hepatitis B vaccine responses during chronic hepatitis C infection: involvement of the PD-1 pathway in regulating CD4(+) T cell responses. Vaccine *29*, 3169–3176.

Morishima, C., Paschal, D.M., Wang, C.C., Yoshihara, C.S., Wood, B.L., Yeo, A.E., Emerson, S.S., Shuhart, M.C., and Gretch, D.R. (2006). Decreased NK cell frequency in chronic hepatitis C does not affect ex vivo cytolytic killing. Hepatology *43*, 573–580.

Napolitani, G., Rinaldi, A., Bertoni, F., Sallusto, F., and Lanzavecchia, A. (2005). Selected Toll-like receptor agonist combinations synergistically trigger a T helper type 1-polarizing program in dendritic cells. Nat. Immunol. *6*, 769–776.

Nookala, S., Srinivasan, S., Kaliraj, P., Narayanan, R.B., and Nutman, T.B. (2004). Impairment of tetanus-specific cellular and humoral responses following tetanus vaccination in human lymphatic filariasis. Infect. Immun. *72*, 2598–2604.

Odumade, O.A., Knight, J.A., Schmeling, D.O., Masopust, D., Balfour, H.H., Jr., and Hogquist, K.A. (2012). Primary Epstein-Barr virus infection does not erode preexisting CD8+ T cell memory in humans. J. Exp. Med. *209*, 471–478.

Pearce, E.L., and Shen, H. (2007). Generation of CD8 T cell memory is regulated by IL-12. J. Immunol. *179*, 2074–2081.

Ramilo, O., Allman, W., Chung, W., Mejias, A., Ardura, M., Glaser, C., Wittkowski, K.M., Piqueras, B., Banchereau, J., Palucka, A.K., and Chaussabel, D. (2007). Gene expression patterns in blood leukocytes discriminate patients with acute infections. Blood *109*, 2066–2077.

Reich, M., Liefeld, T., Gould, J., Lerner, J., Tamayo, P., and Mesirov, J.P. (2006). GenePattern 2.0. Nat. Genet. *38*, 500–501.

Resende Co, T., Hirsch, C.S., Toossi, Z., Dietze, R., and Ribeiro-Rodrigues, R. (2007). Intestinal helminth co-infection has a negative impact on both anti-Mycobacterium tuberculosis immunity and clinical response to tuberculosis therapy. Clin. Exp. Immunol. *147*, 45–52.

Rotger, M., Dalmau, J., Rauch, A., McLaren, P., Bosinger, S.E., Martinez, R., Sandler, N.G., Roque, A., Liebner, J., Battegay, M., et al. (2011). Comparative transcriptomics of extreme phenotypes of human HIV-1 infection and SIV infection in sooty mangabey and rhesus macaque. J. Clin. Invest. *121*, 2391–2400.

Schulz, E.G., Mariani, L., Radbruch, A., and Höfer, T. (2009). Sequential polarization and imprinting of type 1 T helper lymphocytes by interferon-gamma and interleukin-12. Immunity *30*, 673–683.

Stelekati, E., and Wherry, E.J. (2012). Chronic bystander infections and immunity to unrelated antigens. Cell Host Microbe *12*, 458–469.

Subramanian, A., Tamayo, P., Mootha, V.K., Mukherjee, S., Ebert, B.L., Gillette, M.A., Paulovich, A., Pomeroy, S.L., Golub, T.R., Lander, E.S., and Mesirov, J.P. (2005). Gene set enrichment analysis: a knowledge-based approach for interpreting genome-wide expression profiles. Proc. Natl. Acad. Sci. USA *102*, 15545–15550.

Teijaro, J.R., Ng, C., Lee, A.M., Sullivan, B.M., Sheehan, K.C., Welch, M., Schreiber, R.D., de la Torre, J.C., and Oldstone, M.B. (2013). Persistent LCMV infection is controlled by blockade of type I interferon signaling. Science *340*, 207–211.

Vahidnia, F., Petersen, M., Stapleton, J.T., Rutherford, G.W., Busch, M., and Custer, B. (2012). Acquisition of GB virus type C and lower mortality in patients with advanced HIV disease. Clin. Infect. Dis. *55*, 1012–1019.

van Riet, E., Hartgers, F.C., and Yazdanbakhsh, M. (2007). Chronic helminth infections induce immunomodulation: consequences and mechanisms. Immunobiology *212*, 475–490.

Vezys, V., Yates, A., Casey, K.A., Lanier, G., Ahmed, R., Antia, R., and Masopust, D. (2009). Memory CD8 T-cell compartment grows in size with immunological experience. Nature *457*, 196–199.

Wherry, E.J., Blattman, J.N., Murali-Krishna, K., van der Most, R., and Ahmed, R. (2003). Viral persistence alters CD8 T-cell immunodominance and tissue distribution and results in distinct stages of functional impairment. J. Virol. *77*, 4911–4927.

Wilson, E.B., Yamada, D.H., Elsaesser, H., Herskovitz, J., Deng, J., Cheng, G., Aronow, B.J., Karp, C.L., and Brooks, D.G. (2013). Blockade of chronic type I interferon signaling to control persistent LCMV infection. Science *340*, 202–207.

Wojciechowski, S., Jordan, M.B., Zhu, Y., White, J., Zajac, A.J., and Hildeman, D.A. (2006). Bim mediates apoptosis of CD127(lo) effector T cells and limits T cell memory. Eur. J. Immunol. *36*, 1694–1706.

Wortzman, M.E., Lin, G.H., and Watts, T.H. (2013). Intrinsic TNF/TNFR2 interactions fine-tune the CD8 T cell response to respiratory influenza virus infection in mice. PLoS ONE *8*, e68911.

Ye, J., and Maniatis, T. (2011). Negative regulation of interferon-β gene expression during acute and persistent virus infections. PLoS ONE *6*, e20681.

Zhang, Y., Nakata, K., Weiden, M., and Rom, W.N. (1995). Mycobacterium tuberculosis enhances human immunodeficiency virus-1 replication by transcriptional activation at the long terminal repeat. J. Clin. Invest. *95*, 2324–2331.

Zuniga, E.I., Liou, L.Y., Mack, L., Mendoza, M., and Oldstone, M.B. (2008). Persistent virus infection inhibits type I interferon production by plasmacytoid dendritic cells to facilitate opportunistic infections. Cell Host Microbe *4*, 374–386.

Appendix B: Kinetic differences in the induction of interferon stimulated genes by interferon-α and interleukin 28B are altered by infection with hepatitis C virus.

Nikolaus Jilg, Wenyu Lin, Jian Hong, Esperance A Schaefer, David Wolski, James Meixong, Kaku Goto, Cynthia Brisac, Pattranuch Chusri, Dahlene N Fusco, Stephane Chevaliez, Jay Luther, Kattareeya Kumthip, Thomas J Urban, Lee F Peng, Georg M Lauer, and Raymond T Chung.

Hepatology, 2014 vol. 59 (4) pp. 1250-1261.

Summary

This work focuses on gene expression kinetics and profile of hepatocytes in response to type I and type III interferon stimulation. A time-course experiment of primary human hepatocytes stimulated with either IFN-α or IL28B, revealed that while the set of activated genes was similar between interferons, they effected different expression kinetics. Stimulation with IFN-α induced a rapid transient response, whereas the response to IL28B was delayed, but more sustained. A validation experiment using Huh7.5.1 human hepatoma cells that either been infected with a recombinant HCV strain or left uninfected before stimulation with interferons, showed that kinetics in uninfected cells mirrored those in primary hepatocytes. Infected Huh7.5.1 cells, however, displayed impaired induction of ISGs with kinetics closer to those of IL28B. These results suggest that different interferons elicit distinct gene expression kinetics that can be affected by HCV infection.

HEPATOLOGY
Official Journal of the American Association for the Study of Liver Diseases

Kinetic Differences in the Induction of Interferon Stimulated Genes by Interferon-α and Interleukin 28B Are Altered by Infection With Hepatitis C Virus

Nikolaus Jilg,[1] Wenyu Lin,[1] Jian Hong,[1] Esperance A. Schaefer,[1] David Wolski,[1] James Meixong,[1] Kaku Goto,[2] Cynthia Brisac,[1] Pattranuch Chusri,[1] Dahlene N. Fusco,[1] Stephane Chevaliez,[1] Jay Luther,[1] Kattareeya Kumthip,[1] Thomas J. Urban,[3] Lee F. Peng,[1] Georg M. Lauer,[1] and Raymond T. Chung[1]

Several genome-wide association studies (GWAS) have identified a genetic polymorphism associated with the gene locus for interleukin 28B (IL28B), a type III interferon (IFN), as a major predictor of clinical outcome in hepatitis C. Antiviral effects of the type III IFN family have previously been shown against several viruses, including hepatitis C virus (HCV), and resemble the function of type I IFN including utilization of the intracellular Janus kinase signal transducer and activator of transcription (JAK-STAT) pathway. Effects unique to IL28B that would distinguish it from IFN-α are not well defined. By analyzing the transcriptomes of primary human hepatocytes (PHH) treated with IFN-α or IL28B, we sought to identify functional differences between IFN-α and IL28B to better understand the roles of these cytokines in the innate immune response. Although our data did not reveal distinct gene signatures, we detected striking kinetic differences between IFN-α and IL28B stimulation for interferon stimulated genes (ISGs). While gene induction was rapid and peaked at 8 hours of stimulation with IFN-α in PHH, IL28B produced a slower, but more sustained increase in gene expression. We confirmed these findings in the human hepatoma cell line Huh7.5.1. Interestingly, in HCV-infected cells the rapid response after stimulation with IFN-α was blunted, and the induction pattern resembled that caused by IL28B. *Conclusion*: The kinetics of gene induction are fundamentally different for stimulations with either IFN-α or IL28B in hepatocytes, suggesting distinct roles of these cytokines within the immune response. Furthermore, the observed differences are substantially altered by infection with HCV. (HEPATOLOGY 2014;59:1250-1261)

See Editorial on Page 1225

In 2003, a novel family of antiviral cytokines was described and designated type III interferons.[1,2] Since their discovery, the three members comprising this family, interleukin (IL) 28A, also known as interferon (IFN) λ2, IL28B (IFN-λ3), and IL29 (IFN-λ1) have been extensively studied and have in many respects been found to resemble type I interferons. While type III interferons bind to a receptor complex that is distinct from the interferon-α receptor, type I and III interferons have been shown to share a common downstream signaling pathway by way of Janus kinase signal transducer and activator of transcription (JAK-STAT), leading to the induction of interferon stimulated genes (ISGs), like OAS1.[3]

In contrast to the type I interferon receptor that is expressed ubiquitously on mammalian cells, the functional type III interferon receptor appears to be more tissue restricted with preferential expression on the surfaces of epithelial cells, including hepatocytes.[4]

Abbreviations: GWA(S), genome-wide association (study/studies); HCV, hepatitis C virus; Huh, human hepatoma; IFN, interferon; IL, interleukin; IL28B, interleukin-28B; ISG, interferon stimulated gene; JAK-STAT, Janus kinase signal transducer and activator of transcription; PHH, primary human hepatocytes; qPCR, quantitative polymerase chain reaction; RT-PCR, reverse transcription PCR; SNP, single nucleotide polymorphism.

From the [1]Gastrointestinal Unit, Department of Medicine, Massachusetts General Hospital and Harvard Medical School, Boston, MA; [2]Unit of Disease Control Genome Medicine, Institute of Medical Science, University of Tokyo, Tokyo, Japan; [3]Center for Human Genome Variation, Duke University, Durham, NC.

Received March 12, 2013; accepted July 19, 2013.

Supported by NIH AI082630 (RTC), and by the Deutsche Forschungsgemeinschaft (German Research Foundation, DFG) research fellowship Ji 145/1-1 (NJ).

Chronic hepatitis C virus (HCV) is estimated to affect 2%-3% of the world's population and is currently the leading cause of both hepatocellular carcinoma and liver transplantations in both the U.S. and Europe.[5,6] Peginterferon based therapies have been the mainstay of HCV therapy for nearly a decade. However, they are fraught with an unfavorable side effect profile, long duration of treatment, a limited success rate, and high costs.[7] Furthermore, many patients have contraindications to treatment with peginterferon. The parameters that determine therapeutic success or failure in patients treated for HCV are still incompletely understood.

A recent breakthrough in the field was the discovery that genetic variation in the proximity of the IL28B (otherwise known as IFN-λ3) gene is a major predictor of successful therapy with peginterferon and ribavirin.[8-10] In addition, the detected IL28B-associated single nucleotide polymorphisms (SNPs) have been shown to significantly determine spontaneous viral clearance.[11,13] Coupled with the extremely strong correlation between IL28B genotype, the previously known antiviral effect of the IL28B protein makes an important role of the gene product in the course of HCV highly likely. However, the mechanism by which the genetic polymorphism impacts the outcome of viral infection is unknown; thus, further studies to elucidate the mechanism are needed.

Recently, we have shown that IL28B inhibits HCV replication in a hepatoma cell line and that this action depends on an intact JAK-STAT pathway.[3] Thus, IL28B's action seems to resemble the effects of its close relatives IL28A and IL29 as well as IFN-α. While this study was important in order to establish that IL28B, like IL28A, IL29, and IFN is mainly signaling through the JAK-STAT pathway, it did not provide further insight regarding the unique contribution of IL28B in the response to HCV infection and therapy observed in the original genome-wide association studies (GWAS).

In an effort to identify functional differences between the effects of IL28B and IFN-α, we compared the transcriptomes of IL28B and IFN-α stimulated primary human hepatocytes at different doses and over different periods of time. We tested the hypothesis that there are distinct differences in the gene expression patterns of hepatocytes upon stimulation with IFN-α and IL28B, respectively, and that these differences could play a role in differential downstream antiviral action.

Materials and Methods

Cell Cultures and Viruses. The human hepatoma cell line Huh7.5.1 was grown at 37°C in Dulbecco's modified Eagle's medium (DMEM) supplemented with 10% fetal bovine serum (FBS), 100 U/mL penicillin, and 100 μg/mL streptomycin (HyClone Laboratories, South Logan, UT). Viral RNA was made from plasmid Jc1FLAG2(p7-nsGluc2a), which represents an infectious recombinant HCV strain (based on Jc1), that harbors the *Gaussia* luciferase gene, and the RNA was transfected as previously described.[14] Briefly, we used electroporation for the transfection of Jc1FLAG2(p7-nsGluc2a) RNA into Huh7.5.1 cells and collected the supernatants at day 3 posttransfection. We then used these supernatants to inoculate naïve Huh7.5.1 cells with a tissue culture infectious dose 50 ($TCID_{50}$) of 3.24×10^4/mL. $TCID_{50}$ was determined using the method described by Lindenbach et al.[15] with an antibody against HCV core protein. Infection was confirmed by quantitative polymerase chain reaction (qPCR) for viral RNA and western blotting for HCV core protein, and infection with Jc1FLAG2(p7-nsGluc2a) by luciferase assay and qPCR for viral RNA. Primary human hepatocytes (PHH) were obtained after liver resections from three donors for colorectal metastasis from apparently healthy excess liver tissue portions that were not required for pathological diagnosis and therefore discarded if not used for research purposes. Liver resections were received from the University of Pittsburgh through the Liver Tissue and Procurement and Distribution System (LTPADS; Dr. Stephen C. Strom, Pittsburgh, PA) and were isolated under the Institutional Review Board guidelines of the University of Pittsburgh as described.[16] PHH were cultured in HMM (hepatocyte maintenance medium; Lonza, Walkersville, MD) supplemented with HMM Single Quots Kit, except that gentamycin was replaced by 100 U/mL penicillin and 100 μg/mL streptomycin (HyClone Laboratories). The hepatocytes in the microarray experiments were genotyped for an IL28B associated

Address reprint requests to: Raymond T. Chung, M.D., Gastrointestinal Unit, Department of Medicine, Massachusetts General Hospital, 55 Fruit St., Warren 1007, Boston, MA 02114. E-mail: rtchung@partners.org; fax: 617-643-0446.

View this article online at wileyonlinelibrary.com.
DOI 10.1002/hep.26653
Potential conflict of interest: Nothing to report.
Additional Supporting Information may be found in the online version of this article.

Table 1. Primer Sequences for Quantitative RT-PCR

Target Gene	Primer	Nucleotide Sequence (5′ to 3′)
GAPDH	F	ACCTTCCCCATGGTGTCTGA
	R	TCGCAACCCAACGCTACTCG
ACTB	F	CATGTACGTTGCTATCCAGG
	R	CTCCTTAATGTCACGCACGAT
MX1	F	GTTTCCGAAGTGGACATCGCA
	R	GAAGGGCAACTCCTGACAGT
OAS1	F	GATCTCAGAAATACCCCAGCCA
	R	AGCTACCTCGGAAGCACCTT
EIF2AK2	F	TGGAAAGCGAACAAGGAGTAAG
	R	CCATCCCGTAGGTCTGTGAA
ISG15	F	TCCTGGTGAGGAATAACAAGGG
	R	GTCAGCCAGAACAGGTCGTC
STAT1	F	ATGTCTCAGTGGTACGAACTTCA
	R	TGTGCCAGGTACTGTCTGATT
IRF9	F	GTGCTGGGATGATACAGCTAAG
	R	CAGGCGAGTCTTCCAGACAG
IFIT1	F	TCAGGTCAAGGATAGTCTGGAG
	R	AGGTTGTGTATTCCCACACTGTA
IFI6	F	GGTCTGCGATCCTGAATGGG
	R	TCACTATCGAGATACTTGTGGGT
RSAD2	F	CAAGACCGGGGAGAATACCTG
	R	GCGAGAATGTCCAAATACTCACC
HERC5	F	GATGGGCTGCTGTTTACTTTCG
	R	GAGTCACTCTATACCCAACAAGC
HERC6	F	CCCTCAGTGGGCGTAATGTC
	R	AGAGCGATTGTCTCCAAATGTG
JFH-1	F	CTGTCTTCACGCAGAAAGCG
	R	TCGCAACCCAACGCTACTCG

F: forward; R: reverse.

polymorphism at rs12979860 and we obtained the following results: C/C (1602), C/T (1638), T/T (1649).

Interferons. Peginterferon alfa-2b was obtained from Schering (Kenilworth, NJ). For the microarray studies in PHH, we used IL28B derived from an expression system as described.[17] After the protein became commercially available, we used human IL28B from R&D Systems (Minneapolis, MN). We used 0.21 ng/mL peginterferon alfa-2b (equivalent to 6.91×10^{-6} nmol/mL or 15 IU/mL) and 1,000 ng/mL IL28B (4.97×10^{-2} nmol/mL) for the stimulation of PHH. Doses for the Huh7.5.1 cells were 0.43 ng/mL (1.38×10^{-5} nmol/mL or 30 IU/mL) IFN-α and 50 ng/mL (7.46×10^{-4} nmol/l) IL28B.

RNA Extraction. For extraction of total RNA, cells were lysed and processed with the QIA shredder and RNeasy kits (Qiagen, Valencia, CA) according to the manufacturer's protocol. RNA was reconstituted and stored in RNase free water. RNA concentrations were measured using the NanoDrop spectrophotometer (Thermo Scientific NanoDrop Products, Wilmington, DE). For the microarrays, RNA quality was additionally tested by the Agilent Bioanalyzer (Agilent Technologies, Santa Clara, CA).

qRT-PCR. Total RNA was reverse transcribed to complementary DNA (cDNA) with random primers using the Applied Biosystems High Capacity cDNA Reverse Transcription Kit (Invitrogen, Carlsbad, CA). Specific cDNA levels were quantified by real-time PCR using the Bio-Rad IQ5 machine (Bio-Rad Laboratories, Hercules, CA) and Thermo Scientific DyNAmo HS SYBR green qPCR kit (Thermo Fisher Scientific, Waltham, MA). GAPDH expression was used as an internal reference. Primers for the qPCR experiments are listed in Table 1.

Microarrays. The Illumina BeadChip HT-12 was used for microarray analysis according to the manufacturer's protocol (Illumina, San Diego, CA) and to the methods described in Urban et al.[17] A single RNA sample was not available for further analysis and, therefore, no microarray data are available (1602/ IL28B/ 24 hours).

Protein sample preparation and western blotting were performed as described.[31] The following antibodies were used: STAT1 (Tyr701) rabbit monoclonal, and STAT1 mouse monoclonal from Cell Signaling Technology (Beverly, MA), β-actin (A2228) mouse monoclonal from Sigma-Aldrich (St. Louis, MO), and the secondary antibodies antimouse IgG (NA931) and antirabbit IgG (N933, GE Healthcare).

Statistics. Data analysis was carried out using a 2-tailed Student t test with pooled variance. Data are expressed as mean $\pm$ SD of at least three sample replicates, unless stated otherwise. Microarray data was first analyzed as previously.[17] For the identification of relevant interferon stimulated genes in the PHH microarrays, we used gene induction by IL28B at 4, 8, and 24 hours with a q-value (false discovery rate) ≤ 0.05. The hits were further analyzed by means of the database and web-tool STRING (Search Tool for the Retrieval of Interacting Genes/Proteins), a meta-resource that aggregates most of the available information on protein-protein associations, scores and weights it, and augments it with predicted interactions, as well as with the results of automatic literature-mining searches as described in Jensen et al.[35] We fitted cubic splines to the expression data in Fig. 3 to demonstrate trends in expression kinetics.

Results

Transcriptomes of Both IFN-α and IL28B Stimulated PHH Comprise Typical ISGs. In order to identify differential effects of IFN-α and IL28B on the hepatocyte, we sought to determine gene expression patterns using an unbiased approach by transcriptomic microarrays in the currently best model for the isolated study of this cell type, PHH cultures. Interestingly, the

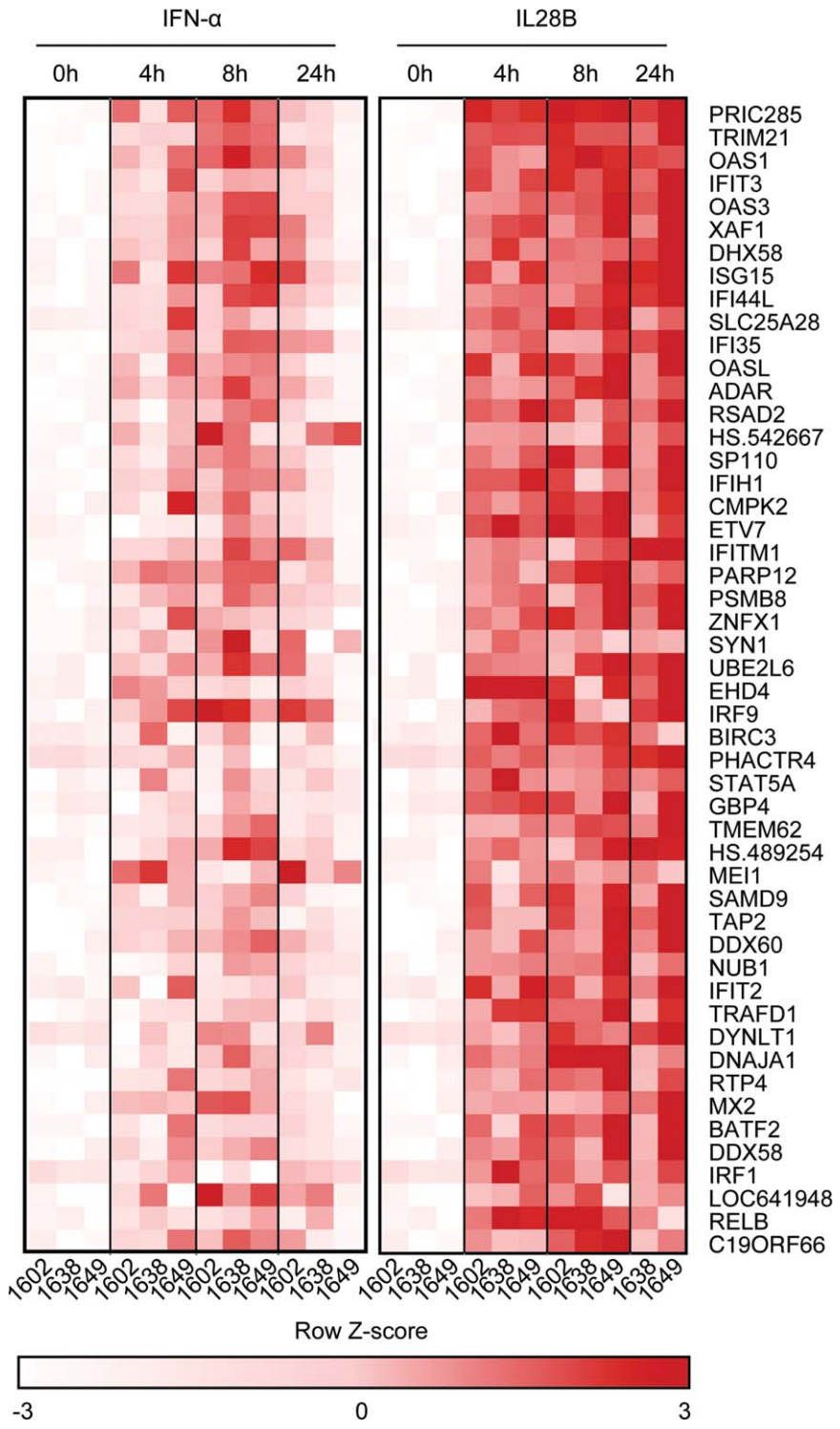

Fig. 1. Gene expression upon stimulation with IFN-α and IL28B in PHH. PHH from three different donors (1602, 1638, 1649) were isolated from liver resections, plated, and cultured as described in the Materials and Methods. The PHH cultures were treated with IFN-α (15 IU/mL) and IL28B (1,000 ng/mL) for 4, 8, and 24 hours. RNA was isolated and, after quality control and reverse transcription to cDNA, gene expression was detected by microarrays. The heatmap shows statistically significant gene induction for IL28B stimulation (false discovery rate, $q \leq 0.05$). Gene expression for the 50 hit genes by IL28B was compared to the respective data after IFN-α induction. Intensity of red correlates with intensity of gene expression compared to the row Z-score.

magnitude of induction was generally much lower for most interferon stimulated genes in PHH compared to hepatoma cells. We stimulated PHH from three different donors with either IFN-α or IL28B over a 24-hour time course, isolated RNA, and determined gene induction by expression microarrays (Fig. 1). We evaluated data from three different donors as described in the Materials and Methods. After sorting the genes by relevant induction by IL28B, we compared the expression of the same genes after IFN-α stimulation. Most of the genes with relevant induction represented known ISGs, which are by definition inducible by IFN-α, after stimulation with both IFN-α and IL28B (Fig. 2A), including OAS1, IFIT3, ISG15, and

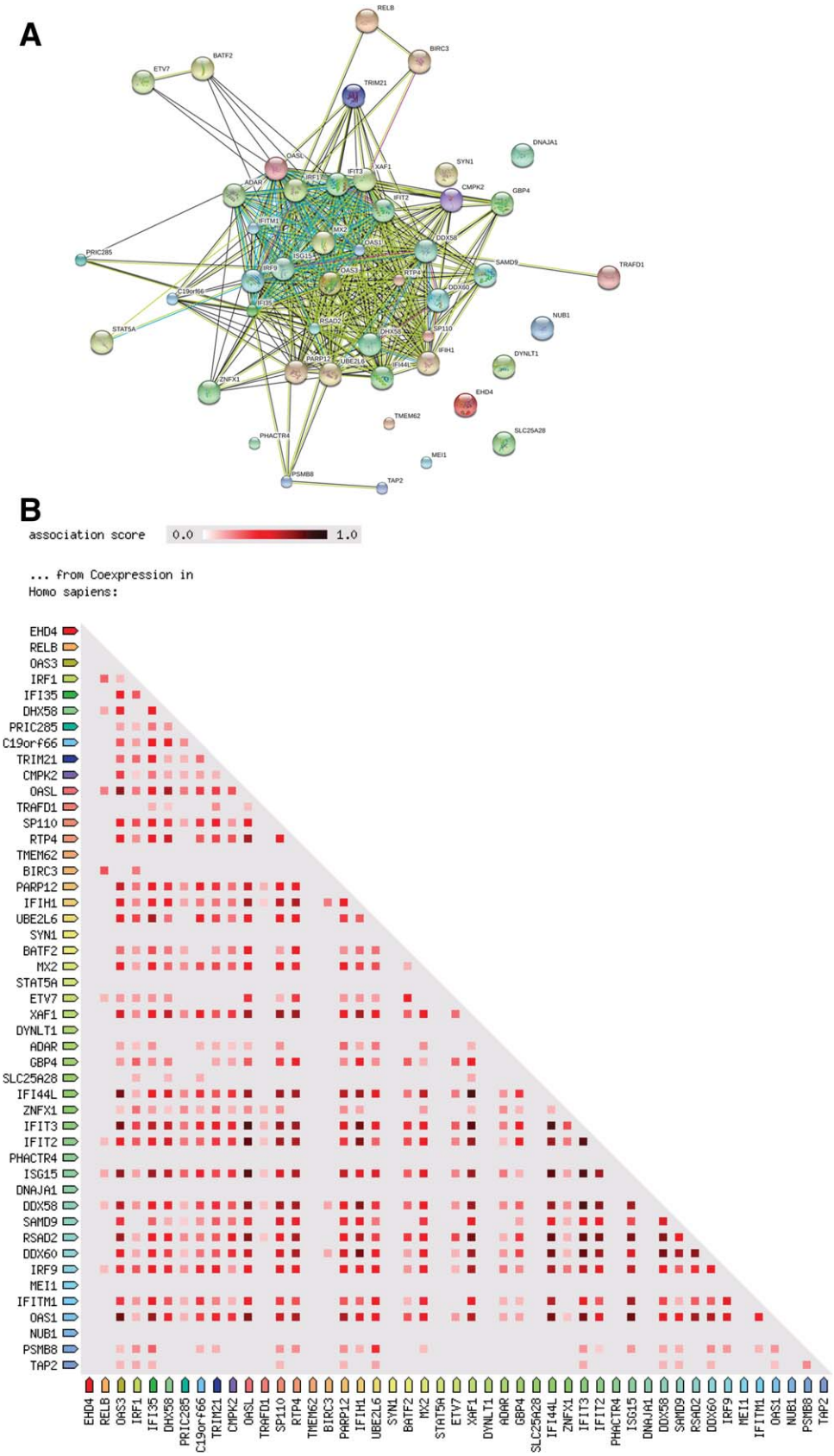

Fig. 2. STRING protein interaction view of significantly induced genes by IFN-α and IL28B in PHH. The 50 genes significantly induced by IL28B were analyzed with the database and web-tool STRING (Search Tool for Retrieval of Interacting Genes/Proteins), a meta-resource that integrates available information on protein-protein associations (http://string-db.org;[33]). (A) Connecting lines between the protein symbols illustrate the many known interactions of the proteins (protein association network), most of the genes are known to be IFN-α induced genes (ISGs). (B) Coexpression view. As illustrated in the figure, many of these proteins are known to be coexpressed under certain conditions. The color intensity reflects the association score (0-1).

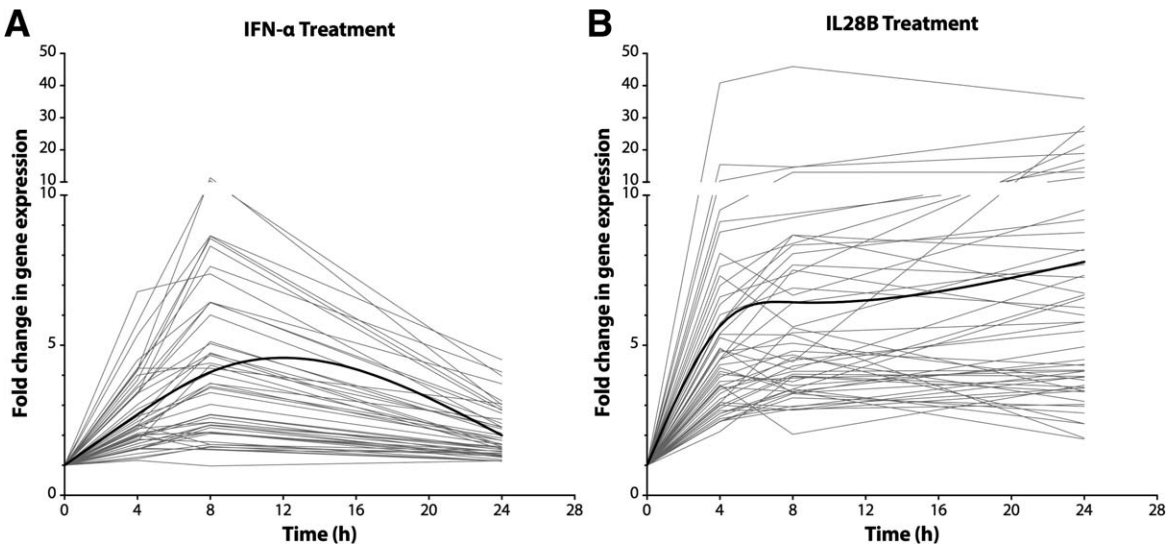

Fig. 3. IFN-α and IL28B induction of 50 genes in PHH over 24 hours suggests general trends. The 50 genes significantly induced by IL28B were analyzed and gene expression at 0, 4, 8, and 24 hours depicted for both IFN-α (15 IU/mL) and IL28B (1 μg/mL) induction.

RSAD2 (Viperin). Many of the significantly induced genes are known to be coexpressed (Fig. 2B). Based on this observation, and in line with previous studies, we concluded that at least a majority of genes substantially induced by IL28B in PHH are shared with those induced by IFN-α, and are therefore typical ISGs. Hence, from these experiments we are not able to identify a unique expression signature of IL28B, which comprises distinct genes from those induced by IFN-α. These findings strongly suggest that IL28B and IFN-α have near complete overlap of signal transduction.

IFN-α Leads to a Rapid but Transient Increase of Gene Expression in PHH, Whereas IL28B Gene Induction Is Slower and Sustained. We next sought to determine the temporal nature of ISG induction by IFN-α and IL28B. When comparing the time courses of induction, we found that many of the IFN-α responsive genes, like MX1, OAS1, and IFI6, were induced at 4 hours, were further up-regulated at 8 hours, and showed lower expression at 24 hours compared to 8 hours. While these genes were also found to be induced by IL28B, the kinetic profile was markedly different: The signal increased steadily over 24 hours with the highest fold-induction value after the longest period of stimulation (Figs. 1,3). The lack of evidence for specific IL28B induced genes and the observation that transcriptomes of IFN-α and IL28B largely overlap in PHH made us consider alternative mechanisms as to how IFN-α and IL28B execute their distinct effects on hepatocytes. Indeed, we observed different *kinetic* profiles when analyzing induction of the same genes by IFN-α and IL28B. We therefore hypothesized that the two cytokines exert their differential effects on innate immunity temporally and therefore further investigated these differences. We analyzed a number of the ISGs induced on the microarrays, MX1 (Fig. 4A), OAS1 (Fig. 4B), RSAD2 (Viperin; Fig. 4C), STAT1 (Fig. 4D), and IRF9 (Fig. 4E), in qRT-PCR experiments from the same RNA extracts. While the magnitude of fold induction differed substantially between genes, the chosen doses led to graphs similar in range for IFN-α and IL28B. We were able to confirm induction of these ISGs by both IFN-α and IL28B on qPCR. As observed in the microarray experiments, we demonstrated that within 24 hours for all but one sample there was maximum induction after 8 hours of treatment with IFN-α, whereas during the same period IL28B led to a monotonic increase of expression. The one exception was a slight shift of the peak to 4 hours in the PHH from one of the donors in IRF9 induction (Fig. 4E).

Typical Patterns of ISG Induction by IFN-α and IL28B Over Time Are Preserved in Huh7.5.1 Cells. While regarded a model closely resembling the *in vivo* situation in many respects, PHH cultured in a monolayer has several limitations. They do not proliferate, rapidly lose cell function, and are only viable for a limited number of days.[16] Moreover, we found that when the hepatoma cell line Huh7.5.1 was used as a robust *in vitro* model for hepatocytes, the magnitude of ISG induction is much higher than in PHH and therefore permits detection of expression differences below a threshold value or below level of detection in PHH. Hence, we chose several of the top induced genes from the microarray experiments and further studied them in Huh7.5.1 cells (Fig. 5). After initial

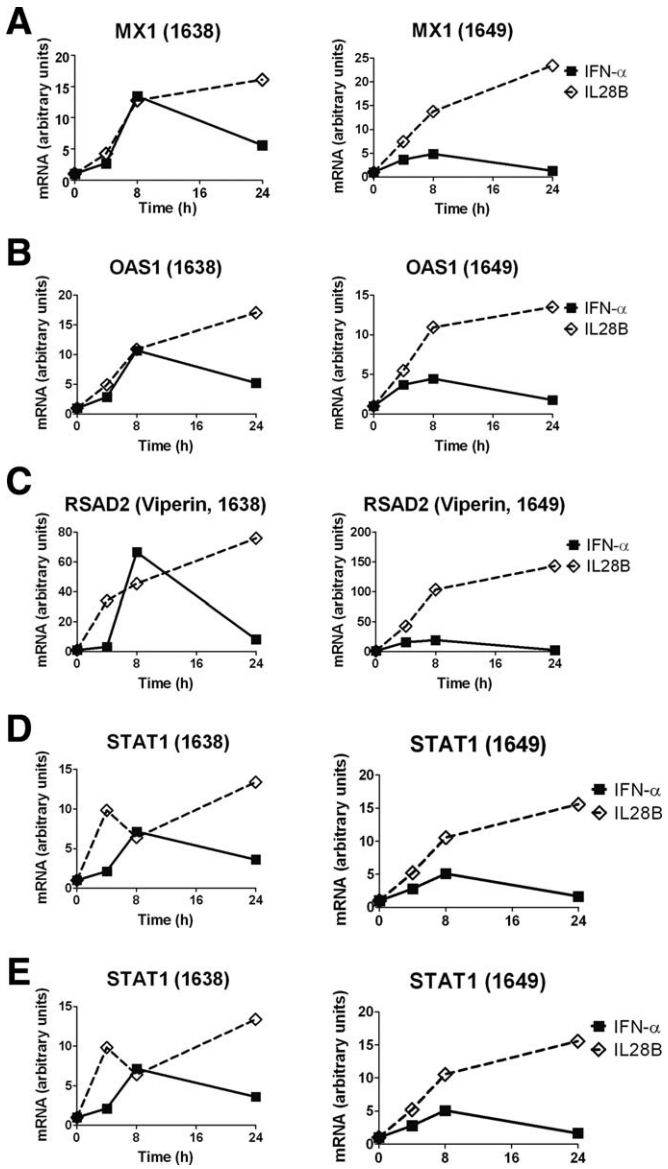

Fig. 4. Kinetic differences in induction of typical ISGs by IFN-α and IL28B in PHH determined by qRT-PCR. IFN-α leads to a rapid but transient increase of gene expression in PHH, whereas IL28B gene induction is slower and sustained. PHH were stimulated with IFN-α (0.21 ng/mL peginterferon alfa-2b, equivalent to 6.91×10^{-6} nmol/mL or 15 IU/mL) and IL28B (1,000 ng/mL) for 0, 4, 8, and 24 hours. (A) MX1, (B) OAS1, (C) RSAD2, (D) STAT1, and (E) IRF9 expression were analyzed by qRT-PCR and normalized to GAPDH expression. The expression of the gene of interest at timepoint 0 was set to 1 and fold inductions determined for the other timepoints. The kinetics are demonstrated in two biological replicates (1638, 1649), largely confirming the trends as seen in the microarray experiments.

dose finding experiments, we submitted Huh7.5.1 cells to a time course over 48 hours of stimulation with IFN-α and IL28B (data not shown and Fig. 5). We studied the expression patterns of the following genes in qPCR experiments: the housekeeping gene ACTB as a non-ISG control, MX1, EIF2AK2 (PKR; Fig. 5A); OAS1, ISG15, STAT1 (Fig. 5B); IRF9, IFIT1 (ISG56), IFI6 (Fig. 5C); RSAD2 (Viperin), HERC5, HERC6 (Fig. 5D). All ISGs, with one exception (IFI6), demonstrated a characteristic expression pattern over 48 hours: IFN-α leads to a rapid increase of expression with a maximum after 8 hours of incubation followed by a decline in the signal. In contrast, IL28B up-regulates the same genes, showing a slower increase of induction that appears more sustained. On the other hand, we detected no changes in gene expression over time upon stimulation with either IFN-α or IL28B in expression of ACTB as a control gene.

Differences in Induction Kinetics by IFN-α and IL28B Are Altered by HCV Infection. We next investigated whether these general and reproducible patterns were preserved upon IFN-α or IL28B stimulation in the setting of infection with HCV. After all, genotypic variation related to *IL28B* profoundly determines therapeutic response in chronic HCV by a yet unidentified mechanism pointing towards an important role of the cytokine in the course of the disease.

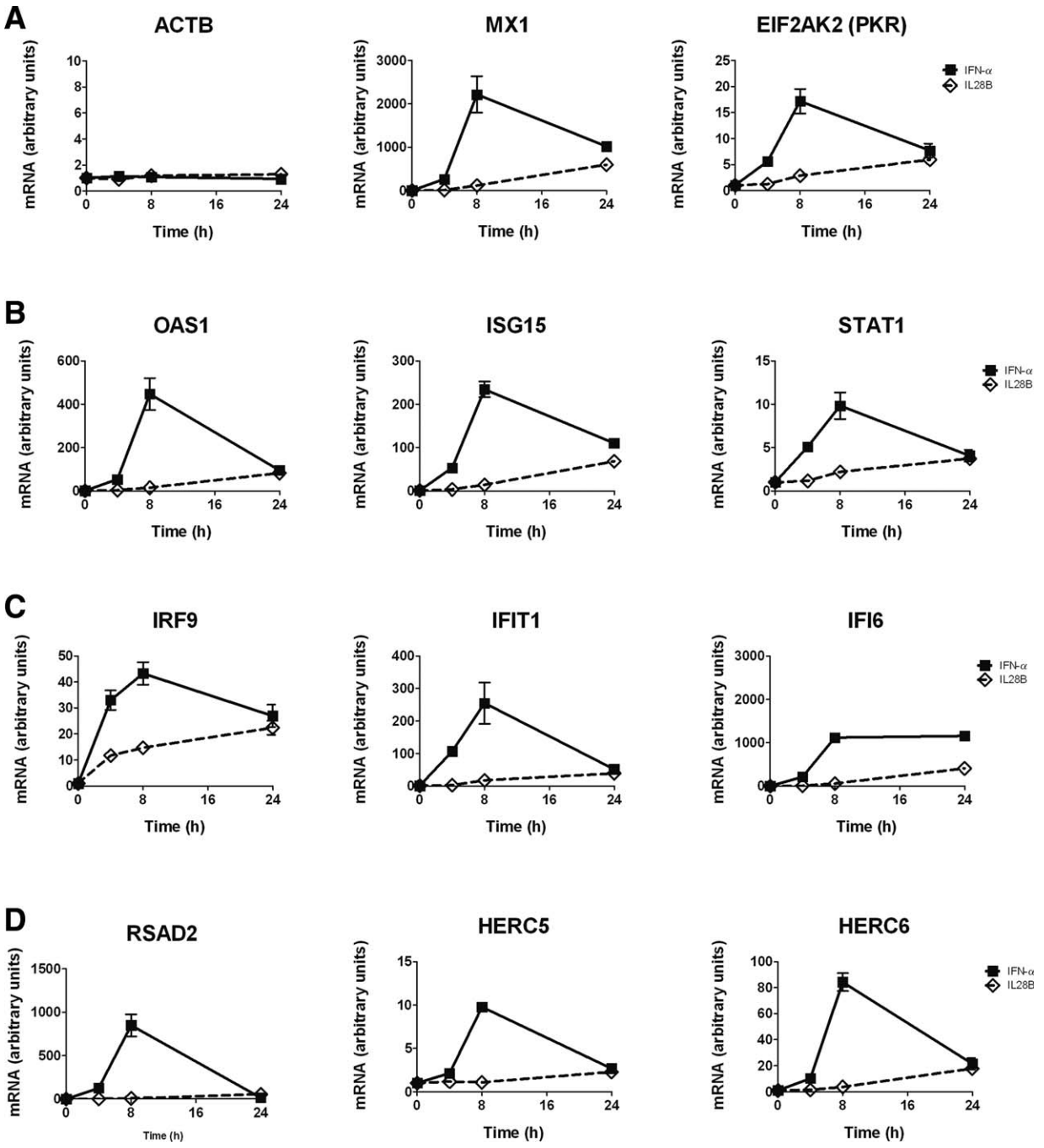

Fig. 5. Kinetic differences in the induction of ISGs by IFN-α and IL28B in hepatoma cells resembles characteristics seen in PHH and suggests the usefulness of Huh7.5.1 culture as a model system. Human hepatoma cells, Huh7.5.1, were plated and cultured as described in the Materials and Methods. One day after seeding, the cells were left untreated or incubated with IFN-α (0.43 ng/mL, equal to 30 IU/mL) or IL28B (50 ng/mL) for 4, 8, and 24 hours. RNA was extracted and analyzed by qRT-PCR. (A) The non-ISG ACTB (β-actin) was used as a negative control. Time courses for the ISGs MX1, EIF2AK2 (PKR), (B) OAS1, ISG15, STAT1, (C) IRF9, IFIT1, IFI6, (D) RSAD2 (Viperin), HERC5, HERC6 are shown. Gene expression at timepoint 0 was set to 1 and further timepoints are measured as fold induction in relation to timepoint 0. Error bars represent SD. Experiments were done in quadruplicate (n = 4).

We treated both uninfected and HCV-infected Huh7.5.1 (after established infection over several days) cells in parallel with IFN-α or IL28B over 48 hours (Fig. 6A-E; Supporting Figure 1A,B). While the overall pattern of IL28B induced gene expression in HCV-infected Huh7.5.1 cells was similar compared to uninfected cells with a slow increase of signal over time, surprisingly, the typical IFN-α response was not preserved in infection: the pattern with early maximum followed by decline of the induction signal observed in

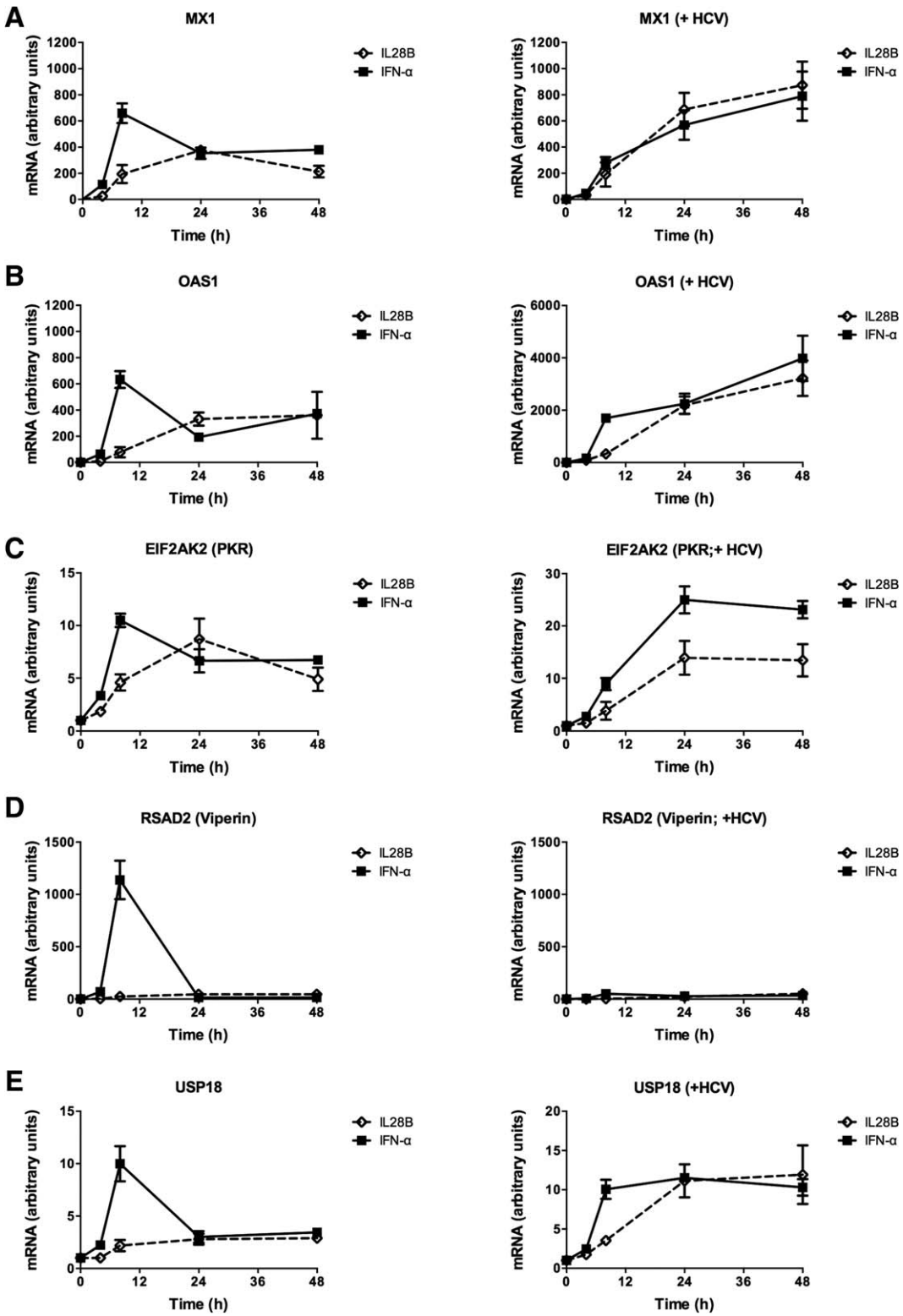

Fig. 6. The pattern of gene induction by IFN-α is profoundly changed after infection with HCV. Viral RNA was made from plasmid Jc1FLAG2(p7-nsGluc2a), an infectious recombinant HCV strain that harbors the *Gaussia* luciferase gene, and the RNA was transfected into Huh7.5.1 cells and supernatants collected at day 3 posttransfection. We then left Huh7.5.1 cells either untreated or used the described infectious supernatants to inoculate naïve Huh7.5.1 cells. After ongoing viral replication in the system for 5 days we continued with the gene induction experiments in both uninfected and infected Huh7.5.1 cells. Induction kinetics for several ISGs after stimulation with IFN-α (0.43 ng/mL, equal to 30 IU/mL) or IL28B (50 ng/mL) for 0, 4, 8, and 24 hours in Huh7.5.1 in the absence and presence of HCV infection are shown. For (A) MX1, (B) OAS1, (C) EIF2AK2 (PKR), (D) RSAD2 (Viperin), and (E) USP18, gene induction is shown in uninfected Huh7.5.1 and compared to the kinetics in cells that were previously infected with Jc1Gluc. Error bars represent SD. Experiments were done in quadruplicate.

uninfected Huh7.5.1 was blunted in the HCV-infected cells, and the course of gene expression over time became similar for IFN-α and IL28B-treated cells, reminiscent of a type III response. We assessed the effect of the cytokines on viral replication in the same samples over time and detected comparable antiviral effects (Supporting Figure 1C) and no clear pattern of increased or decreased expression for a selected number of representative ISGs (Supporting Figure 1D)

Differential Kinetics in Gene Expression Are Not Explained by Alteration in STAT1 Phosphorylation. Next, we investigated whether the observed RNA levels of ISGs were reflected in STAT1 phosphorylation patterns under the different conditions: we therefore studied phosphorylated STAT1 (pSTAT1) and STAT1 expression over time by western blot (Supporting Fig. 2). After optimization of relevant timepoints (time course up to 48 hours, data not shown) we saw an increase in the pSTAT1 signal with a maximum within 6 hours of stimulation followed by a decline. There were no apparent differences in the phosphorylation pattern observed in IFN-α or IL28B stimulated uninfected or infected cells. We conclude that STAT 1 phosphorylation patterns do *not* explain the distinct kinetic ISG mRNA patterns and that the basis for these distinct patterns potentially lie outside of the IFN signal transduction pathway.

Discussion

In order to better understand the role and function of IL28B, we sought to characterize differences in gene induction by IFN-α and IL28B. While our comprehensive transcriptomic analysis in *ex vivo* cultured PHH did not primarily reveal distinct genes induced by IL28B, there were significant kinetic differences when looking at the expression profiles of the studied typical ISGs. For many of these genes, the response to IFN-α was a fast and sharp increase followed by a decline in expression within 24 hours, whereas the IL28B response was slower but more sustained. This led us to confirm and further investigate these patterns in a more stable cell culture model that is permissive for robust HCV infection, human hepatoma cells. In infected cells, we obtained a similar temporal response to IL28B and IFN-α. Therefore, interestingly, the kinetic difference we found previously was substantially altered after infection with HCV.

We compared IFN-α and IL28B induced genes in PHH over 24 hours in expression microarrays. When we sorted the genes by relevance in the IL28B induced samples, we found known IFN-α-stimulated genes. This concurs with the initial reports describing type III IFNs, in which the authors detected intracellular signal transduction by way of the same JAK-STAT pathway that transduces the type I IFN signal.[1,2] Several publications analyze microarrays in PHH treated with IFN-α: In 2002 Radaeva et al.[18] published gene expression in PHH detected on an Affymetrix chip comprising 12,000 known genes and found 44 up-regulated >2-fold, including MX1, the OAS family and PKR, and nine genes down-regulated by greater than 50%. He et al.[19] compared transcriptomes of PHH after stimulation with IFN-α and IFN-γ at 6 hours and 18 hours. There were more IFN-α up-regulated genes at 6 hours than at 18 hours, whereas the opposite was true for IFN-γ. In HCV replicon cells, Marcello et al.[20] compared the effects of IFN-α and IL29 (IFN-λ1) and found several different patterns of gene regulation over 24 hours. However, the replicon model is limited to intracellular stages of the viral life cycle and may not be directly comparable to our experiments. Another group found different kinetics of RSAD2 and IFI44 induction between IFN-α and IL28B stimulation in PHH, as well as overlapping and distinct genes when comparing transcriptomes.[21] Based on our findings we speculate that genes previously described as being induced by solely one cytokine are ascribable to false negatives in the comparison samples, since the magnitude of induction appears to be considerably lower in PHH compared to cell lines and thus some genes have fallen below the threshold of significance. Interestingly, Doyle et al.[4] treated HepG2 cells with IL-29 or IFN-α for 1, 6, and 24 hours. The gene expression profiles upon stimulation with both cytokines were very similar with induction of typical ISGs, like PKR and MX1 at 6 hours and declining signals thereafter. Therefore, in contrast to what we describe for IL28B, the kinetics for IL29 induced genes may rather resemble IFN-α induction.

PHH are exquisitely sensitive to perturbations, lose cell functions and viability rapidly in culture, and do not proliferate.[16] Moreover, their use is limited by availability and quality of surgical specimens and the complex isolation procedure. It is important to note that due to the nature of hepatocyte extraction, there is a risk of contamination with other cell types in the PHH cultures. While on daily microscopic examination we were unable to detect any other cell types but hepatocytes in the cultures used for our studies, we cannot fully exclude that some of the effects that we see may be due to nonhepatocyte cells present in the cultures. Huh7.5.1 cells therefore appear as a valid model system to analyze kinetics. Based on our data

from two lines of investigation, we conclude that IFN-α and IL28B exert their differential effects through temporal expression differences. We further hypothesize that these differences may play a critical role in the antiviral immune response and that IFN-α and IL28B may complement each other's effects. Cell type-dependent expression of IL28RA and production of type III IFNs may facilitate tissue-specific regulation of antiviral effects, therefore allowing for fine-tuned responses that are able to match the organ and cell specificity of viruses. There is accumulating evidence that the type III IFNs function as a first line of antiviral defense in epithelial tissues like the gut, human liver, and lung, e.g., upon infection with influenza virus, whereas lack of local receptor expression, for instance in the central nervous system (CNS), makes use of the system in other tissues unlikely.[22-26]

Viruses have developed sophisticated mechanisms to counteract the effects of IFN.[27] HCV is notorious for its ability to evade host antiviral effector functions: mitochondrial antiviral-signaling protein (MAVS, also known as IPS-1), for example, is inactivated by the viral protease NS3/4, likely to diminish IFN induction. Further, HCV inhibits JAK-STAT signaling through a variety of mechanisms.[28-32]

In this study, we observed that HCV's modulation of the type I ISG response to resemble a type III response does not appear to be mediated by classical IFN signaling. Rather, they suggest that HCV may be acting through other, nonclassical mechanisms to sustain ISG expression, including induction of alternate transduction pathways or posttranscriptional regulation of ISGs. Blunting a rapid IFN response may be beneficial to survival of the virus. Once infection has stabilized, viral products may set up an effective antiinflammatory armamentarium that is able to suppress downstream effects of IFN-α. This is compatible with the clinical reality that signs of active inflammation *early* in the disease are predictive of viral clearance in HCV.[33,34] This response may be important in many viral infections to rapidly induce innate antiviral action and protect the host from systemic spread of viruses.

We selected differing doses of IFN-α and IL28B for the PHH experiments because our pilot studies indicated that higher concentrations of IL28B were required to produce comparable levels of peak ISG induction. These data are supported by our findings in Fig. 3. This apparent dose disparity may be attributable to the two cytokine's differential affinity for their cognate receptors. We also performed experiments using much higher doses of IFN-α and lower doses of IL28B and found no difference in the induction kinetics of ISGs (not shown), suggesting that the two IFNs retain their fundamental induction patterns over a wide range of concentrations.

Mechanisms that could potentially explain outcome differences upon HCV infection in patients with different IL28B-related genotypes include: alterations in IL28B expression, mRNA splicing, half-life, or cytokine-receptor affinity or specificity.[13] The literature on IL28A and IL28B expression levels is controversial, with some studies detecting slightly higher expression levels of the cytokines in the clearance associated genotype, e.g., in peripheral blood mononuclear cells (PBMCs),[9,10] and others being unable to find any such correlations in PBMCs and liver tissue, respectively.[8,17] An interesting recent contribution describes a novel gene that may be an additional member of the type III IFN family and contains a functional SNP related to both the IL28B genotype and outcome in HCV[35]: Depending on genotype, a protein is either made or not made. Strikingly, the favorable IL28B genotype as well as viral clearance are associated with nonproduction of the protein. The functional role of this novel gene, named IFNL4 (IFN-λ4), and the mechanism of action of its protein are unknown. Another recent study detected the same polymorphism, but found a correlation with IL28B expression.[37]

In summary, we demonstrate functional differences of IFN-α and IL28B by showing distinct kinetic induction patterns for many typical ISGs in hepatocytes. Furthermore, we demonstrate that the kinetic patterns of gene induction are altered during HCV infection. Given their common downstream signaling but temporal differences in gene induction, we speculate that IFN-α and IL28B play complementary roles with a massive, early IFN-α response and slower but more sustained gene induction by IL28B.

Acknowledgment: The authors thank F.V. Chisari (Scripps Research Institute, La Jolla, CA) for Huh7.5.1 cells, T. Wakita (National Institute for Infectious Diseases, Tokyo, Japan), and Charles M. Rice (Rockefeller University, New York, NY) for the infectious HCV strains JFH1 and Jc1Gluc. Normal human hepatocytes were obtained through the Liver Tissue Cell Distribution System (S.C. Strom, University of Pittsburgh, Pittsburgh, PA) which was funded by NIH Contract #N01-DK-7-004/HHSN26l7200700004C. We thank David Goldstein (Duke University, NC) for facilitating the microarray experiments and T.F. Baumert (INSERM U748, Strasbourg, France) for helpful suggestions.

References

1. Sheppard P, Kindsvogel W, Xu W, Henderson K, Schlutsmeyer S, Whitmore TE, et al. IL-28, IL-29 and their class II cytokine receptor IL-28R. Nat Immunol 2003;4:63-68.
2. Kotenko SV, Gallagher G, Baurin VV, Lewis-Antes A, Shen M, Shah NK, et al. IFN-lambdas mediate antiviral protection through a distinct class II cytokine receptor complex. Nat Immunol 2003;4:69-77.
3. Zhang L, Jilg N, Shao RX, Lin W, Fusco DN, Zhao H, et al. IL28B inhibits hepatitis C virus replication through the JAK-STAT pathway. J Hepatol 2011;55:289-298.
4. Doyle SE, Schreckhise H, Khuu-Duong K, Henderson K, Rosler R, Storey H, et al. Interleukin-29 uses a type 1 interferon-like program to promote antiviral responses in human hepatocytes. Hepatology 2006; 44:896-906.
5. Alter MJ. Epidemiology of hepatitis C virus infection. World J Gastroenterol 2007;13:2436-2441.
6. Lavanchy D. Evolving epidemiology of hepatitis C virus. Clin Microbiol Infect 2011;17:107-115.
7. Fried MW, Shiffman ML, Reddy KR, Smith C, Marinos G, Gonçales FL Jr, et al. Peginterferon alfa-2a plus ribavirin for chronic hepatitis C virus infection. N Engl J Med 2002;347:975-982.
8. Ge D, Fellay J, Thompson AJ, Simon JS, Shianna KV, Urban TJ, et al. Genetic variation in IL28B predicts hepatitis C treatment-induced viral clearance. Nature 2009;461:399-401.
9. Suppiah V, Moldovan M, Ahlenstiel G, Berg T, Weltman M, Abate ML, et al. IL28B is associated with response to chronic hepatitis C interferon-alpha and ribavirin therapy. Nat Genet 2009;41:1100-1104.
10. Tanaka Y, Nishida N, Sugiyama M, Kurosaki M, Matsuura K, Sakamoto N, et al. Genome-wide association of IL28B with response to pegylated interferon-alpha and ribavirin therapy for chronic hepatitis C. Nat Genet 2009;41:1105-1109.
11. Thomas DL, Thio CL, Martin MP, Qi Y, Ge D, O'Huigin C, et al. Genetic variation in IL28B and spontaneous clearance of hepatitis C virus. Nature 2009;461:798-801.
12. Rauch A, Kutalik Z, Descombes P, Cai T, Di Iulio J, Mueller T, et al. Genetic variation in IL28B is associated with chronic hepatitis C and treatment failure: a genome-wide association study. Gastroenterology 2010;138:1338-1345, 1345.e1-7.
13. Afdhal NH, McHutchison JG, Zeuzem S, Mangia A, Pawlotsky JM, Murray JS, et al. Hepatitis C pharmacogenetics: state of the art in 2010. Hepatology 2011;53:336-345.
14. Marukian S, Jones CT, Andrus L, Evans MJ, Ritola KD, Charles ED, et al. Cell culture-produced hepatitis C virus does not infect peripheral blood mononuclear cells. Hepatology 2008;48:1843-1850.
15. Lindenbach BD, Evans MJ, Syder AJ, Wölk B, Tellinghuisen TL, Liu CC, et al. Complete replication of hepatitis C virus in cell culture. Science 2005;309:623-626.
16. Strom SC, Pisarov LA, Dorko K, Thompson MT, Schuetz JD, Schuetz EG. Use of human hepatocytes to study P450 gene induction. Methods Enzymol 1996;272:388-401.
17. Urban TJ, Thompson AJ, Bradrick SS, Fellay J, Schuppan D, Cronin KD, et al. IL28B genotype is associated with differential expression of intrahepatic interferon-stimulated genes in patients with chronic hepatitis C. Hepatology 2010;52:1888-1896.
18. Radaeva S, Jaruga B, Hong F, Kim WH, Fan S, Cai H, et al. Interferon-alpha activates multiple STAT signals and down-regulates c-Met in primary human hepatocytes. Gastroenterology 2002;122:1020-1034.
19. He XS, Nanda S, Ji X, Calderon-Rodriguez GM, Greenberg HB, Liang TJ. Differential transcriptional responses to interferon-alpha and interferon-gamma in primary human hepatocytes. J Interferon Cytokine Res 2010;30:311-320.
20. Marcello T, Grakoui A, Barba-Spaeth G, Machlin ES, Kotenko SV, MacDonald MR, et al. Interferons alpha and lambda inhibit hepatitis C virus replication with distinct signal transduction and gene regulation kinetics. Gastroenterology 2006;131:1887-1898.
21. Thomas E, Gonzalez VD, Li Q, Modi AA, Chen W, Noureddin M, et al. HCV infection induces a unique hepatic innate immune response associated with robust production of type III interferons. Gastroenterology 2012;142:978-988.
22. Jewell NA, Cline T, Mertz SE, Smirnov SV, Flaño E, Schindler C, et al. Lambda interferon is the predominant interferon induced by influenza A virus infection in vivo. J Virol 2010;84:11515-11522.
23. Sommereyns C, Paul S, Staeheli P, Michiels T. IFN-lambda (IFN-lambda) is expressed in a tissue-dependent fashion and primarily acts on epithelial cells in vivo. PLoS Pathog 2008;4:e1000017.
24. Pott J, Mahlakõiv T, Mordstein M, Duerr CU, Michiels T, Stockinger S, et al. IFN-lambda determines the intestinal epithelial antiviral host defense. Proc Natl Acad Sci U S A 2011;108:7944-7949.
25. Mordstein M, Neugebauer E, Ditt V, Jessen B, Rieger T, Falcone V, et al. Lambda interferon renders epithelial cells of the respiratory and gastrointestinal tracts resistant to viral infections. J Virol 2010;84:5670-5677.
26. Mordstein M, Kochs G, Dumoutier L, Renauld JC, Paludan SR, Klucher K, et al. Interferon-lambda contributes to innate immunity of mice against influenza A virus but not against hepatotropic viruses. PLoS Pathog 2008;4:e1000151.
27. Wang BX, Fish EN. The yin and yang of viruses and interferons. Trends Immunol 2012;33:190-197.
28. Baril M, Racine ME, Penin F, Lamarre D. MAVS dimer is a crucial signaling component of innate immunity and the target of hepatitis C virus NS3/4A protease. J Virol 2009;83:1299-1311.
29. Lin W, Kim SS, Yeung E, Kamegaya Y, Blackard JT, Kim KA, et al. Hepatitis C virus core protein blocks interferon signaling by interaction with the STAT1 SH2 domain. J Virol 2006;80:9226-9235.
30. Lin W, Choe WH, Hiasa Y, Kamegaya Y, Blackard JT, Schmidt EV, et al. Hepatitis C virus expression suppresses interferon signaling by degrading STAT1. Gastroenterology 2005;128:1034-1041.
31. Kumthip K, Chusri P, Jilg N, Zhao L, Fusco DN, Zhao H, et al. Hepatitis C virus NS5A disrupts STAT1 phosphorylation and suppresses type I interferon signaling. J Virol 2012;86:8581-8591.
32. Taylor DR, Shi ST, Romano PR, Barber GN, Lai MM. Inhibition of the interferon-inducible protein kinase PKR by HCV E2 protein. Science 1999;285:107-110.
33. Gerlach JT, Diepolder HM, Zachoval R, Gruener NH, Jung MC, Ulsenheimer A, et al. Acute hepatitis C: high rate of both spontaneous and treatment-induced viral clearance. Gastroenterology 2003;125:80-88.
34. Bochud PY, Bibert S, Kutalik Z, Patin E, Guergnon J, Nalpas B, et al. IL28B alleles associated with poor hepatitis C virus (HCV) clearance protect against inflammation and fibrosis in patients infected with non-1 HCV genotypes. Hepatology 2012;55:384-394.
35. Jensen LJ, Kuhn M, Stark M, Chaffron S, Creevey C, Muller J, et al. STRING 8 — a global view on proteins and their functional interactions in 630 organisms. Nucleic Acids Res 2009;37:D412-416.
36. Prokunina-Olsson L, Muchmore B, Tang W, Pfeiffer RM, Park H, Dickensheets H, et al. A variant upstream of IFNL3 (IL28B) creating a new interferon gene IFNL4 is associated with impaired clearance of hepatitis C virus. Nat Genet 2013;45:164-171.
37. Bibert S, Roger T, Calandra T, Bochud M, Cerny A, Semmo N, et al. IL28B expression depends on a novel TT/-G polymorphism which improves HCV clearance prediction. J Exp Med 2013;210.

Appendix C: Liver environment and HCV replication affect human T-cell phenotype and expression of inhibitory receptors.

Daniela C Kroy, Donatella Ciuffreda, Jennifer H Cooperrider, Michelle Tomlinson, Garrett D Hauck, Jasneet Aneja, Christoph Berger, David Wolski, Mary Carrington, E John Wherry, Raymond T Chung, Kenneth K Tanabe, Nahel Elias, Gordon J Freeman, Rosemarie H de Kruyff, Joseph Misdraji, Arthur Y Kim, and Georg M Lauer.

Gastroenterology, 2014 vol. 146 (2) pp. 550-561.

Summary

This study investigates the immunophenotypic profiles of CD8 T cells in HCV infection in the context of varying cell localization. In a multi-color flow cytometric approach, it compares the expression of multiple inhibitory receptors (PD-1, 2B4, CD160, Tim-3, LAG-3) in HCV- and CMV-specific CD8 T cells from paired peripheral blood and liver samples of patients with untreated chronic, treated chronic and resolved HCV infection. The data show that liver-resident T cells generally have a rather distinct phenotype compared to those in the blood, with higher expression of inhibitory receptors even in healthy livers. Virus-specific T cells in the liver then express even higher levels of 2B4 and PD-1 and cells in untreated chronic infection also express Tim-3, while cells in patients with sustained virologic response and those specific to CMV lack Tim-3 but express higher levels of LAG-3 and display a different memory phenotype and capacity to proliferate.

These results demonstrate that expression of inhibitory receptor expression and memory phenotype of CD8 T cells in viral infection is dependent on both cellular localization and for specific T cells on the level of viral control.

Gastroenterology 2014;146:550–561

Liver Environment and HCV Replication Affect Human T-Cell Phenotype and Expression of Inhibitory Receptors

Daniela C. Kroy,[1] Donatella Ciuffreda,[1] Jennifer H. Cooperrider,[1] Michelle Tomlinson,[1,2] Garrett D. Hauck,[1] Jasneet Aneja,[1] Christoph Berger,[3] David Wolski,[1] Mary Carrington,[3,4] E. John Wherry,[5,6] Raymond T. Chung,[1] Kenneth K. Tanabe,[7] Nahel Elias,[8] Gordon J. Freeman,[9] Rosemarie H. de Kruyff,[10] Joseph Misdraji,[2] Arthur Y. Kim,[11] and Georg M. Lauer[1]

[1]Gastrointestinal Unit, [2]Department of Pathology, [7]Divison of Surgical Oncology, [8]Transplantation Unit, and [11]Infectious Disease Division, Massachusetts General Hospital and Harvard Medical School, Boston, Massachusetts; [3]Ragon Institute of Massachusetts General Hospital, Massachusetts Institute of Technology, and Harvard University, Boston, Massachusetts; [4]Cancer and Inflammation Program, Laboratory of Experimental Immunology, SAIC-Frederick, Inc, Frederick National Laboratory for Cancer Research, Frederick, Maryland; [5]Department of Microbiology and [6]Institute for Immunology, University of Pennsylvania Perelman School of Medicine, Philadelphia, Pennsylvania; [9]Department of Medical Oncology, Dana-Farber Cancer Institute and Harvard Medical School, Boston, Massachusetts; and [10]Division of Immunology, Children's Hospital and Harvard Medical School, Boston, Massachusetts

BACKGROUND & AIMS: There is an unclear relationship between inhibitory receptor expression on T cells and their ability to control viral infections. Studies of human immune cells have been mostly limited to T cells from blood, which is often not the site of infection. We investigated the relationship between T-cell location, expression of inhibitory receptors, maturation, and viral control using blood and liver T cells from patients with hepatitis C virus (HCV) and other viral infections. **METHODS:** We analyzed 36 liver samples from HCV antibody–positive patients (30 from patients with chronic HCV infection, 5 from patients with sustained virological responses to treatment, and 1 from a patient with spontaneous clearance) with 19 paired blood samples and 51 liver samples from HCV-negative patients with 17 paired blood samples. Intrahepatic and circulating lymphocytes were extracted; T-cell markers and inhibitory receptors were quantified for total and virus-specific T cells by flow cytometry. **RESULTS:** Levels of the markers PD-1 and 2B4 (but not CD160, TIM-3, or LAG-3) were increased on intrahepatic T cells from healthy and diseased liver tissues compared with T cells from blood. HCV-specific intrahepatic $CD8^+$ T cells from patients with chronic HCV infection were distinct in that they expressed TIM-3 along with PD-1 and 2B4. In comparison, HCV-specific $CD8^+$ T cells from patients with sustained virological responses and T cells that recognized cytomegalovirus lacked TIM-3 but expressed higher levels of LAG-3; these cells also had different memory phenotypes and proliferative capacity. **CONCLUSIONS:** T cells from liver express different inhibitory receptors than T cells from blood, independent of liver disease. HCV-specific and cytomegalovirus-specific $CD8^+$ T cells can be differentiated based on their expression of inhibitory receptors; these correlate with their memory phenotype and levels of proliferation and viral control.

Keywords: Immune Regulation; Costimulation; T-Cell Exhaustion; Inflammation.

Inhibitory and costimulatory T-cell receptors regulate T-cell responses to allow for effective control of pathogens and tumor cells while limiting immunopathology and autoimmunity.[1,2] A disturbed balance between stimulatory and inhibitory signals can lead to ineffective T-cell responses that are unable to clear infected or malignant hepatocytes.[3] Increased expression of a variety of T-cell inhibitory receptors such as PD-1, 2B4, LAG-3, TIM-3, and CD160 has been described for chronic infections caused by lymphocytic choriomeningitis virus, simian immunodeficiency virus, human immunodeficiency virus 1, hepatitis B virus, and hepatitis C virus (HCV),[4–7] among others, showing that this pathway enabling viral persistence is widely operative in chronic infections in animals and humans. Dissecting the mechanisms leading to T-cell exhaustion generates opportunities for immunotherapeutic interventions by reversing T-cell inhibition, as shown by the recent success of PD-1 blockade in human malignancies.[8] To optimize the impact of these therapies while minimizing the risk of immunopathologies and autoimmunity, it is paramount to develop our understanding of the coregulation patterns of inhibitory receptors, because T-cell regulation is likely adapted to the infecting pathogen as well as the immunological features of the site of infection.

HCV infection offers the rare opportunity to study the immune correlates required for viral control mediated by virus-specific T cells, because an estimated 20% to 30% of infected patients are able to clear infection spontaneously and others control HCV on therapy.[9] Furthermore, because HCV infection is limited to hepatocytes, access to liver tissue allows comparison of T cells from the site of infection with those circulating in the blood. Previous studies of HCV

Abbreviations used in this paper: **CMV, cytomegalovirus; HCV, hepatitis C virus; IHL, intrahepatic lymphocyte; PBMC, peripheral blood mononuclear cell.**

0016-5085/$36.00
http://dx.doi.org/10.1053/j.gastro.2013.10.022

infection have shown the up-regulation of T-cell inhibitory receptors, especially PD-1,[5,10] on HCV-specific T cells and the association of continuous antigenic stimulation with higher expression levels of PD-1.[11,12] Emerging data further suggest that coexpression of multiple T-cell inhibitory receptors on HCV-specific CD8 T cells in the blood leads to a more severely exhausted phenotype than expression of PD-1 alone, with a variety of additional inhibitory receptors suggested as important.[13–15] Although these data suggest that T-cell exhaustion through expression and engagement of T-cell inhibitory receptors may be a causative factor leading to persistent HCV infection, these studies were predominantly performed on circulating T cells in blood. Recent studies in chronically HCV infected livers have shown that intrahepatic T cells, in comparison to T cells in the blood, express higher levels of PD-1 and lower levels of the T-cell maturation marker CD127.[5,16,17] In addition, coexpression of PD-1 with TIM-3 has been suggested to identify HCV-specific T cells with advanced exhaustion.[13,18] These studies provide a rationale to fully define the expression of a larger set of inhibitory receptors on intrahepatic T cells in chronic HCV infection. They also suggest that the liver might represent a special microenvironment in the context of T-cell regulation that needs better definition to interpret profiles of intrahepatic T cells adequately.

Based on the previous findings in HCV infection and the remaining gaps in our understanding of how HCV-specific T cells are regulated, we tested the following hypotheses: (1) intrahepatic T cells are in general characterized by T-cell inhibitory expression patterns that are distinct from T cells in the blood, (2) coexpression patterns of T-cell inhibitory receptors on intrahepatic T cells are distinct in different disease types, and (3) in the case of HCV infection, distinct levels of viral control are directly associated with differential expression of T-cell inhibitory receptors and with different T-cell phenotypes. To this end, we studied bulk CD4 and CD8 T-cell responses in blood and liver from subjects with a variety of liver conditions and also intrahepatic virus-specific CD8 T-cell responses targeting HCV and cytomegalovirus (CMV). Importantly, we were able to study intrahepatic T cells in not only persistent but also resolved HCV infection, allowing us to define differences in T-cell properties that can be directly attributed to persistent viremia. The results suggest an overarching influence of the liver environment on all intrahepatic T cells but also identify unique T-cell phenotypes that correspond to different levels of viral control.

Materials and Methods

Subjects

Eighty-seven liver specimens were obtained from explanted or resected liver tissue from subjects recruited at Massachusetts General Hospital. The study was approved by the local institutional review board ("Cell mediated immunity in hepatitis C virus infection"; protocol no. 1999-P-004983/54; Massachusetts General Hospital no. 90-7246).

Liver tissue was obtained from liver explants in end-stage liver disease and from liver resection for malignant or benign lesions. When intrahepatic lesions were present, the tissue for this study was collected from the most distant section of the specimen. One HCV antibody–positive RNA-negative subject was undergoing a second liver transplant and was being treated with tacrolimus.

Overall, we analyzed 36 HCV antibody–positive liver tissues (30 chronically infected, 5 with sustained virological response, and 1 after spontaneous clearance) with 19 paired blood samples and 51 HCV-negative liver tissues with 17 paired blood samples. The patient characteristics are described in Table 1.

Intrahepatic lymphocytes (IHLs) were extracted by mechanical disruption of liver tissue. The cell suspension was washed twice in R10 (RPMI 1640 with 10% fetal bovine serum), followed by centrifugation at 300 rpm to remove cell debris and hepatocytes. The final washing step was followed by centrifugation at 1500 rpm to pellet the IHLs. Peripheral blood mononuclear cells (PBMCs) were extracted and cryopreserved as previously described.[5]

HLA Typing

High-resolution HLA typing was performed at NCI Frederick. Samples were genotyped for HLA-A/B/C by the polymerase

Table 1. Clinical Characteristics of Patient Cohort (N = 87)

Cohort	n (%)	Average age (*y*)	Male (%)	Cirrhosis (%)	Jaundice (%)	Average alanine aminotransferase level (*U/L*)	Average aspartate aminotransferase level (*U/L*)
Viral hepatitis	43 (50)	59.4	90	73	42	58	82
HCV	36 (83)	59.8	89	60	43	64	90
Chronic HCV: malignancy (19), ESLD (11)	30	60.3	87	89	52	70	99
Resolved HCV: malignancy (5), rejection (1)	6	57.2	100	60	40	31	43
Hepatitis B virus: malignancy (6), ESLD (1)	7 (17)	57.9	100	57	43	36	47
Nonviral: malignancy (20), other liver diseases (16)	36 (43)	55.8	50	22	25	60	65
Control: benign liver lesions (8)	8 (7)	48.7	17	0	0	28	23

ESLD, end-stage liver disease.

chain reaction/sequence-specific oligonucleotide probing typing protocol and polymerase chain reaction sequence-based typing. All HLA class I loci were defined to 4-digit resolution with the exceptions of A*74:01/2, B*81, Cw*17, and Cw*18, which were determined to 2 digits.

Flow Cytometry

For expression analysis of T-cell inhibitory receptors on bulk $CD4^+$ and $CD8^+$ PBMCs and IHLs, 0.3 to 0.5 million cells were stained with viability dye (L23105; Invitrogen, Carlsbad, CA) for 30 minutes at room temperature, followed by a washing step with phosphate-buffered saline and incubation with surface antibodies for 30 minutes on ice (CD3-Pacific Blue [BD Biosciences, Franklin Lakes, NJ; 558117], CD4 APC-Cy7 [BD Biosciences 557871], CD8 AF700 [BD Biosciences 557945], PD-1 PerCp/Cy5.5 [BioLegend, San Diego, CA; 329914] or PE-Cy7 [BioLegend 109110], CD160 PE [eBioscience, San Diego, CA; 12-1601-81] or AF488 [eBioscience 53-1609-42], CD244 PC5 [Beckman Coulter, Brea, CA; IM2658] or PerC-pyCy5.5 [BioLegend 329514], LAG-3 FITC [Lifespan Biosciences, Seattle, WA; LS-B2237] or PerCp [R&D, Minneapolis, MN; FAB2319C], TIM-3 APC [clone 11G8, Rosemary de Kruyff], CCR7 APC-Cy7 [BioLegend 353212], CD45RA Qdot605 [eBioscience 93-0458-42]). The cells were washed twice with phosphate-buffered saline/2% fetal calf serum and then fixed in 1% formalin/phosphate-buffered saline. Flow cytometry was performed on an LSR-II flow cytometer (Becton Dickinson, Franklin Lakes, NJ) and the data were analyzed using FlowJo software (Tree Star Inc, Ashland, OR). Gating for the different antibodies was determined by fluorescence minus 1 with sample flow plots shown in Supplementary Figure 1. Due to application of different flow cytometry panels, CD160 or TIM-3 staining is missing in some patients (Figure 4*C* and *D*). For staining with HCV-peptide tetramers or pentamers, the samples were incubated with tetrameric or pentameric complexes for an additional 30 minutes at room temperature after addition of the viability dye, followed by a washing step, as described previously.[19] A list of the used multimers is provided in Supplementary Table 1.

Statistical Analysis

All data were normally distributed. When comparing continuous variables within 2 groups, Student *t* test (paired and unpaired) was used as applicable. *P* values were corrected using Bonferroni method whenever applicable. All statistical tests were performed using GraphPad Prism software version 5 (GraphPad Software, La Jolla, CA) and SAS version 9.3 (SAS Institute, Cary, NC).

For Figure 4, we acknowledge that the n value of 15 and the n value of 8 include 2 patients in both of these experiments who contributed more than one observation (11-13 and 10-96 for chronic HCV; 10N and 10V for resolved HCV). To account for this discrepancy, we recalculated our sample size. Assuming a moderate intraclass correlation coefficient of 0.5, which in our opinion is a conservative estimate, we determined our effective sample size to be 12 and 6.6, respectively (calculation not shown). This technique is justifiable considering that the statistical significance remains unchanged even if said observations are removed from the analysis.

SPICE Analysis

To analyze coexpression profiles of different T-cell inhibitory receptors on $CD4^+$ and $CD8^+$ T cells as well as on HLA multimer-positive $CD8^+$ T cells, we used SPICE, which is a freeware analysis program provided by the National Institutes of Health (http://exon.niaid.nih.gov/spice/). Data analysis was based on the "Boolean gates" function in FlowJo (TreeStar Inc).

Results

Expression of PD-1 and 2B4, but Not CD160, LAG-3, or TIM-3, Is Higher in Intrahepatic CD4 and CD8 T-Cell Populations Compared With Circulating T Cells

To compare the expression levels of different T-cell inhibitory receptors between intrahepatic and peripheral lymphocytes, we analyzed bulk $CD4^+$ and $CD8^+$ T cells using liver tissue–derived lymphocytes and matched PBMCs from 19 patients with chronic HCV infection and 14 HCV-negative patients. The clinical characteristics are shown in Table 1, and a flow cytometry sample is shown in Supplementary Figure 1. We detected higher expression levels for PD-1, as previously described,[5,16,17] but could also detect much higher expression of 2B4 on bulk $CD4^+$ and $CD8^+$ T cells in the liver compared with matched PBMCs in HCV-infected subjects (Figure 1*A* and *B*, *first and third graphs*). Interestingly, the same differential expression levels of PD-1 and 2B4 between the liver and periphery could be observed in HCV-negative individuals (Figure 1*A* and *B*, *second and fourth graphs*). Because the liver contains virtually no naïve T cells, we also compared the 2 compartments while limiting the analysis to the non-naïve cell pool ($CD45RA^-$ $CCR7^-$) in blood and liver. Removing naïve T cells, which typically do not express inhibitory receptors, from the analysis did not alter the general pattern of differential expression of inhibitory receptors in liver versus blood, although the differences were less pronounced (Supplementary Figure 2).

In contrast to PD-1 and 2B4, the global expression levels of CD160, TIM-3, and LAG-3 did not differ significantly between intrahepatic and peripheral $CD4^+$ and $CD8^+$ T cells in either HCV antibody–positive or HCV-negative patients, and overall their expression levels were generally much lower compared with those observed for PD-1 and 2B4 (Figure 1*C*–*E*). One exception was that CD160 expression was higher on intrahepatic CD8 T cells from HCV-negative liver tissues (Figure 1*C*, *fourth graph*). Altogether, our data show that, irrespective of HCV status, intrahepatic CD4 and CD8 T cells are characterized by the global up-regulation of PD-1 and 2B4, while expression levels of TIM-3, LAG-3, and CD160 are comparable to what is observed in blood.

Expression Patterns of Inhibitory T-Cell Receptors on IHLs Are Similar in All Liver Disease Types and Even in Healthy Liver

Given the surprising finding that T-cell inhibitory receptor expression patterns were similar in HCV antibody–positive

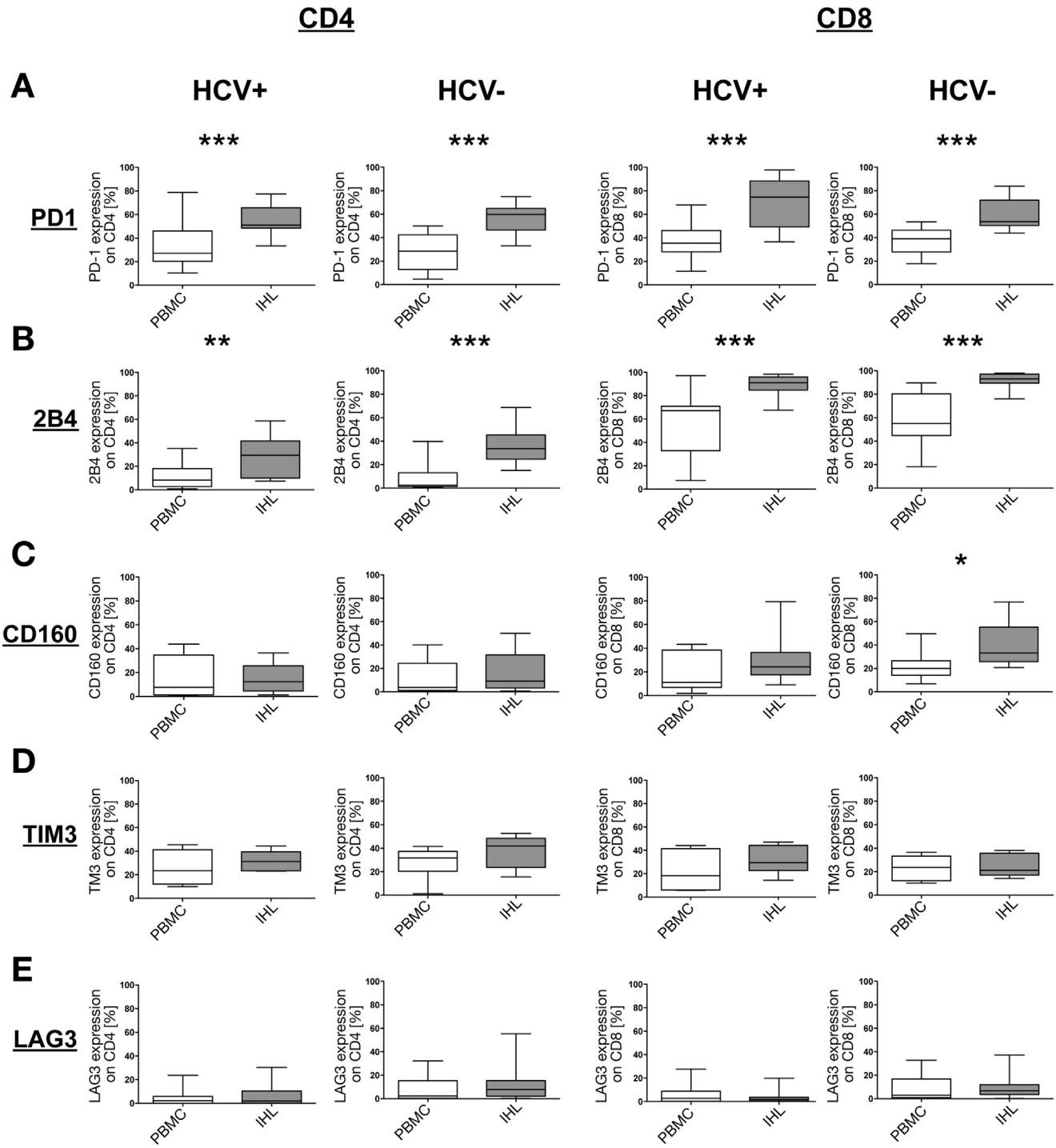

Figure 1. Expression analysis of PD-1, 2B4, CD160, TIM-3, and LAG-3 on $CD4^+$ (*2 left graphs*) and $CD8^+$ T cells (*2 right graphs*) for patient-matched PBMCs and IHLs. The analysis includes 19 chronically HCV-infected and 14 HCV-negative patients (*$P < .05$, **$P < .01$, ***$P < .001$, paired *t* test). (*A*) PD-1, (*B*) 2B4, (*C*) CD160, (*D*) TIM-3, and (*E*) LAG-3 expression on $CD4^+$ and $CD8^+$ T cells on PBMCs versus IHLs (percentage).

and HCV-negative liver tissues, we extended our analysis to a total of 81 liver tissues, allowing us to compare a variety of different infectious and noninfectious liver pathologies. Thirty liver tissues were from HCV antibody–positive subjects and 51 from HCV-negative subjects with different liver diseases, including 8 tissues without any signs of infection, inflammation, or malignancy (obtained from subjects with resections of liver adenomas or cysts). We did not

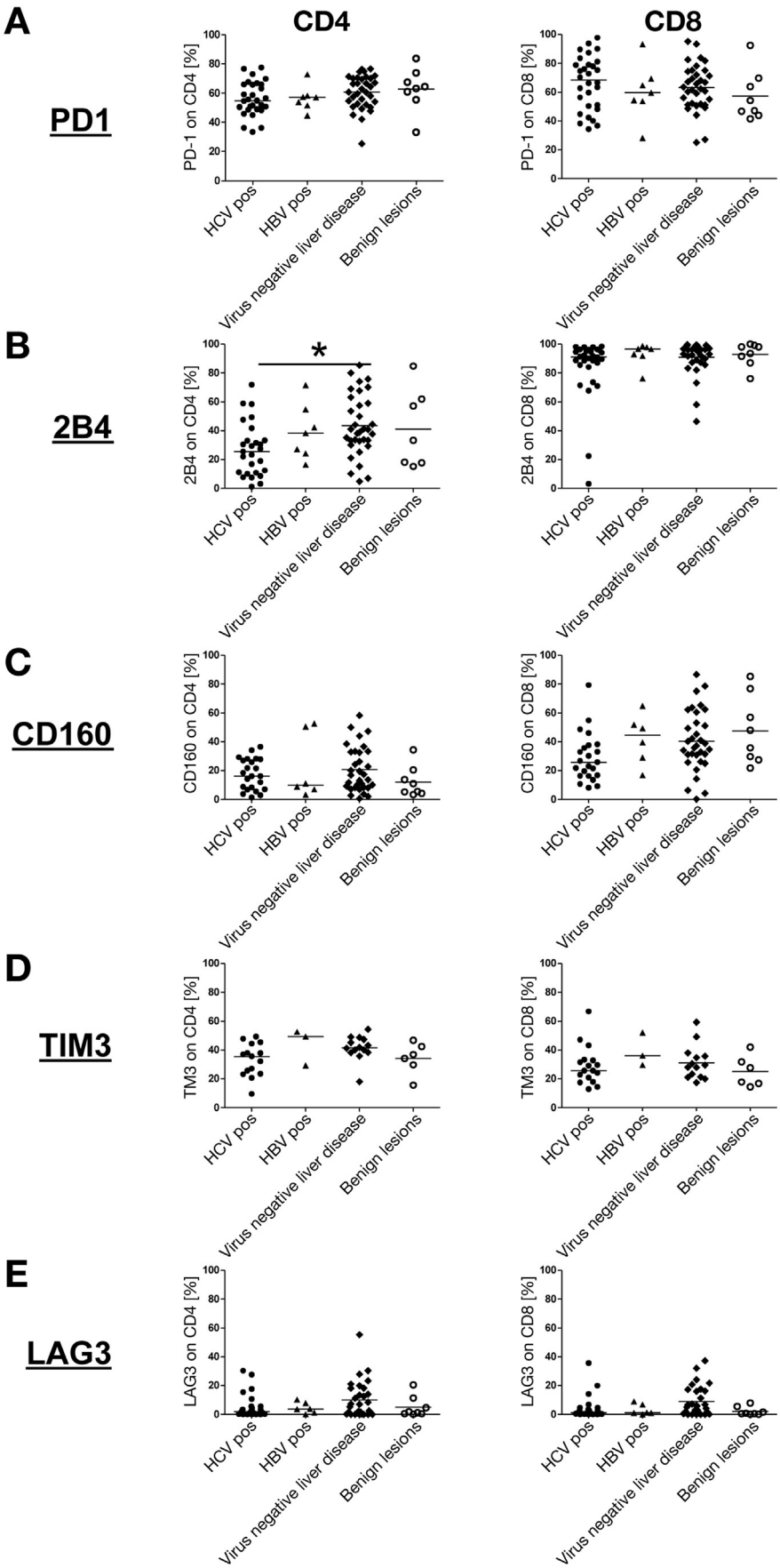

Figure 2. Inhibitory receptor expression on $CD4^+$ and $CD8^+$ IHLs in 4 different subgroups: HCV positive (30), hepatitis B virus positive (7), virus negative with other liver disease (36), and benign liver lesions (8). (*A*) PD-1, (*B*) 2B4, (*C*) CD160, (*D*) TIM-3, and (*E*) LAG-3 expression on $CD4^+$ (*left graphs*) and $CD8^+$ IHLs (*right graphs*). *P* values $<.008$ were considered positive using unpaired *t* tests with Bonferroni correction.

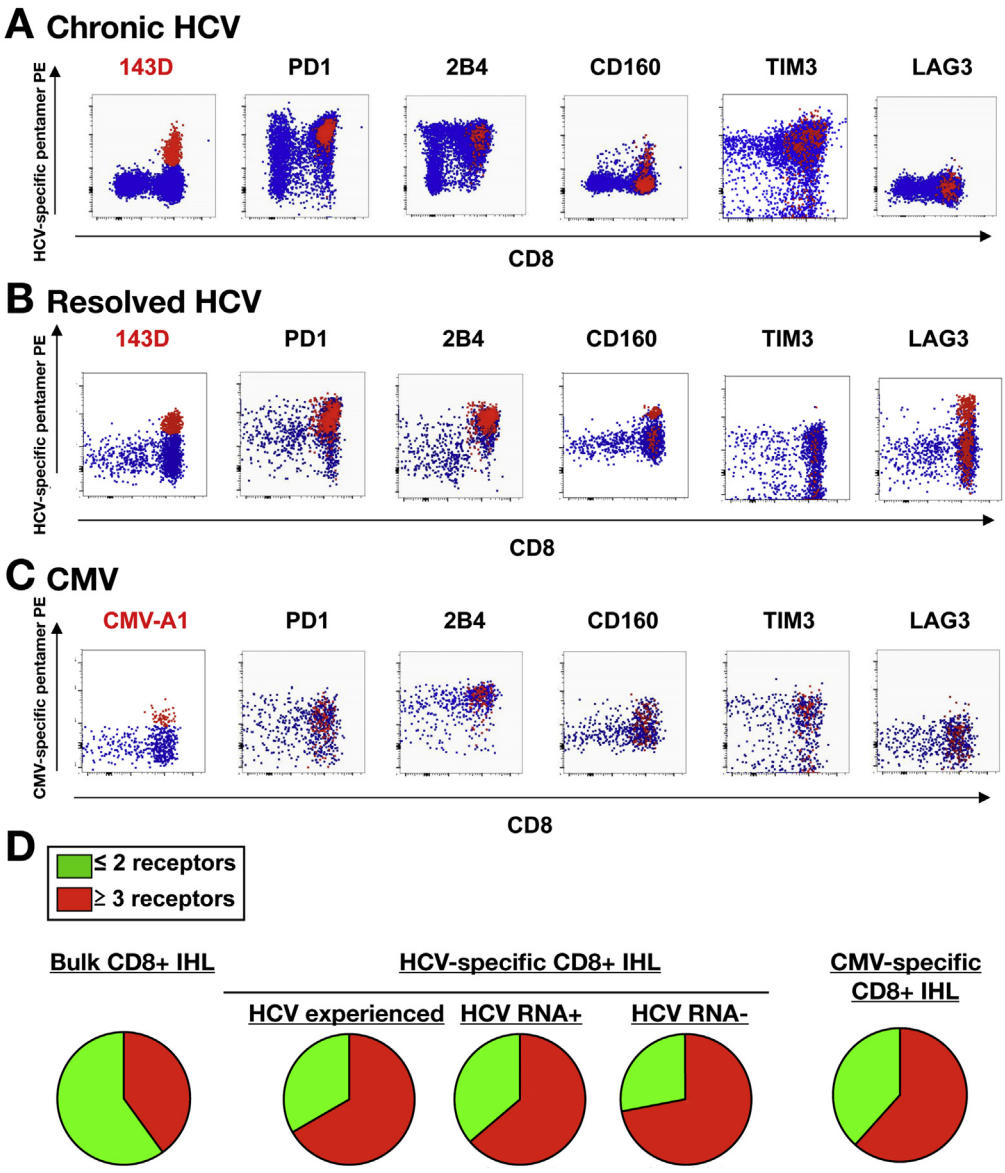

Figure 3. Representative flow plots for analysis of virus-specific IHLs (*red dots*) and PD-1, 2B4, CD160, TIM-3, and LAG-3 in comparison to bulk $CD8^+$ IHLs for (*A*) a chronically infected HCV patient, (*B*) a patient with resolved HCV, and (*C*) an intrahepatic CMV-specific response. (*D*) Coexpression patterns of T-cell inhibitory receptors in different T-cell populations by SPICE analysis (each SPICE diagram represents all experiments performed in this subgroup): total intrahepatic CD8 T-cell population (*left panel*), intrahepatic HCV-specific CD8 T-cell responses (*middle panels*, separated into all responses combined, responses in resolved HCV infection and responses in chronic HCV infection), and intrahepatic CMV responses (*right panel*). The *green sections* represent T cells with coexpression of 2 or fewer inhibitory receptors, and the *red sections* represent coexpression of 3 or more inhibitory receptors.

detect any major differences in the expression levels of T-cell inhibitory receptors between different liver pathologies, including IHLs from control liver tissue from patients with benign lesions (Figure 2). We did not find any correlation between expression of inhibitory receptors and alanine aminotransferase levels (Supplementary Figure 3, *left graphs*) or the presence or absence of cirrhosis (Supplementary Figure 3, *right graphs*), and patients younger or older than 60 years (data not shown) also failed to show significant differences. When we analyzed the correlation between inhibitory receptor expression and viral load, we could not detect any expression pattern relationship (data not shown). These data identify an expression pattern of T-cell inhibitory receptors on intrahepatic bulk $CD4^+$ and $CD8^+$ T cells that is characteristic of the liver environment and not a function of liver disease etiology or liver pathology.

HCV-Specific IHLs in Chronic Hepatitis C Are Characterized by Coexpression of Multiple T-Cell Inhibitory Receptors That Correlate With the Degree of Viral Control

We next assessed to what degree virus-specific CD8 T cells coexpress the different T-cell inhibitory receptors using class I multimers specific for HCV and CMV epitopes. Sixteen HCV antibody–positive subjects were assessed with 22 CD8 T-cell responses to 14 HCV antigens. Furthermore, 11 CMV antigens of 4 HCV antibody–positive and 7 HCV-negative patients could be identified directly ex vivo. Representative example stainings on specific cells are presented in Figure 3. Using the Boolean gate function in FlowJo together with SPICE analysis, we integrated the expression data for the different T-cell regulatory receptors. Interestingly, a significantly higher proportion of HCV-

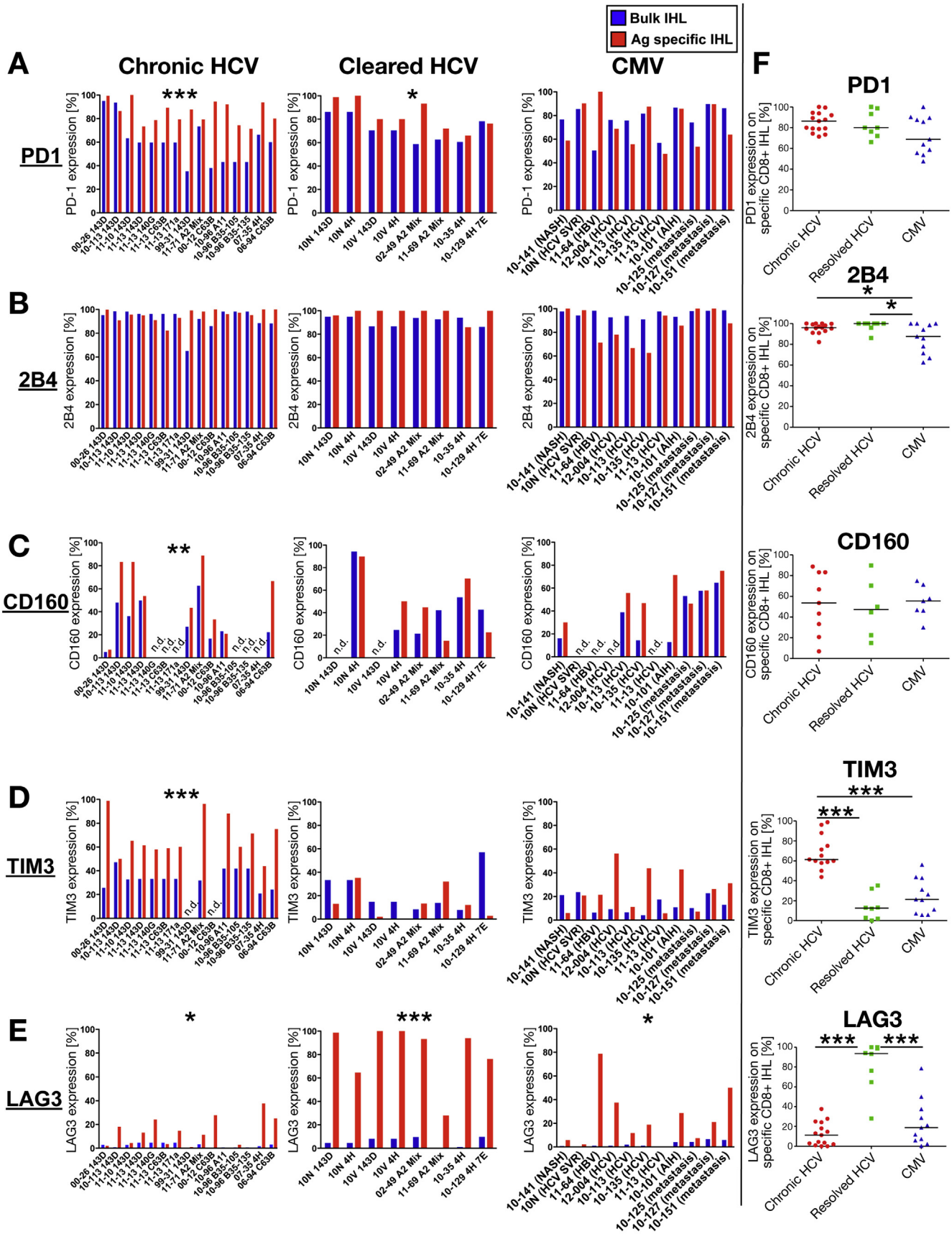

Figure 4. Expression of T-cell inhibitory receptors on bulk CD8$^+$ IHLs (*blue bars*) compared with HCV-specific CD8$^+$ IHLs (*red bars*). (*A–E*, *left graphs*) Patients with chronic HCV infection, (*A–E*, *middle graphs*) patients with resolved HCV, and (*A–E*, *right graphs*) CMV-specific IHLs. (*F*) IHL results for (*A*) PD-1, (*B*) 2B4, (*C*) CD160, (*D*) TIM-3, and (*E*) LAG-3. *$P < .01$, ***$P < .0001$ in paired and unpaired *t* tests with Bonferroni correction.

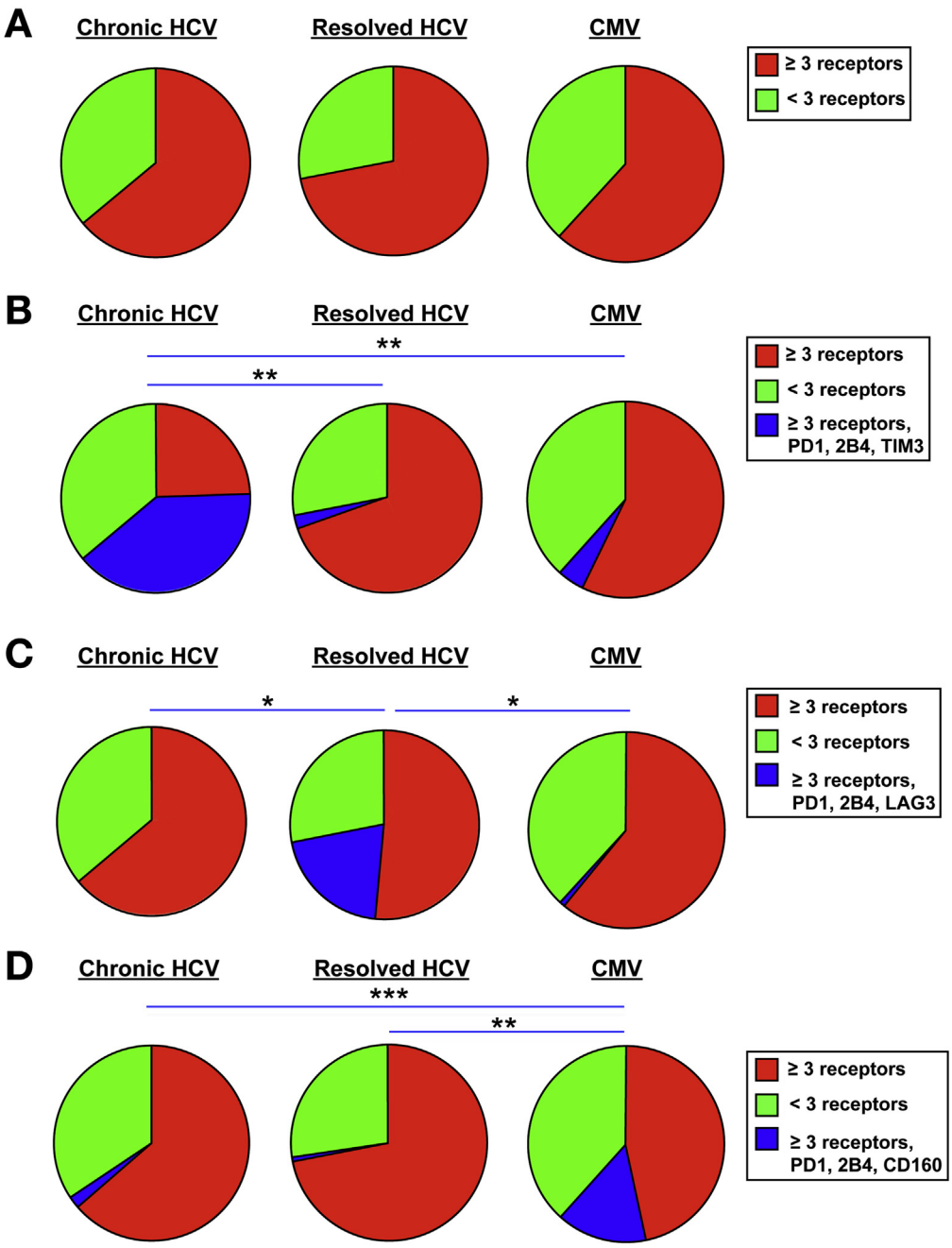

Figure 5. SPICE coexpression analysis of T-cell inhibitory receptors (PD-1, 2B4, CD160, TIM-3, and LAG-3) on HCV-specific IHLs from 4 chronically infected patients, 3 patients with resolved infection, and 3 patients with CMV infection (*$P < .05$, **$P < .01$, ***$P < .001$, nonparametrical statistical comparison by a partial permutation test). (*A*) Coexpression of inhibitory receptors on HCV-specific $CD8^+$ IHLs compared with patients with resolved infection. (*B*) The predominant receptor combination on HCV-specific $CD8^+$ IHLs in chronically infected patients is the combination of PD-1, 2B4, and TIM-3. (*C*) The combination of PD-1 with 2B4 and LAG-3 is the dominating receptor combination on HCV-specific $CD8^+$ IHLs in patients with resolved HCV infection. (*D*) CMV-specific IHLs display coexpression of PD-1 with 2B4 and CD160.

specific $CD8^+$ T cells express 3 or more inhibitory receptors compared with the total $CD8^+$ population (Figure 3*D*). This was observed for both the 15 CD8 responses in 10 subjects with persistent viremia and the 8 responses in 6 patients who were HCV antibody–positive and HCV RNA negative. Of these subjects with resolved HCV infection for a minimum of 5 years, 5 achieved a sustained virological response after therapy and one resolved HCV spontaneously.

Looking at individual T-cell inhibitory receptors, we found that PD-1 expression, although already generally high on all IHLs (Figure 1), was further increased on HCV-specific T cells compared with bulk IHLs by paired analysis (Figure 4*A*, *left graphs*), which is in line with previous studies.[5] There was no significant difference in the expression of 2B4 between specific and bulk $CD8^+$ IHLs (Figure 4*B*, *left graphs*), whereas CD160 expression was increased on some HCV-specific cells (Figure 4*C*, *left graphs*). Expression levels of PD-1, 2B4, and CD160 in CMV-specific responses were even more closely aligned with those of the bulk CD8 T-cell population.

In contrast to the results for PD-1, 2B4, and CD160, expression levels of TIM-3 and LAG-3 were distinct between specific and bulk CD8 T cells and, more importantly, between T cells associated with different levels of viral control. Although TIM-3 was detected in only a minority of intrahepatic bulk $CD8^+$ T cells, a majority of HCV-specific cells in

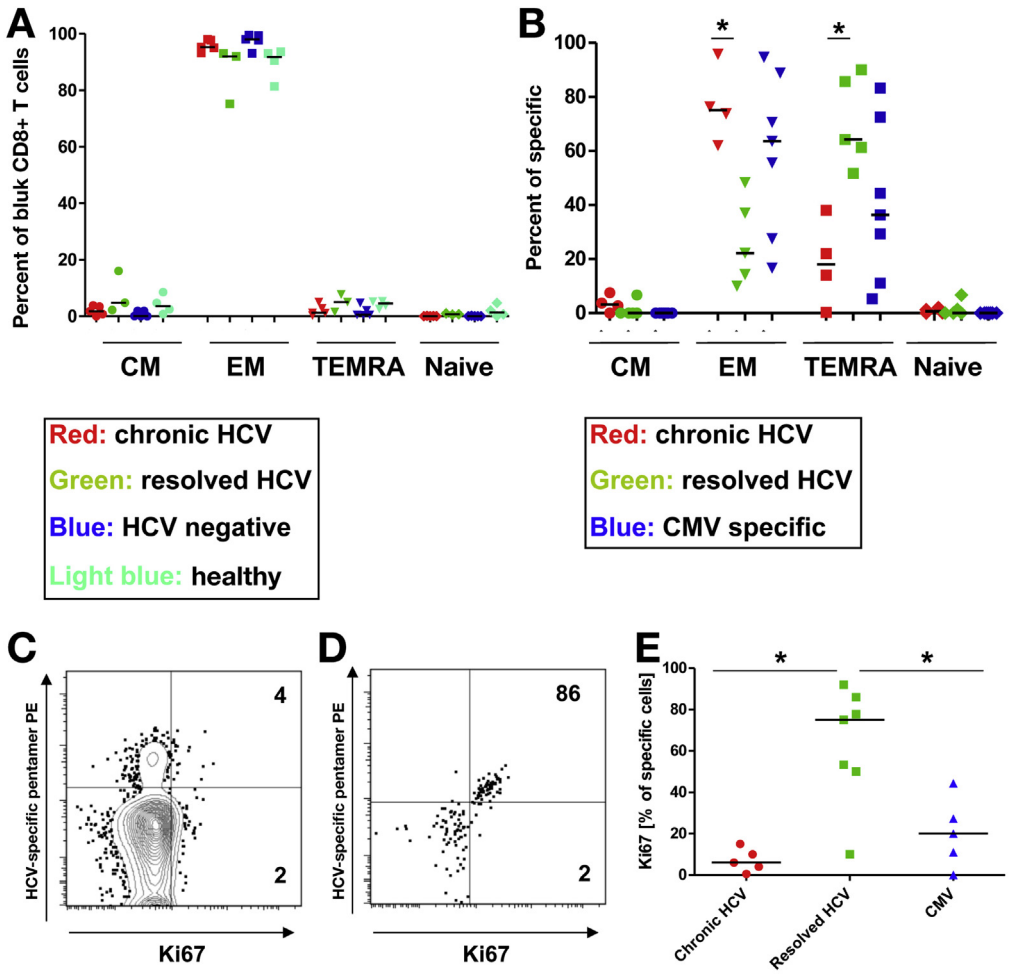

Figure 6. Memory phenotype and proliferation marker for IHLs in chronic and resolved infection. We defined central memory (CM, CD45RA$^-$/CCR7$^+$), effector memory (EM, CD45RA$^-$/CCR7$^-$), effector memory RA (TEMRA, CD45RA$^+$/CCR7$^-$), and naive (CD45RA$^+$/CCR7$^+$) CD8$^+$ T-cell subsets for (*A*) total intrahepatic CD8 lymphocytes in patients with chronic HCV infection (*red dots*, n = 5), resolved HCV infection (*green dots*, n = 3), HCV-negative liver disease (*blue dots*, n = 5), and healthy liver tissue (*light blue dots*, n = 4) and (*B*) intrahepatic virus-specific CD8 T cells in patients with chronic HCV infection (*red dots*, n = 4), resolved HCV infection (*green dots*, n = 5), and intrahepatic CMV-specific populations (*blue dots*, n = 7). *$P < .01$ in unpaired *t* test with Bonferroni correction. (*C* and *D*) Ki-67 expression. Examples of Ki-67 analysis are shown for intrahepatic HCV-specific CD8 responses in (*C*) a patient with chronic HCV infection and (*D*) a patient with resolved HCV infection. *E* summarizes Ki-67 expression for virus-specific intrahepatic CD8 responses in chronic and resolved HCV infection and for CMV-specific populations. *$P < .01$ in unpaired *t* test with Bonferroni correction.

chronic HCV infection were TIM-3 positive (Figure 4*D*, *left graphs*). HCV-specific CD8 T cells in resolved HCV infection rarely displayed elevated levels of TIM-3. These cells, however, almost universally expressed LAG-3 (Figure 4*E*), distinguishing them from all other T-cell populations we studied. CMV responses were on the lower side of both TIM-3 and LAG-3 expression, although individual responses expressing these molecules were observed (Figure 4*A*–*E*).

The coexpression of 3 or more inhibitory receptor molecules differentiated HCV-specific CD8 T-cell responses from bulk CD8 populations in the liver (Figures 3*D* and 5). Expression of TIM-3 in addition to PD-1 and 2B4 was characteristic of HCV-specific T cells in chronic HCV infection (Figure 5*B*), whereas coexpression of LAG-3 with PD-1 and 2B4 was predominantly observed in subjects who controlled HCV successfully (Figure 5*C*). CMV-specific responses contained few cells coexpressing either TIM-3 or LAG-3 but instead had a significant proportion of CD160-coexpressing cells (Figure 5*D*). Together the data show that virus-specific CD8$^+$ T cells have a distinct inhibitory receptor expression profile compared with other intrahepatic T cells and that distinct inhibitory receptor profiles are associated with different levels of viral control.

The Expression Pattern of Inhibitory Receptors in Chronic Versus Resolved Infection Defines HCV-Specific T Cells With Differences in Memory Phenotype and Proliferation

To determine whether the different patterns of inhibitory receptor expression associated with different levels of viral control translate into distinct T-cell memory

phenotypes and T-cell functions, we analyzed the virus-specific $CD8^+$ T-cell populations in the liver for the memory molecules CD45RA and CCR7 as well as for the proliferation marker Ki-67.

No differences in the distribution of different memory phenotypes were observed on bulk $CD8^+$ IHLs from the different subgroups. Bulk $CD8^+$ IHLs are almost universally effector memory cells ($CCR7^-$, $CD45RA^-$), regardless of the disease status (Figure 6*A*; chronic HCV, resolved HCV, HCV-negative diseased tissue, healthy controls). HCV-specific $CD8^+$ T cells in chronic infection were of the same effector memory phenotype, whereas those from resolved infection were mostly TEMRA cells (terminally differentiated RA^+ effector cells; $CCR7^-$, $CD45RA^+$) (Figure 6*B*) that expressed Ki67 as a marker of recent proliferation (Figure 6*C*–*E*). CMV responses displayed a phenotype that was a mix of those detected in chronic HCV and resolved HCV infection, with both $CD45RA^-$ and $CD45RA^+$ cells and a minority of cells expressing Ki-67 (Figure 6*B* and *E*). These data indicate that different degrees of viral control are associated with different inhibitory receptor patterns, with distinct memory development and with different functional properties of those T cells.

Discussion

The first aim of this study was to establish the general differences in inhibitory receptor expression profiles between T cells circulating in the blood and those residing in the liver. Previous reports described increased expression of PD-1 on intrahepatic T cells and associated this observation with T-cell exhaustion in chronic viral hepatitis C.[16,17] Studying PD-1 and 4 additional inhibitory receptors, we found that some, but not all, are expressed by more T cells in the liver compared with blood. This differential expression was only observed for PD-1 and 2B4, whereas CD160, TIM-3, and LAG-3 were expressed at similar levels in blood and liver. These differences in expression between liver and blood were similar for both CD4 and CD8 T cells, although they were more pronounced in the CD8 T-cell population. Importantly, differences in inhibitory receptor expression levels between T cells in the liver and those in the blood were not just a consequence of intrahepatic T-cell populations consisting entirely of antigen-experienced T cells and PBMCs consisting of a significant proportion of naïve, inhibitory receptor–negative T cells. Exclusion of naïve T cells from analysis in PBMCs did not change the overall pattern.

Having hypothesized that elevated expression of inhibitory receptors on IHLs was a consequence of T-cell exhaustion in viral infection and also malignancy, we were surprised to find that the IHL phenotype characterized by increased expression of 2B4 and PD-1 was actually not limited to diseases known for exhausted T cells expressing T-cell inhibitory receptors. Expression patterns of the 5 receptors on intrahepatic T cells were identical to those observed in HCV infection for all liver tissues, whether it was hepatic tissue surrounding cancer or from sterile inflammation as seen in nonalcoholic steatohepatitis. Most importantly, IHLs from liver tissue without infection, inflammation, or malignancy displayed the same patterns, indicating that higher expression levels of PD-1 and 2B4 are not driven by pathological processes (Figure 2 and Supplementary Figure 4). Our interpretation of these data is that higher expression levels of PD-1 and 2B4 are a physiological response to the liver environment and not a reflection of a failing immune response in disease. As an example, the expression of 2B4 and PD-1 on intrahepatic T cells could be important for the prevention of tissue damage by liver-infiltrating lymphocytes, both in scenarios with large numbers of such cells (eg, viral hepatitis) or with few IHLs in normal liver tissue. In this context, it will be important to determine whether T cells acquire this phenotype on entering the liver or whether T cells with this phenotype are specifically recruited to this site. In either case, our data suggest that expression of inhibitory receptors on T cells cannot be automatically equated with a pathological immune response; rather, we need to define the physiological roles of T-cell inhibitory receptors for adaptation to tissue microenvironments. We describe the characteristic inhibitory receptor expression patterns for intrahepatic T cells as a starting point for future investigations into the relationship between tissue environment and physiological T-cell regulation and an important standard for the interpretation of studies on liver resident T cells in disease.

Defining the baseline pattern of inhibitory receptor expression of T cells in liver tissues allowed us to determine what further differentiates virus-specific T cells in this specific microenvironment. The analysis of HCV-specific T cells from persistent and resolved HCV infection and T cells specific for CMV allowed us to directly assess the impact of viral replication on T-cell phenotype. The first important finding from studying both HCV- and CMV-specific T cells was that virus-specific T cells are more susceptible to regulation by coinhibitory pathways, because a majority coexpressed 3 or more inhibitory receptors, in contrast to most other CD8 T-cells coexpressing 2 or fewer receptors. Because this pattern was found in T cells from both chronic and resolved HCV infection and those targeting CMV, a chronic infection with controlled viremia, expression of multiple different inhibitory receptors may not be pathological per se but rather enable the critical regulation of T cells to balance the need for sufficient antiviral activity with the threat of excessive immunological response.

Although the coexpression of PD-1 and 2B4 with additional inhibitory receptors was a unifying feature of virus-specific T cells, certain coexpression patterns of the inhibitory receptors, memory phenotypes, and functional properties were distinct between T cells in different settings of viral control. It was previously suggested that coexpression of TIM-3 and PD-1 defines more severely exhausted T cells than those expressing PD-1 alone.[13,18] Our data strongly support an even more critical role for TIM-3, because the differential expression of TIM-3, but not that of PD-1, was the defining feature of T cells in persistent HCV infection compared with resolved HCV and CMV infection. Our interpretation of these findings is not that the

PD-1 pathway is irrelevant for T-cell exhaustion in HCV infection but that PD-1 expression alone is not a sufficient marker for exhausted T cells and needs to be understood within a complex network of T-cell regulation. The fact that HCV-specific T cells coexpressing TIM-3 were functionally deficient was supported by the finding that they did not express Ki-67, a marker of proliferation, despite high levels of antigen expression. These data conform to our recent observation that most intrahepatic HCV-specific T cells in chronic infection express the T-box transcription factor Eomes, but not T-bet, characteristic of terminally exhausted T cells that have undergone extensive division and have lost further proliferative potential.[20] Accordingly, these intrahepatic T cells display an effector memory phenotype with low expression of both CCR7 and CD45RA. These findings differ from what has been described for circulating TIM-3–expressing T cells in chronic viral infection, which are central memory T cells[13] with high T-bet expression.[21] Together, our data on intrahepatic HCV-specific T cells in chronic HCV infection suggest that TIM-3 expression is the hallmark of a distinct intrahepatic T-cell population that has differentiated into a phenotype unable to sustain an effective antiviral response.

Although the critical role of TIM-3 for T cells in persistent viral infection was not surprising based on previous studies, the up-regulation of LAG-3 on HCV-specific T cells in the liver after eradication of HCV was unexpected. Indeed, we and others have seen extremely few LAG-3–expressing T cells in human samples in general,[22] in contrast to mouse lymphocytes that almost universally express LAG-3 on activation.[23] The PD-1–, 2B4–, and LAG-3–coexpressing populations were almost completely compartmentalized to the liver, and within the liver they represent a unique and rare phenotype of CD45RA-positive memory T cells, in contrast to the rest of the intrahepatic CD8 + T-cell population that consists almost exclusively of CD45RA-negative effector memory cells. This CD45RA-positive memory phenotype was originally described as terminally differentiated with short-term survival,[24] but recent evidence suggests a critical role for cells with this phenotype in long-term antiviral memory.[25] It is striking that these cells were maintained in the liver many years after presumed complete eradication of HCV and also continued to display markers of recent proliferation. It is also noteworthy that intrahepatic CMV-specific T cells displayed phenotypes on a continuum between what we observe for HCV with and without viremia, with most CMV-specific populations expressing LAG-3 and TIM-3 at levels between the extremes of controlled and viremic HCV. This fits the clinical picture of CMV as a controlled chronic infection with latency and intermittent episodes of viral replication. To what degree LAG-3 is directly regulating this T-cell phenotype and thus is not an inhibitory receptor and whether the expression of LAG-3 is critical to maintain small memory T-cell populations after viral control needs to be determined.

In summary, we find that elevated expression of T-cell inhibitory receptors is not necessarily a sign of an exhausted T-cell response. We actually have identified a T-cell inhibitory receptor signature for T cells in both healthy and diseased liver, which suggests a physiological role for the expression of PD-1 and 2B4 on IHLs and which serves as a point of reference for interpreting studies on T cells in this important microenvironment. We further show that virus-specific T cells in the liver are characterized by inhibitory receptor coexpression patterns that correlate with the status of viral control and that are associated with differences in memory phenotype and functional properties in addition to the differences in transcriptional regulation that we reported recently.[20] Further development of safe and effective immunological interventions through modulation of T-cell coinhibitory pathways will require our understanding of the physiological role of these pathways and the downstream effects of these distinct inhibitory receptor coexpression patterns on T-cell function and T-cell differentiation in humans.

Supplementary Material

Note: To access the supplementary material accompanying this article, visit the online version of *Gastroenterology* at www.gastrojournal.org, and at http://dx.doi.org/10.1053/j.gastro.2013.10.022.

References

1. Odorizzi PM, Wherry EJ. Inhibitory receptors on lymphocytes: insights from infections. J Immunol 2012; 188:2957–2965.
2. Peggs KS, Quezada SA, Allison JP. Cancer immunotherapy: co-stimulatory agonists and co-inhibitory antagonists. Clin Exp Immunol 2009;157:9–19.
3. Wherry EJ. T cell exhaustion. Nat Immunol 2011; 12:492–499.
4. **Day CL, Kaufmann DE**, Kiepiela P, et al. PD-1 expression on HIV-specific T cells is associated with T-cell exhaustion and disease progression. Nature 2006; 443:350–354.
5. Kasprowicz V, Schulze Zur Wiesch J, Kuntzen T, et al. High level of PD-1 expression on hepatitis C virus (HCV)-specific CD8+ and CD4+ T cells during acute HCV infection, irrespective of clinical outcome. J Virol 2008; 82:3154–3160.
6. Raziorrouh B, Schraut W, Gerlach T, et al. The immunoregulatory role of CD244 in chronic hepatitis B infection and its inhibitory potential on virus-specific CD8+ T-cell function. Hepatology 2010;52:1934–1947.
7. Blackburn SD, Shin H, Haining WN, et al. Coregulation of CD8+ T cell exhaustion by multiple inhibitory receptors during chronic viral infection. Nat Immunol 2009; 10:29–37.
8. Ribas A. Tumor immunotherapy directed at PD-1. N Engl J Med 2012;366:2517–2519.
9. Lauer GM, Walker BD. Hepatitis C virus infection. N Engl J Med 2001;345:41–52.
10. Urbani S, Amadei B, Tola D, et al. PD-1 expression in acute hepatitis C virus (HCV) infection is associated with HCV-specific CD8 exhaustion. J Virol 2006;80:11398–11403.
11. Rutebemberwa A, Ray SC, Astemborski J, et al. High-programmed death-1 levels on hepatitis C virus-specific

T cells during acute infection are associated with viral persistence and require preservation of cognate antigen during chronic infection. J Immunol 2008;181:8215–8225.
12. Kasprowicz V, Kang YH, Lucas M, et al. Hepatitis C virus (HCV) sequence variation induces an HCV-specific T-cell phenotype analogous to spontaneous resolution. J Virol 2010;84:1656–1663.
13. McMahan RH, Golden-Mason L, Nishimura MI, et al. Tim-3 expression on PD-1+ HCV-specific human CTLs is associated with viral persistence, and its blockade restores hepatocyte-directed in vitro cytotoxicity. J Clin Invest 2010;120:4546–4557.
14. Bengsch B, Seigel B, Ruhl M, et al. Coexpression of PD-1, 2B4, CD160 and KLRG1 on exhausted HCV-specific CD8+ T cells is linked to antigen recognition and T cell differentiation. PLoS Pathog 2010;6:e1000947.
15. Schlaphoff V, Lunemann S, Suneetha PV, et al. Dual function of the NK cell receptor 2B4 (CD244) in the regulation of HCV-specific CD8+ T cells. PLoS Pathog 2011;7:e1002045.
16. Radziewicz H, Ibegbu CC, Fernandez ML, et al. Liver-Infiltrating lymphocytes in chronic human hepatitis C virus infection display an exhausted phenotype with high levels of PD-1 and low levels of CD127 expression. J Virol 2007;81:2545–2553.
17. Golden-Mason L, Palmer B, Klarquist J, et al. Upregulation of PD-1 expression on circulating and intrahepatic hepatitis C virus-specific CD8+ T cells associated with reversible immune dysfunction. J Virol 2007;81:9249–9258.
18. Golden-Mason L, Palmer BE, Kassam N, et al. Negative immune regulator Tim-3 is overexpressed on T cells in hepatitis C virus infection and its blockade rescues dysfunctional CD4+ and CD8+ T cells. J Virol 2009;83:9122–9130.
19. **Lauer GM, Lucas M**, Timm J, et al. Full-breadth analysis of CD8+ T-cell responses in acute hepatitis C virus infection and early therapy. J Virol 2005;79:12979–12988.
20. Paley MA, Kroy DC, Odorizzi PM, et al. Progenitor and terminal subsets of CD8+ T cells cooperate to contain chronic viral infection. Science 2012;338:1220–1225.
21. Sakhdari A, Mujib S, Vali B, et al. Tim-3 negatively regulates cytotoxicity in exhausted CD8+ T cells in HIV infection. PloS One 2012;7:e40146.
22. Baitsch L, Legat A, Barba L, et al. Extended co-expression of inhibitory receptors by human CD8 T-cells depending on differentiation, antigen-specificity and anatomical localization. PloS One 2012;7:e30852.
23. Grosso JF, Kelleher CC, Harris TJ, et al. LAG-3 regulates CD8+ T cell accumulation and effector function in murine self- and tumor-tolerance systems. J Clin Invest 2007;117:3383–3392.
24. Geginat J, Lanzavecchia A, Sallusto F. Proliferation and differentiation potential of human CD8+ memory T-cell subsets in response to antigen or homeostatic cytokines. Blood 2003;101:4260–4266.
25. Akondy RS, Monson ND, Miller JD, et al. The yellow fever virus vaccine induces a broad and polyfunctional human memory CD8+ T cell response. J Immunol 2009;183:7919–7930.

Author names in bold designate shared co-first authorship.

Received March 15, 2013. Accepted October 4, 2013.

Reprint requests
Address requests for reprints to: Georg M. Lauer, MD, PhD, Gastrointestinal Unit, Massachusetts General Hospital and Harvard Medical School, 55 Fruit Street, Boston, Massachusetts 02114. e-mail: glauer@mgh.harvard.edu; fax: (617) 643-0446.

Conflicts of interest
The authors disclose no conflicts.

Funding
Supported by Deutsche Forschungsgemeinschaft (Kr3839/1-1 to D.C.K.), National Institutes of Health (NIH) grant U19 AI082630 (to G.M.L., E.J.W., R.T.C., G.J.F., and J.M.), NIH grant U19 AI066345 (to G.M.L., A.Y.K.), NIH grant R01 AI105035 (to G.M.L.), NIH grant P01 AI054456 (to R.D.K. and G.J.F.), and NIH grant R01 A1089955 (to R.D.K. and G.J.F.). This project was funded in whole or in part with federal funds from the Frederick National Laboratory for Cancer Research under contract no. HHSN261200800001E. The content of this publication does not necessarily reflect the views or policies of the Department of Health and Human Services, nor does mention of trade names, commercial products, or organizations imply endorsement by the US government. This research was also supported in part by the Intramural Research Program of the NIH, Frederick National Laboratory, Center for Cancer Research.

Page intentionally left blank

David WOLSKI

Integrative analysis of CD8 T-cell responses in the context of adaptive immunity to acute Hepatitis C virus infection

Résumé

Le virus de l'hépatite C (VHC) établit généralement une infection chronique. Néanmoins, environ 20% des sujets vont résoudre spontanément l'infection. Il existe des preuves solides que les cellules T CD8 sont essentielles au contrôle du VHC. Dans la première partie de ma thèse, nous avons identifié un nouveau marqueur de la dysfonction des lymphocytes T, CD39, comme étant régulé positivement au cours de l'infection chronique par le VHC, le VIH et dans un modèle d'infection chronique par LCMV. Dans une deuxième partie, nous avons utilisé une approche d'analyse intégrative pour étudier la régulation transcriptionnelle des cellules T CD8 au cours de la phase aiguë de l'infection par le VHC. Nous avons identifié des changements précoces dans la régulation transcriptionelle d'importantes fonctions effectrices, de voies métaboliques et du nucléosome par les cellules T CD8 des patients souffrant d'une infection persistante. Certains de ces changements corrèlent avec l'absence des cellules T CD4 spécifiques du VHC et sont associés avec l'âge et le sexe du sujet infecté. Nos résultats suggèrent que la dysfonction des lymphocytes T CD8 au cours de l'infection par le VHC est liée à des événements précoces dans la régulation des gènes, non seulement amplifiés par une inflammation chronique et une absence des cellules T CD4 auxiliaires, mais qui pourraient également être infuencés par des facteurs de l'hôte tels que l'âge et le sexe.

Mots clés : Virus de l'hépatite C, Lymphocytes T CD8, Régulation Transcriptionnelle, Dysfonction des Lymphocytes T, Lymphocytes T CD4 auxiliaires.

Résumé en anglais

Infection with Hepatitis C virus typically establishes chronic infection, but about 20% of subjects clear HCV spontaneously. There is strong evidence that functional CD8 T cells are critical for HCV control. In the first part of my thesis we identified a new marker for exhausted T cells, CD39, that we showed to be upregulated in chronic HCV infection, progressive HIV infection and in chronic infection with LCMV. In the second part we used an integrative analysis approach to study transcriptional regulation of CD8 T cells in the acute phase of HCV infection with different outcomes. We found early transcriptional changes in key immune effector pathways as well as metabolic and nucleosomal processes in CD8 T cells from patients with persistent infection. Some of these changes track with a lack of HCV-specific CD4 T cells exhibit associations with subject age and sex. Our findings suggest that CD8 T cell exhaustion in HCV infection is linked to early gene regulatory events that are not only amplified by chronic inflammation and a lack of CD4 help, but might also be influenced by disease-relevant host factors such as patient age and sex.

Keywords: Hepatitis C virus, CD8 T cells, transcriptional regulation, T cell exhaustion, CD4 help